

Technical Report Documentation Page

1. Report No. FHWA/TX-11/0-4889-1	2. Government Accession No.	3. Recipient's Catalog No.	
4. Title and Subtitle Laboratory and Field Evaluations of External Sulfate Attack in Concrete		5. Report Date February 2010, Rev. January 2011	
		6. Performing Organization Code	
7. Author(s) Thanos Drimalas, John C. Clement, Kevin J. Folliard, Raj Dhole, and Michael D.A. Thomas		8. Performing Organization Report No. 0-4889-1	
9. Performing Organization Name and Address Center for Transportation Research The University of Texas at Austin 1616 Guadalupe, Suite 4.202 Austin, TX 78701		10. Work Unit No. (TRAIS)	
		11. Contract or Grant No. 0-4889	
12. Sponsoring Agency Name and Address Texas Department of Transportation Research and Technology Implementation Office P.O. Box 5080 Austin, TX 78763-5080		13. Type of Report and Period Covered Technical Report 9/1/2004–8/31/2009	
		14. Sponsoring Agency Code	
15. Supplementary Notes Project performed in cooperation with the Texas Department of Transportation and the Federal Highway Administration.			
16. Abstract Sulfate attack is a complex form of deterioration that has damaged concrete structures throughout the world. Sulfate attack is particularly complex because the source of sulfates can be external or internal (delayed ettringite formation), and the distress can be chemical in nature, due to alteration of hydration of products, or physical in nature, due to phase changes in the penetrating sulfate solution. Although sulfate attack has been recognized as a cause of concrete distress for many years, it remains a controversial, confusing, and complex topic. There are many unresolved issues, far too many to be tackled in a single investigation. The research described in this report aims to address several of these lingering issues, especially those that are particularly relevant to the state of Texas.			
17. Key Words Sulfate, sulfate-resistance, sulfate attack, delayed ettringite formation, DEF, concrete distress	18. Distribution Statement No restrictions. This document is available to the public through the National Technical Information Service, Springfield, Virginia 22161; www.ntis.gov .		
19. Security Classif. (of report) Unclassified	20. Security Classif. (of this page) Unclassified	21. No. of pages 190	22. Price

Form DOT F 1700.7 (8-72) Reproduction of completed page authorized



Laboratory and Field Evaluations of External Sulfate Attack in Concrete

Thanos Drimalas

John C. Clement

Kevin J. Folliard

Raj Dhole

Michael D. A. Thomas

CTR Technical Report:	0-4889-1
Report Date:	February 2010, Rev. January 2011
Project:	0-4889
Project Title:	Sulfate Resistance of Concrete Exposed to External Sulfate Attack
Sponsoring Agency:	Texas Department of Transportation
Performing Agency:	Center for Transportation Research at The University of Texas at Austin

Project performed in cooperation with the Texas Department of Transportation and the Federal Highway Administration.

Center for Transportation Research
The University of Texas at Austin
1616 Guadalupe, Ste. 4.202
Austin, TX 78701

www.utexas.edu/research/ctr

Copyright (c) 2010
Center for Transportation Research
The University of Texas at Austin

All rights reserved
Printed in the United States of America

Disclaimers

Author's Disclaimer: The contents of this report reflect the views of the authors, who are responsible for the facts and the accuracy of the data presented herein. The contents do not necessarily reflect the official view or policies of the Federal Highway Administration or the Texas Department of Transportation (TxDOT). This report does not constitute a standard, specification, or regulation.

Patent Disclaimer: There was no invention or discovery conceived or first actually reduced to practice in the course of or under this contract, including any art, method, process, machine manufacture, design or composition of matter, or any new useful improvement thereof, or any variety of plant, which is or may be patentable under the patent laws of the United States of America or any foreign country.

Engineering Disclaimer

NOT INTENDED FOR CONSTRUCTION, BIDDING, OR PERMIT PURPOSES.

Project Engineer: David W. Fowler
Professional Engineer License State and Number: Texas No. 27359
P. E. Designation: Researcher

Acknowledgments

The authors express appreciation to the TxDOT Project Director (Kevin Pruski), members of the PMC Committee, and the staff and undergraduate research assistants at the Concrete Durability Center.

Table of Contents

Chapter 1. Introduction.....	1
1.1 Introduction.....	1
1.2 Research objectives.....	1
1.3 Outline of Report	3
Chapter 2. Literature Review	5
2.1 Types of Sulfates	5
2.1.2 Calcium Sulfate.....	5
2.1.3 Sodium Sulfate.....	6
2.1.4 Magnesium Sulfate	6
2.2 Physical Sulfate Attack.....	7
2.3 Preventing Sulfate Attack	8
2.3.1 Permeability	8
2.3.2 Sulfate Resistant Cements.....	9
2.3.3 Supplementary Cementing Materials.....	9
2.3.4 Physical Sulfate Attack	11
2.4 Characterization of Sulfate Exposure Conditions.....	11
2.4.2 Water Samples	12
2.4.3 Soil Samples.....	12
2.5 Structures Suffering from Sulfate Attack	13
2.6 Test Methods and Specifications	13
Chapter 3. Materials used in Research Project.....	15
3.1 Aggregates	15
3.2 Cement	15
3.3 Supplementary Cementing Materials.....	15
Chapter 4. ASTM C 1012 Testing	17
4.1 Expansion Limits	17
4.2 Cement Selection for ASTM C 1012 Testing.....	18
4.2.1 Producer Variability	19
4.2.2 Cement Study Results	20
4.3 Evaluation of Class C Fly Ashes	21
4.3.1 Expansions	21
4.3.2 X-Ray Diffraction	27
4.3.3 Scanning Electron Microscopy	28
4.4 Evaluation of Ternary Blends	34
4.4.1 Expansions	35
4.4.2 X-Ray Diffraction	37
4.4.3 Scanning Electron Microscopy	39
4.5 Modified ASTM C 1012 Testing.....	40
4.6 Fly Ash Investigation.....	44
4.7 Summary	45
Chapter 5. Outdoor Exposure Site.....	47
5.1 Outdoor Sulfate Exposure Site Design and Test Procedure	47

5.1.1 Exposure Site Design	48
5.1.2 Concrete Prism Testing Regime	49
5.1.3 Mortar Bar Testing Using ASTM C 1012	51
5.1.4 Sulfate Profiling	51
5.1.5 Physical Sulfate Attack Testing	52
5.2 Results and Discussion	53
5.2.2 Calcium Sulfate	54
5.2.3 Supplementary Cementing Materials	58
5.2.4 Sodium Sulfate	65
5.2.5 Magnesium Sulfate	82
5.2.6 Prisms Constructed for Phase II	93
5.3 Discussion	102
5.4 Conclusions	103
Chapter 6. Sulfate Resistance of High-Calcium Fly Ash Concrete	105
6.1 Introduction	105
6.2 Materials	105
6.3 Combined Physical-Chemical Sulfate Attack on Concrete (Phase 1)	106
6.4 Sulfate Resistance of Mortars Containing Class C Fly Ash Blended with Other Pozzolans	119
6.5 Strategies for Increasing the Sulfate Resistance of Mortars Containing Class C Fly Ash: Gypsum Addition, Low W/CM and HVFA	127
6.5.1 Gypsum Addition	127
6.5.2 Low W/CM	129
6.5.3 High-Volume Fly Ash Mortars	130
6.6 Characterization of Class C Fly Ashes	134
6.6.1 Characterization using X-Ray Diffraction	134
6.6.2 Characterization using SEM-EDXA	139
6.7 Analysis of Fly Ash Hydration Products in Sulfate Environments	141
6.8 Summary	144
Chapter 7. Evaluation of Concrete Structures for Potential Deterioration to External Sulfate Attack	145
7.1 Experimental Methods	145
7.1.1 Water Samples	146
7.1.2 Soil Samples	146
7.1.3 Concrete Powder Samples	147
7.1.4 Concrete Cores	147
7.2 Results and Discussion	147
7.2.1 Childress District	147
7.2.2 Paris District	150
7.2.3 El Paso District	154
7.3 Conclusions	163
Chapter 8. Conclusions, Recommendations, and Guidelines for Sulfate Resistant Concrete	165
References	169

List of Figures

Figure 2.1: Solubility Curve for Sodium Sulfate /Water System (Berkeley 1904)	7
Figure 2.2: Relationship between C ₃ A Content in fly ash to 6 month expansion in ASTM C 1012 testing (Shashiprakash and Thomas 2001).....	10
Figure 2.3: The use ternary blends with silica fume and Class C fly ash reduces the expansion of mortars compared to only using Class C fly ash as a pozzolan. (Shashiprakash and Thomas 2001).....	11
Figure 4.1: Variability in Cement Performance from a Producer with Time	20
Figure 4.2: ASTM C 1012 Results of Cements Tested	21
Figure 4.3: Expansions of FA1 at Different Replacement Dosages	24
Figure 4.4: Expansions of FA2 at different replacement dosages	25
Figure 4.5: Expansion of FA8 fly ash at different replacements	26
Figure 4.6: FA8 after 56 days in ASTM C 1012 testing.....	27
Figure 4.7: SEM and EDS Spectrum of 25% FA2 after 18 months storage in sodium sulfate solution. Ettringite formation has occurred in pockets in the sample	30
Figure 4.8: SEM Image and EDS Spectrum of 20% FA1after 18 months of storage showing gypsum formation around aggregates	31
Figure 4.9: SEM Image and EDS spectrum of possible conversion of gypsum into ettringite in 20% FA1 mortar after 18 months storage in sodium sulfate.....	32
Figure 4.10: SEM and EDS analysis of 40% FA1 after 18 months in sodium sulfate solution.....	33
Figure 4.11: SEM and EDS analyses of 35% FA2 after 18 months of storage in sodium sulfate	34
Figure 4.12: Mortar mixtures with 20% FA1 and ternary blends.....	36
Figure 4.13: Mortar mixtures with 40% FA1 and ternary blends.....	36
Figure 4.14: Relationship between ettringite, gypsum, and CH from mortars of ternary blends of FA1 and FA2.....	39
Figure 4.15: SEM Image and EDS spectrum of 40% FA1 with 5% SF after 18 months of storage in sodium sulfate storage. Gypsum band is found along the samples edge and around aggregates.....	40
Figure 4.16: Mortar mixtures containing Type I/II Cement placed into three different soak solutions.....	41
Figure 4.17: Mortar mixtures containing Type V Cement placed into three different soak solutions	42
Figure 4.18: ASTM C 1012 mortar mixture with Type I/II cement and 20% FA8.....	43
Figure 4.19: ASTM C 1012 mortar mixture with Type V cement and 40% FA1	43
Figure 4.20: Quantitative XRD Rietveld analyses for FA1, FA2, and FA8. FA1 and FA2 have similar crystalline composition but perform drastically different in ASTM C 1012 Testing.....	44

Figure 5.1: Outdoor sulfate exposure site located in Austin, TX. From left to right, the trenches contain calcium sulfate, sodium sulfate and magnesium sulfate.....	48
Figure 5.2: The placement of prisms from each mixture into the outdoor exposure site or in the modified ASTM C 1012 testing.....	50
Figure 5.3: Placement of prisms in each outdoor exposure trench. The units are in terms of inches.....	50
Figure 5.4: Prisms were cut into cubes to allow for milling for sulfates. Slices were also removed for SEM analysis.....	52
Figure 5.5: Temperature Cycle for mortars subjected to physical sulfate attack.....	53
Figure 5.6: Mixture designations used throughout this chapter.....	53
Figure 5.7: Concrete prism with a 0.4 w/cm placed vertically in the outdoor calcium sulfate exposure site. In this photograph, the left side shows the portion of the prism that was below the soil level.....	56
Figure 5.8: Semi-quantitative Rietveld analysis showing differences in cement types for prisms at 0.4w/cm, placed indoors in calcium sulfate	57
Figure 5.9: Quantitative Analysis showing differences in cement types for prisms at 0.7 w/cm placed indoors in calcium sulfate.....	58
Figure 5.10: Semi-quantitative XRD analysis of profiled prisms containing Class C fly ash at a 0.4 w/cm to determine phase content at different milled depths	60
Figure 5.11: Quantitative XRD analysis of profiled prisms containing Class C fly ash at a 0.4 w/cm to determine phase content at different milled depths	61
Figure 5.12: Concrete Prisms Exposed to 33000 ppm Calcium Sulfate, Type I Cement at 0.4 w/cm.....	64
Figure 5.13: Concrete Prisms Exposed to 33000 ppm Calcium Sulfate, Type I Cement at 0.7 w/cm.....	64
Figure 5.14: C1-7 Prism submerged in the outdoor sodium sulfate exposure site after 18 months.....	67
Figure 5.15: Mixture C5-7 after 18 months of outdoor exposure to sodium sulfate. This prism was placed vertically, with the section on the left fully submerged below sulfate-saturated soil.....	68
Figure 5.16: Quantitative XRD Rietveld analyses of concrete prisms at 0.4 w/cm, placed indoors in sodium sulfate solutions after 18 months	69
Figure 5.17: Semi-quantitative XRD Rietveld analysis of concrete prisms at 0.7 w/cm, placed indoors in sodium sulfate solutions after 18 months	70
Figure 5.18: Quantitative XRD Analysis of Concrete prisms at 0.4 w/cm placed in sodium sulfate solutions for 18 months	76
Figure 5.19: Quantitative XRD analysis of prisms at 0.7 w/cm placed tested indoors in sodium sulfate solutions.....	77
Figure 5.20: Damage to prisms exposed to 33000 ppm sodium sulfate	79
Figure 5.21: Concrete Prisms Exposed to 33000 ppm Sodium Sulfate exhibiting excellent performance	81

Figure 5.22: Semi-quantitative XRD Analysis of concrete prisms at 0.4 w/cm placed in indoor magnesium sulfate conditions	84
Figure 5.23: Semi-quantitative XRD Rietveld analysis of prisms placed in magnesium sulfate conditions	85
Figure 5.24: Semi-quantitative XRD Rietveld analysis of prisms containing SCMs in indoor magnesium sulfate conditions	89
Figure 5.25: Semi-quantitative XRD Rietveld Analysis of prisms with SCMs placed indoors in magnesium sulfate solution	90
Figure 5.26: Damage to Prisms Exposed to 33000 ppm Magnesium Sulfate	92
Figure 5.27: Updated Outdoor Sulfate Exposure Site	94
Figure 5.28: Surface Scaling in 1500 ppm Sodium Sulfate in Soil Contact Zone.....	96
Figure 5.29: Surface Scaling in 10000 ppm Sodium Sulfate in Soil Contact Zone.....	97
Figure 5.30: Physical Sulfate Attack in 10000 ppm Sodium Sulfate Above Soil Contact Zone	98
Figure 5.31: Physical sulfate testing of non-air-entrained mortars containing Type V cement (w/cm=0.7)	100
Figure 5.32: Physical sulfate testing of air-entrained and non-air-entrained mortars (w/cm=0.7) immersed in 30% sodium sulfate solution and subjected to temperature changes.....	101
Figure 5.33: Mortar specimens before and after physical sulfate testing. The mixture contained Type V cement at 0.7w/cm. The disk on the left was prior to testing and the disk on the right went through 150 cycles.	101
Figure 6.1: Effect of w/cm on the Change in Relative Dynamic Modulus of Control Mixes Exposed to Wet-dry Cycling in 5% Na ₂ SO ₄ Solution (NSD).....	108
Figure 6.2: Effect of w/cm on the expansion of Control Mixes Exposed to Wet-Dry Cycling in 5% Na ₂ SO ₄ Solution (NSD).....	109
Figure 6.3: Effect of w/cm on the Expansion of Control Mixes Immersed in 5% Na ₂ SO ₄ Solution (NSS)	110
Figure 6.4: Effect of w/cm on the Expansion of Control Mixes Immersed in Saturated-CaSO ₄ Solution (CSS)	110
Figure 6.5: Visual Appearance of Control Mixtures after Immersion in 5% Na ₂ SO ₄ Solution (NSS)	111
Figure 6.6: Visual Appearance of Control Mixtures after Immersion in Saturated CaSO ₄ Solution (CSS)	112
Figure 6.7: Change in Relative Dynamic Modulus of Concrete with TK Fly Ash (23.54% CaO) Exposed to Wet-Dry Cycling in 5% Na ₂ SO ₄ Solution (NSD)	113
Figure 6.8: Expansion of Concrete with TK Fly Ash (23.54% CaO) Exposed to Wet-Dry Cycling in 5% Na ₂ SO ₄ Solution (NSD).....	113
Figure 6.9: Change in Relative Dynamic Modulus of Concrete with Fly Ash WL (28.98% CaO) and RL (12.76% CaO) Exposed to Wet-Dry Cycling in 5% Na ₂ SO ₄ Solution (NSD)	114

Figure 6.10: Expansion of Concrete with Fly Ash WL (28.98% CaO) and RL (12.76% CaO) Exposed to Wet-Dry Cycling in 5% Na ₂ SO ₄ Solution (NSD)	114
Figure 6.11: Expansion of Concrete with Fly Ash TK (23.54% CaO) Immersed in 5% Na ₂ SO ₄ Solution (NSS).....	115
Figure 6.12: Expansion of Concrete with Fly Ash WL (28.98 CaO) and RL (12.76% CaO) Immersed in 5% Na ₂ SO ₄ Solution (NSS)	116
Figure 6.13: Summary of Expansion Data for Concrete Mixes.....	117
Figure 6.14: Summary of Relative Dynamic Modulus Data for Concrete Mixes	118
Figure 6.15: Expansion of Mortar Bars with Different Fly Ashes (ASTM C 1012 – 5% Na ₂ SO ₄ Solution)	122
Figure 6.16: Expansion of Mortar Bars with Blended (Type F – Type C) Fly Ashes (ASTM C 1012 – 5% Na ₂ SO ₄ Solution).....	123
Figure 6.17: Effect of the CaO Content of Fly Ash on the Expansion of Mortar Bars with 25 to 30% Fly Ash (ASTM C 1012 – 5% Na ₂ SO ₄ Solution).....	124
Figure 6.18: Effect of the CaO Content of Blended Fly Ash on the Expansion of Mortar Bars with 25 to 30% Fly Ash (ASTM C-1012 – 5% Na ₂ SO ₄ Solution)	125
Figure 6.19: Summary of Expansion Results for Mortars Containing Ultra-Fine Fly Ash (UFFA) or Silica Fume (SF) – ASTM C 1012).....	127
Figure 6.20: Expansion of Mortar Bars with TK Fly Ash and Added Gypsum (ASTM C 1012 – 5% Na ₂ SO ₄ Solution).....	128
Figure 6.21: Expansion of Mortar Bars with WL Fly Ash and Added Gypsum (ASTM C 1012 – 5% Na ₂ SO ₄ Solution).....	129
Figure 6.22: Effect of w/cm on the Expansion of Mortar Bars with WL Fly Ash (ASTM C 1012 – 5% Na ₂ SO ₄ Solution)	130
Figure 6.23: Expansion of HVFA Mortar Bars with TK Fly Ash (ASTM C 1012 – 5% Na ₂ SO ₄ Solution).....	131
Figure 6.24: Expansion of HVFA Mortar Bars with PS Fly Ash (ASTM C 1012 – 5% Na ₂ SO ₄ Solution).....	132
Figure 6.25: Expansion of HVFA Mortar Bars with WL Fly Ash (ASTM C 1012 – 5% Na ₂ SO ₄ Solution)	132
Figure 6.26: Expansion of HVFA Mortar Bars with Blends of PS and RL Fly Ash (ASTM C 1012 – 5% Na ₂ SO ₄ Solution).....	133
Figure 6.27: Expansion of HVFA Mortar Bars with Blends of PS and RL Fly Ash and Reduced w/cm = 0.40 (ASTM C 1012 – 5% Na ₂ SO ₄ Solution).....	133
Figure 6.28: Crystalline Composition of Class F Fly Ashes Determined by XRD Rietveld Method	135
Figure 6.29: Crystalline Composition of Class C Fly Ashes Determined by XRD Rietveld Method	136
Figure 6.30: Normalized Glass Composition of Fly Ashes Determined by Subtraction of Oxide Content of Crystalline Components from Bulk Oxide Composition	138
Figure 6.31: Ternary CaO-SiO ₂ -Al ₂ O ₃ Diagram Showing Location of Glass in Six Fly Ashes Glass Composition Determined by Rietveld Analysis.....	139

Figure 6.32: Ternary CaO-SiO ₂ -Al ₂ O ₃ Diagram Showing Location of Glass in Seven Fly Ashes Glass Composition Determined by SEM-EDXA.....	140
Figure 6.33: Ternary CaO-SiO ₂ -Al ₂ O ₃ Diagram Showing Location of Glass in Seven Fly Ashes Bulk Composition of Fly Ash Determined by Chemical Analysis	141
Figure 6.34: Relationship between the CaO Content of Fly Ash and the Quantity of Sulfate Phases produced in Lime-Fly Ash Pastes after Curing (prior to sulfate exposure).....	142
Figure 6.35: Relationship between the CaO Content of Fly Ash and the Quantity of Ettringite produced in Lime-Fly Ash Pastes exposed to 5% Na ₂ SO ₄	143
Figure 6.36: Relationship between the CaO Content of Fly Ash and the Quantity of Ettringite Produced in Lime-Fly Ash Pastes exposed to 5% Na ₂ SO ₄	144
Figure 7.1: Site Locations evaluated within this chapter.....	145
Figure 7.2: Calibration curve for sulfate using the turbidimeter	146
Figure 7.3: Damage to the lower part of a wall below US 83 in Childress District	148
Figure 7.4: Damage to a bridge column on FM 2278, south of Childress, Texas	149
Figure 7.5: Deterioration commonly found in culverts in the Paris District. The distress begins near the base of the culvert and continues up the side, likely in line with the highest level of water.	151
Figure 7.6: Deterioration of a culvert above the soil level, with no deterioration visible below the level of the soil (after excavation).....	152
Figure 7.7: Deteriorated concrete columns from a bridge in the Paris District	153
Figure 7.8: Riprap deterioration occurring on the embankment below a bridge	155
Figure 7.9: Riprap deterioration at Site 31 in the El Paso District	156
Figure 7.10: Deteriorated Riprap at Site 32 located on FM 652 in the El Paso District.....	157
Figure 7.11: ROW marker deteriorating in West Texas.....	158
Figure 7.12: Location of the removed and replaced ROW markers along SH 54 north of Van Horn, TX	159
Figure 7.13: Placement of new ROW marker in the existing location of the deteriorated ROW marker.....	160
Figure 7.14: The sulfate content of soils taken from each of the ROW locations using ASTM C 1580 and TEX-135-E Test Methods	161
Figure 7.15: Rietveld Analyses from ROW markers in the El Paso District.....	162
Figure 7.16: New ROW marker with Class C fly ash at 0.4 w/cm after 3 months of exposure in gypsiferous soils.....	163

List of Tables

Table 2.1: Cement Chemistry notations used throughout this report	5
Table 2.2: Sulfate Exposure classification for water-soluble sulfates in soil or sulfates in water (ACI 2001)	12
Table 3.1: Chemical data for the portland cements used in this study	15
Table 3.2: Chemical Analysis of Fly Ashes Tested in the Study.....	16
Table 3.3: Chemical Analysis of other SCMs Tested in the Study	16
Table 4.1: Composition of Cements Used in Study.....	19
Table 4.2: Expansion Measurements from FA1 in ASTM C 1012 Testing	22
Table 4.3: Expansion Measurements for FA2 in ASTM C 1012 Testing	23
Table 4.4: Semi-quantitative Rietveld analysis of select mortar mixtures at 18 months.....	28
Table 4.5: Mortar mixtures with FA-4, FA5, FA-6, FA7, and FA-8.....	35
Table 4.6: Semi-quantitative Rietveld analysis of ternary blends with FA1 and FA2	38
Table 4.7: Testing matrix for fly ashes FA-1, FA-2, FA-8 various fly ash replacements combined with Type II and Type V cement in different soak solutions.....	41
Table 5.1: Expansion and Mass Change Data from Mixtures Placed in Calcium Sulfate Conditions	55
Table 5.2: Expansion and Mass Change Data from Mixtures with Class C fly ash Placed in Calcium Sulfate Conditions	59
Table 5.3: Comparison between mortar bars and concrete prisms evaluated using calcium sulfate solution in ASTM C 1012 storage conditions.....	62
Table 5.4: Expansion and Mass Change for Phase I Prisms Exposed to a 5% Calcium Sulfate Solution in Outdoor Exposure Site	63
Table 5.5: Expansion and Mass Change Data for Mixtures without SCMs, exposed to Sodium Sulfate Solution	66
Table 5.6: Expansion and Mass Change Data for Concrete with Type I Cement and Class C fly ash, exposed to sodium sulfate solution.....	72
Table 5.7: Expansion and Mass Change Data for Concrete with Type I/II Cement and Class C fly ash, exposed to sodium sulfate solution.....	72
Table 5.8: Expansion and Mass Change Data for Concrete with Type V Cement and Class C fly ash, exposed to sodium sulfate solution.....	73
Table 5.9: Expansion and Mass Change Data for Concrete with ternary SCM blends exposed to sodium sulfate solution	74
Table 5.10: Expansion and Mass Change Data for Concrete with Various Cements (Type I, II, or V) in combination with Class F fly ash and exposed to sodium sulfate solution.....	75
Table 5.11: Comparison between mortar bars and concrete prisms evaluated using sodium sulfate solution in ASTM C 1012 storage.....	78

Table 5.12: Expansion and Mass Change for Phase I Prisms Exposed to a 5% Sodium Sulfate Solution in Outdoor Exposure Site	82
Table 5.13: Expansion and Mass Change Data for Mixtures without SCMs, exposed to Magnesium Sulfate Solution.....	83
Table 5.14: Expansion and Mass Change Data for Concrete with Type I Cement and Class C fly ash, exposed to magnesium sulfate solution	86
Table 5.15: Expansion and Mass Change Data for Concrete with Type I/II Cement and Class C fly ash, exposed to magnesium sulfate solution	86
Table 5.16: Expansion and Mass Change Data for Concrete with ternary SCM blends exposed to magnesium sulfate solution	88
Table 5.17: Comparison between mortar bars and concrete prisms evaluated using magnesium sulfate solution in ASTM C 1012 storage conditions	91
Table 5.18: Expansion and Mass Change for Phase I Prisms Exposed to a 5% Magnesium Sulfate Solution in Outdoor Exposure Site.....	93
Table 5.19: Mixtures Cast for Phase II Outdoor Sulfate Exposure	94
Table 5.20: Expansion and Mass Change for Phase II Prisms Exposed to a 1500 ppm Calcium Sulfate Solution	95
Table 5.21: Expansion and Mass Change for Phase II Prisms Exposed to a 1500 ppm Sodium Sulfate Solution	95
Table 5.22: Expansion and Mass Change for Phase II Prisms Exposed to a 10000 ppm Sodium Sulfate Solution	96
Table 5.23: Final mixtures for Outdoor Exposure Study.....	98
Table 6.1: Details of Cementing Materials	106
Table 6.2: Summary of Concrete Mixes	107
Table 6.3: Performance Criteria.....	119
Table 6.4: Ranking of Concrete Based on Performance	119
Table 6.5: Details of Binary Mixes with Class F or Class C Fly Ash for ASTM C 1012 Tests	120
Table 6.6: Details of Ternary Mixtures with Blends of Class F and Class C Fly Ash for ASTM C 1012 Tests	120
Table 6.7: Details of Mixes with Blends of Fly Ash, Ultra-Fine Fly Ash and Silica Fume for ASTM C 1012 Tests.....	121
Table 6.8: Details of Mixes with Blends of Fly Ash, Ultra-Fine Fly Ash and Silica Fume for ASTM C 1012 Tests.....	126
Table 6.9: Details of Mortar Mixes with Added Gypsum for ASTM C 1012 Tests	128
Table 6.10: Details of Mortar Mixes with Lower w/cm for ASTM C 1012 Tests	129
Table 6.11: Details of Mortar Mixes with High-Volume Fly Ash for ASTM C 1012 Tests.....	131
Table 6.12: Quantities of Phases in Lime-Fly Ash Pastes Prior to Sulfate Exposure	142
Table 6.13: Quantities of Phases in Lime-Fly Ash Pastes after Exposure to 5% Na ₂ SO ₄ for 90 days.....	143
Table 7.1: Sulfate content of concrete powders from locations in the Childress District	149

Table 7.2: Quantitative XRD Rietveld Analyses from columns SO and NO in the Childress District	150
Table 7.3: Quantitative Rietveld analyses taken from two sections from a culvert at Site 22.....	151
Table 7.4: XRD results from Site 57 in the Paris District	153
Table 7.5: Sulfate content of concrete powder taken from the riprap at site 31	156
Table 7.6: Concrete Mixtures made for ROW Markers in West Texas.....	160

Chapter 1. Introduction

1.1 Introduction

Sulfate attack is a complex form of deterioration that has damaged concrete structures throughout the world. Sulfate attack is particularly complex because the source of sulfates can be external or internal (delayed ettringite formation), and the distress can be chemical in nature, due to alteration of hydration of products, or physical in nature, due to phase changes in the penetrating sulfate solution. This project and final report focus exclusively on external sulfate attack, but includes both chemical and physical manifestations of this form of attack.

The research described herein was funded by the Texas Department of Transportation (TxDOT) under TxDOT Project 4889, “Sulfate Resistance of Concrete Exposed to External Sulfate Attack” and was initiated as a joint research project between The University of Texas at Austin and the University of New Brunswick. The project was initiated in September 2004 and was completed in August 2009 (although outdoor test specimens are still being monitored by the research team in Austin and in other sites in Texas). This report focuses primarily on the work performed to date at The University of Texas at Austin but also includes a brief synopsis of research performed at the University of New Brunswick. The remainder of this chapter provides a brief summary of the project objectives and describes how the remaining chapters are organized and presented.

1.2 Research Objectives

Although sulfate attack has been recognized as a cause of concrete distress for many years, it remains a controversial, confusing, and complex topic. There are many unresolved issues, far too many to be tackled in a single investigation. The research described in this report aims to address several of these lingering issues, especially those that are particularly relevant to the state of Texas. The key technical issues that were evaluated include:

Sulfate resistance of concrete containing ASTM C 618 Class C fly ash. This is particularly an issue in Texas, where Class C fly ash is widely available, and in some parts of the state (e.g., Lubbock); it is the only type of fly ash available. Research under this project aimed to determine the impact of fly ash chemistry and mineralogy on sulfate resistance and to identify the mechanisms responsible for the poor sulfate resistance exhibited by certain Class C fly ashes. Lastly, and perhaps most importantly from a practical point of view, research was initiated to identify methods by which concrete containing Class C fly ash can be made sulfate resistant (i.e., incorporation of silica fume or ultra-fine fly ash in ternary systems).

Sulfate resistance of concrete exposed to gypsiferous soils. There is much debate today regarding the potential for deterioration of concrete exposed to gypsiferous or gypsum-bearing soils. Because gypsum (calcium sulfate) is much less soluble than other common forms of sulfate, such as sodium sulfate and magnesium sulfate, it has been suggested that there is less potential for sulfate-induced distress. This uncertainty related to this solubility-related issue is compounded by the fact that the vast majority of laboratory studies have used more aggressive sulfate solutions, primarily sodium sulfate, and as such, there is a general lack of information on how damaging gypsum can be to concrete.

Given that gypsum is by far the most common form of sulfate in soils and groundwater in Texas, this is obviously a critical issue and was a key focus of this study.

Determination of Severity of Exposure. The general approach recommended by the American Concrete Institute (ACI), as well as other agencies, to preventing sulfate attack starts with defining the severity of exposure to which a given concrete structure will be subjected. This involves sampling either groundwater or soils from the subject site and analyzing it for sulfate content. The measured sulfate content would then be used to select an appropriate preventive measure, such as concrete mixtures with lower water/cementitious materials (w/cm) ratios, and potentially containing low-C₃A cements and/or supplementary cementing materials (SCMs). The measurement of sulfates in groundwater is quite straightforward and is not a contentious issue as one only has to measure the sulfate concentration using appropriate analytical techniques. However, when one attempts to measure the concentration of sulfates in a soil sample, the inherent issue regarding the solubility of different sulfate forms becomes critical. The issue is that one must extract sulfate from the subject soil by diluting it with water, and as such, the solubility of the sulfate contained in the soil affects the values obtained for a given extraction ratio (or water:soil ratio). There is no clear consensus on what specific extraction ratio should be used for soil analysis, with values ranging from 1:1 to as high as 20:1 (currently recommended in ACI 201 – Guide to Durable Concrete). Sodium and magnesium sulfate are very soluble and are not impacted much by changes in extraction ratio, as even lower extraction ratios (i.e., 1:1 or 2:1) tend to extract most of the sulfates from the subject soil. Gypsum-based soils, however, are highly impacted by varying extraction ratios as increases in extraction ratios yield proportionally higher sulfate contents. Because the sulfate concentration generated from soil analysis is directly linked to levels of sulfate protection, this is clearly a key issue, especially in Texas, where gypsum is the primary sulfate form. As such, significant focus was placed under this project on determining the severity of deterioration of various materials and mixtures in gypsiferous soils and gypsum-based aqueous solutions.

Resistance of Concrete to Physical Sulfate Attack. In recent years, a relatively new form of sulfate-induced distress has been recognized, one in which sulfates penetrate into concrete and lead to deterioration without chemically altering the hydration products within the concrete (Folliard and Sandberg, 1994). This distress, known as physical salt attack or physical sulfate attack, results from phase changes within the penetrating sulfate solution, which triggers crystallization pressures that can physically degrade concrete. Research was initiated under this TxDOT project to determine which salts can cause this form of distress and how this deterioration can be prevented.

Correlation between laboratory tests and field performance. To date, there is very little correlation between accelerated laboratory tests (using ASTM C 1012 or other standard tests) and the actual performance of concrete subjected to external sulfates. This is particularly relevant given that physical salt attack may be more prevalent than previously thought in the field and is not considered or triggered in standard, accelerated laboratory tests such as ASTM C 1012. This project attempted to correlate the performance of various concrete mixtures exposed to various sulfate types and concentrations in the laboratory and in the field.

The above research objectives were addressed in this project through a combination of laboratory tests, forensic and mechanistic evaluations, field studies, and the development of outdoor sulfate exposure sites in Texas. This comprehensive research project culminated in one Ph.D. dissertation (Drimalas, 2007) and one MS thesis (Clement, 2009) at The University of Texas at Austin and one Ph.D. dissertation (Dhole, 2009) at the University of New Brunswick. The present report is intended to serve as a broad overview of the research described in these three dissertations/theses. The reader is urged to refer to these publications for more detailed technical information on this TxDOT-funded project, as well as for a comprehensive literature review on external sulfate attack.

1.3 Outline of Report

The remainder of this report is organized into the following chapters:

Chapter 2 presents a brief review of literature on sulfate attack, with primary emphasis on external sulfate attack.

Chapter 3 describes the materials used throughout this experimental study.

Chapter 4 presents an overview of key findings of laboratory testing of mortar and concrete (following ASTM C 1012 or variations thereof).

Chapter 5 presents an overview of the outdoor exposure site testing at the University of Texas at Austin.

Chapter 6 summarizes the research conducted at the University of New Brunswick, as described in detail in Dhole (2009).

Chapter 7 summarizes the findings of various field investigations of transportation structures in the state of Texas exposed to sulfate-rich conditions.

Chapter 8 briefly summarizes the main conclusions from this study and provides guidance on assuring durability in sulfate-rich environments

Chapter 2. Literature Review

External sulfate attack, sometimes referred to as the “classical form of sulfate attack” is quite complex and still not fully understood. Sulfates can enter concrete through many external sources such as soils and groundwater. Sulfate can be of natural origin or derived from agricultural fertilizers or industrial effluents (Neville 1996). The specific types of sulfates that are found in soils and groundwater are discussed next.

2.1 Types of Sulfates

The complexity of sulfate attack begins first with the variety of sulfates that can damage concrete. The most common sulfates that interact with concrete are calcium, sodium, and magnesium sulfate, which are listed in order of their aggressiveness. Each of these sulfate forms are discussed separately next, but one should bear in mind that it is common to find mixed sulfates present in the same groundwater or soil sample. Table 2.1 provides cement chemistry notations used throughout this report.

Table 2.1: Cement Chemistry notations used throughout this report

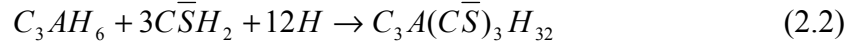
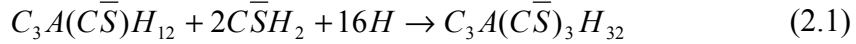
Chemical Name	Cement Chemistry Notation
Ettringite	$\text{C}_3\text{A}(\text{C}\bar{\text{S}})_3\text{H}_{32}$
Calcium Monosulfoaluminate	$\text{C}_3\text{A}(\text{C}\bar{\text{S}})\text{H}_{12}$
Gypsum	$\text{C}\bar{\text{S}}\text{H}_2$
Tricalcium Aluminate	C_3A or C_3AH_6
Sodium Sulfate	$\text{N}_2\bar{\text{S}}\text{H}_{10}$
Magnesium Hydroxide	$\text{Mg}(\text{OH})_2$
Calcium Hydroxide	CH
Aluminum Hydroxide	AH_3
Sodium Hydroxide	NH
Silica Gel	S

2.1.2 Calcium Sulfate

Calcium sulfate (gypsum) is generally believed to be the least aggressive of the three sulfates, mainly due to its lower solubility. The solubility of gypsum is approximately 1440 ppm, which is significantly less than that of sodium sulfate and magnesium sulfate. There are essentially two different schools of thought on the issue of gypsum solubility and its impact on sulfate attack. One school of thought is that the inherently low solubility of gypsum limits its concentration in groundwater (or in the pore water of soil), and this low concentration limits the potential damage to concrete (Rebel et al 2005). The other school of thought is that once calcium sulfate ions enter concrete, its solubility increases as it encounters the highly-alkaline pore

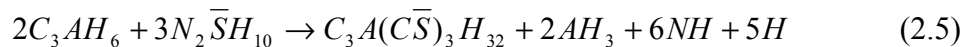
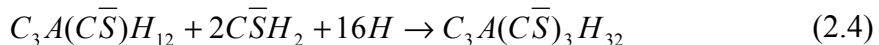
solution within the concrete, and the higher sulfate concentrations can then more aggressively attack the hydrated cement paste (Hansen and Pressler 1947).

Specifically, as shown in equation 2.1, calcium sulfate will react with monosulfoaluminate and water to form ettringite, which can result in expansion and cracking. Calcium sulfate also reacts with tricalcium aluminate to form ettringite as shown in Equation 2.2.



2.1.3 Sodium Sulfate

Attack from sodium sulfate is more complex than attack from calcium sulfate because more phases are affected. Sodium sulfate may attack concrete in two different ways. The first form of attack (Equation 2.3) involves sodium sulfate reacting with calcium hydroxide (portlandite) to form gypsum. Gypsum can then react with monosulfoaluminate (Equation 2.4) to form ettringite. Once the calcium hydroxide is depleted, gypsum formation will discontinue. Once the monosulfoaluminate becomes depleted, excess gypsum will form in the system and ettringite formation will cease (Gollop and Taylor 1992). The second form of attack (Equation 2.5) involves sodium sulfate reacting with tricalcium aluminate to form ettringite.



Tian and Cohen (2000) studied the expansion of alite (C_3S) caused by the formation of gypsum. In the case of a pure alite paste, no aluminum should be available to form ettringite. Cement pastes made with and without silica fume were placed in a 5% sodium sulfate solution. After 360 days in sodium sulfate, the alite paste, without silica fume, began to expand, and x-ray diffraction analyses showed that this expansion was due to gypsum formation (Tian and Cohen 2000). These findings suggest that gypsum formation can, in fact, lead to expansion, in addition to the loss of mass or cohesion that is typically observed when gypsum forms.

2.1.4 Magnesium Sulfate

Magnesium sulfate is the most complex of the three types of sulfates. It can react with all hydrated cement products and is generally considered to be the most damaging form of sulfate. Magnesium sulfate will react with calcium silicate to form gypsum plus magnesium hydroxide and a silica gel, as shown in Equation 2.6. This formation of magnesium hydroxide (brucite) is known to form a barrier which may provide protection to the concrete and it also tends to internally affect pore solution pH. Brucite formation does have its downfall in that it needs a high amount of calcium hydroxide to form. Once the CH is depleted, the magnesium sulfate will seek more calcium. In this case, decalcification of the C-S-H will occur, due to a removal of calcium (Gollop and Taylor 1992).



2.2 Physical Sulfate Attack

The previous examples of external sulfate attack due to interactions with calcium, sodium, and magnesium sulfate resulted in chemical alterations of the hydrated cement paste, for example leading to the formation of gypsum or ettringite or to the decalcification of C-S-H. However, damage triggered by external sulfates may also be physical in nature, without any such chemical alterations. A common form of physical salt attack in concrete occurs when sodium sulfate penetrates into concrete and phase changes occur between anhydrous sodium sulfate (thenardite) and decahydrate sodium sulfate (mirabilite). These phase changes, typically triggered by changes in temperature, lead to significant crystallization pressures that can impart stresses and cracking in concrete. Neville (2004) reported that this transformation of thenardite to mirabilite can result in tensile hoop stresses stressing the range of 1450-2900 psi (10-20 MPa). This stress is quite high and could easily damage concrete (Neville 2004).

In the early 1990's, Folliard and Sandberg (1994) proposed that crystallization of sodium sulfate within concrete, triggered by temperature changes, was the predominant cause of distress due to physical salt or sulfate attack. Figure 2.4 shows the solubility curve for sodium sulfate, which shows the change between thenardite and mirabilite at approximately 91 °F (33 °C). After cycling concrete specimens in 30% sodium sulfate solution from 41° to 86 °F (5° to 30 °C), substantial mass loss occurred in the samples. X-ray diffraction on these samples did not show any sign of ettringite formation or any other deleterious product from chemical attack. In parallel tests, it was shown that the total volume of the sodium sulfate/water solution increased by approximately 3 % as crystallization was triggered upon a temperature drop. In essence, this type of distress is similar to freeze-thaw distress in that physical distress is triggered by a volume change of the water or solution inside concrete. Samples cycled from 95° to 230 °F (35° to 110 °C) did not show any weight loss and the majority of these samples gained weight (Sandberg and Folliard 2004), confirming that the distress only occurs when temperatures drop below about 91 °F (33 °C) and when a high concentration of sodium sulfate is present in the pores of concrete.

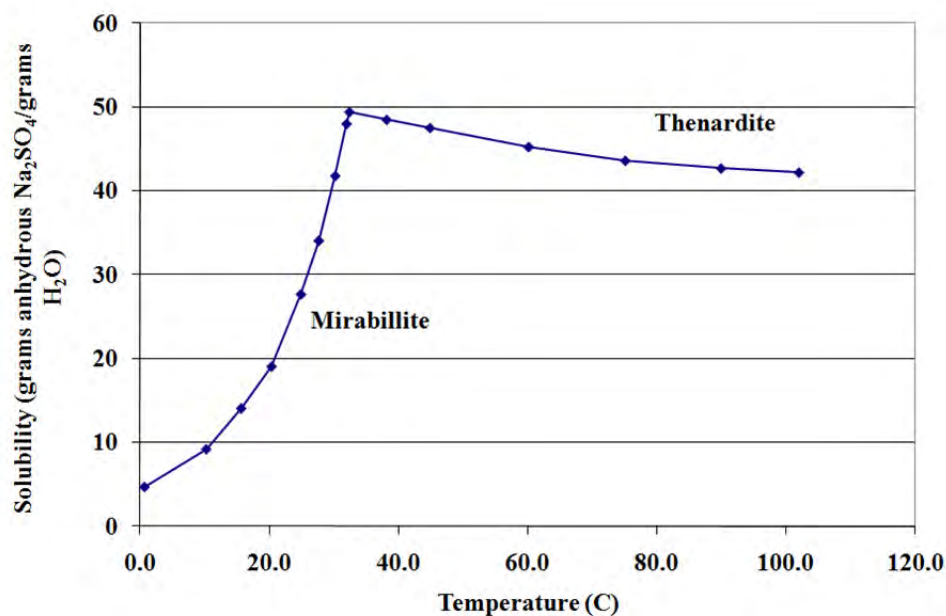


Figure 2.1: Solubility Curve for Sodium Sulfate /Water System (Berkeley 1904)

Since the 1940's, the Portland Cement Association (PCA) has studied the long-term durability of concrete specimens stored in outdoor environments in Sacramento, California. The PCA study is comprised of four research phases since its inception and has focused on the areas of cement content, cement composition, cement types, SCMs, w/cm, and various types of coatings. The fourth phase, initiated in 1982, is comprised of research on mineral admixture replacements, w/cm, and coatings. Concrete beams measuring 6 in x 6 in x 30 in (150 mm x 150 mm x 760 mm) were cast and shipped to Sacramento, California one year after being cast. The beams were then halfway submerged in soil containing 10% sodium sulfate. The beams were annually inspected and assigned a rating between 1 and 5, with 5 showing the most deterioration (Stark 1989).

The first PCA bulletin report in 1989 reported that the most important parameter influencing sulfate resistance was the w/cm of concrete (Stark 1989). It was also reported that cement type (e.g., Type I vs. Type II vs. Type V) had minimal influence on sulfate resistance for concrete mixtures with either low or high w/cm, but a significant difference was noted for mixtures with intermediate w/cm values. Interestingly, mixtures containing fly ash or GGBFS reduced sulfate resistance in 29 of 30 mixtures, when compared to a control mixture. Beams with coatings were reported to behave well, but it was proposed that this protection may only be temporary as the epoxy coating showed signs of peeling away from the concrete (Stark 1989). The distress reported in concrete beams was attributed to external, chemical sulfate attack in this 1989 bulletin, and there was no mention of other distress mechanisms.

In 2002, a second bulletin on the PCA site determined that damage on the concrete beams was only occurring above the soil level, and that very little damage was reported below ground or in parallel tests in which beams were stored indoors (without substantial variations in temperature). Stark (2002) proposed that the main mechanism of distress was physical sulfate (or salt) attack, a form of distress that had been identified as being a key deterioration factor in various papers published between the 1989 and 2002 PCA bulletins, some of which are described next. The main findings from this 2002 bulletin suggest that physical sulfate attack is a much more significant form of distress in field concrete than had been previously reported and suggests that the overall topic of sulfate attack is even more complex than ever.

2.3 Preventing Sulfate Attack

External sulfate attack can be prevented through proper material selection and mixture proportioning. This section briefly summarizes viable means of preventing sulfate attack, including discussions on the universal importance of reducing permeability and the direct benefits of using lower w/cm, sulfate-resistant cements, and SCMs.

2.3.1 Permeability

Concrete with a low w/cm yields a microstructure with reduced porosity and permeability which reduces the rate of ingress of sulfate ions. Cement paste with a w/cm of 0.7 is approximately 10 times more permeable to that a comparable mixture with a 0.55 w/cm (Powers et al 1954). A significant correlation between higher permeability and greater expansion was reported with concretes exposed to 5% sodium sulfate (Khatri 1997), and Al-Amouti (2002) reported similar findings for concrete exposed to sodium sulfate, but not with magnesium sulfate solutions. To achieve low permeability, one must not only use a low w/cm (i.e., less than 0.45) but also ensure adequate curing. As described later, the incorporation of SCMs into concrete mixtures is the most powerful method of reducing sulfate ingress.

2.3.2 Sulfate Resistant Cements

Sulfate-resistant cement was developed to limit the C₃A in the cement to prevent sulfate attack. The lower C₃A cement primarily reduces the amount of ettringite that can form. However, sulfate-resistant cement does not stop the attack on calcium hydroxide and C-S-H (Mehta 1993). ASTM C-150 limits the C₃A content of Type V cement to 5 % and the C₃A content of Type II cement to 8 % maximum. It is also generally believed that the alumina in the aluminoferrite phase of portland cement can participate in sulfate attack, and as such, ASTM C 150 states that the C₄AF + 2C₃A in Type V cement should not exceed 25%, unless specific performance tests show satisfactory results (ACI 201.2R-01). In localities that do not have availability of Type V cement, the use of Type II cement with suitable SCMs can provide comparable sulfate resistance to Type V cement (ACI 2001). The U.S. Bureau of Reclamation has shown Type V cement to be beneficial in its long term studies and considers sulfate-resistant cement to be a viable means of improving performance in a sulfate environment (Eglinton 1998).

Gollop and Taylor (1995) employed various analytical techniques to investigate the microstructure of cement paste cubes with ordinary portland and sulfate-resistant cements after 6 months submerged in magnesium and sodium sulfate solutions. Sulfate-resistant cement cubes still provided the same deleterious. Brucite formation was noticed along the edge of the sample but again at a lesser degree than that found in the ordinary portland cement cube (Gollop and Taylor 1995).

2.3.3 Supplementary Cementing Materials

Most SCMs, when used in sufficient dosages, can be quite effective in preventing sulfate attack by lowering permeability, reducing CH content, and diluting the reactive components emanating from the portland cement. Many studies have been conducted to show the benefits of incorporating various SCMs in concrete to improve sulfate resistance, and only a select few of these are cited herein for conciseness.

Generally, ground-granulated blast furnace slag (GGBFS) is quite effective in controlling sulfate attack, with replacement levels from 25 to 50% providing moderate to severe exposure protection, respectively. Mortars containing 45 to 72% GGBFS (by mass replacement of cement) were reported by Hooton and Emery (1990) to provide satisfactory sulfate resistance after 10 years of storage in 3000 mg/l sodium sulfate solution. One potential issue with slag is that the typical 1% sulfur content in blast furnace slags occurs mainly as sulfide in glass phase and is released upon hydration as other constituents. The release of the sulfide cannot be ignored when considering the effects on sulfate attack (Taylor and Gollop 1997). ACI 201.2R-01 recommends the use of between 40 and 70 % by mass of slag to control sulfate attack (ACI 201 2001).

Many studies have shown that low calcium fly ash is generally more effective than high calcium fly ash in preventing sulfate-induced expansion and cracking. Dunstan (1980) worked with creating a resistance factor R that based the sulfate resistance of fly ash on calcium and iron oxide content of the fly ash. In the study, higher calcium oxide fly ash would fail the resistance factor. Tikalsky also studied a variety of fly ashes and found that high calcium fly ashes do not perform well in sulfate environments (Tikalsky and Carrasquillo 1993).

The use of Class F fly ash (CaO content less than 20%) has long been found to be effective for sulfate resistance when dosages between 25 and 35% by mass are used. However, some high-lime Class C fly ashes produce concrete with poor sulfate resistance, sometimes even worse than control mixtures without fly ash. Shashiprakash and Thomas (2001) found that this led to increased expansion when compared with the high-C₃A cement used on its own. The

reasons why high-lime ashes were less effective than low-lime ashes in controlling sulfate attack were identified as:

- Some high-calcium fly ashes contain C₃A (also some CH)
- Lower consumption of lime due to reduced pozzolanicity
- Presence of reactive calcium-aluminates in glass phase
- Production of reactive aluminate hydrates (e.g. Dunstan's gehlenite)

Figure 2.2 shows the strong relationship between the CaO content of the fly ash and the expansion at six months in ASTM C 1012 testing. More research is needed to better differentiate the behavior of different high-lime ashes; using CaO as an index of potential expansion may not hold for all fly ashes.

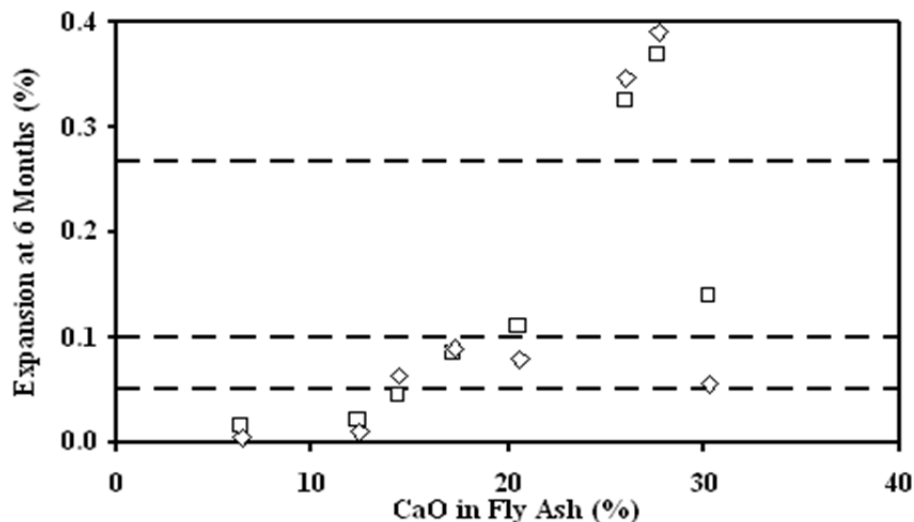


Figure 2.2: Relationship between C₃A Content in fly ash to 6 month expansion in ASTM C 1012 testing (Shashiprakash and Thomas 2001)

In addition to linking the mineralogy and chemistry of fly ashes to sulfate resistance, Shashiprakash and Thomas (2001) also performed significant research on combining high-CaO ashes with silica fume, with emphasis on mixtures between 3% and 6% percent silica fume (by mass of total cementitious materials). Figure 2.3 shows the effects of just a small dosage of silica fume (3%) on the sulfate resistance of concrete with a high-calcium fly ash.

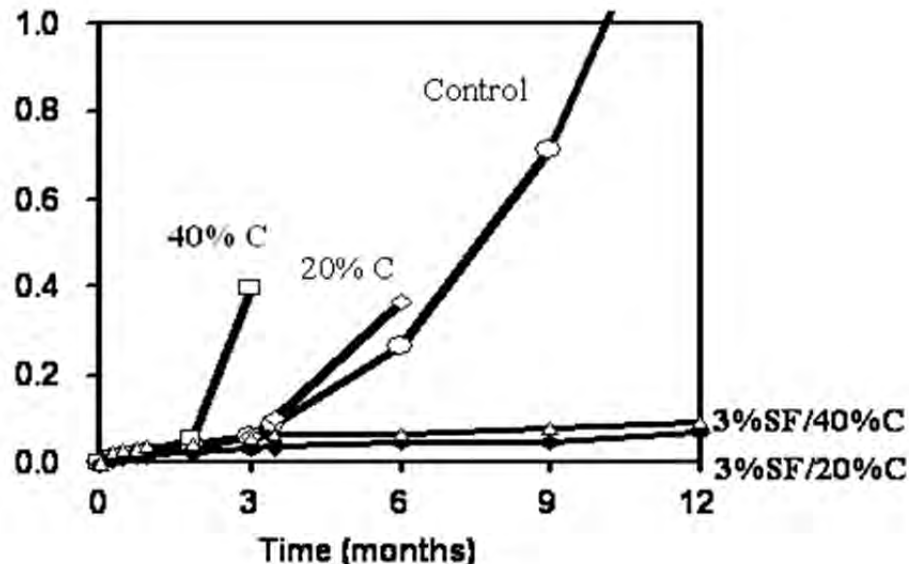


Figure 2.3: The use ternary blends with silica fume and Class C fly ash reduces the expansion of mortars compared to only using Class C fly ash as a pozzolan. (Shashiprakash and Thomas 2001)

Metakaolin is a pozzolan that has shown great performance in cases of alkali aggregate reaction (AAR), chloride ingress, and carbonation (Lee 2004). In the case of sulfate attack, the deterioration depends on the type of sulfate. Khatib and Wild (1998) show that a minimum of 20% metakaolin is needed to produce durable concrete when exposed to sodium sulfate. In magnesium sulfate solutions, the opposite is true. Lee (2004) showed that an increase of metakaolin increased expansions and deterioration on mortars and pastes.

2.3.4 Physical Sulfate Attack

There have been only limited studies on methods of preventing physical sulfate attack. Folliard and Sandberg (1994) reported that low w/cm concrete mixtures are quite effective in preventing physical sulfate attack, especially when SCMs are used. They also showed that air-entrainment is helpful in reducing but not eliminating physical sulfate attack. With time, it was shown that air-entrained voids ultimately become filled with salts, and they are no longer accessible to the salt solution as it increases in volume.

2.4 Characterization of Sulfate Exposure Conditions

Various methods of preventing sulfate attack have been discussed in this chapter, with a wealth of data available from various laboratory studies. Ideally, the level of protection against sulfate attack should be matched to the specific exposure conditions in which the subject concrete will be cast. An example of this approach of selecting mitigation measures based on severity of exposure is shown in Table 2.2 (after ACI 201-2R-01). To establish this link, it is essential to accurately assess exposure conditions by either analyzing the local groundwater or soil sample, each of which are discussed next.

Table 2.2: Sulfate Exposure classification for water-soluble sulfates in soil or sulfates in water (ACI 2001)

Severity of potential exposure	Water-soluble sulfate (SO_4) in soil, percent by mass	Sulfate (SO_4) in water, ppm	(w/cm) by mass, max.	Cementitious material requirements
Class 0 exposure	0.00 to 0.10	0 to 150	No special requirements for sulfate resistance	No special requirements for sulfate resistance
Class 1 exposure	>0.10 and <0.20	>150 and <1500	0.50	C 150 Type II or Equivalent
Class 2 exposure	0.20 to <2.0	1500 to <10,000	0.45	C 150 Type V or Equivalent
Class 3 exposure	2.0 or greater	10,000 or greater or greater	0.40	C 150 Type V plus pozzolan or slag

2.4.2 Water Samples

The measurement of sulfates from groundwater from a new construction site is fairly straightforward and essentially without controversy. The water can directly be analyzed for sulfate content using widely available analytical methods or diluted to be read by an instrument that measures sulfates.

2.4.3 Soil Samples

Since not all sites have groundwater present for sampling, soil samples must be taken to analyze the amount of sulfates. A few issues arise when sampling soil. First, there is no clear consensus or guidance on how many samples to extract and evaluate from a given site. Within a single site, a large variability of sulfate concentrations is quite common. This variation in sulfate content impacts not only sampling regimes but also the actual sulfate resistance of concrete ultimately cast on that site. For example, a foundation in Italy exhibited severe deterioration from sulfate attack on only certain piers, due to local variations in sulfate content (Tulliani 2002). The flow of groundwater can move sulfates throughout the soil or even the natural soils in different areas can contain different amounts of sulfates. Rainfall and drainage may also affect the locations and concentrations of sulfate within a given site. A statistical number of samples should be taken and measured; however, this increases the cost of testing, and as stated previously, no definitive guidance exists on how to properly sample soils from a given site.

The second major problem that occurs with sulfates and soils is the analytical techniques needed to measure the sulfates. There are two methods of measuring sulfates from a given soil sample -- either water soluble or acid soluble sulfate determination. Acid soluble determination is fairly rare and somewhat complex, and in addition, this method can trigger the release of sulfates from soils that would otherwise not be released under realistic field conditions. Water soluble sulfate testing is more common; however there are many versions of this test and they all provide different results, mostly due to variations in the extraction ratio.

For water-soluble sulfate determination, the extraction ratio can easily change the results of a sulfate concentration from a given sample, especially when the soil contains gypsum. The extraction ratio is the mass of water per mass of soil. There is no clear consensus on what extraction ratio should be used and values range in practice from as low as 1:1 to as high as 20:1. Sodium and magnesium sulfate are very soluble and are not impacted much by changes in extraction ratio, as even lower extraction ratios (i.e., 1:1 or 2:1) tend to extract most of the sulfates from the subject soil. Gypsum-based soils, however, are highly impacted by varying extraction ratios as increases in extraction ratios yield proportionally higher sulfate contents. Because the sulfate concentration generated from soil analysis is directly linked to levels of sulfate protection, this is clearly a key issue, especially in Texas, where gypsum is the primary sulfate form. For gypsum-bearing soils, higher extraction ratios tend to result in classifying the soil as a higher degree of severity, thereby requiring more stringent preventive measures.

2.5 Structures Suffering from Sulfate Attack

Cases of sulfate attack in field structures are fairly uncommon, mainly because most agencies have already adopted specifications and guidelines aimed at preventing deterioration. Even when sulfate attack does occur, it is not clear how damaging the distress can be in the long term, but Mehta (2000) has suggested that the “threat” of structural failure due to sulfate attack is less than that for other distress mechanisms, such as corrosion or alkali-aggregate reaction. One major issue is that there is a general lack of correlation between accelerated laboratory test methods and actual field performance, which is discussed next.

2.6 Test Methods and Specifications

There exists a general lack of correlation between the performance of concrete subjected to standard test methods and concrete subjected to realistic field conditions (Santhanam et al 2001). Two current ASTM test methods for assessing sulfate attack are ASTM C 1012 and ASTM C 452. ASTM C 452 is a test method for the potential expansion of portland cement mortars exposed to sulfate. In this standard, gypsum is added to the cement prior to mixing to produce 7% SO₃ by mass of cement and gypsum. The additional gypsum allows for ettringite formation to occur internally without the need for external sulfates to enter the specimens. Mortars are then placed in limewater and measured for expansion. This test method is not very common because it is intended only to be used as a test for portland cement, and thus has limited applicability to more varied systems, such as mixtures containing SCMs.

ASTM C 1012 is one of the most common tests used in practice and is often included in specifications and guidelines. The test involves casting mortar bars, typically containing a high-C₃A cement (with or without SCMs) and standard Ottawa sand, allowing the mixture to reach a minimum strength of 2850 PSI (20 MPa), and then immersing the specimens in 5% sodium sulfate solution for up to 18 months. This is the most common test method for determining sulfate resistance and is the test method chosen for equivalent testing in ACI 201.2R. One concern with this test is that the pH of the sulfate solution will change with time, as will the pH of the pore solution (due to leaching). To minimize this pH effect, the sulfate solution is required to be replaced each time a measurement is conducted. However, at intervals of longer measurements periods, the pH may change considerably, thereby affecting the progression of sulfate attack. Mehta (1974) has proposed a test set-up that automatically adjusts the pH of the soak solution to minimize this effect, but the complexity of this approach has hindered its use in standard test methods.

Both of the aforementioned test methods deal with the chemical process of sulfate attack and do not adequately assess the physical component of sulfate attack that may occur in the field. As mentioned in Section 2.2.2, PCA showed that physical salt damage was the predominant damage in their exposure site in Sacramento (Stark 2002). An important finding from this exposure site is that more testing needs to be conducted with specimens in the field or simulated outdoor testing in the laboratory to evaluate both physical and chemical attack.

Bellmann and Stark (2006) suggested that test methods that use a high sulfate concentration do not accurately reflect field observations. High sulfate concentrations in laboratory testing results in gypsum formation, whereas ettringite (or sometimes thaumasite) formation is favored under realistic field conditions.

The overall approach to defining severity of exposure and then matching this to a level of protection was previously shown in Table 2.2 and is typical of standard practice in North America and elsewhere. This table results in a situation where concrete placed in a higher severity of classification requires a lower C₃A content of the portland cement, a lower w/cm ratio, and sometimes the use of suitable SCMs. In lieu of this prescriptive approach, performance testing, typically using ASTM C 1012, is often employed to determine if a proposed combination of materials will provide comparable sulfate resistance. For example, an equivalent and acceptable approach to producing concrete for Class 3 exposure could consist of Type I cement with 30% Class F fly ash, with an 18-month expansion (ASTM C 1012) value of less than 0.1%.

Chapter 3. Materials used in Research Project

A wide range of materials were chosen for this study to evaluate the performance of Class C fly ash in a sulfate environment. ASTM C 1012 was selected as the standard testing procedure for this research, not because it is deemed to be the best test or the test most linked to field performance, but rather because it is the test most commonly used, specified, and included in national and international guidelines (such as ACI 201 and ACI 318).

3.1 Aggregates

A crushed limestone coarse aggregate and manufactured limestone sand were used in all concrete mixtures. These aggregates were procured from central Texas sources, and prior testing at the Concrete Durability Center (CDC) found these aggregates to be non-reactive with regard to alkali-silica reaction (ASR). It was deemed important to select aggregates not susceptible to ASR to ensure that any damage occurring either in the laboratory or in the outdoor exposure site could be attributed solely to sulfate-induced distress. For the mortar mixtures described in this chapter, as per ASTM C 1012, a standard graded ASTM C 778 Ottawa sand was used for all mixtures.

3.2 Cement

Type I cement, designated herein as C1, with a C₃A content of 11%, was used for ASTM C 1012 Testing. As per the guidance in ACI 201.2R, a portland cement with a minimum of 8% C₃A must be used to evaluate the performance of cement/supplementary cementing combinations. Table 3.1 provides the composition of the Type I cement. In addition to testing mixtures with Type I cement, mixtures were cast containing Type II and Type V cements.

Table 3.1: Chemical data for the portland cements used in this study

Chemical Data	C1	C2	C5
SiO ₂ (%)	20.12	19.38	20.55
Al ₂ O ₃ (%)	5.21	4.79	4.19
Fe ₂ O ₃ (%)	1.93	3.17	5.32
CaO (%)	63.78	65.24	63.36
SO ₃ (%)	3.4	2.43	3.81
MgO (%)	1.56	1.44	0.83
Na ₂ O (%)	0.78	0.16	0.32
C ₃ A (%)	11	7.4	2.11

3.3 Supplementary Cementing Materials

A range of fly ashes, with CaO contents from 15 to 29%, were included in this investigation. Table 3.2 details the chemical analyses of the 8 Class C fly ashes used in the mortar mixtures. A Class F fly ash (FA-9) was also included in the testing. Other SCMs were also included in this study, which were tested separately or in conjunction with the various fly

ashes in ternary blends. Specific information regarding these other SCMs is included in Table 3.3.

Table 3.2: Chemical Analysis of Fly Ashes Tested in the Study

CHEMICAL TESTS	FA-1 (TK)	FA-2	FA-3 (PS)	FA-4	FA-5	FA-6	FA-7	FA-8 (WL)	FA-9* (RL)
Silicon Dioxide (SiO ₂), %	38.57	41.32	33.14	34.47	33.35	36.36	37.16	30.76	48.48
Aluminum Oxide (Al ₂ O ₃), %	18.84	19.25	18.12	20.35	18.74	17.44	20.55	17.75	25.01
Iron Oxide (Fe ₂ O ₃), %	6.69	6.48	6.65	5.65	6.69	6.08	6.06	5.98	3.56
Sum of SiO ₂ , Al ₂ O ₃ , Fe ₂ O ₃ , %	64.1	67.05	57.91	60.47	58.78	59.88	63.77	54.49	77.05
Calcium Oxide (CaO), %	23.54	21.58	27.49	26.5	27.3	25.68	24.76	28.98	15.92
Magnesium Oxide (MgO), %	4.76	4.43	5.45	4.7	5.83	6.15	4.29	6.55	2.5
Sulfur Trioxide (SO ₃), %	1.43	1.25	2.71	1.71	1.85	2.03	1.23	3.64	0.72
Sodium Oxide (Na ₂ O), %	1.71	1.43	1.91	1.76	1.93	1.9	1.63	2.15	0.3
Potassium Oxide (K ₂ O), %	0.65	0.78	0.3	0.46	0.38	0.46	0.45	0.3	0.71
Total Alkalies (as Na ₂ O), %	2.14	1.94	2.11	2.06	2.18	2.2	1.93	2.35	0.77
PHYSICAL TESTS	FA-1	FA-2	FA-3	FA-4	FA-5	FA-6	FA-7	FA-8	FA-9
Loss on Ignition, %	0.28	0.16	0.4	0.25	0.21	0.58	0.13	0.44	0.55

*FA9 was not evaluated in this chapter but is included in research described in Chapter 4

Table 3.3: Chemical Analysis of other SCMs Tested in the Study

Chemical Tests	Silica Fume (SF)	UFF A	Slag
SiO ₂ (%)	93.17	50.65	35.91
Al ₂ O ₃ (%)	--	26.64	11.98
Fe ₂ O ₃ (%)	2.1	4.66	0.94
CaO (%)	0.8	10.85	44.1
MgO (%)	0.3	2.23	8.9
SO ₃ (%)	0.2	1	1.63

Chapter 4. ASTM C 1012 Testing

ASTM C 1012 is an accelerated test procedure that exposes mortar specimens to a 5% sodium sulfate solution, with length change being the primary index. Some of the key features of this test method are described next.

As per ASTM C 1012, a standard mortar mixture is cast with 1 part portland cement and 2.75 parts sand. For the control portland cement mixture, the w/cm is fixed at 0.485, and for mixtures incorporating SCMs, water is removed to obtain a flow of ± 5 of that of the control portland cement mixture. The mortar bars have dimensions of 1 in X 1 in X 11.25 in (25 mm X 25 mm X 286 mm) with stainless steel gauge studs embedded into the ends for length measurements. Nine mortar cubes (2 in x 2 in or 50 mm x 50 mm) are also cast from each mixture. After casting the mortar bars and cubes, they are sealed and placed into a 95 °F (35 °C) water bath for 23 ± 0.5 hours. After curing, the specimens are demolded and two of the cubes are tested for strength. Once the compressive strength of the cubes has reached 2850psi ± 100 psi (20MPa ± 0.70 MPa), the bars are then placed into a 5% sodium sulfate solution (352 moles of Na₂SO₄ per m³). Appendix A in Drimalas 2007 and Clement 2009 provides the mortar strengths from each of the mixtures. Otherwise, the bars and cubes are placed into a saturated limewater bath until strength is achieved. Upon immersion in the sulfate solution, expansion measurements are taken every 1, 2, 3, 4, 8, 13, 15 weeks and 4, 6, 9, 12, 18 months thereafter.

The remainder of this chapter is organized as follows:

- Section 4.1 describes the expansion limit criteria from ACI.2R-01
- Section 4.2 describes the importance of cement selection for ASTM C 1012 testing
- Section 4.3 describes the evaluation of Class C fly ash in sulfate environments
- Section 4.4 describes the evaluation of ternary blends in sulfate environments
- Section 4.5 describes modified mixtures placed into ASTM C 1012 environments (modified solutions and use of Type II and Type V cements)
- Section 4.6 characterization of Class C fly ash

4.1 Expansion Limits

Expansion limits (and immersion times at which expansion limits are applied) vary considerably from one agency/source to another and also depending on the severity of sulfate exposure. In this report, expansion limits from ACI 201.2R-01 are nominally used to compare and evaluate the performance of mortars exposed to sulfate solutions. Table 2.2 in the chapter 2, from ACI 201.2R-01, shows the four classes of exposure, increasing in order of severity as one progresses downward in the table. The severity is determined based on the sulfate concentration in either the groundwater or soil. As discussed previously in this final report and as will be discussed in more detail later in this chapter, there are several unresolved issues when measuring sulfates in soil, especially when gypsiferous soils are encountered. As one moves from the less severe to more severe exposure classes, more stringent prescriptive guidelines are provided, which include lower w/cm, the use of sulfate-resistant cements, and the use of SCMs. The last column in Table 2.2 shows the different cementitious requirements for each of the exposure classes. Type II or Type V portland cement (as per ASTM C 150) is specified in Class 1-3

exposures, but “equivalent” materials are allowed for these exposure classes, with equivalency based on ASTM C 1012 test results, as described next.

As shown in Table 2.2, “equivalent” cementitious materials can be used in lieu of Type II or Type V cements, which is particularly important for Type V equivalency as there exist very few Type V cements in the United States. Equivalency is judged based on ASTM C 1012 testing, with various expansion limits and test durations, depending on the specific exposure class. An equivalent for Type II cement in Class 1 exposure would be any type of ASTM C 150 or C 1157 cement with fly ash, silica fume, or slag that yields an expansion less than 0.10% after 6 months. An equivalent for Type V cement in Class 2 exposure has two criteria. The first criterion requires the expansion to be less than 0.05% percent after six months, provided that these materials were previously qualified by performance testing. If the materials were not previously qualified, an expansion limit of 0.10% after one year is specified. For Class 3 exposure, an ASTM C 150 Type V or ASTM C 1157 Type HS cement must be used with a suitable dosage of SCM to achieve an expansion less than 0.10% after 18 months of testing using ASTM C 1012.

4.2 Cement Selection for ASTM C 1012 Testing

In order to test a mortar mixture, cement with C3A content greater than 8% is needed according to ACI 201.2R-01. This cement solely in the test would have to fail at least the 0.1% expansion limit at 6 months. If the cement mixture passes this expansion limit at six months, then clearly one cannot use this threshold when testing this cement in combination with fly ash or other supplementary cementing materials (SCMs). After testing a few cements, results showed that high C3A cement can pass the test at 6 months. Cements from six producers around the state of Texas were thus used in the current study. Five of the cements were Type I and one was Type I/II, as per ASTM C 150. Table 4.1 presents the chemical composition of the cements as determined by Rietveld analysis.

Table 4.1: Composition of Cements Used in Study

Compound	% Contained in Each Cement						
	C1	C2	C3	C4	C5	C6	C7
C3S	36.51	61.62	48.55	58.92	60.11	61.45	45.39
C2S	23.63	15.81	22.73	22.01	12.19	13.49	23.75
C4AF	4.63	9.02	3.34	6.47	7.04	7.43	8.90
C3Ac	6.15	1.91	6.98	4.99	5.25	3.11	2.74
C3Ao	1.77	2.33	2.21	0.95	1.91	5.20	3.56
Periclase	0.00	1.30	0.80	0.00	0.19	0.85	0.22
Arcanite	2.39	0.00	0.00	0.00	0.00	0.00	1.21
Anhydrite	0.26	0.00	0.00	0.00	0.17	0.33	0.00
Bassanite	2.15	2.11	4.38	1.95	3.55	4.80	5.66
Gypsum	0.68	1.32	9.01	0.65	2.51	0.00	0.00
Calcite	4.55	0.00	0.00	0.00	2.41	0.00	4.15
Quartz	0.44	0.00	0.00	0.00	0.16	0.00	0.00
Lime	0.30	0.00	0.00	0.00	0.20	0.90	0.38
Portlandite	0.99	2.40	0.44	1.15	0.00	0.00	0.00
Amorphous	15.50	2.19	1.55	2.92	4.28	2.44	4.03
Cement Type	Type I	Type I	Type I	Type I	Type I	Type I	Type II

4.2.1 Producer Variability

Cements designated C1 and C4 are from the same source, but were acquired one year apart. Cement from this producer is commonly used at the Concrete Durability Center (CDC) in Austin, Texas and has been evaluated five times since this project began. Figure 4.1 shows the expansion of mortar bars tested in accordance with ASTM C 1012. The expansion results varied considerably between cements, with three samples passing the six-month, 0.10 percent expansion limit and two failing this limit. This variability in performance from one cement sources, as a function of production date, raises some concern about using “standard” cements for ASTM C 1012. Certainly, this validates the need to always test a control sample, along with SCM mixtures, so that proper comparisons can be made. Six-month expansion criteria should only be used for ranking SCM mixtures when the parallel control mixture exceeds the designated expansion limit.

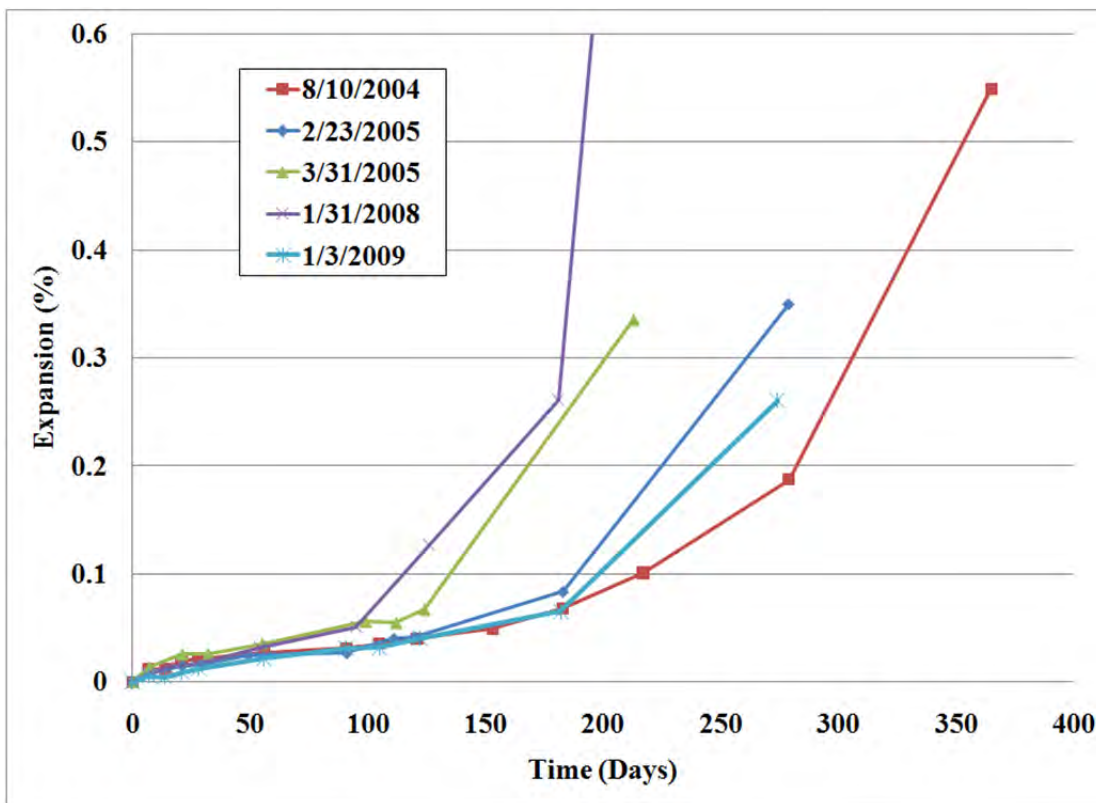


Figure 4.1: Variability in Cement Performance from a Producer with Time

4.2.2 Cement Study Results

Figure 4.2 presents the ASTM C 1012 test results for the cements listed in Table 4.1. The only cements to pass expansion limits at six months were C7 and C4. C7 is sold as a Type II cement, and is thus expected to pass this requirement. C4 was discussed in the previous section and is sold as a Type I cement, and depending on when it was produced, it may or may not pass six month expansion limits. A detailed study should be performed in the future on cements C2, C3, C5, and C6 to determine if variability in these cements could lead to erroneous interpretations of mixtures incorporating SCMs in ASTM C 1012 testing.

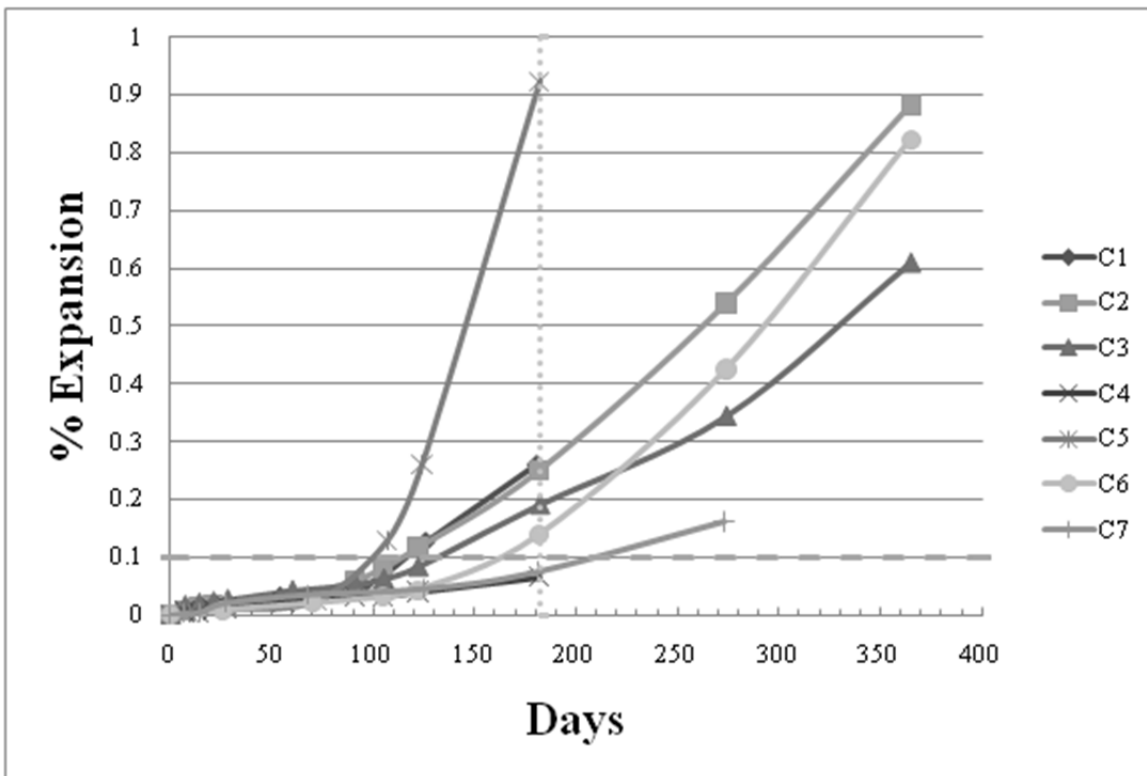


Figure 4.2: ASTM C 1012 Results of Cements Tested

4.3 Evaluation of Class C Fly Ashes

4.3.1 Expansions

A comprehensive testing program involving 8 fly ashes and other SCMs was performed, and for convenience, Tables 4.2 and 4.3 summarizes the key data, including the dosages of SCMs used for FA1 and FA2. The data for FA3-FA8 are provided in Appendix B in Drimalas 2007. For conciseness, the expansion values at 6, 12, and 18 months are included in the table as these test ages correspond to age-specific criteria set forth in ACI 201.2R for “equivalent” sulfate resistance. Expansion values that are in bold font indicate expansions in excess of 0.1%, which is a typical expansion limit for the different test ages, depending on the exposure class in ACI 201.2R. The “X” designation in the table represents mortars that had deteriorated and were not measurable. This section discusses only the expansion results for control mixtures (without fly ash) and mixtures containing fly ash; discussion on the behavior of mixtures containing ternary blends (portland cement, Class C fly, and either silica fume or ultra-fine fly ash) is provided in Section 4.4.

Table 4.2: Expansion Measurements from FA1 in ASTM C 1012 Testing

FA1	Ternary	6 Month	9 Month	12 Month	18 Month
20%		0.043	0.100	0.134	0.900
20%	3% SF	0.060	0.074	0.192	X
20%	5% SF	0.028	0.042	0.074	0.261
20%	6% UFFA	0.037	0.045	0.079	0.244
20%	9% UFFA	0.037	0.038	0.053	0.099
20%	20% Slag	0.028	0.040	0.062	0.106
20%	25% Slag	0.027	0.038	0.052	0.056
25%		0.041	0.092	0.340	X
25%	3% SF	0.036	0.062	0.132	0.395
25%	5% SF	0.027	0.045	0.079	0.194
25%	6% UFFA	0.036	0.044	0.048	0.065
25%	9% UFFA	0.037	0.051	0.069	0.084
25%	20% Slag	0.036	0.054	0.088	0.107
25%	25% Slag	0.039	0.056	0.076	0.091
30%		0.072	0.085	0.229	X
30%	3% SF	0.034	0.058	0.199	0.621
30%	5% SF	0.034	0.051	0.074	0.138
30%	6% UFFA	0.038	0.053	0.077	0.094
30%	9% UFFA	0.028	0.041	0.052	0.057
35%		0.060	0.113	0.398	X
35%	3% SF	0.039	0.062	0.106	0.213
35%	5% SF	0.039	0.047	0.056	0.095
35%	6% UFFA	0.041	0.066	0.084	0.083
35%	9% UFFA	0.038	0.069	0.094	0.097
40%		0.118	0.257	0.511	X
40%	3% SF	0.045	0.072	0.072	0.090
40%	5% SF	0.027	0.046	0.052	0.073
40%	6% UFFA	0.044	0.057	0.073	0.077
40%	9% UFFA	0.040	0.057	0.075	0.071

Table 4.3: Expansion Measurements for FA2 in ASTM C 1012 Testing

FA2	Ternary	6 Month	9 Month	12 Month	18 Month
20%		0.055	0.117	0.359	0.995
20%	3% SF	0.039	0.055	0.075	0.201
20%	5% SF	0.035	0.052	0.074	0.162
20%	6% UFFA	0.024	0.031	0.040	0.069
20%	9% UFFA	0.034	0.042	0.054	0.080
20%	20% Slag	0.038	0.058	0.089	0.133
20%	25% Slag	0.048	0.063	0.077	0.085
25%		0.070	0.130	0.470	X
25%	3% SF	0.028	0.037	0.047	0.103
25%	5% SF	0.032	0.039	0.057	0.073
25%	6% UFFA	0.058	0.068	0.080	0.094
25%	9% UFFA	0.069	0.075	0.099	0.090
25%	20% Slag	0.046	0.064	0.090	0.136
25%	25% Slag	0.047	0.037	0.085	0.237
30%		0.051	0.073	0.098	0.191
30%	3% SF	0.060	0.077	0.092	0.124
30%	5% SF	0.072	0.079	0.087	0.100
30%	6% UFFA	0.053	0.067	0.098	0.110
30%	9% UFFA	0.064	0.063	0.075	0.105
35%		0.046	0.070	0.108	0.161
35%	3% SF	0.042	0.062	0.083	0.135
35%	5% SF	0.026	0.049	0.077	0.087
35%	6% UFFA	0.064	0.070	0.088	0.100
35%	9% UFFA	0.064	0.072	0.088	0.109
40%		0.054	0.074	0.075	0.102
40%	3% SF	0.032	0.037	0.048	0.057
40%	5% SF	0.065	0.080	0.091	0.092
40%	6% UFFA	0.061	0.066	0.080	0.099
40%	9% UFFA	0.067	0.080	0.098	0.144

With regard to mixtures containing Class C fly ash, almost all mixtures exhibited faster deterioration and often higher expansions compared to the control specimens (note some mixtures showed little expansion before completely deteriorating, as discussed later in this section). To supplement the tabular representation of the expansion results provided in Table 4.2 and 4.3, some of the key results are shown graphically next to highlight key trends in behavior.

Figure 4.3 shows the behavior of mortar containing fly ash FA1. This mixture begins to expand earlier than the control, and the onset of expansion occurs earlier as the dosage of fly ash is increased. Only the mixture containing 20% FA1 (by mass replacement of portland cement) was intact at the end of the 18 month test; all other mixtures with higher dosages of FA1 deteriorated prior to this time and subsequent measurements were not possible. The increased storage duration of the mortar bars for 18 months shows that 20% FA1 lasts for that period unlike the other replacements; however, it has the highest ultimate expansion compared to the other replacement levels at one year. Increasing the dosage of FA1 tended to increase the expansions. In fact, the mixture containing 40% FA1 “failed” the aforementioned 0.1% expansion limit at 6 months. The increasing replacement dosages of Class C fly ash deteriorated the mortar bars at faster rates due to greater amounts of reactive phases placed into the system.

Similar findings by Tikalsky and Carrasquillo (1993) showed a decrease in sulfate resistance with Class C fly ash.

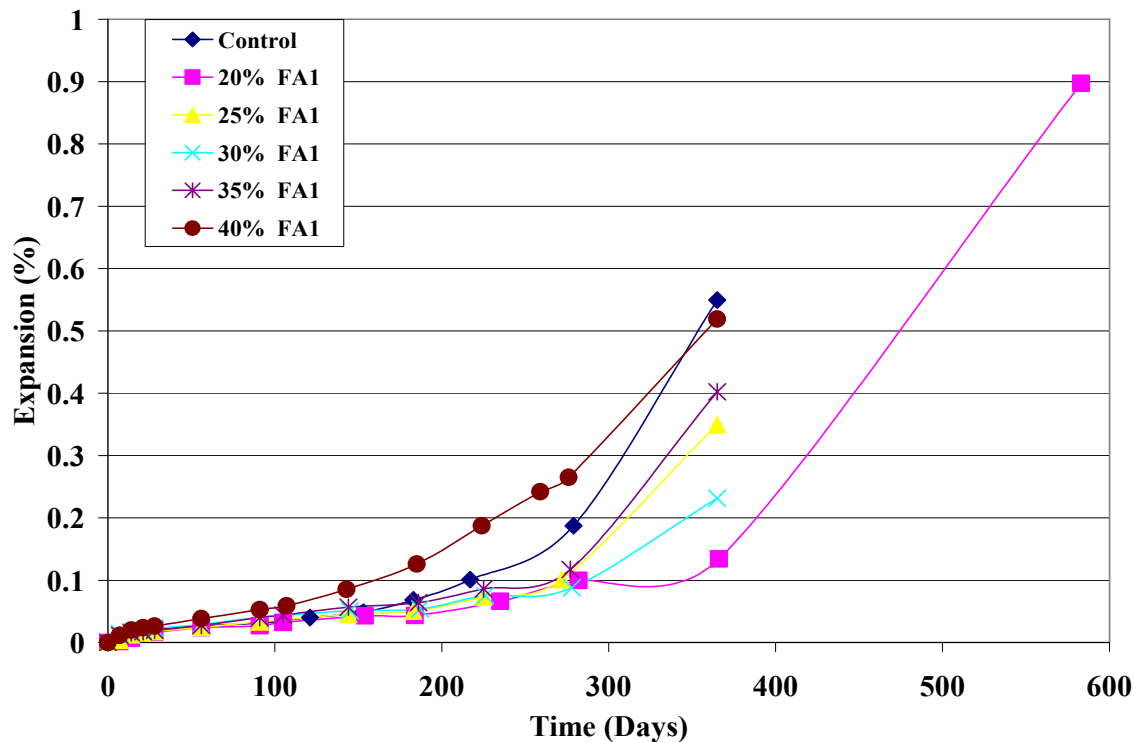


Figure 4.3: Expansions of FA1 at Different Replacement Dosages

All but one of the other Class C fly ashes tested in this program performed similarly to FA1, with increasing fly ash dosages leading to increasing deterioration. The only exception was FA2, which had similar bulk chemistry to FA1, but performed quite differently in ASTM C 1012 testing, as shown in Figure 4.4. Increasing the dosage of FA2 did not result in an increase in expansion, and in fact, after six months, all of the mixtures containing FA2 showed exhibited expansions less than 0.1%. After one year, mixtures containing 20 and 25% FA2 expanded more than the nominal 0.1% expansion limit, mixtures containing 30 and 35% FA2 were approximately at this expansion limit, and the mixture containing 40% FA2 was below this expansion limit. After 18 months, all the mixtures containing FA2 expanded greater than 0.1%.

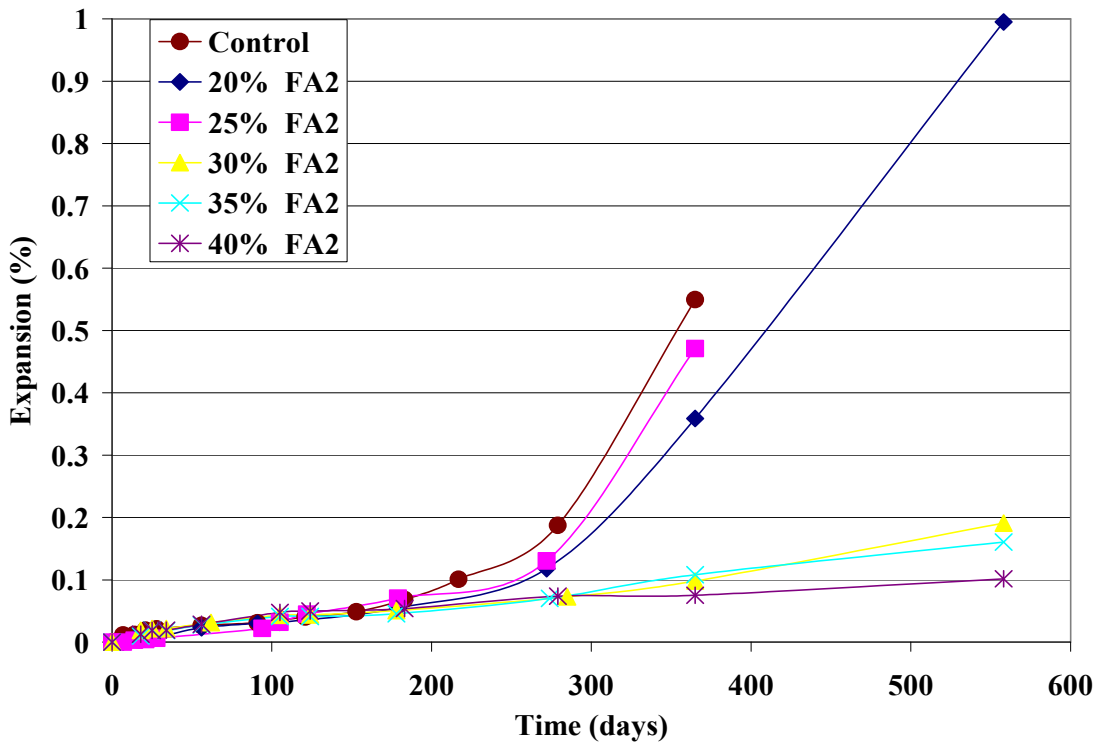


Figure 4.4: Expansions of FA2 at different replacement dosages

Interestingly, the mode of failure of mortar bars containing FA2 was quite similar to that of control specimens specifically high expansions were observed without bulk disintegration of the specimens. Microstructural observations of the mortar bars containing FA2, after exposure to sulfate solution, are described later in Section 4.3.2

As previously described, mortar containing fly ashes FA3-FA8 all showed similar behavior to FA1, with increasing deterioration of specimens observed, especially at higher fly ash dosages. Expansion results are shown in Appendix B in Drimalas 2007. In fact, most of the mixtures containing these fly ashes showed significant deterioration without observed expansions, or the specimens completely deteriorated from one measurement age to the next, making it impossible to correlate failure to a level of expansion. Figure 4.5 illustrates the expansions observed for mortars containing FA8 in which deterioration occurred after minimal times exposed to sulfate solution and without actually passing the nominal 0.1% expansion threshold. Figure 4.6 shows a photograph of mortar bars containing 40% FA8 after only 56 days immersion in sodium sulfate solution in the ASTM C 1012 test. The bars have completely deteriorated, yet expansion was not detected prior to failure. The deterioration of mortar containing FA2 (as well as most of the other high-calcium ashes in this study) is also quite interesting as the mode of failure seems to change as the percent replacement of fly ash for portland cement increases. At lower replacement levels the bars would increase in expansion and break eventually; however at higher replacement levels the bars deteriorate so quickly that they would fail prior to significant expansion. Clearly, this creates yet another interesting challenge when using ASTM C 1012. The technical viability of using expansion limits when testing certain Class C fly ashes clearly comes into question here as the dramatic deterioration occurs without

measured increases in expansion. More discussion on the mechanisms responsible for this behavior and the practical implications of such behavior is provided later in this chapter.

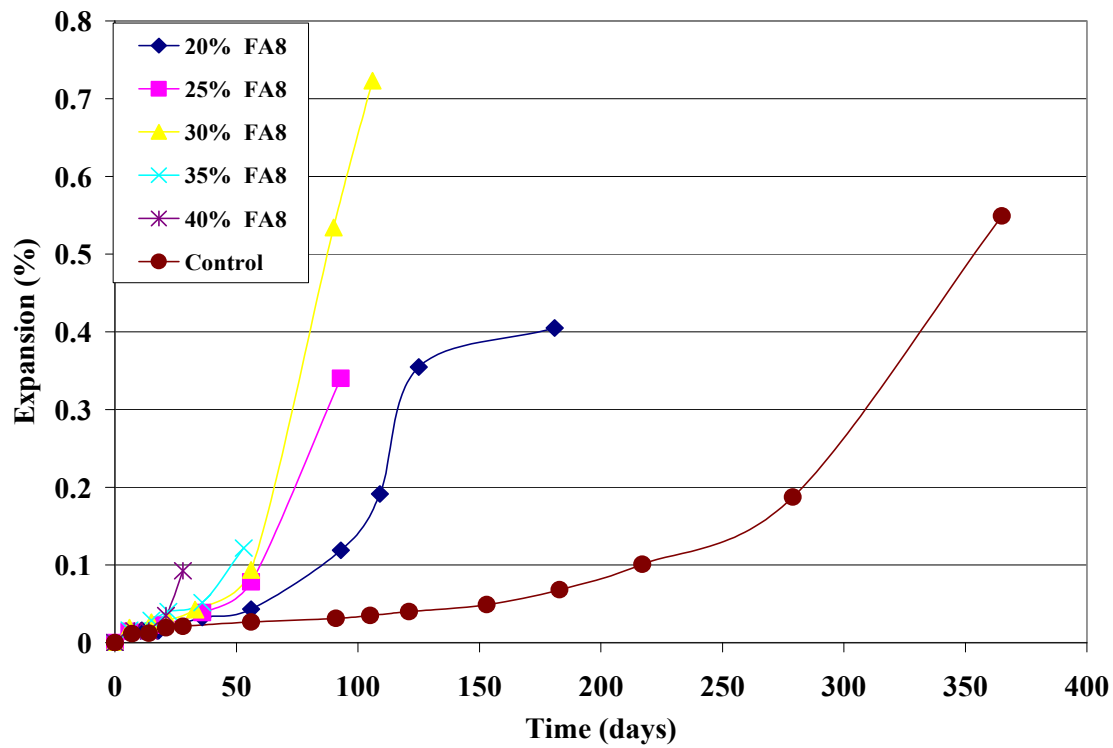


Figure 4.5: Expansion of FA8 fly ash at different replacements



Figure 4.6: FA8 after 56 days in ASTM C 1012 testing

Although the sulfate resistance of most of the Class C fly ashes studied in this program was quite poor, options were identified for improving the durability of mortar or concrete containing these types of ashes. The incorporation of an additional SCM in ternary blends helped to improve the sulfate resistance, as described later in this chapter, and parallel research at the University of New Brunswick showed that the use of higher replacement levels of these ashes (i.e., greater than 60%) actually improved sulfate resistance, as did the addition of small amounts of gypsum (i.e., 0.5% by mass) to mortar mixtures containing these problematic high-calcium ashes.

4.3.2 X-Ray Diffraction

X-ray diffraction (XRD) analysis was used to analyze the composition of mortars after 18 months of storage in sodium sulfate solution. Because of the relatively small size of the mortar bars, the entire cross section of a given bar was cut and crushed and subsequently analyzed by XRD. As such, the average composition of a given mortar bar was analyzed, generating data/information on the impact of sulfate attack on bulk or general behavior. Nevertheless, the data generated from XRD analyses of mortar bars provide an insightful means of determining what hydration products are being attacked and what reaction products are being formed. Furthermore, by applying advanced semi-quantitative XRD techniques, specifically Rietveld analysis, it is possible to estimate the type and amount of hydration or reaction products present within a given specimen.

Table 4.4 provides semi-quantitative Rietveld analysis of mortar bars containing Class C fly ash after 18 months of sulfate exposure (ASTM C 1012). For mortar mixture 25% FA2 after 12 months, the bars had expanded by 0.47%; however all the bars had broken and were not measurable at 18 months. Semi-quantitative analysis of these specimens identified ettringite as the primary constituent, consisting of 65% of the matrix. Similar results were found for mortar

bars containing the other Class C fly ashes after 18 months of testing. These large amounts of ettringite forming within the bars are possibly too high due to the ratio of cement and sand in the prepared mortar bar. This high amount of ettringite could be contributed to the full deterioration of these mortar bars that fell apart within the storage container. These deteriorated bars were removed from the storage container and not hammered due to the bars had broken into small pieces. Although the classic symptoms of sulfate attack were observed in mortar bars containing each of the Class C fly ashes, specifically the presence of ettringite and gypsum and the general reduction in portlandite and monosulfate concentration, it was not possible to distinguish major differences between the different fly ash-containing mortars or to elucidate major differences for a given fly ash as the dosage of fly ash was varied. The inability to differentiate between different fly ashes and dosages was likely due to the fact that the specimens had undergone such high levels of distress prior to analyses and/or the method of analyzing the entire cross section of a given mortar bar does not allow for detailed quantification of distress. More detailed evaluations of concrete affected by sulfate attack are described in Chapter 4, where concrete prisms, because of their larger size, were analyzed as a function of distance from the sulfate solution using profile grinding and subsequent XRD analysis.

Table 4.4: Semi-quantitative Rietveld analysis of select mortar mixtures at 18 months

Mixture	Ettringite (%)	Gypsum (%)	Monosulfate (%)	Portlandite (%)
20% FA2	48.13	8.62	0.02	0.38
25% FA2	64.59	5.02	0.09	0.55
20% FA3	48.72	5.13	0.14	0.66
25% FA3	32.81	7.85	1.41	3.33
30% FA3	50.66	2.1	0.06	0.06
30% FA4	49.12	3.28	0.42	0.59
25% FA6	45.92	3.35	0.95	3.83
30% FA6	41.64	1.52	1.38	5.39
35% FA6	29.17	3.47	5.1	6.4

4.3.3 Scanning Electron Microscopy

In order to better understand the mechanisms occurring with Class C fly ash and sulfate attack, scanning electron images with energy dispersive spectroscopy (EDS) were taken for analysis. Figure 4.7 is a SEM image of 25% FA2 after 18 months of storage in sodium sulfate solution. Throughout the sample, ettringite pockets are found in the paste. Ettringite was more prevalent in the paste rather than around the aggregates. The selected area in the image was chosen for EDS analysis. EDS provides the chemical analysis of this area comprising with amounts of Ca, S, and Al in this region and EDS confirms that these pockets are ettringite. Small amounts of gypsum throughout the sample were identified with EDS. With expansion initiating several months before the analysis of these specimens, it is possible that gypsum may have formed earlier and subsequently converted to ettringite.

Comparing FA1 and FA2 at lower replacements, 20% FA2 had expanded early compared to 20% FA1 which expanded after 1 year. Figure 4.8 is a SEM image of 20% FA1 after 18 months of storage in sodium sulfate. There are many large bands of gypsum that surround many

of the aggregates in the system. There was more gypsum observed around aggregates and very little ettringite was detected within the paste. The EDS spectrum shows large amounts of Ca and S, reflecting gypsum in the system. In parts of the mortar bars, it is evident that gypsum could be converting to ettringite. The late expansion of 20% FA1 is noticed from the conversion of gypsum to ettringite in the sample. At 20% FA1 replacement there is less reactive calcium aluminates than compared to 40% which may suggest attack is occurring more on the calcium hydroxide in the 20% FA1 mortar bars and could contribute to the later formation of ettringite from its conversion from gypsum. Figure 4.9 shows this possible conversion in an area of ettringite and gypsum formed in the same area. Gypsum and ettringite are in this same area as seen in the EDS spectrum.

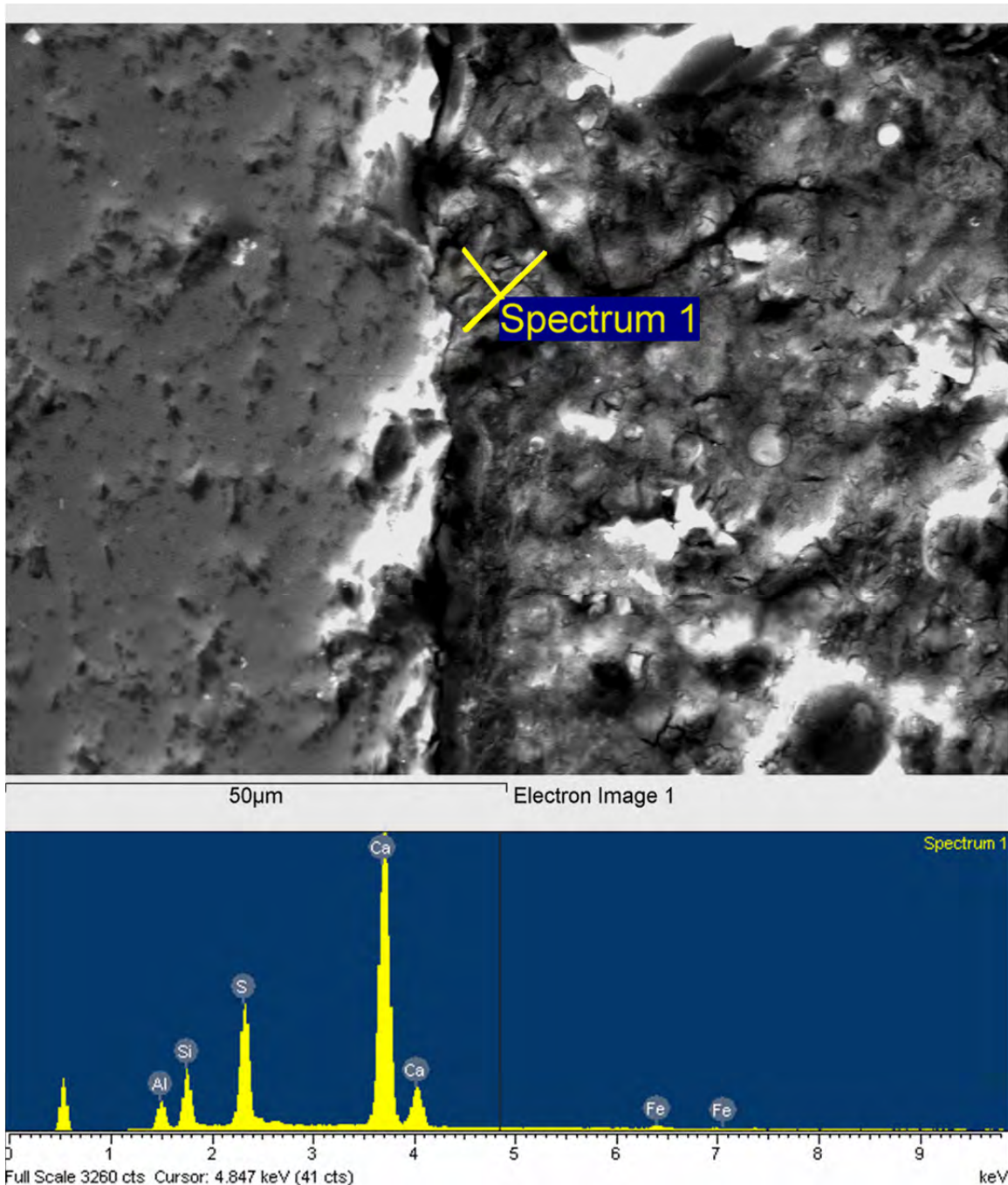


Figure 4.7: SEM and EDS Spectrum of 25% FA2 after 18 months storage in sodium sulfate solution.
Ettringite formation has occurred in pockets in the sample

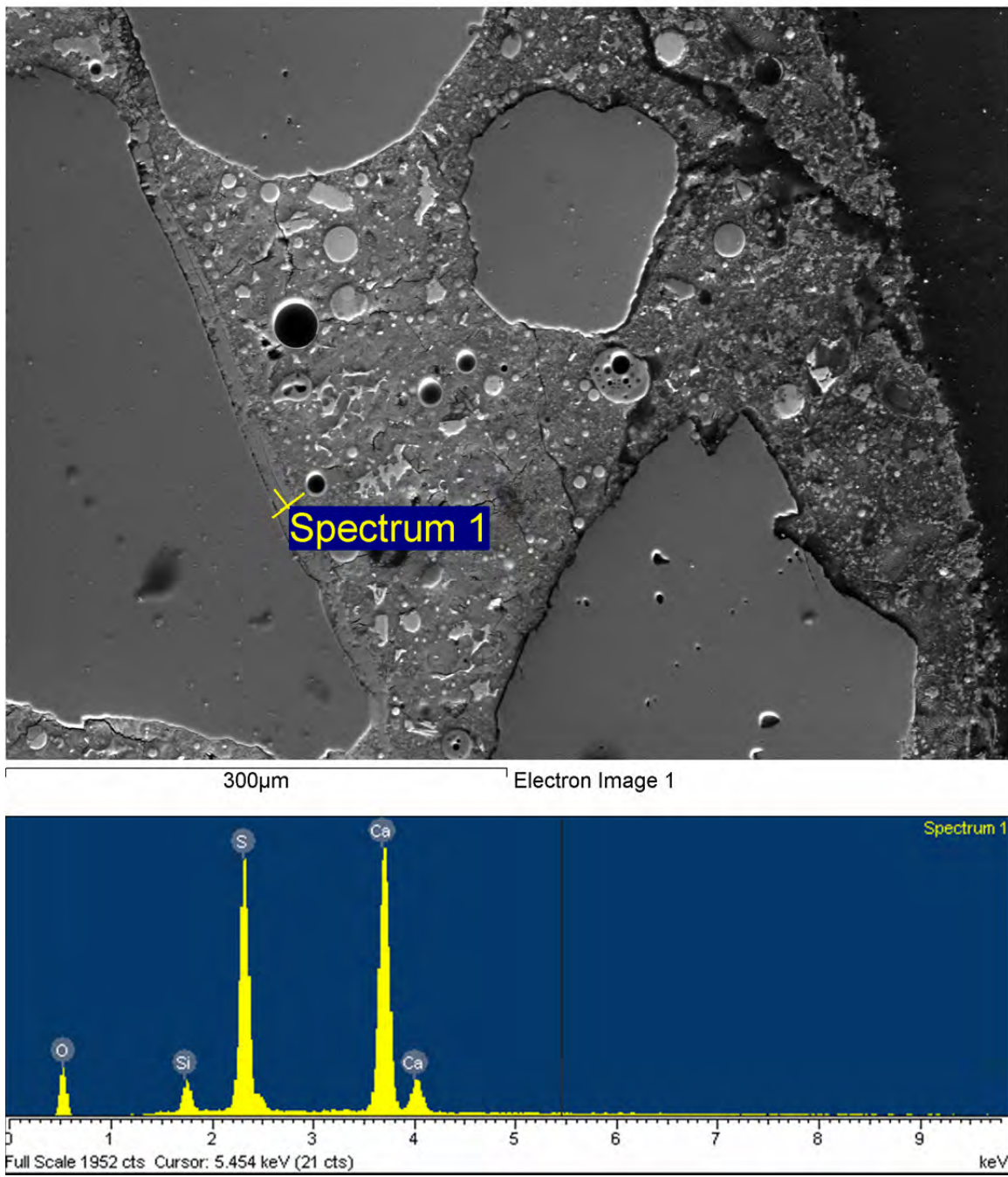


Figure 4.8: SEM Image and EDS Spectrum of 20% FA after 18 months of storage showing gypsum formation around aggregates

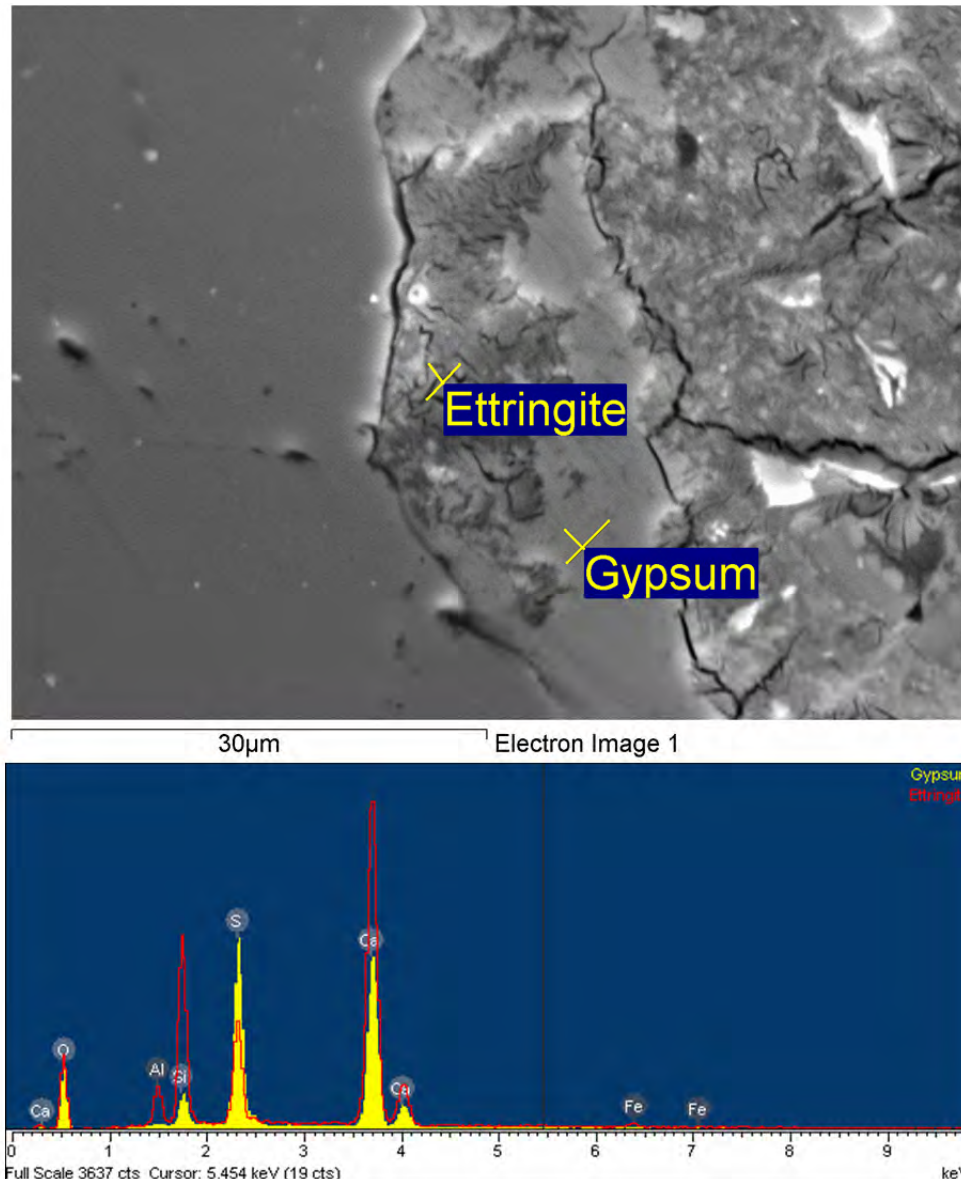


Figure 4.9: SEM Image and EDS spectrum of possible conversion of gypsum into ettringite in 20% FA1 mortar after 18 months storage in sodium sulfate

At the higher end of the replacement dosages, 40% FA1 and 35% FA2 were analyzed to determine the differences between the two fly ash responses. Figure 4.10 and 4.11 show SEM and EDS analyses of 40% FA1 and 35% FA2. In the SEM images of 40% FA1, there are many cracks throughout the hydrated paste. Ettringite formation is visible throughout the paste, with small amounts of gypsum near aggregates. The EDS spectrum confirms the small area of gypsum occurring near the aggregate. In comparison, 35% FA2 has gypsum formation lining aggregates and very small amounts of ettringite. Gypsum deposits are found lining aggregates and in some cases branching into the paste and connecting to other aggregates. The bands are similar to ettringite filled cracks often observed in delayed ettringite formation, but in this case the cracks are filled with gypsum. The gypsum bands that form around the aggregates have not converted to ettringite possibly due to aluminates from monosulfoaluminate not being available.

In addition, the FA2 may not present any reactive calcium aluminates that may react at later times to react with gypsum to form ettringite. There are a few small areas that have ettringite filled voids within the sample. The bulk chemistries of these two ashes were quite similar, but subsequent quantification of the glassy phases showed distinct differences in composition, as described later in this chapter.

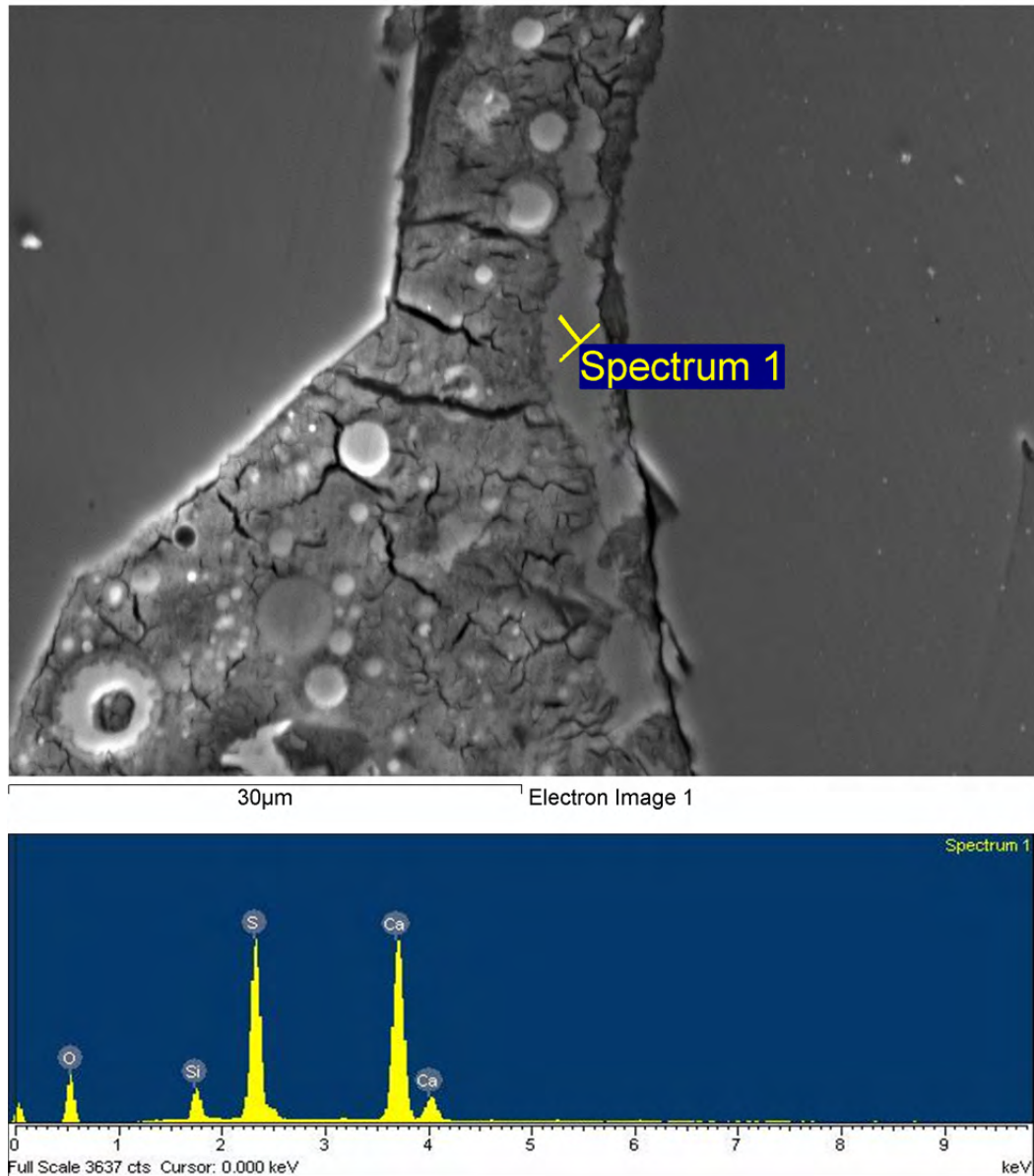


Figure 4.10: SEM and EDS analysis of 40% FA1 after 18 months in sodium sulfate solution

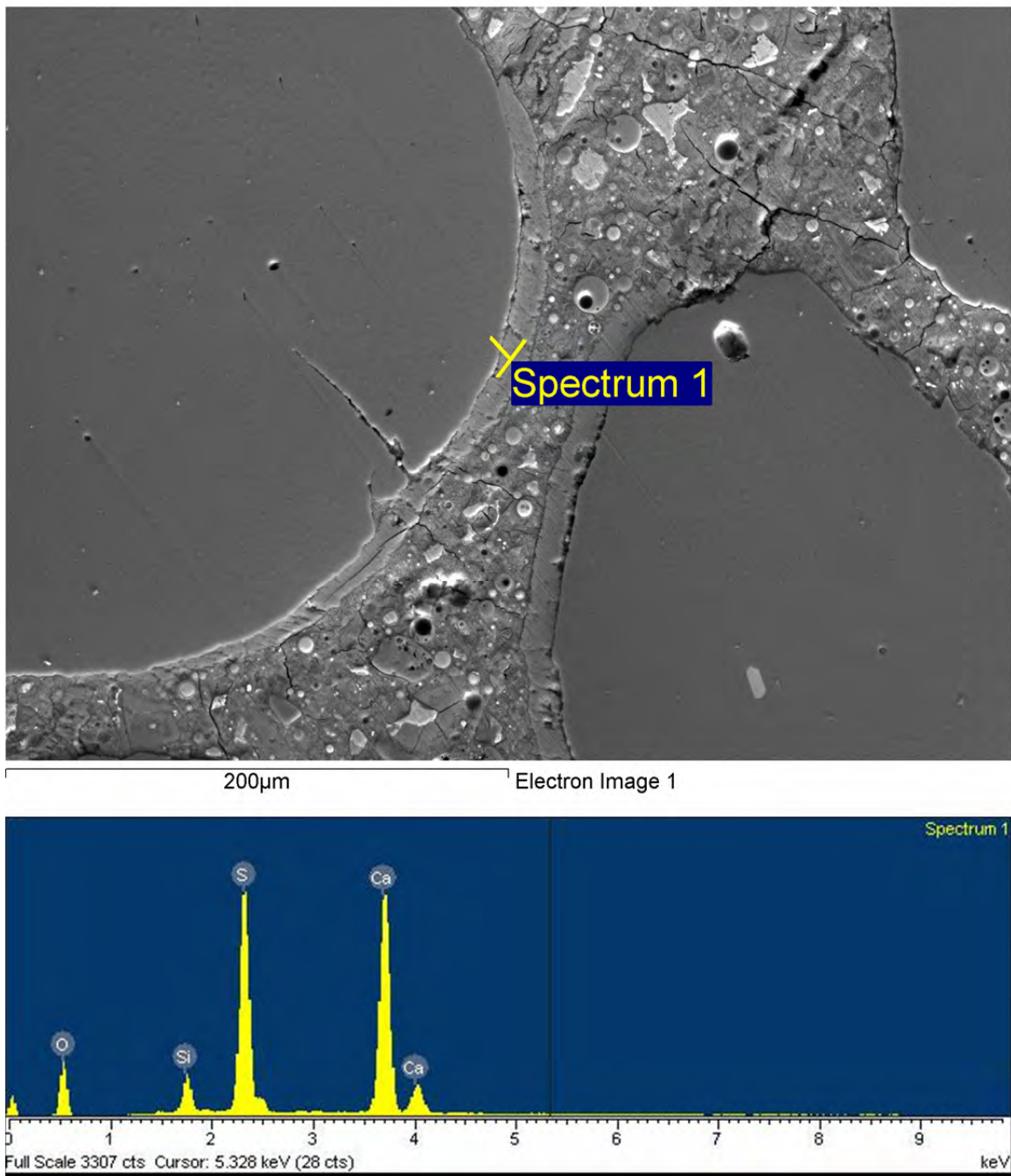


Figure 4.11: SEM and EDS analyses of 35% FA2 after 18 months of storage in sodium sulfate

4.4 Evaluation of Ternary Blends

This section describes the results of ASTM C 1012 testing performed on mortar mixtures containing ternary blends of Class C fly ash plus an additional SCM (silica fume, ultra fine fly ash (UFFA), or GGBFS). For convenience and to allow for direct comparison between the

performance of ternary blends and mixtures containing only Class C fly ash, the expansion data were previously included in Table 4.2 and 4.3. The majority of testing reported herein involved ternary blends including FA1, FA2, or FA3.

4.4.1 Expansions

Twenty four ternary blends were made with FA1, FA2, and FA3 at replacements between 20 and 40%. At all replacement levels, 3 and 5% silica fume, and 6% and 9% UFFA fly ash were used as a ternary blends. At 20 and 25% Class C fly ash replacements, 20 and 25% slag replacements were used. Replacement dosages of 30% Class C fly ash did not include slag as part of the ternary blend. An additional 8 ternary mixtures per fly ashes FA4, FA-5, FA-6, FA-7, and FA-8 were cast and are shown in Table 4.5.

Table 4.5: Mortar mixtures with FA-4, FA5, FA-6, FA7, and FA-8

% Fly Ash	% Silica Fume		
	0%	5%	7%
20	x		x
25	x		x
30	x	x	x
35	x	x	x
40	x	x	x

When adding either silica fume or ultra-fine fly ash to mortar containing FA1, significant improvements in sulfate resistance were realized. All of these ternary blends reduced expansions at six months below 0.1% expansion criteria at 6 months, and the majority satisfied the aforementioned requirements for Class 2 equivalent sulfate resistance, as per ASTM C 1012. At 18 months, ternary blends at the lower replacement levels of Class C fly ash performed worse than those at higher replacement dosages. In almost all cases, ternary blends with 6 and 9% UFFA exhibited excellent sulfate resistance. A surprising trend noticed was an increase in protection of ternary blends as the replacement levels of FA1 increased, which was the opposite when FA1 was used separately (without silica fume or ultra-fine fly ash). Figure 4.12 and 4.13 provide the ternary blends for 20 and 40% FA1. The decrease in expansion with ternary blends at higher replacement dosages may be related to reductions in permeability, which slow down and reduce the ingress of sulfate solution into the bars. GGBFS performed well in a ternary blend with either 20 or 25% FA1 with 25% GGBFS. The performance of GGBFS is substantial as it usually takes at least a 50% replacement dosage to control sulfate attack. The addition of Class C fly ash and GGBFS may provide a combination that removes nearly 50% of the cement.

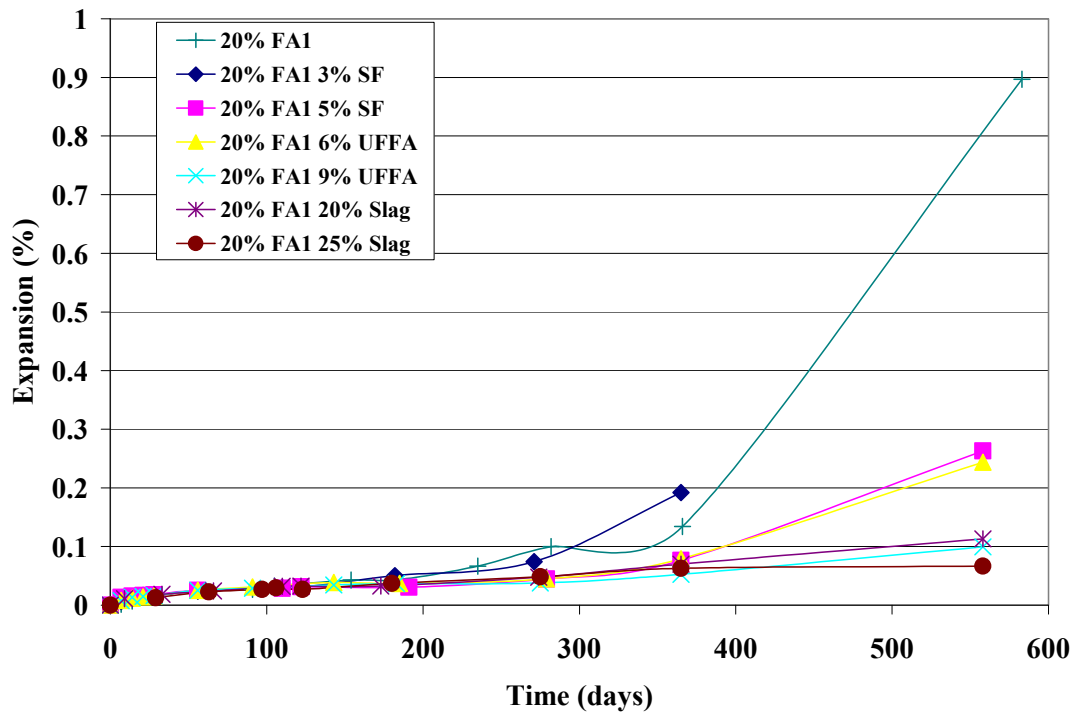


Figure 4.12: Mortar mixtures with 20% FA1 and ternary blends

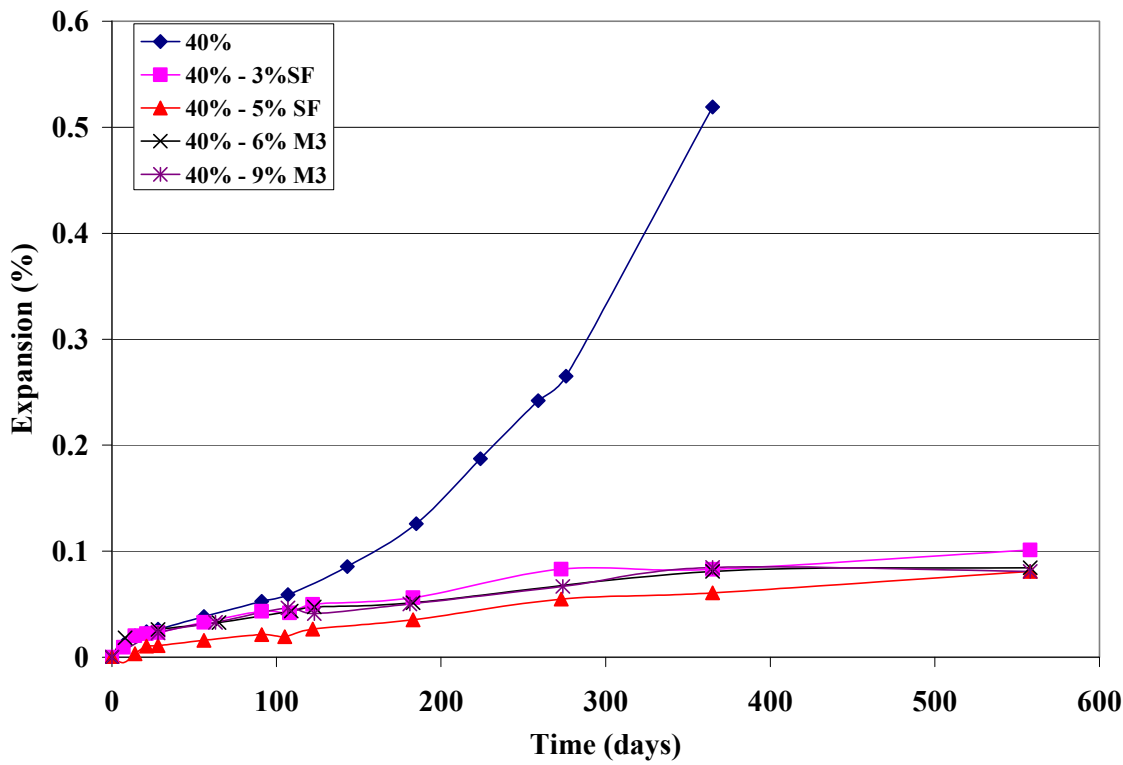


Figure 4.13: Mortar mixtures with 40% FA1 and ternary blends

Ternary blends with FA2 performed well at 6 months and at 1 year. All the ternary blends passed the 6 month criteria of 0.1% expansion; however, at 1 year three mixtures containing UFFA barely failed at 0.1%. At 18 months, the performance of ternary blends declined slightly. Many of the mixtures that failed had expansions close to 0.1% expansion. Although the sulfate resistance was improved through the use of ternary blends, FA2 did not respond as well as FA1, and it was difficult to reduce expansions to meet the criteria set forth for Class 3 exposure, as per ACI 201.2R.

Ternary blends cast with FA3, a fly ash that failed rapidly when tested by itself, performed similarly to ternary blends containing FA1 in that as the replacement levels of Class C fly ash increased, the performance of ternary blends improved. Silica fume at a 3% dosage in ternary blends did not perform well at any replacement level, but did perform better than only using FA3. In all cases, UFFA performed better than silica fume. Mortars with 40% FA3 disintegrated after 6 months while all the ternary blends were still intact and measurable at 18 months. Slag did not perform as well in ternary blends with FA3.

4.4.2 X-Ray Diffraction

X-ray diffraction analyses were performed on a wide range of mortar specimens containing ternary blends, with samples scanned from 5° to $65^\circ 2\theta$, at a .01 degree step size per 2 seconds. Semi-quantitative Rietveld analysis was conducted on all samples. As previously described in Section 4.3.2, abundant amounts of ettringite were detected in mixtures containing Class C fly ash after exposure to sulfate solution. Ettringite concentrations in mixtures containing only Class C fly ash were found to range between 30 and 65% of the total specimen mass in deteriorated specimens. When sulfate resistance was achieved through the use of ternary blends, the composition of the mortar bars after testing in ASTM C 1012 changed significantly. Table 4-6 provides semi-quantitative results from ternary blends with FA1 and FA2. For example, 25% FA2 with 9% UFFA, expanded only 0.09% at 18 months, meeting all expansion limits set forth by ACI 201.2R, even for the most severe exposure class. Semi-quantitative Rietveld analysis yielded an ettringite content of 26%, which is far less than the 65% shown in Table 4.7. The gypsum content was the same between mortars; however only trace amounts of monosulfate and portlandite were found in 25% FA2 mortars. All of the monosulfate and calcium hydroxide had converted to ettringite in the 25% FA2 bars. The ternary blends show greater monosulfate and portlandite content after 18 months. The silica fume, UFFA, and slag create less permeable system. In addition create a greater pozzolanicity that does not allow growth of deleterious products to form in the transition zone around aggregates.

Table 4.6: Semi-quantitative Rietveld analysis of ternary blends with FA1 and FA2

Mixture	Ettringite (%)	Gypsum (%)	Monosulfate (%)	Portlandite (%)
25% FA1 3% SF	43.51	5.83	1.41	5.24
25% FA1 20% Slag	39.08	6.46	1.53	3.35
25% FA1 25% Slag	25.85	12.43	4.2	1.05
30% FA1 3% SF	65.7	6.36	0.32	0.57
30% FA1 5% SF	44.88	4.6	0.97	2.67
30% FA1 9% UFFA	23.15	5.04	3.15	3.44
35% FA1 5% SF	54.64	5.08	1.11	2.37
35% FA1 6% UFFA	34.33	5.93	0.94	1.73
35% FA1 9% UFFA	37.5	6.5	3.46	2.74
20% FA2 3% SF	26.07	7.14	4.75	7.09
20% FA2 5% SF	35.26	8.84	1.86	5.17
20% FA2 6% UFFA	28.22	5.98	4.33	7.16
20% FA2 9% UFFA	40.29	7.27	3.15	3.45
20% FA2 20% Slag	34.44	6.26	4.17	3.59
20% FA2 25% Slag	25.32	8.55	4.16	3.73
25% FA2 6% UFFA	25.18	6.57	4.11	5.64
25% FA2 9% UFFA	26.17	6.31	3.98	4.09
25% FA2 3%SF	30.66	8.08	7.21	5.89
25% FA2 5%SF	33.41	10.12	0.22	0.11
25% FA2 20% Slag	41.28	7.14	1.3	0.43
25% FA2 25% slag	38.69	5.4	0.93	0.01

Figure 4.14 shows ettringite, gypsum, and CH contents from nearly 50 ternary blends with FA1 and FA2 related to expansion at 18 months. An increase of expansion relates primary to ettringite formation. There was little correlation between gypsum content and expansion. The concentration of CH did tend to decrease with increasing expansion. It should again be noted that the approach followed herein for quantifying the type and amount of hydration or reaction products was based on analyzing full cross sections of mortar bars, and as such, the results are averaged across a section that can be comprised of both damaged mortar (at surface exposed to sulfate solution) and undamaged mortar at the center of a given specimen. Nevertheless, this technique did allow for the identification of general trends in reaction products formed and their link to observed expansion and/or deterioration.

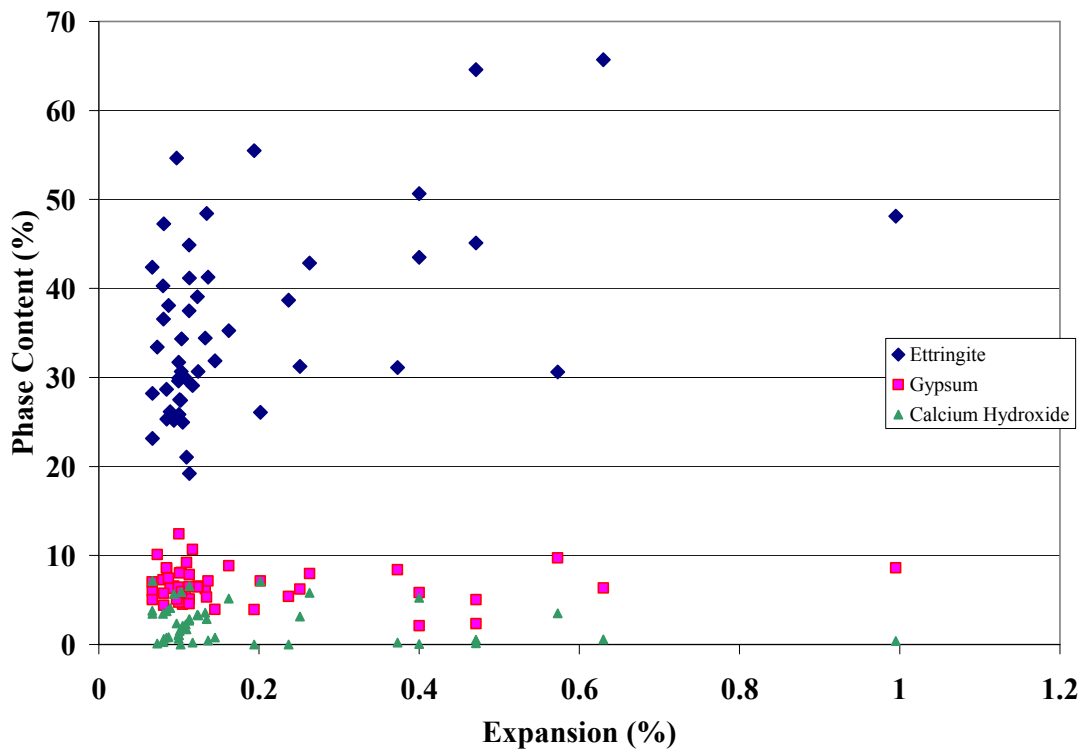


Figure 4.14: Relationship between ettringite, gypsum, and CH from mortars of ternary blends of FA1 and FA2

4.4.3 Scanning Electron Microscopy

Figure 4.15 shows an SEM image and EDS spectrum of 40% FA1 with 5% SF. In the image, a long band of gypsum runs along the samples edge. This band runs along the entire sample along the edge of the sample nearest to the sodium sulfate solution. The Ca and S in the EDS spectrum confirm the gypsum band in the image. In comparison with 40% FA1 in Figure 3.8, there is much less ettringite in the paste and around aggregates. Semi-quantitative XRD results show only 0.8% monosulfate in the 40% FA1 with 5% SF sample which suggests that gypsum has not converted to ettringite. Ternary blends with 6 and 9% UFFA also did well in suppressing expansion, even at 18 months. The use of these ternary blends significantly reduces the permeability of mortar, minimizing the ingress of sulfates and preventing chemical alterations of the matrix. This physical effect is also accompanied by the chemical effect of the pozzolanic reaction, resulting in lower CH contents and concomitant reductions in attack on this vulnerable phase.

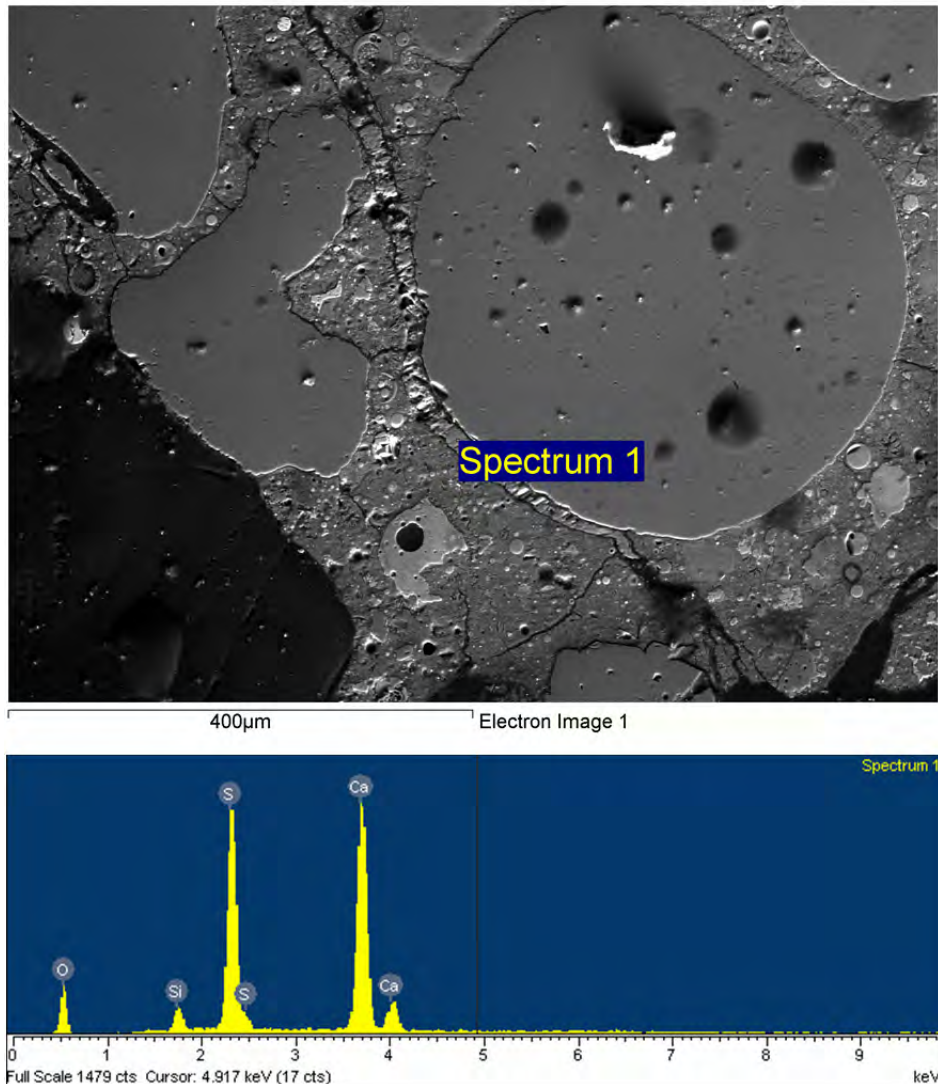


Figure 4.15: SEM Image and EDS spectrum of 40% FA1 with 5% SF after 18 months of storage in sodium sulfate storage. Gypsum band is found along the samples edge and around aggregates

4.5 Modified ASTM C 1012 Testing

The section evaluates mixtures that don't fit the regular criteria of ASTM C 1012 testing. This section includes three fly ashes (FA-1, FA2, and FA-3) in calcium sulfate, sodium sulfate, and magnesium sulfate with either Type II or Type V cement. Table 4.7 provides the matrix used in this section.

Table 4.7: Testing matrix for fly ashes FA-1, FA-2, FA-8 various fly ash replacements combined with Type II and Type V cement in different soak solutions

Cement Type	Fly Ash Replacement	Soak Solutions (5%)		
		Calcium Sulfate	Sodium Sulfate	Magnesium Sulfate
Type II	20%	X	X	X
Type II	30%	X	X	X
Type II	40%	X	X	X
Type V	20%	X	X	X
Type V	30%	X	X	X
Type V	40%	X	X	X

Figure 4.16 and 4.17 provide the expansion values for the controls containing Type I/II and Type V cement. All three mixtures with Type V cement in the three soaking solutions pass the test at 18 months. The controls with Type II cement fail at 1 year with sodium sulfate and the mixture in magnesium sulfate fails the 0.1 % expansion criteria at 18 months. Type I/II placed in calcium sulfate passes at 18 months. According to ACI 318, the Type I/II cement would meet the S1 exposure class and the Type V cement would meet S3 exposure conditions.

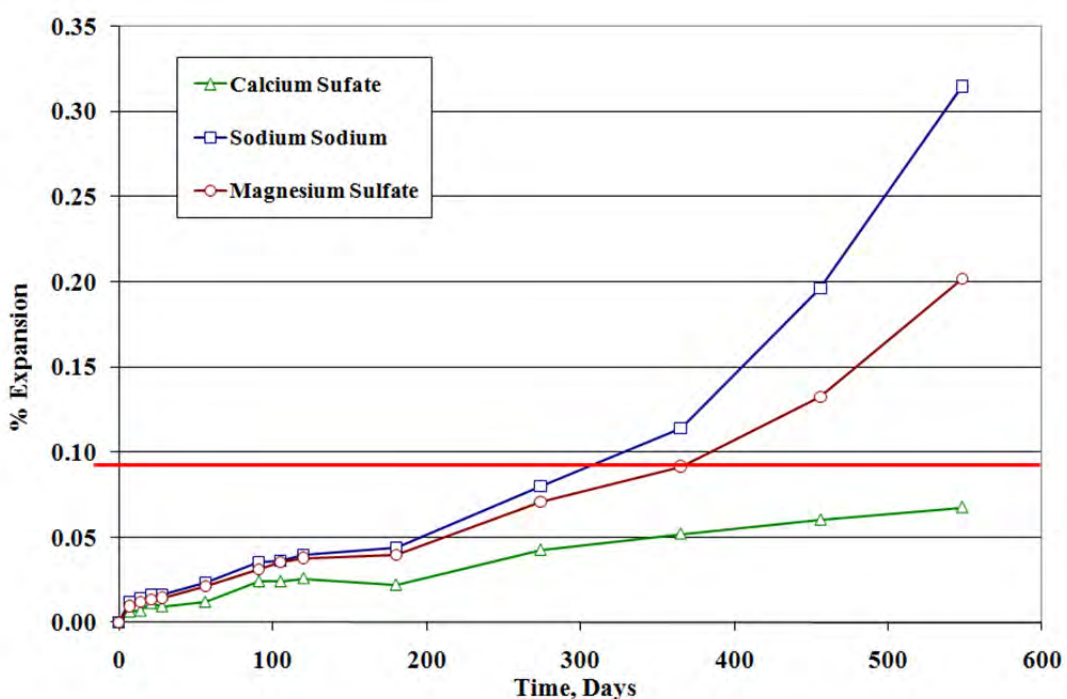


Figure 4.16: Mortar mixtures containing Type I/II Cement placed into three different soak solutions

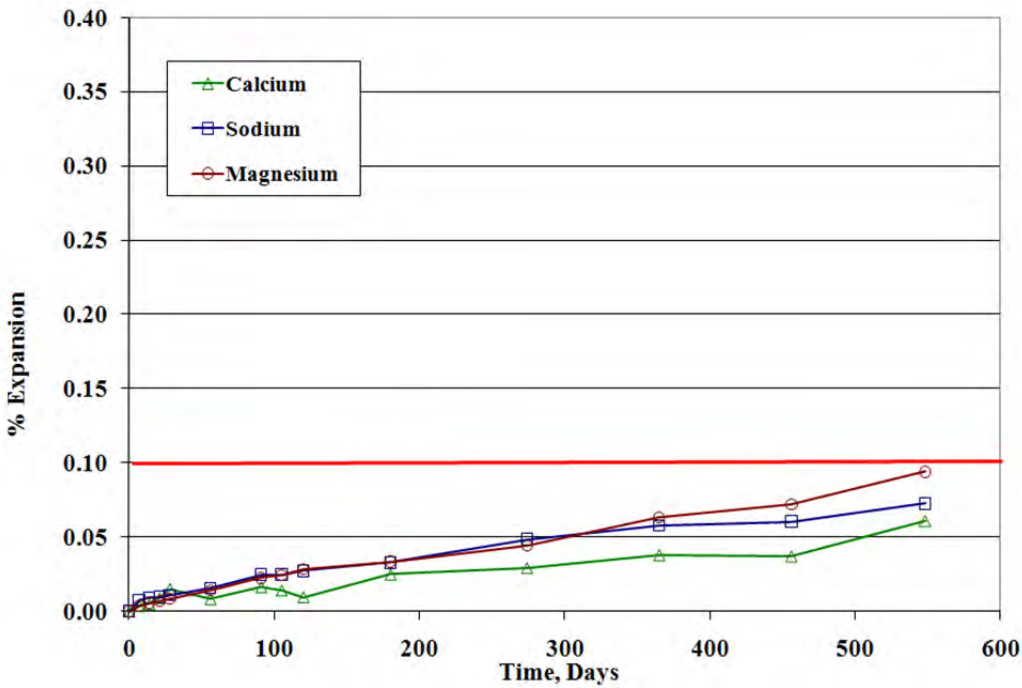


Figure 4.17: Mortar mixtures containing Type V Cement placed into three different soak solutions

Similar to section 4.2 the addition of Class C fly ash into mixtures increases the rate of expansion and fails the test at earlier times. The addition of Class C fly ashes increases the C3A content within the mixture of these mixtures which contain lower C3A content cements, and the addition of their reactive amorphous glassy phase increases the expansion values. Figure 4.18 and 4.19 show the effects of adding Class C fly ash into a mixture with either Type II or Type V cements. Figure 4.18 shows the addition of FA-8 with Type II cement. Mixtures in sodium and magnesium sulfate fail at 6 months while those in calcium sulfate fail the expansion limit at 1 year. Figure 4.19 shows the addition 40% FA-1 (lower reactive Class C fly ash) with Type cement. The mixtures placed into sodium and magnesium sulfate fail at 4 months and the mixture placed into calcium sulfate fails at 6 months. Overall, the calcium sulfate soak solution provides conditions with the least amount of expansion. The lower solubility of this solution may allow this soak solution to outperform the others. Sodium and magnesium sulfate solutions tend to provide the same rate of expansions.

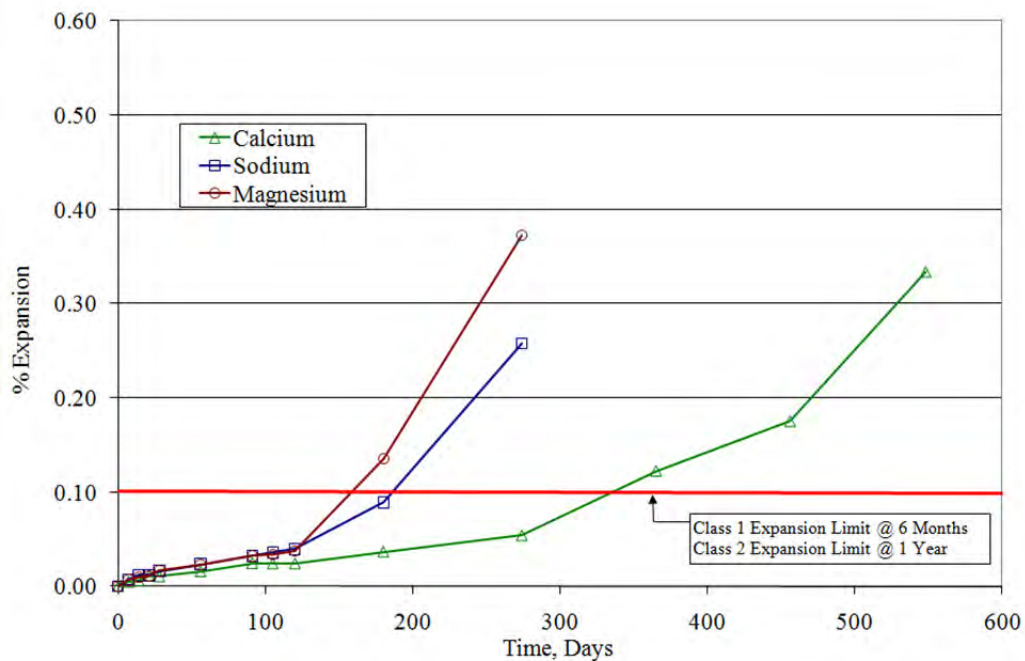


Figure 4.18: ASTM C 1012 mortar mixture with Type I/II cement and 20% FA8

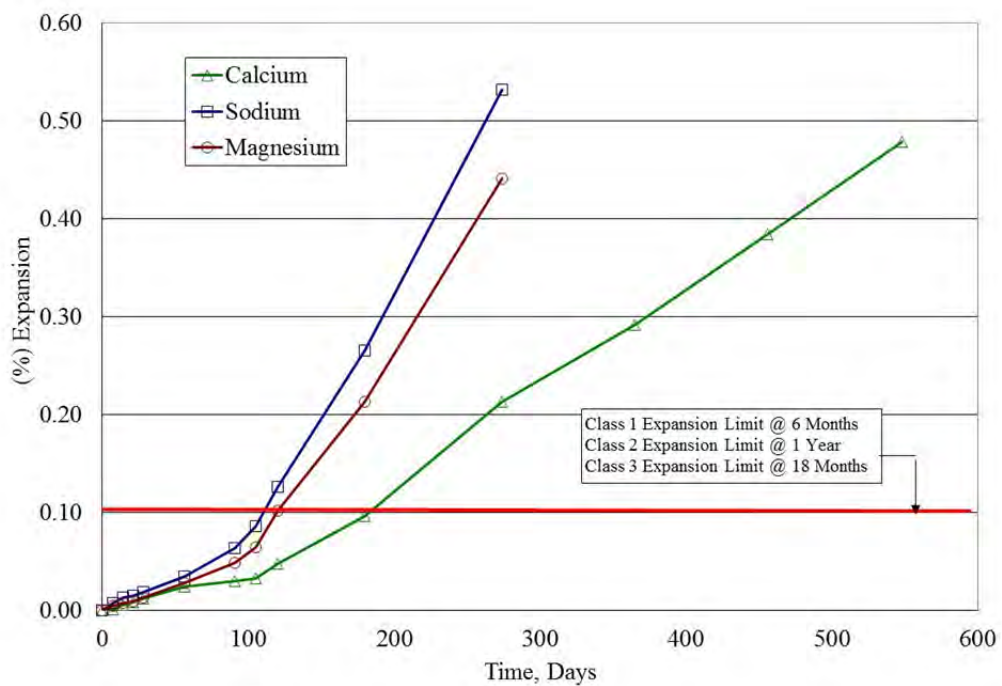


Figure 4.19: ASTM C 1012 mortar mixture with Type V cement and 40% FA1

4.6 Fly Ash Investigation

The bulk chemical compositions of the Class C fly ashes used in this study were previously provided in Table 3.2. However, as previously described, fly ash with similar chemical compositions exhibits starkly different behavior when tested using ASTM C 1012. As such, it is necessary to go beyond chemical composition and to try to better quantify the mineralogy of fly ash, including both the crystalline and amorphous phases. Figure 4.20 shows the XRD Rietveld analyses for FA1, FA2, and FA8. FA1 and FA2 showed similar crystalline phase compositions, and these were quite different from the crystalline composition of FA8.

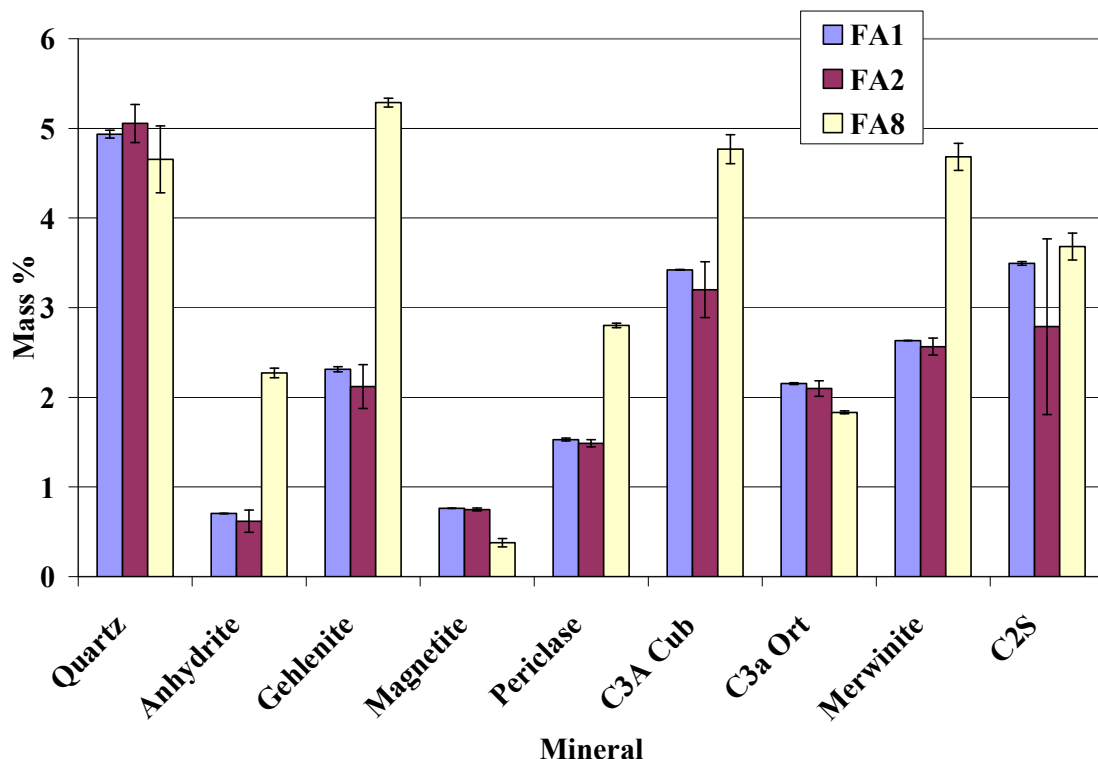


Figure 4.20: Quantitative XRD Rietveld analyses for FA1, FA2, and FA8. FA1 and FA2 have similar crystalline composition but perform drastically different in ASTM C 1012 Testing

As previously described in Section 4.3, FA1 and FA2 exhibit drastically different behavior in ASTM C 1012 testing, despite similarities in crystalline compositions, suggesting strongly that one must evaluate the amorphous or glassy phases to determine if the differences in behavior can be elucidated. FA8, which was one of the worst performers in ASTM C 1012, was found to have significant differences in its crystalline content and composition, when compared to FA1 and FA2.

A detailed evaluation of the amorphous or glassy phases is currently ongoing in research both at the University of New Brunswick and The University of Texas at Austin through the use of scanning electron microscopy. Scanning electron microscopy was used to analyze the bulk and glassy phases of the ashes. The chemical analysis of the glassy phases was then plotted onto

a calcium-aluminum-silicon ternary diagram. Fly ashes that exhibited the worst sulfate resistance in ASTM C 1012 testing show a tendency towards containing more calcium aluminates in the glassy phase. This is especially evident for FA8, which exhibited the most significant deterioration in ASTM C 1012. Research at the University of New Brunswick links the composition of the glassy phase to early hydration products and ultimately to the mechanism of failure when mortar containing Class C fly ash is exposed to sulfate solutions. The research conducted at the University of New Brunswick will be discussed in Chapter 6.

4.7 Summary

This chapter summarized a comprehensive study in which a wide range of high-calcium fly ashes were evaluated to determine their sulfate resistance when tested according to ASTM C 1012. All tests were conducted for 18 months (except for those specimens that failed prior to this age) in order to generate data that can be used as inputs for selecting preventive measures for ensuring sulfate resistance as per ACI 201.2R. The following are significant findings from this chapter

- High-calcium fly ashes evaluated in this study showed poor sulfate resistance with a decrease in performance as the replacement dosages increased. The addition of reactive phases caused the mortars to deteriorate.
- The formation of ettringite were determined to cause the deteriorating expansions occurring in the mortar bars. Calcium hydroxide and monosulfate was depleted in these systems to form gypsum and ettringite.
- The incorporation of a second SCM (silica fume, UFFA, or GGBFS) helped to restore sulfate resistance. This can allow agencies to use ternary blends in areas that may not be able to use Class C fly ash in sulfate prone areas. The use of these second SCMs in the mixtures created a less permeable system which slowed down the progression of attack. The increased pozzolanic activity from the additional SCMs helped prevent further deterioration.
- Mechanistic studies using XRD and SEM identified the key modes of failure such as ettringite formation being greater in specimens with solely Class C fly ash. Monosulfate and portlandite were also depleted from attack in these same mortar bars.
- Lastly, detailed evaluations of the mineralogy of Class C fly ashes were performed using Rietveld analyses for the crystalline phases and SEM (and EDS) analyses for the glassy phases, and work at UNB has found a link between the mineralogy of the glassy phase and sulfate resistance. The glassy phase has more reactive calcium aluminates which tend to destruct the mortars containing these fly ashes. The fly ashes that behave worse in sulfate environments tend to have more of these reactive calcium aluminates.

Chapter 5. Outdoor Exposure Site

ASTM C 1012 is the most common test method used to predict sulfate attack and it is specified in many guidelines for the evaluation of external sulfate attack. However, there is a lack of correlation between standard test methods and concrete subjected to sulfate-bearing soils in-situ. The research described in this chapter aims at helping to bridge the gap between laboratory and field performance of concrete subjected to external sulfates. Before describing this work, a brief background is presented on some past work aimed at addressing this same linkage between the laboratory and the field.

Based on the recent findings of laboratory and field evaluations, there seems to be a significant disconnect between the performance of concrete exposed to external sulfates in the laboratory (where specimens are stored in sulfate solutions at constant temperature) and concrete exposed to realistic field conditions, where evaporation fronts and concentration gradients exist and where temperature fluctuations are commonplace. To attempt to elucidate these key differences in behavior and to attempt to better correlate standard laboratory tests with field performance, a comprehensive research program was initiated at the Concrete Durability Center (CDC) at The University of Texas at Austin. This included the development of an outdoor sulfate exposure site and the evaluation of concrete mixtures subjected to different sulfate solutions at this outdoor site and in parallel laboratory tests. Mechanistic work is also presented that aimed to identify the cause and extent of distress of the various concrete specimens exposed to the different test conditions.

5.1 Outdoor Sulfate Exposure Site Design and Test Procedure

The development of an outdoor sulfate exposure site began in 2005 at the Concrete Durability Center (CDC) in Austin, Texas. Figure 5.1 shows the outdoor sulfate exposure site. The design of this site was based loosely on the PCA site in Sacramento, but various modifications were employed to evaluate a more comprehensive range of exposure conditions and test parameters. Detailed information on the key features of this site in Austin, Texas is presented next.



Figure 5.1: Outdoor sulfate exposure site located in Austin, TX. From left to right, the trenches contain calcium sulfate, sodium sulfate, and magnesium sulfate.

5.1.1 Exposure Site Design

The exposure site consists of three 13 ft x 16 ft (4 m x 5 m) trenches, each having a depth of 18 in (450 mm). After excavation, a 0.045 in (1.14 mm) ethylene propylene diene terpolymer (EPDM) pond liner made by Firestone was placed for confinement of sulfates in each trench. A sandy loam used for residential foundations in Austin, Texas was used as the fill material in the trenches, filled to a depth of 8 in (200 mm). Testing of this loam confirmed sulfates were not present. Sulfate solutions (sodium, magnesium, and calcium) were then added to each of the three trenches. The trench containing sodium sulfate was filled with solution to obtain a concentration of 5% sodium sulfate, which matches the sulfate concentration used in ASTM C 1012. For comparison, the PCA site contained a 10% sodium sulfate solution, but this concentration was deemed to be too aggressive and not indicative of realistic soils. The other two trenches for the current study were matched to the total sulfate concentration contained in the sodium sulfate trench, but contained calcium sulfate and magnesium sulfate. The sulfate solutions were initially kept at a height 3 in (75 mm) above the soil. The trenches were subsequently monitored and allowed to evaporate until the solutions just reached the soil level and were then filled with water. As such, the concentrations of sulfates in the trenches are at a minimum when the levels are at their highest (and initial) level and at a maximum when the water has evaporated to the point where the solution reaches the soil level.

For the magnesium and sodium sulfate trenches, the high solubility of these salts allowed for easy filling of the trenches. For example, for the sodium sulfate trench, anhydrous sodium sulfate was simply dissolved in water and added to the trench to yield a concentration of 5% sodium sulfate in the water-filled pores of the soil. A similar approach was followed for magnesium sulfate, but in this case, the *sulfate ion* concentration was matched to that of the sodium sulfate trench, thereby allowing for a more direct comparison between the two trenches. For the gypsum trench, the limited solubility of gypsum did not allow for complete dissolution of the calcium sulfate into water. Rather gypsum was added to water until it precipitated out of solution (1440 ppm), and additional gypsum powder was added to the soil to reach the target

concentration (same sulfate ion concentration as sodium sulfate trench) and mixed thoroughly. This, in essence, is what is encountered in heavily concentrated gypsum soils, and it helps to explain why high extraction ratios tend to result in higher values of gypsum in the extracted solution.

5.1.2 Concrete Prism Testing Regime

Forty concrete mixtures, each comprised of 24 concrete prisms, were cast for placement in the outdoor sulfate exposure site. The initial round of mixtures consisted of 30 mixtures followed by 10 mixtures looking at more specific mixtures. Details of these concrete mixtures are provided later in this chapter. Concrete prisms with dimensions of 3 in x 3 in x 11.25 in (75 mm x 75 mm x 285 mm) were selected, rather than larger prisms used at the PCA exposure site, to allow for expansion measurements, mass loss, and dynamic modulus testing in standard laboratory equipment at the CDC. The prisms were demolded 24 hours after casting. After demolding, the prisms were cured in a fog room (73 °F (23 °C), 100% RH) for 28 days. At 28 days of age the prisms were placed in either the outdoor exposure site or in a modified ASTM C 1012 testing regime.

Figure 5.2 shows the testing program and the disposition of the 24 concrete prisms per mixture. A total of 15 prisms were stored in the sulfate exposure site, either completely submerged or stored vertically with 6 in (150 mm) of the prism submerged in the sulfate-bearing soil. The other 9 prisms were placed in a modified ASTM C 1012 storage condition in solutions containing calcium, sodium, or magnesium sulfate (matched to the same concentration as trenches containing same solution). Because larger prisms were used than those typically used in ASTM C 1012, larger storage containers with the appropriate ratio of the volume of sulfate-bearing solution to volume of concrete were necessary. To address the issue of the limited solubility of gypsum, solutions were prepared with the target sulfate concentration (to match the sulfate ion concentration of the 5% sodium sulfate solution), resulting in large amounts of sulfate precipitating out of solution. The specimens stored in this solution were elevated off of the bottom of the container at a height sufficiently high to prevent the bars from being in contact with the precipitant. As such, the bars were stored in a solution surrounded by saturated gypsum solution but the bars were not in intimate or direct contact with “solid” gypsum.

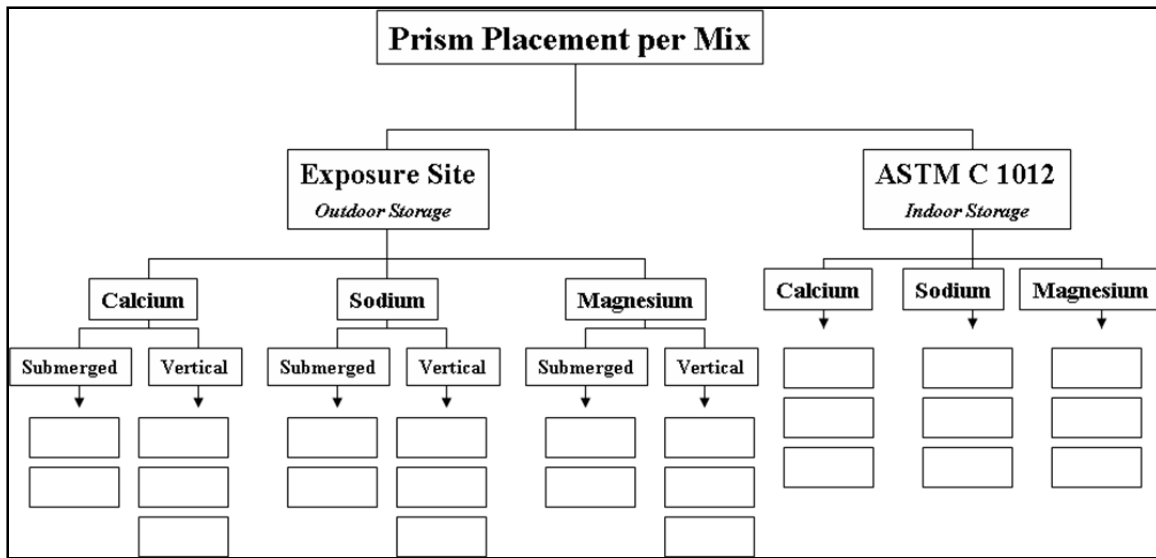


Figure 5.2: The placement of prisms from each mixture into the outdoor exposure site or in the modified ASTM C 1012 testing

The concrete prisms were strategically placed in the outdoor sulfate exposure sites to provide multiple storage conditions per mixture. Figure 5.3 shows how each mixture was placed in the respective sulfate trench. From each mixture in each trench, two prisms were placed below the soil level, roughly 2 in (51 mm) above the bottom of the trench, and three prisms were placed vertically. The vertical prisms were halfway submerged to provide the following three areas of exposure: submerged (in sulfate solution below grade), soil/solution interface zone (wetting/drying zone), and non-contact zone (above solution but subject to wicking action for some salts).

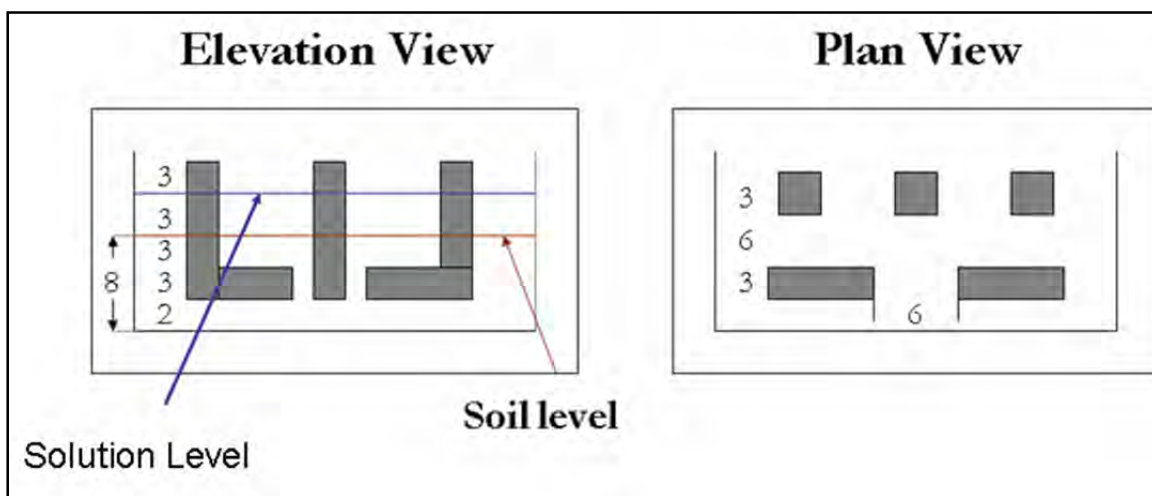


Figure 5.3: Placement of prisms in each outdoor exposure trench. The units are in terms of inches.

Prisms in each trench were measured (for mass change, length change, and dynamic modulus as per resonant frequency) after the following durations of exposure: 1, 2, 3, 4, 6, 9, 12, and 18 months. The prisms were removed from the exposure site one day prior to each

measurement. Once removed from the exposure site, the prisms were wrapped with moist towels and placed in a temperature and humidity controlled environment at 73 °F (23 °C) and a RH < 50% to ensure that thermal or moisture effects would not substantially impact the properties measured.

The remaining nine prisms from each mixture were placed in a modified ASTM C 1012 storage condition as noted above. Measurements on these prisms were taken at the same intervals of those in the exposure site. The sulfate solution was changed at each measurement period to a new solution. Each mixture was stored in its own container in a temperature controlled environment of 73 °F (23 °C). The prisms were elevated from the bottom of the container to reduce friction and raise the prisms that were in gypsum solutions above the super saturated gypsum.

5.1.3 Mortar Bar Testing Using ASTM C 1012

Mortar bars comprised of the same materials tested in the outdoor exposure site and in concrete prism testing (modified ASTM C 1012 storage condition) were also tested in accordance with ASTM C 1012. This procedure is provided in detail in section 3.2.2. Typically ASTM C 1012 only subjects mortar specimens to 5% sodium sulfate. However, to allow for comparisons with the concrete prisms previously described, mortar bars were also placed in calcium and magnesium sulfate solutions with sulfate concentrations equal to that in the 5% sodium sulfate solution.

5.1.4 Sulfate Profiling

Concrete prisms tested as per the modified version of ASTM C 1012 were removed at 18 months and progressively milled to a depth of .12 in (3 mm) to generate concrete powder samples to be analyzed by x-ray diffraction for the presence of hydration products and potentially detrimental reaction products from sulfate attack. For comparison, concrete prisms stored vertically at the outdoor exposure site were removed for milling and subsequent profile analysis. Figure 5.4 shows the process of how concrete cubes were cut from the prisms for milling. Each vertical prism was cut into 3 zones with a wet saw. Each zone has two concrete specimens removed, a 3 in (75 mm) cube cut for milling and a smaller slice for scanning electron microscopy. The specimens were cut into cubes to mill between saw cuts to have a one dimensional entrance of sulfates. The cubes were placed on a lathe that was attached to a drill press. The drill press allowed for vertical movement which determined the depth of the mill. The lathe moved the specimen horizontally through the diamond tipped bit that turned the concrete into a powder. A 1 in (25 mm) wide path was used for milling and the samples were milled every 0.12 in (3 mm) to a depth of 0.48 in (12 mm) and analyzed by either XRD. For convenience, units of mm will be used when sulfate milling is discussed. Once the powder was collected it was sieved through the No. 325 (45 micron) sieve and steps followed in 3.2.3 were followed for preparation of the powder for the SEM.

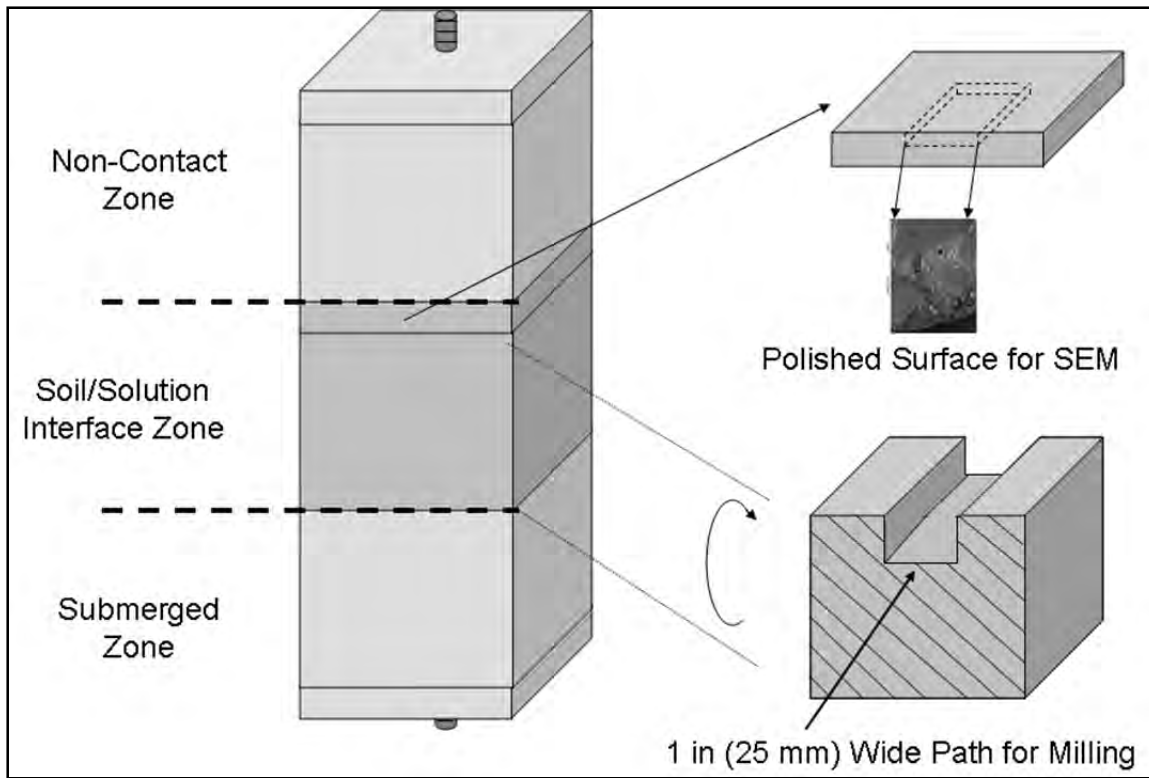


Figure 5.4: Prisms were cut into cubes to allow for milling for sulfates. Slices were also removed for SEM analysis.

5.1.5 Physical Sulfate Attack Testing

In addition to the concrete and mortar testing program previously described, a test procedure modified from Folliard and Sandberg (1994) was employed for evaluating physical sulfate attack. Mortar mixtures were cast into discs measuring 2 in (50 mm) in diameter and 1 in (25 mm) thick. Twenty-four hours after casting the discs were demolded and placed into solutions containing 10, 20, 30% sodium sulfate and 10, 20, 30% magnesium sulfate. Eight mortar mixtures were made with Type I and Type V cement at either 0.4 or 0.7 w/cm. Corresponding air-entrained mixtures were also cast. The mortar disks in the containers were enclosed with a lid and were subjected to 150 temperature cycles, as shown in Figure 5.5. This temperature cycling, which takes 11 hours for a single cycle, was selected because Folliard and Sandberg reported that this cycle triggers the most damaging transition between thenardite and mirabilite, resulting in the most significant concrete deterioration. The samples were removed at different cycle periods and weighed to measure if any mass changes occurred.

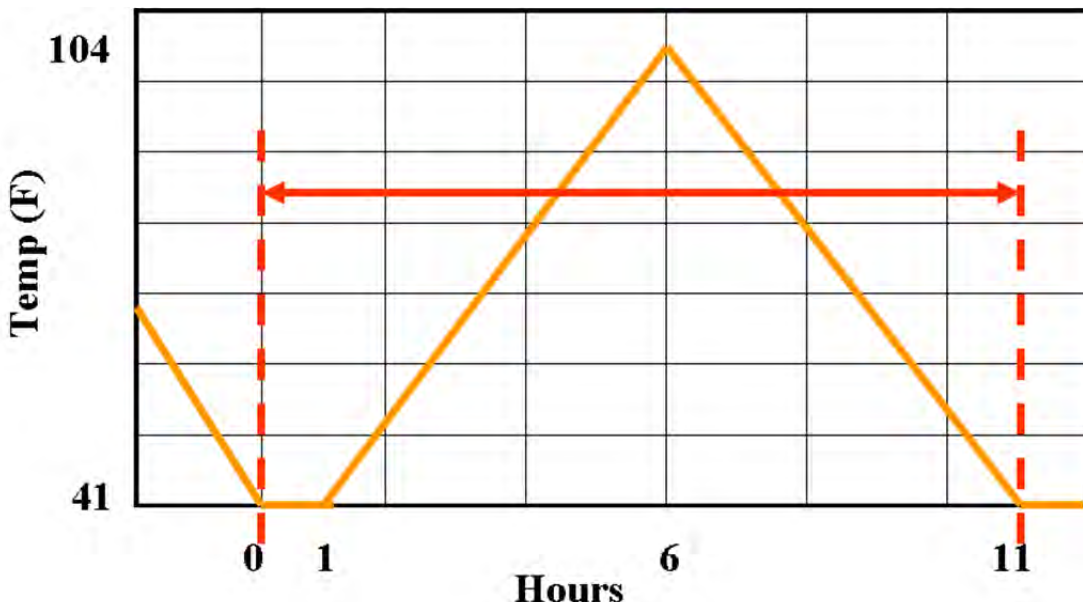


Figure 5.5: Temperature Cycle for mortars subjected to physical sulfate attack

5.2 Results and Discussion

This section summarizes the results of laboratory and outdoor testing related to external sulfate attack. It is divided into four sub-sections with each of the first three providing results from each type of sulfate condition, and the fourth section comparing mixtures from all three sulfate conditions. Calcium sulfate is discussed in the first section followed by sodium sulfate and then magnesium sulfate. Within each section the following are discussed for mixtures up to 18 months: effects of cement composition, w/cm, supplementary cementing materials, and the comparison of concrete prisms to mortar bars. At the end of each section, describes the long-term conditions of these mixtures at 45 months. Semi-quantitative Rietveld analyses were used to understand the mechanisms occurring in the specimens. Figure 5.6 provides the mixture designation for the mixtures discussed in this chapter. For example, the designation in Figure 5.6 is for a mixture with Type I/II cement, 20% Class C fly ash at a w/cm of 0.4. If this mixture did not contain SCMs, the designation would be C2-4.

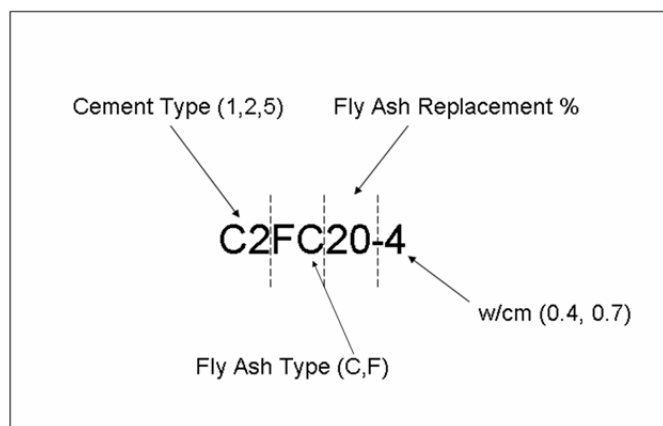


Figure 5.6: Mixture designations used throughout this chapter

5.2.2 Calcium Sulfate

Cement Composition and w/cm

Expansions and Mass Change up to 18 months

Mixtures containing Type I cement (without SCMs) were the only ones to show any expansion in calcium sulfate conditions. These were not significant expansions greater than 0.1%. Table 5.1 provides the expansion and mass change for these mixtures. Mixtures C1-4 and C1-7 exhibited expansions of 0.05% and 0.09% at 18 months, respectively, in the modified ASTM C 1012 indoor testing. However, these mixtures exhibited very little mass loss compared to the submerged and vertically placed prisms in the outdoor calcium sulfate exposure site. Interestingly, these prisms that exhibited mass loss outdoors did not show any appreciable expansion at 18 months. In a visual inspection of the prisms at 18 months, the indoor prisms showed minor cracking along the sides. The prisms placed in the outdoor exposure site showed deterioration below the soil level which leads to the mass loss.

Table 5.1: Expansion and Mass Change Data from Mixtures Placed in Calcium Sulfate Conditions

Mix ID	Age (Months)	Calcium Sulfate 1012		Calcium Submerged		Calcium Vertical	
		Expansion (%)	Mass Change (%)	Expansion (%)	Mass Change (%)	Expansion (%)	Mass Change (%)
C1.4	3	-0.01	0.48	0.01	0.39	-0.01	0.07
C1.4	6	0.01	0.54	0.01	-0.19	0.00	-0.01
C1.4	9	0.02	0.71	0.01	-0.35	-0.01	-0.05
C1.4	12	0.02	0.63	0.02	-0.59	0.00	-0.28
C1.4	18	0.05	0.43	0.02	-1.44	0.01	-0.28
C1.7	3	0.00	0.27	0.00	0.03	0.00	-0.12
C1.7	6	0.01	0.32	0.00	-1.15	0.00	-0.33
C1.7	9	0.02	0.37	0.01	-1.70	0.01	-0.64
C1.7	12	0.05	0.29	0.02	-1.83	0.01	-0.64
C1.7	18	0.09	0.40	0.03	-3.72	0.00	-0.68
C2.4	3	0.01	0.18	-0.02	0.40	-0.01	-0.09
C2.4	6	-0.01	0.26	0.00	0.42	0.01	-0.02
C2.4	9	0.00	0.25	0.01	0.18	0.02	-0.02
C2.4	12	0.00	0.25	0.00	0.15	0.00	0.01
C2.4	18	-0.01	0.23	-0.02	0.17	0.00	0.07
C2.7	3	0.00	0.22	0.00	-0.06	-0.01	-0.09
C2.7	6	-0.01	0.27	0.00	-0.42	-0.01	-0.15
C2.7	9	0.00	0.31	0.01	-0.56	0.00	-0.25
C2.7	12	0.01	0.39	-0.01	-0.73	-0.01	-0.28
C2.7	18	0.00	0.35	0.01	-1.85	-0.01	-0.84
C5.4	3	0.01	0.36	-0.01	0.26	0.00	-0.07
C5.4	6	0.01	0.40	-0.01	0.30	0.00	0.06
C5.4	9	0.01	0.39	0.00	0.26	0.00	0.07
C5.4	12	0.02	0.36	0.00	0.27	-0.01	-0.12
C5.4	18	0.02	0.30	0.01	0.27	0.00	0.05
C5.7	3	0.01	0.40	0.01	0.01	0.01	0.05
C5.7	6	0.01	0.39	0.01	0.01	0.01	0.11
C5.7	9	0.01	0.65	0.02	0.01	0.01	0.13
C5.7	12	0.01	0.28	0.01	0.01	0.01	0.12
C5.7	18	0.02	0.37	0.02	0.02	0.02	0.15

Figure 5.7 shows a vertical prism from mixture C1-4. This vertically placed prism exhibiting deterioration occurring below the soil level. The deterioration that is occurring on these prisms is significant. Many debates do occur if whether gypsum causes damage to concrete structures. There is not an increase in expansion which many might not consider as damage, but if the concrete is deteriorating on the outside this is considered as damage. The low solubility of gypsum is probably preventing the sulfates from entering at a higher rate as seen with sodium and magnesium sulfates. Prisms containing Type I/II and Type V cements did not expand at either 0.4 or 0.7 w/cm in any calcium sulfate condition. From mixtures containing Type I/II cement, only prisms cast from mixture C2-7 showed any appreciable mass loss.



Figure 5.7: Concrete prism with a 0.4 w/cm placed vertically in the outdoor calcium sulfate exposure site. In this photograph, the left side shows the portion of the prism that was below the soil level.

Sulfate Profiling

Figure 5.8 depicts the semi-quantitative x-ray Rietveld analyses from the milling of concrete prisms at 0.4 w/cm in indoor modified ASTM C 1012 testing after 18 months of storage. Semi-quantitative analyses are compared separately between w/cm ratios as the cement content in the mixture can change the amount of hydration products formed. This could lead to different amounts of ettringite/gypsum formed and a dissimilar amount of calcium hydroxide depleted. In the outer 3 mm of the prism, ettringite formation was similar between each of the cement types. It is not uncommon to see this ettringite formation with Type V cement, Mehta (1993) mentions that sulfate resistant cements do not stop sulfate attack since calcium hydroxide can still be attacked. Further into the prisms, ettringite formation decreased. The gypsum content in the outer layer showed an increase from Type I to Type V cements. Calcium hydroxide (portlandite) was not attacked (no observed depletion) in the C1-4 mixture; however, it is lowered in the C2-4 and C5-4 mixtures which could entail how the ettringite formed in these two mixtures.

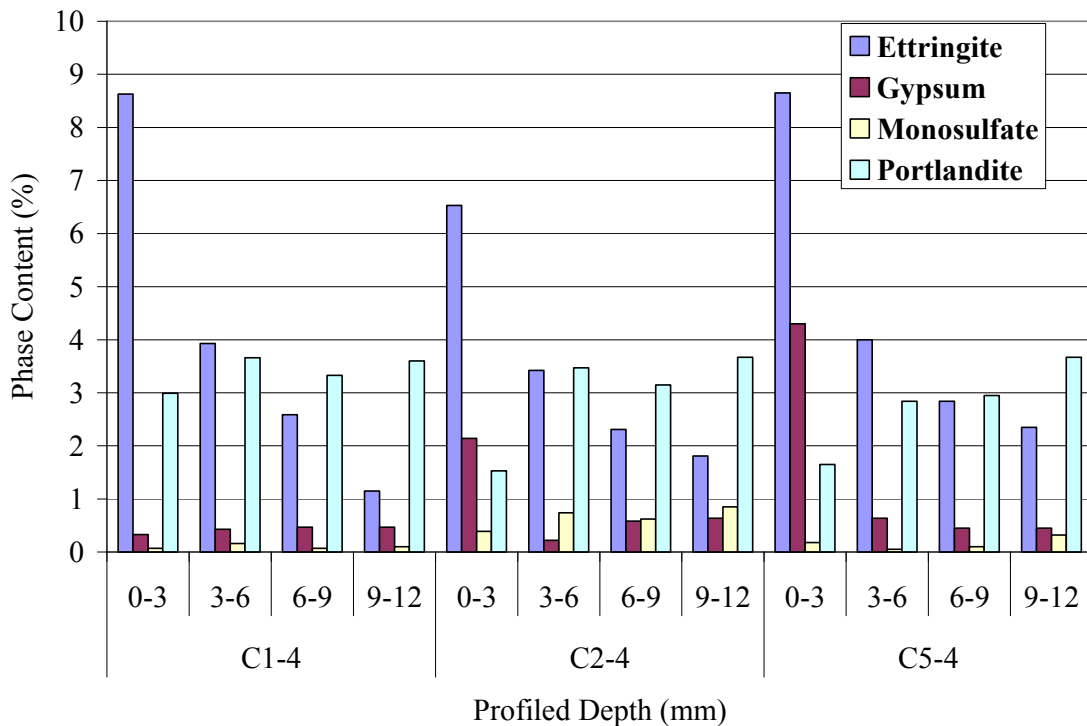


Figure 5.8: Semi-quantitative Rietveld analysis showing differences in cement types for prisms at 0.4w/cm, placed indoors in calcium sulfate

Figure 5.9 depicts the quantitative x-ray analyses from the milling of concrete prisms at 0.7 w/cm in the modified ASTM C 1012 testing after 18 months of storage. Similar to the 0.4 w/cm prisms, ettringite formation occurred with these mixtures as well; however, these lower quality mixtures allowed for further penetration of solution into the concrete, allowing for ettringite to form further into the concrete. In addition, greater gypsum formation was shown in the outer layer of the concrete. Unlike the lower w/cm mixtures, the calcium hydroxide was more depleted in the outer regions in all the mixtures.

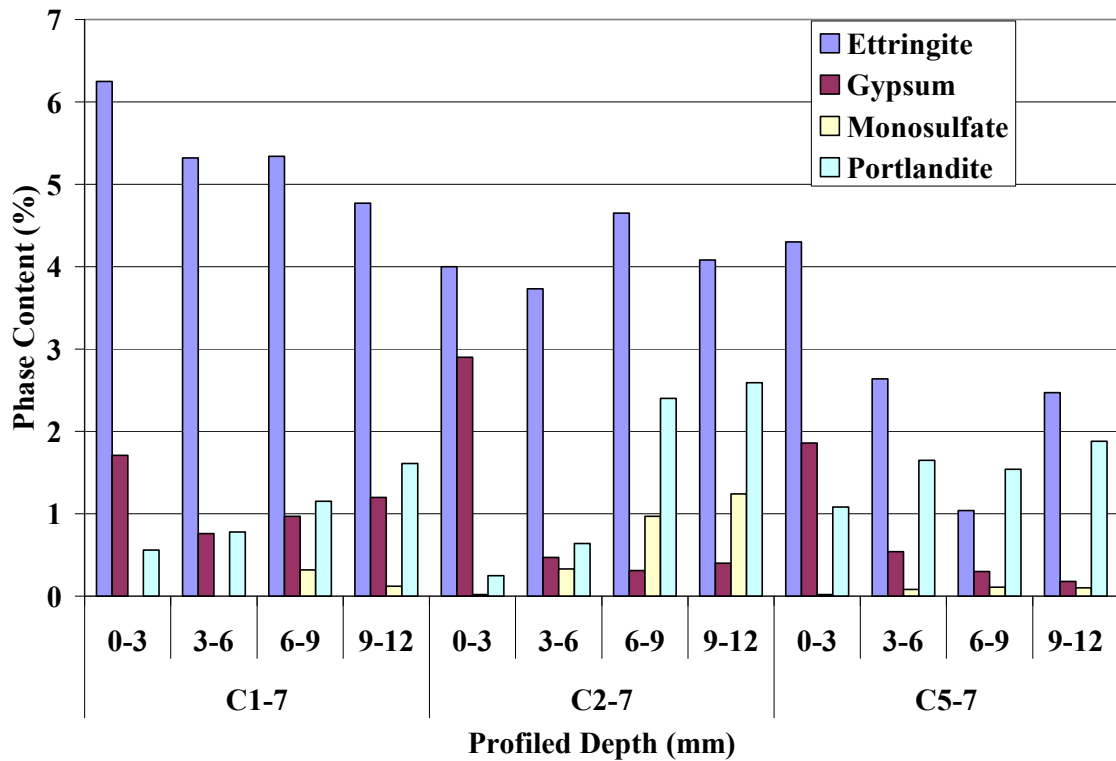


Figure 5.9: Quantitative Analysis showing differences in cement types for prisms at 0.7 w/cm placed indoors in calcium sulfate

5.2.3 Supplementary Cementing Materials

Expansions and Mass Change

Concrete mixtures containing either Class C or Class F fly ash did not increase in expansion in any of the calcium sulfate conditions. Table 5.2 shows the expansion and mass change data from mixtures containing Type I and Type I/II cement with Class C fly ashes.

Table 5.2: Expansion and Mass Change Data from Mixtures with Class C fly ash Placed in Calcium Sulfate Conditions

Mix ID	Age (Months)	Calcium Sulfate 1012		Calcium Submerged		Calcium Vertical	
		Expansion (%)	Mass Change (%)	Expansion (%)	Mass Change (%)	Expansion (%)	Mass Change (%)
C1FC20-4	3	0.00	0.00	-0.01	0.19	0.00	0.04
C1FC20-4	6	0.00	0.00	0.00	0.26	0.01	0.11
C1FC20-4	9	0.00	0.00	0.00	0.27	0.02	0.12
C1FC20-4	12	0.00	0.00	0.02	0.27	0.01	0.01
C1FC20-4	18	0.00	0.00	0.03	0.19	0.04	0.10
C1FC20-7	3	0.00	0.29	-0.01	0.19	0.00	0.04
C1FC20-7	6	0.01	0.36	0.00	0.26	0.01	0.11
C1FC20-7	9	0.03	0.44	0.01	0.27	0.02	0.12
C1FC20-7	12	0.03	0.52	0.02	0.27	0.01	0.01
C1FC20-7	18	0.07	0.60	0.03	0.18	0.04	0.11
C1FC40-4	3	0.02	0.05	0.01	0.12	0.01	0.12
C1FC40-4	6	0.03	0.28	0.01	0.05	-0.01	0.03
C1FC40-4	9	0.03	0.11	0.01	0.03	0.01	0.05
C1FC40-4	12	0.04	-0.05	0.03	-0.05	0.01	-0.17
C1FC40-4	18	0.08	0.19	0.05	-0.22	0.03	-0.19
C1FC40-7	3	0.03	0.23	0.00	0.04	0.00	-0.07
C1FC40-7	6	0.03	0.21	-0.01	0.12	0.00	0.00
C1FC40-7	9	0.05	0.37	-0.06	0.12	-0.02	-0.07
C1FC40-7	12	0.03	0.32	-0.04	0.08	0.00	-0.19
C1FC40-7	18	0.05	0.37	-0.04	0.05	0.01	-0.22
C2FC20-4	3	0.01	0.17	0.00	0.20	0.00	0.01
C2FC20-4	6	0.01	0.17	0.01	0.22	0.00	-0.03
C2FC20-4	9	0.01	0.35	0.01	0.30	-0.01	-0.04
C2FC20-4	12	0.00	0.27	0.02	0.30	0.01	0.03
C2FC20-4	18	0.01	0.27	0.01	0.26	0.00	0.07
C2FC20-7	3	0.03	0.42	0.00	-0.40	0.00	-0.07
C2FC20-7	6	0.03	0.37	0.01	-0.64	0.01	-0.20
C2FC20-7	9	0.02	0.50	0.02	-1.00	0.01	-0.34
C2FC20-7	12	0.04	0.13	0.03	-2.00	0.02	-0.26
C2FC20-7	18	0.02	-0.51	0.04	-3.10	-0.01	-0.33
C2FC40-4	3	0.04	0.20	0.00	-0.04	-0.01	0.07
C2FC40-4	6	0.04	0.31	0.00	0.03	-0.01	0.10
C2FC40-4	9	0.03	0.34	0.00	0.09	-0.02	-0.11
C2FC40-4	12	0.06	0.44	0.00	0.02	-0.02	0.05
C2FC40-4	18	0.07	0.48	-0.03	0.04	-0.04	0.06
C2FC40-7	3	0.01	0.29	0.01	0.05	0.01	0.00
C2FC40-7	6	0.01	0.33	0.00	0.19	0.00	0.06
C2FC40-7	9	0.01	0.44	0.01	0.22	0.01	-0.13
C2FC40-7	12	0.03	0.73	0.00	0.15	0.00	0.01
C2FC40-7	18	0.03	0.76	0.00	0.12	0.00	0.02

In many cases, including mixtures with Class C fly ash, the expansions were less than the controls shown in section 5.2.1. However, after 18 months of exposure the prisms did show signs of deteriorations similar to Figure 5.7. Mixtures with Type V cement and Class C fly ashes, and mixtures with all three cements with ternary blends and Class F fly ash are shown in Appendix C in Drimalas 2007.

Sulfate Profiling

Figure 5.10 provides quantitative XRD Rietveld analyses on prisms with Class C fly ash at 0.4 w/cm placed indoors in calcium sulfate. Similar to mixtures without SCMs, ettringite formation was the greatest in the outer layer and decreased with increasing depth into the concrete. The difference in calcium hydroxide content between mixtures containing 20 and 40% Class C fly is likely due to the diluting effect of replacing additional portland cement with fly ash and perhaps due to increased pozzolanic activity with increasing fly ash dosage.

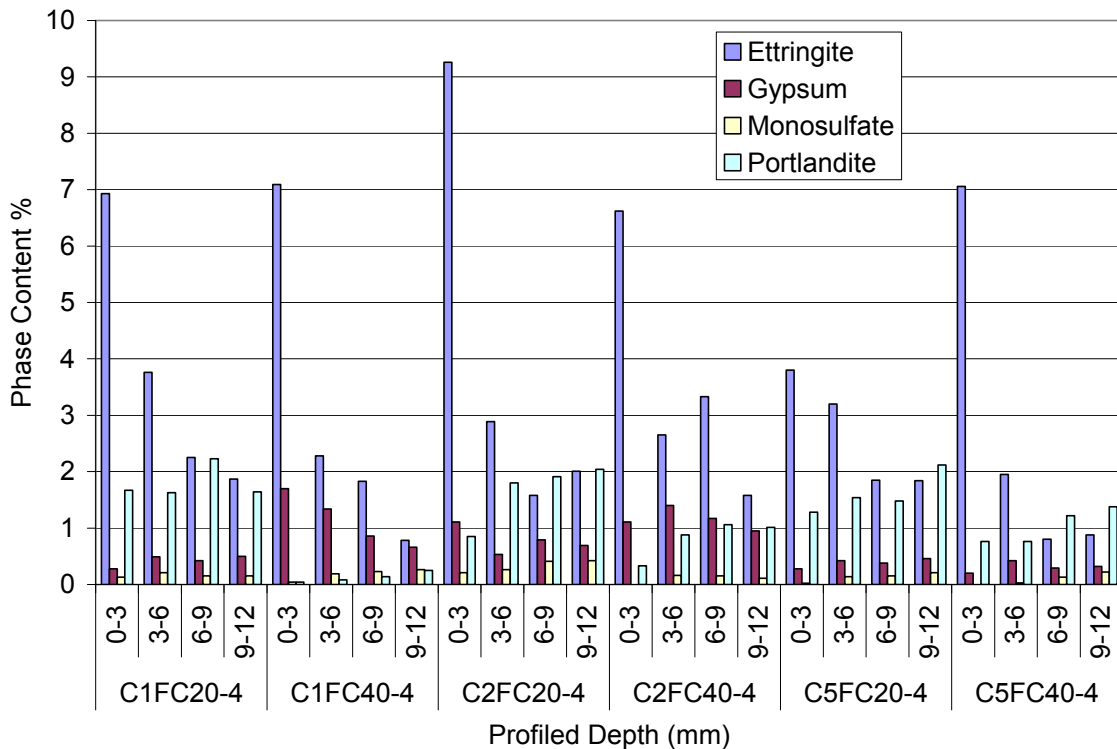


Figure 5.10: Semi-quantitative XRD analysis of profiled prisms containing Class C fly ash at a 0.4 w/cm to determine phase content at different milled depths

Figure 5.11 shows the semi-quantitative XRD analysis of prisms at 0.7 w/cm in the modified ASTM C 1012 calcium sulfate solutions. The progression of attack into concrete containing SCMs does not penetrate as deep as the control mixtures at the same w/cm. C5FC40-7 had less ettringite formation than C5FC20-7, which suggests that decreased permeability may reduce penetration of sulfates in prisms containing fly ash.

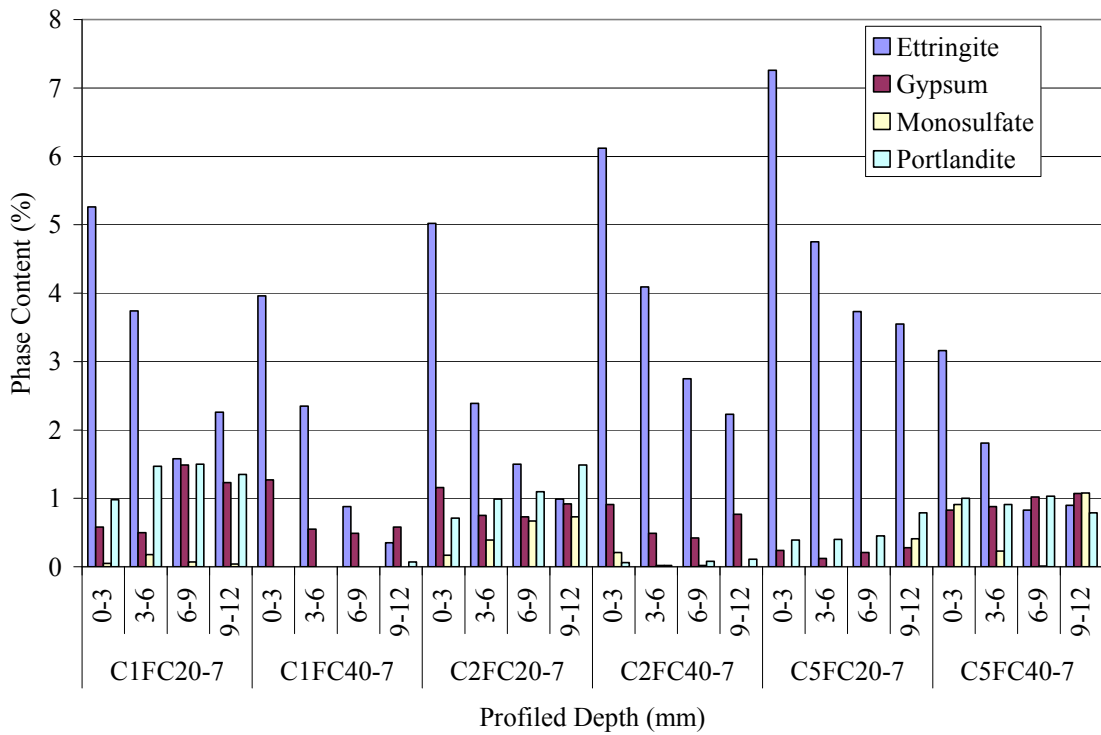


Figure 5.11: Quantitative XRD analysis of profiled prisms containing Class C fly ash at a 0.7 w/cm to determine phase content at different milled depths

Mortar and Concrete comparisons

Modified ASTM C 1012 testing of mortars containing Type I/II and Type V cements and immersed in calcium sulfate solution was performed to compare with concrete prisms subjected to the same testing regime. Table 5.3 summarizes the expansions of these mixtures, as well as similar mixtures containing Class C fly ash. Mixtures that are bolded have failed the commonly applied 0.1% expansion criteria. Both control mixtures had similar expansion values at 18 months. The Type I/II control mixture (C2) had an expansion of 0.07% and the Type V control mixture (C5) had an expansion of 0.06% at 18 months. These mortar mixtures expanded more than concrete prisms containing the same blend of cementitious materials and at approximately the same w/cm ratio (as previously detailed in Table 5.2). This increase in expansion may be due to the higher paste content of the mortar mixtures or may also be size-related, as the concrete prisms have large cross sections, making it more difficult for gypsum to reach the interior core of the specimens. Mortars containing 20% Class C fly ash showed very little expansion, but mortars containing 40% Class C fly ash expanded beyond 0.1% within 6 months in calcium sulfate condition. Similar concrete mixtures did not expand at either 0.4 or 0.7 w/cm at 18 months. The reasons for this difference in behavior may be similar to those discussed above (e.g., paste content, specimen size, etc.). It is interesting to note that mortar containing these “sulfate resistant” cements still expanded when higher dosages of Class C fly were used, highlighting the key role that fly ash mineralogy plays in expansion and distress in sulfate environments.

Table 5.3: Comparison between mortar bars and concrete prisms evaluated using calcium sulfate solution in ASTM C 1012 storage conditions

Age (Months)	Mixture	Concrete* Expansion (%)	Mortar** Expansion (%)	Mixture	Concrete* Expansion (%)	Mortar** Expansion (%)
3	Type I/II Cement	0.01	0.02	Type V Cement	0.01	0.02
6		-0.01	0.02		0.01	0.03
9		0.00	0.04		0.02	0.03
12		0.00	0.05		0.02	0.04
18		-0.01	0.07		0.02	0.06
3		0.01	0.02		0.04	0.02
6	Type I/II Cement 20% FA1	0.01	0.03	Type V Cement 20% FA1	0.03	0.03
9		0.01	0.04		0.06	0.04
12		0.00	0.06		0.07	0.04
18		0.01	0.09		0.05	0.04
3		0.04	0.02		0.03	0.03
6	Type I/II Cement 40% FA1	0.04	0.06	Type V Cement 40% FA1	0.02	0.1
9		0.03	0.14		0.07	0.21
12		0.06	0.24		0.06	0.29
18		0.07	0.36		0.06	0.48

* w/cm = 0.40

** w/cm = 0.43 – 0.48 (based on meeting target flow value)

Expansions and mass loss at 45 months

Expansion and mass change at 45 months of the 30 mixtures cast are presented in Table 5.4. Expansion values in bold indicate an expansion of over 0.1% length change, the limit established in the Phase I report.

It is important to note that excessive expansion had occurred in four of the mixtures exposed to calcium sulfate. Mixtures containing only portland cement as the binder at 0.4 and 0.7 w/cm suffered severe damage. Figures 5.12 and 5.13 show these prisms, samples to the left of the labeling card are the upright prisms; samples to the right were stored below the soil line. Also, two mixtures containing Type II cement showed severe distress, a 0.7 w/cm control and 0.7w/cm with 20% Class C fly ash. Damage in the latter two mixtures could be attributed to the higher permeability associated with high w/cm. Following the trend seen in Phase I, mixtures with 20% Class C fly ash performed worse than mixtures with 40% Class C fly ash. This could be due to a slight reduction in permeability from the use of SCMs. It should also be noted that damage did not extend above the soil line on the upright samples, a trend that is not true for sodium and magnesium sulfate. This fact may present challenges when evaluating field structures, as excavation may become necessary to reach a level with adequate moisture to cause damage to the structure.

The use of a low w/cm and moderate sulfate resistant cement does show significant protection after 45 months. Figure 5.14 shows the resistance of a Type I/II cement binder at a 0.4 w/cm in the 33,000ppm calcium sulfate site. Damage has not occurred on these specimens after 45 months in this aggressive environment.

Table 5.4: Expansion and Mass Change for Phase I Prisms Exposed to a 5% Calcium Sulfate Solution in Outdoor Exposure Site

Mix Description			Age Months	Calicium Sulfate				
				Up Exp %	Mass %	Submerged Exp %	Mass %	
1	0.4	Type I	-	45	0.11	-3.7	0.17	-12.7
2	0.7	Type I	-	45	x	-25.8	x	-15.7
3	0.4	Type I	20% C	45	0.01	-0.1	0.03	0.3
4	0.7	Type I	20% C	45	0.05	0.0	0.07	-0.1
5	0.4	Type I	40% C	45	0.00	-0.3	0.05	0.2
6	0.7	Type I	40% C	45	0.00	-0.2	-0.05	0.1
7	0.4	Type V	-	45	-0.01	-0.3	0.03	0.0
8	0.7	Type V	-	45	0.02	0.1	0.02	0.3
9	0.4	Type V	20% C	45	0.00	0.2	0.03	0.6
10	0.7	Type V	20% C	45	0.03	0.0	0.06	-0.1
11	0.4	Type V	40% C	44	0.01	0.0	0.01	0.2
12	0.7	Type V	40% C	44	-0.01	0.0	-0.01	0.2
13	0.4	Type I/II	-	44	0.02	-0.2	0.04	0.1
14	0.7	Type I/II	-	44	-0.13	-1.7	x	-12.0
15	0.4	Type I/II	20% C	44	0.01	-0.1	0.03	0.3
16	0.7	Type I/II	20% C	43	0.02	-0.7	0.24	-3.7
17	0.4	Type I/II	40% C	43	-0.02	-0.1	0.01	-0.1
18	0.7	Type I/II	40% C	43	0.00	-0.2	0.01	0.0
19	0.4	Type I/II	20% F	42	-0.01	-0.1	0.02	0.3
20	0.7	Type I/II	20% F	42	-0.01	-0.3	0.03	-0.2
21	0.4	Type I/II	30%C 3SF	42	0.01	-0.2	0.03	0.1
22	0.7	Type I/II	30%C 3SF	42	0.02	-0.2	0.01	0.1
23	0.4	Type I	20% F	41	-0.02	-0.2	0.02	0.2
24	0.7	Type I	20% F	41	-0.01	-0.1	-0.02	-0.1
25	0.4	Type I	30%C 3SF	40	0.00	-0.2	0.00	0.0
26	0.7	Type I	30%C 3SF	40	-0.01	-0.3	-0.02	0.1
27	0.4	Type V	20% F	39	0.00	-0.2	0.01	0.2
28	0.7	Type V	20% F	39	0.01	-0.2	0.02	0.2
29	0.4	Type V	30%C 3SF	38	-0.02	-0.1	-0.01	0.1
30	0.7	Type V	30%C 3SF	38	-0.07	0.0	-0.08	0.0



Figure 5.12: Concrete Prisms Exposed to 33000 ppm Calcium Sulfate, Type I Cement at 0.4 w/cm



Figure 5.13: Concrete Prisms Exposed to 33000 ppm Calcium Sulfate, Type I Cement at 0.7 w/cm



Figure 5.14: Concrete Prisms Exposed to 33000 ppm Calcium Sulfate, Type I/II Cement at 0.4 w/cm

5.2.4 Sodium Sulfate

Cement Composition and w/cm

Expansion and Mass Change

The concrete prisms in sodium sulfate conditions did not perform as well as their counterparts in calcium sulfate. Expansion measurements were taken for 18 months or until they were not measurable due to deterioration. Table 5.5 gives the expansion and mass change data for prisms placed into either the outdoor sodium sulfate exposure site or placed in modified ASTM C 1012 storage conditions containing sodium sulfate solutions in the laboratory. Mixtures containing Type I cement performed worse than mixtures containing Type I/II cement. Mixtures containing Type V cement did not show any significant expansions in any sodium sulfate storage condition. Mixture C1-4 performed well for 12 months, but expanded to 1.08% at 18 months in indoor testing. In outdoor testing, the same mixture failed at 9 months in the submerged conditions and failed at 12 months in the vertical condition. The outdoor prisms stored in sodium sulfate are also affected by physical sulfate attack, explaining why deterioration was more rapid and severe.

Table 5.5: Expansion and Mass Change Data for Mixtures without SCMs, exposed to Sodium Sulfate Solution

Mix	Age (months)	Sodium Sulfate 1012		Sodium Submerged		Sodium Vertical	
		Expansion (%)	Mass Change (%)	Expansion (%)	Mass Change (%)	Expansion (%)	Mass Change (%)
C1-4	3	0.00	0.21	0.02	0.02	0.02	-0.06
C1-4	6	0.03	0.48	0.03	0.02	0.02	-0.18
C1-4	9	0.04	0.79	0.10	0.05	0.05	-1.38
C1-4	12	0.07	1.10	0.43	0.43	0.43	-2.21
C1-4	18	1.08	-3.67	Broken	Broken	Broken	Broken
C1-7	3	0.02	0.32	0.06	0.24	0.07	-0.37
C1-7	6	0.10	0.53	0.52	0.71	0.23	-0.46
C1-7	9	0.20	0.72	1.20	1.21	0.54	-0.52
C1-7	12	0.28	0.86	1.40	1.44	0.69	-0.67
C1-7	18	0.36	1.05	1.82	0.65	1.13	-1.08
C2-4	3	0.00	-0.09	0.00	-0.09	0.01	-0.12
C2-4	6	0.01	-0.06	0.01	0.21	0.01	0.05
C2-4	9	0.01	0.00	0.01	0.29	0.01	0.04
C2-4	12	0.01	0.12	0.03	0.35	0.01	0.10
C2-4	18	0.01	0.21	0.11	0.12	0.04	0.04
C2-7	3	-0.02	0.20	0.01	0.17	-0.01	-0.15
C2-7	6	0.02	0.23	0.02	0.17	0.01	-0.14
C2-7	9	0.03	0.27	0.05	0.36	0.03	-0.20
C2-7	12	0.07	0.43	0.08	0.38	0.06	-0.20
C2-7	18	0.11	0.46	0.21	0.55	0.12	-0.14
C5-4	3	0.00	0.00	0.00	0.04	0.00	-0.17
C5-4	6	0.01	-0.01	0.01	0.12	0.01	-0.07
C5-4	9	0.03	-0.02	0.01	0.20	0.01	-0.15
C5-4	12	0.02	0.03	0.00	0.29	0.00	-0.07
C5-4	18	0.03	0.05	0.01	0.35	0.01	-0.04
C5-7	3	0.00	0.23	0.02	0.31	0.01	-0.17
C5-7	6	0.02	0.24	0.03	0.40	0.01	-0.17
C5-7	9	0.02	0.23	0.04	0.46	0.00	-0.30
C5-7	12	0.02	0.27	0.04	0.56	0.00	-0.25
C5-7	18	0.03	0.32	0.06	0.57	0.04	-0.13

In the outdoor sulfate exposure site, mixture C1-7 expanded more than 0.1% after 6 months and more than 1% after 18 months. Despite this excessive expansion, the prisms were still intact and measurable after 18 months. Mixture C1-4 exceeded the 0.1% expansion threshold at 9 months (submerged) and 12 months (vertical) and the prisms were completely deteriorated and immeasurable at 18 months. Interestingly, the higher w/cm prisms tended to gain mass and show expansion, yet would not deteriorate to the level of mixtures at 0.4 w/cm. It is possible that the higher w/cm mixtures were able to accommodate expansive products, such as ettringite, more within the more porous matrix, resulting in a mass gain as more sulfate solution enters the system. Figure 5.15 shows an image of a submerged prism from mixture C1-7 in the outdoor sulfate site after 18 months of exposure. While the bar appears to be in good condition, it has expanded by 1.8%. However, at this time it is unclear as to why this increase in mass and significant expansion does not result in cracking or deterioration as seen in the lower w/cm concretes. A possible conclusion is the porosity allows for ettringite formation to form within these areas.

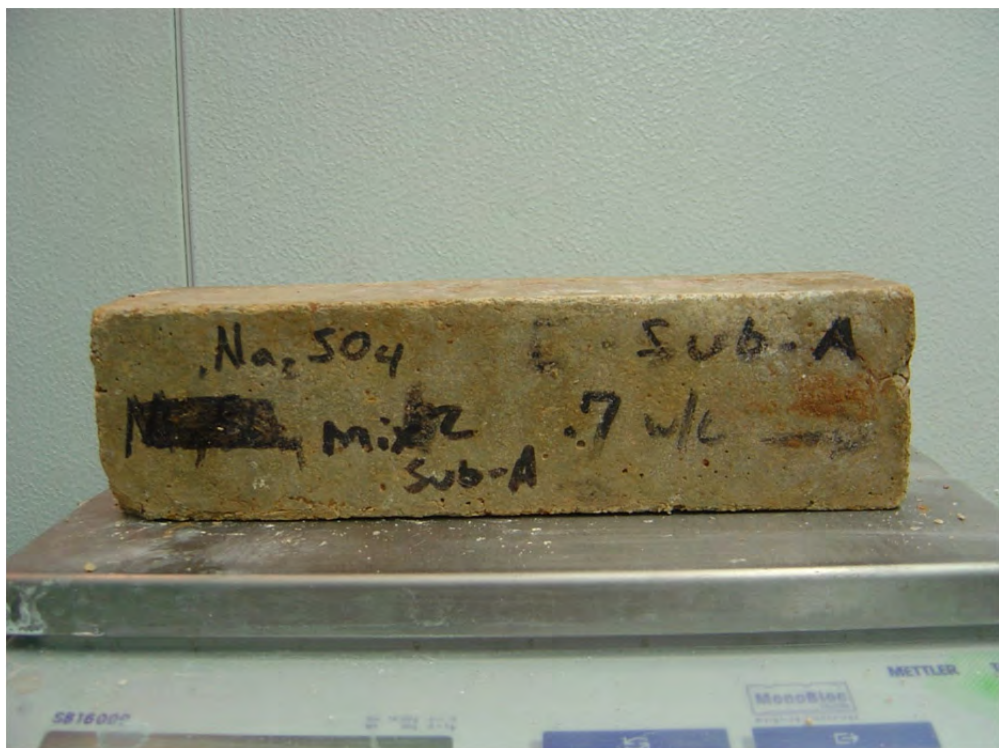


Figure 5.15: C1-7 Prism submerged in the outdoor sodium sulfate exposure site after 18 months

Mixture C2-7 failed the 0.1% expansion criteria at 18 months in all exposure conditions, while the lower w/cm mixture, C2-4, failed the 0.1% criteria at 18 months only in the submerged specimens stored outdoors. There are no significant mass changes associated with any of these prisms. However, vertically placed prisms containing Type I/II or Type V cements did show signs of deterioration occurring in the section exposed to the atmosphere (no-contact with soil zone). Figure 5.16 shows a prism from mixture C5-7 placed vertically after 18 months of exposure in the sodium sulfate exposure site. The top of the prism (right part in the picture) does have visible paste loss. This may be attributed to physical sulfate attack and is discussed in more detail later in this chapter. Similar distress was found at the PCA (2002) exposure site in Sacramento, California which they contributed to physical sulfate attack.

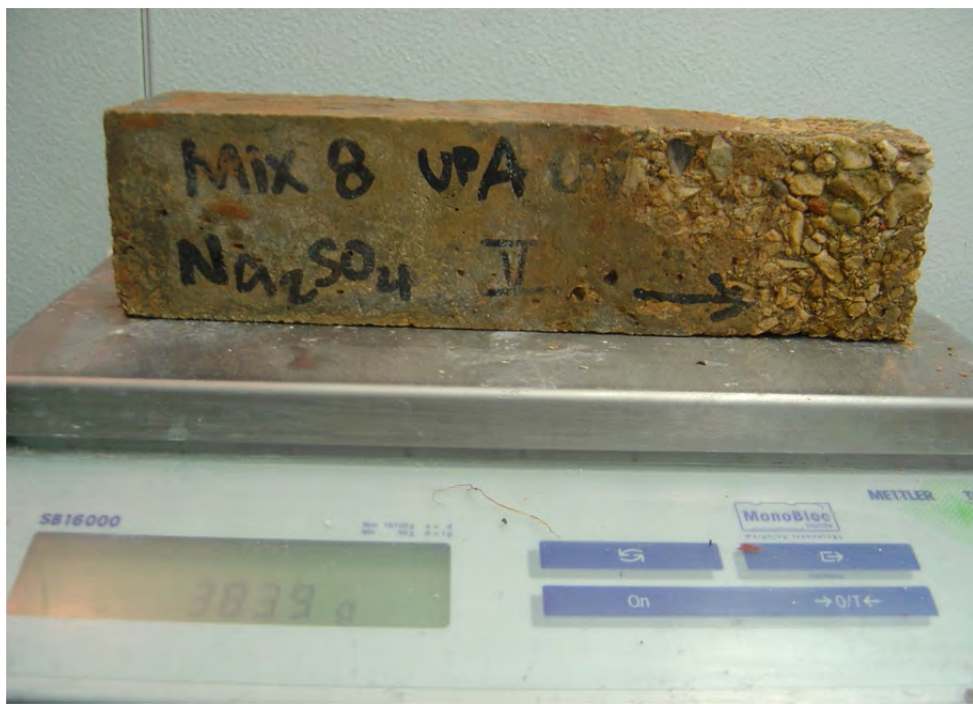


Figure 5.16: Mixture C5-7 after 18 months of outdoor exposure to sodium sulfate. This prism was placed vertically, with the section on the left fully submerged below sulfate-saturated soil.

Sulfate Profiling

Figure 5.17 shows the semi-quantitative XRD analyses of concrete prisms with various cement types subjected to modified ASTM C 1012 storage conditions after 18 months. Ettringite content is higher in the C1-4 prisms, compared to prisms comprised of the Type I/II and V cements. This is expected due to the higher C₃A content of the Type I cement (C1). Also, the additional ettringite formation from mixture C1-4 may be the consequence of the depletion of calcium hydroxide, leading to the formation of gypsum. This then combines with monosulphoaluminate to form ettringite. See equation 2.3. Mixtures with Type I/II and Type V cement show no signs of chemical alteration or deterioration.

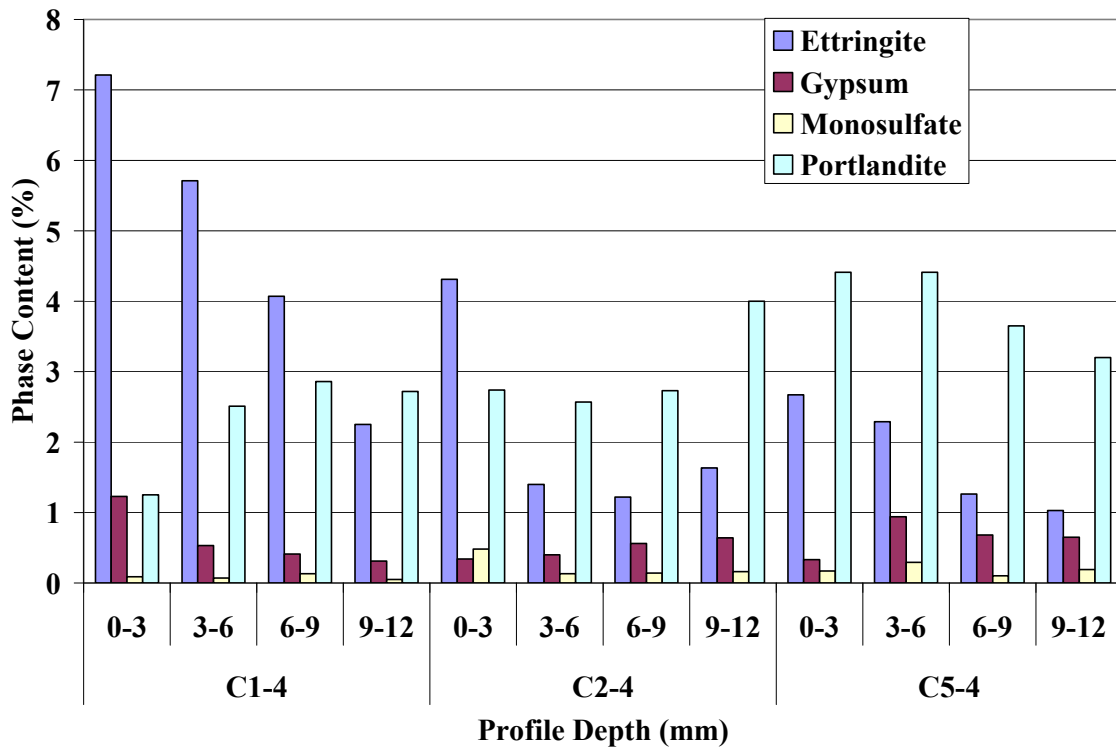


Figure 5.17: Quantitative XRD Rietveld analyses of concrete prisms at 0.4 w/cm, placed indoors in sodium sulfate solutions after 18 months

In Figure 5.18, the semi-quantitative XRD analyses for concrete prisms at a 0.7 w/cm subjected to modified ASTM C 1012 storage conditions are presented. Mixture C1-7 shows the most ettringite formation in the outer layer of the prism. A slight decrease in the amount of ettringite occurs as a function of distance into the prism. Gypsum formation is low in mixture C1-7 in all the layers compared to mixtures C2-7 and C5-7. Mixtures with Type I/II and Type V cement do not show a decreasing amount of ettringite formation, perhaps suggesting that the all reaction products that can lead to ettringite formation have been consumed.

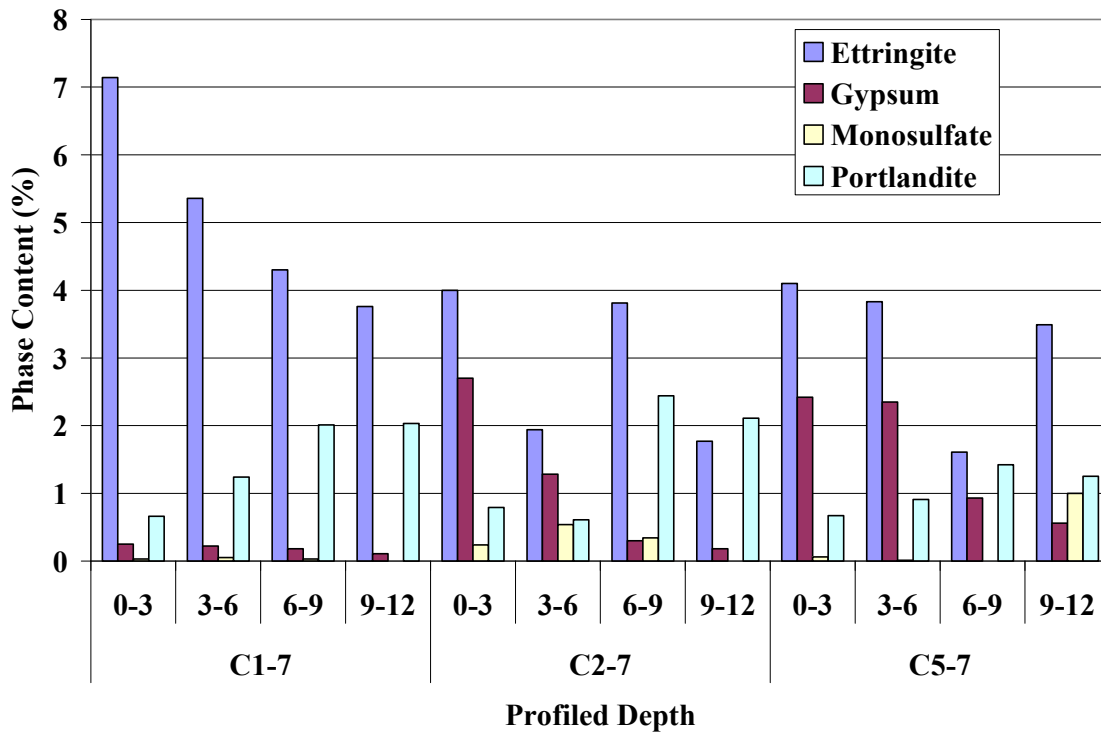


Figure 5.18: Semi-quantitative XRD Rietveld analysis of concrete prisms at 0.7 w/cm, placed indoors in sodium sulfate solutions after 18 months

Semi-quantitative XRD analyses were also performed on prisms in the outdoor sulfate exposure site. Figure 5.19 presents the semi-quantitative XRD analyses of Type V mixtures in the submerged and non-contact zones. In this figure, gypsum formation is greater in the submerged zones in both mixtures. The gypsum formation in the outdoor submerged conditions is greater than the prisms from the same mixture in the modified ASTM C 1012 testing. This may be attributed to the average higher temperature for the outdoor site, compared to the indoor testing environment. Higher temperatures tend to increase rates of ionic movement and accelerate chemical reactions. The portion of the beams in the “non-contact” zone show very little alterations or excessive amounts of gypsum; this may be attributed to the fact that gypsum shows very little propensity for wicking, in contrast to sodium sulfate, which tends to wick considerably in the vertical direction.

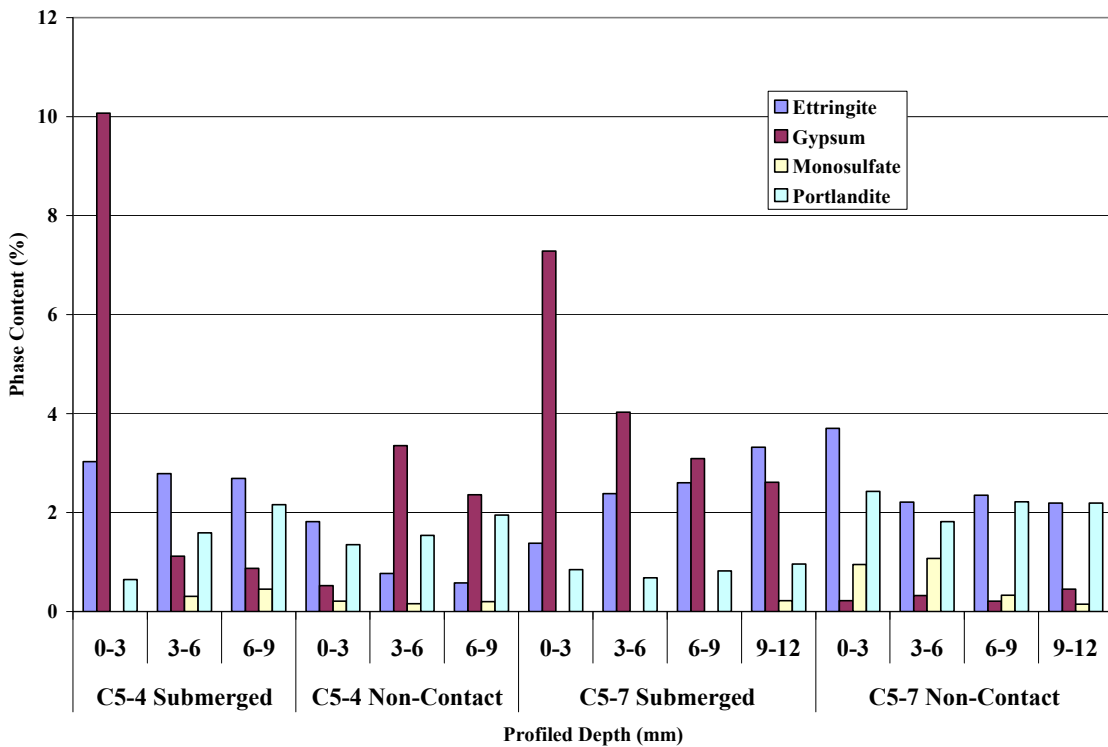


Figure 5.19: Semi-quantitative XRD analysis from mixtures containing sulfate resistant cement at in the outdoor sulfate exposure site

Supplementary Cementing Materials

Expansion and Mass Change

This section summarizes the measured expansions and mass changes for concrete mixtures containing SCMs (with a primary focus on Class C fly ash). The use of Class C fly ash will be discussed first followed by mixtures containing Class F fly ash. Table 5.6 shows the expansion and mass change data for mixtures containing Type I cement and Class C fly ash. Mixtures with higher w/cm (0.7) performed substantially worse than mixtures with lower w/cm ratio. For example, mixture C1FC20-7 failed the 0.1% expansion criteria at 3 months while mixture C1FC20-4 failed at 1 year for the submerged conditions and 18 months for the other two conditions. Mass loss was significant during the expansion of these prisms, with a mass loss of greater than 1% for prisms that expanded greater than 0.1%. The addition of Class C fly ash showed more deterioration (but not expansion) compared to the control specimens. An increasing replacement dosage of Class C fly ash was found to generally cause more deterioration in mortar bars tested using ASTM C 1012, as described in Chapter 4. However, for the concrete mixtures shown in Table 5.6, mixtures with 20% Class C fly ash (C1FC20-4 and C1FC20-7) performed worse than those containing 40% Class C fly ash (C1FC40-4 and C1FC40-7). One possible explanation is that higher fly ash contents tend to reduce permeability more than lower fly ash contents, and this effect may be even more important for larger, concrete specimens and for specimens exposed to temperature variations and wetting and drying cycles.

Table 5.6: Expansion and Mass Change Data for Concrete with Type I Cement and Class C fly ash, exposed to sodium sulfate solution

Mix	Age (months)	Sodium Sulfate 1012		Sodium Submerged		Sodium Vertical	
		Expansion (%)	Mass Change (%)	Expansion (%)	Mass Change (%)	Expansion (%)	Mass Change (%)
C1FC20-4	3	0.01	0.09	0.01	-0.08	0.01	-0.09
C1FC20-4	6	0.02	-0.02	0.02	-1.24	0.02	-0.32
C1FC20-4	9	0.02	-0.49	0.03	-3.18	0.02	-0.64
C1FC20-4	12	0.05	-1.58	0.23	-3.81	0.07	-1.34
C1FC20-4	18	Broken	Broken	Broken	Broken	Broken	Broken
C1FC20-7	3	0.25	-0.28	0.50	-5.31	0.40	-1.55
C1FC20-7	6	Broken	Broken	Broken	Broken	Broken	Broken
C1FC20-7	9	--	--	--	--	--	--
C1FC20-7	12	--	--	--	--	--	--
C1FC20-7	18	--	--	--	--	--	--
C1FC40-4	3	0.03	0.36	0.00	-0.17	0.00	-0.18
C1FC40-4	6	0.03	-0.53	0.00	-2.35	0.01	-0.93
C1FC40-4	9	0.08	-0.83	0.01	-3.88	0.02	-1.20
C1FC40-4	12	0.12	-1.30	0.03	-3.94	0.07	-1.58
C1FC40-4	18	0.48	-3.30	0.10	-4.43	0.12	-2.47
C1FC40-7	3	0.05	-1.45	0.01	-0.84	0.02	-1.26
C1FC40-7	6	0.18	-2.88	0.09	-7.58	0.11	-4.55
C1FC40-7	9	0.64	-4.08	Broken	-13.97	0.14	-6.23
C1FC40-7	12	Broken	Broken	--	Broken	Broken	Broken
C1FC40-7	18	--	--	--	--	--	--

Mixtures containing Type I/II cement with Class C fly ash are shown in Table 5.7, with expansion and mass change data collected during the 18 month exposure to sodium sulfate conditions. Similar to Type I cement, mixtures with Type I/II cement did not perform well at higher w/cm ratios, and mass loss was observed to occur along with expansion in the prisms. At the lower w/cm ratio of 0.4, mixtures containing Type I/II cement exhibited better sulfate resistance than similar mixtures containing Type I cement.

Table 5.7: Expansion and Mass Change Data for Concrete with Type I/II Cement and Class C fly ash, exposed to sodium sulfate solution

Mix	Age (months)	Sodium Sulfate 1012		Sodium Submerged		Sodium Vertical	
		Expansion (%)	Mass Change (%)	Expansion (%)	Mass Change (%)	Expansion (%)	Mass Change (%)
C2FC20-4	3	0.01	-0.01	0.00	0.13	-0.01	-0.04
C2FC20-4	6	0.01	0.01	0.01	0.22	0.00	-0.06
C2FC20-4	9	0.02	0.09	0.02	0.37	0.01	-0.01
C2FC20-4	12	0.00	-0.39	0.05	0.28	0.03	-0.02
C2FC20-4	18	0.04	-0.07	0.15	-0.49	0.06	-1.32
C2FC20-7	3	.05	0.28	0.01	-0.24	0.01	-0.25
C2FC20-7	6	Broken	Broken	Broken	-9.67	0.11	-2.03
C2FC20-7	9	--	--	--	Broken	Broken	-6.99
C2FC20-7	12	--	--	--	--	--	--
C2FC20-7	18	--	--	--	--	--	--
C2FC40-4	3	0.01	0.03	0.00	-0.20	0.00	-0.12
C2FC40-4	6	0.01	0.08	0.01	-0.96	0.00	-0.22
C2FC40-4	9	0.01	0.14	0.05	-1.54	0.01	-0.29
C2FC40-4	12	0.04	0.24	0.14	-1.57	0.03	-0.31
C2FC40-4	18	0.07	0.30	0.33	-3.01	0.03	-0.51
C2FC40-7	3	0.07	-1.44	0.05	-5.49	0.02	-2.66
C2FC40-7	6	0.24	-0.64	0.21	-31.35	Broken	-8.36
C2FC40-7	9	0.15	-14.28	Broken	Broken	--	Broken
C2FC40-7	12	0.20	-14.36	--	--	--	--
C2FC40-7	18	0.31	-14.56	--	--	--	--

Table 5.8 presents the expansion and mass loss data for the mixtures containing Type V cement with Class C fly ash. Expansion was only observed for mixtures containing 20% Class C

fly ash at the higher w/cm ratio of 0.7. After 6 months, prisms from mixture C5FC20-7 placed in the outdoor sulfate conditions expanded past 0.1%. At 9 months, the prisms from the same mixture exceeded this same expansion threshold when tested indoors using ASTM C 1012 storage conditions. Interestingly, all three cements tested with either 20 or 40% Class C fly ash showed greater deterioration at the lower replacement dosage. A mixture that uses Type V cement may not always be suitable if a Class C fly ash is used in the mixture. The addition of reactive phases from Class C fly ash into a mixture could allow for the formation of deleterious products.

Table 5.8: Expansion and Mass Change Data for Concrete with Type V Cement and Class C fly ash, exposed to sodium sulfate solution

Mix	Age (months)	Sodium Sulfate 1012		Sodium Submerged		Sodium Vertical	
		Expansion (%)	Mass Change (%)	Expansion (%)	Mass Change (%)	Expansion (%)	Mass Change (%)
C5FC20-4	3	0.00	0.11	0.01	0.28	0.01	0.01
C5FC20-4	6	0.02	0.12	0.02	0.37	0.02	0.06
C5FC20-4	9	0.03	0.14	0.03	0.47	0.02	0.03
C5FC20-4	12	0.03	0.19	0.02	0.48	0.02	0.02
C5FC20-4	18	0.02	0.23	0.03	0.54	0.01	0.04
C5FC20-7	3	0.01	0.08	0.05	-0.24	0.03	-0.12
C5FC20-7	6	0.05	0.15	0.23	-0.10	0.10	-0.31
C5FC20-7	9	0.15	0.33	0.49	-0.98	0.27	-1.06
C5FC20-7	12	0.24	0.50	0.67	-1.06	0.42	-1.26
C5FC20-7	18	0.42	0.68	Broken	Broken	0.45	-8.60
C5FC40-4	3	0.00	0.11	0.00	0.12	0.00	-0.08
C5FC40-4	6	0.00	0.19	0.00	0.21	0.00	-0.09
C5FC40-4	9	0.03	0.16	0.01	0.22	0.01	-0.11
C5FC40-4	12	0.03	0.25	-0.01	0.26	0.01	-0.06
C5FC40-4	18	0.05	0.31	0.06	0.28	-0.01	-0.03
C5FC40-7	3	0.00	-0.12	0.00	0.05	0.00	-0.16
C5FC40-7	6	0.02	-0.11	0.01	-0.51	0.00	-0.47
C5FC40-7	9	0.02	-0.03	0.03	-1.80	0.01	-1.04
C5FC40-7	12	0.03	0.06	0.04	-1.91	0.02	-1.21
C5FC40-7	18	0.04	0.12	0.04	-1.88	0.02	-1.29

Table 5.9 shows the expansion and mass change data for ternary blends containing 30% Class C fly ash and 3% silica fume. Ternary blend mixtures at 0.4 w/cm passed the 0.1% expansion criteria for all time periods, whereas mixtures C1FC30SF3-7 and C2FC30SF3-7 failed the expansion criteria at 6 months. These prisms exhibited mass loss but were still cohesive until the 18 month measurements.

Table 5.9: Expansion and Mass Change Data for Concrete with ternary SCM blends exposed to sodium sulfate solution

Mix	Age (months)	Sodium Sulfate 1012		Sodium Submerged		Sodium Vertical	
		Expansion (%)	Mass Change (%)	Expansion (%)	Mass Change (%)	Expansion (%)	Mass Change (%)
C1FC30S3-4	3	0.02	0.09	0.00	-0.08	0.00	-0.15
C1FC30S3-4	6	0.04	0.19	0.02	-0.18	0.02	-0.15
C1FC30S3-4	9	0.02	0.20	0.02	-0.42	0.02	-0.15
C1FC30S3-4	12	0.04	0.23	0.01	-0.86	0.00	-0.16
C1FC30S3-4	18	0.04	0.25	0.02	-0.82	0.00	-0.16
C1FC30S3-7	3	0.03	-0.53	0.05	-3.66	0.04	-1.37
C1FC30S3-7	6	0.09	-1.23	0.20	-4.76	0.27	-2.25
C1FC30S3-7	9	0.18	-2.83	0.42	-5.16	0.35	-3.08
C1FC30S3-7	12	0.28	-0.53	1.18	-6.75	Broken	-7.36
C1FC30S3-7	18	Broken	Broken	broken	broken	Broken	Broken
C2FC30S3-4	3	0.00	-0.02	0.02	-0.02	0.01	-0.07
C2FC30S3-4	6	0.01	0.01	0.03	-0.08	0.02	-0.14
C2FC30S3-4	9	0.02	-0.07	0.04	-0.03	0.02	-0.14
C2FC30S3-4	12	0.03	0.07	0.05	-0.04	0.03	-0.10
C2FC30S3-4	18	0.03	0.09	0.09	-0.30	0.05	-0.25
C2FC30S3-7	3	0.03	-0.02	0.07	-0.12	0.06	-1.20
C2FC30S3-7	6	0.17	-0.79	0.18	-3.62	0.14	-2.02
C2FC30S3-7	9	0.31	-1.28	0.34	-4.70	0.16	-0.24
C2FC30S3-7	12	0.56	-2.65	0.47	-5.21	0.18	-2.89
C2FC30S3-7	18	Broken	-4.65	0.78	-15.42	Broken	-3.96
C5FC30S3-4	3	0.00	0.10	0.00	-0.06	0.00	-0.10
C5FC30S3-4	6	0.01	0.13	0.00	-0.08	0.00	-0.06
C5FC30S3-4	9	0.00	0.19	0.00	-0.05	0.00	-0.05
C5FC30S3-4	12	0.00	0.19	-0.01	-0.07	-0.01	-0.06
C5FC30S3-4	18	0.01	0.20	-0.01	-0.01	-0.01	-0.04
C5FC30S3-7	3	0.01	0.05	0.00	0.16	0.00	-0.08
C5FC30S3-7	6	0.02	0.42	0.02	0.19	0.01	-0.13
C5FC30S3-7	9	0.02	0.21	0.03	0.20	0.01	-0.14
C5FC30S3-7	12	0.04	0.24	0.03	0.19	0.00	-0.17
C5FC30S3-7	18	0.07	0.45	0.04	0.18	0.01	0.12

Table 5.10 summarizes the expansion and mass change data for mixtures with Class F fly ash in the three sodium sulfate conditions. The use of 20% Class F fly ash suppressed expansion when used with Type V cement at all w/cm ratios and it suppressed expansion in low w/cm mixtures with Type I and Type I/II cement. Mixtures CIFF20-7 and C2FF20-7 expanded in all three sodium sulfate exposure conditions at 6 months. The mixtures that expanded also lost mass, but the form of deterioration was different. The prisms did not show the same disintegration form of attack as was noticed with the Class C fly ash. The pieces that broke off from the prisms were still solid and the loss of cohesion often observed with Class C fly ash was not observed.

Table 5.10: Expansion and Mass Change Data for Concrete with Various Cements (Type I, II, or V) in combination with Class F fly ash and exposed to sodium sulfate solution

Mix	Age (months)	Sodium Sulfate 1012		Sodium Submerged		Sodium Vertical	
		Expansion (%)	Mass Change (%)	Expansion (%)	Mass Change (%)	Expansion (%)	Mass Change (%)
C1FF20-4	3	0.01	0.06	0.01	0.06	0.00	-0.12
C1FF20-4	6	0.02	0.15	0.01	0.11	0.00	-0.10
C1FF20-4	9	0.03	0.21	0.02	0.16	0.00	-0.08
C1FF20-4	12	0.03	0.29	0.02	-0.57	-0.01	-0.55
C1FF20-4	18	0.06	0.16	0.02	-0.19	0.00	-0.34
C1FF20-7	3	0.03	0.26	0.03	0.01	0.03	-0.38
C1FF20-7	6	0.08	0.23	0.12	0.03	0.11	-0.82
C1FF20-7	9	0.39	-0.99	0.40	-0.10	0.34	-1.22
C1FF20-7	12	Broken	Broken	Broken	-0.94	Broken	-1.74
C1FF20-7	18	Broken	Broken	Broken	Broken	Broken	-13.57
C2FF20-4	3	0.00	0.00	0.00	-0.01	0.00	-0.08
C2FF20-4	6	0.00	0.00	0.00	0.11	-0.01	-0.12
C2FF20-4	9	0.00	0.06	0.00	0.19	0.01	-0.08
C2FF20-4	12	0.01	0.16	0.01	0.22	0.01	-0.03
C2FF20-4	18	0.00	0.23	0.01	0.27	0.01	0.03
C2FF20-7	3	0.00	0.00	0.00	0.24	-0.02	0.08
C2FF20-7	6	0.02	0.07	0.07	0.42	0.01	-0.03
C2FF20-7	9	0.06	0.15	0.17	0.50	0.08	-0.01
C2FF20-7	12	0.15	0.36	0.25	0.62	0.12	0.04
C2FF20-7	18	0.26	0.49	0.65	0.10	0.47	-0.81
C5FF20-4	3	0.00	0.12	0.00	-0.06	0.00	-0.07
C5FF20-4	6	0.01	0.12	0.00	0.03	0.02	-0.09
C5FF20-4	9	0.02	0.13	0.01	0.13	0.01	-0.04
C5FF20-4	12	0.02	0.14	0.00	0.20	-0.01	0.02
C5FF20-4	18	0.03	0.12	0.01	0.30	-0.01	0.05
C5FF20-7	3	0.01	0.19	0.02	-0.01	0.01	-0.05
C5FF20-7	6	0.01	0.22	0.01	0.01	0.00	-0.16
C5FF20-7	9	0.02	0.23	0.02	0.19	0.03	-0.20
C5FF20-7	12	0.03	0.22	0.03	0.29	0.02	-0.14
C5FF20-7	18	0.06	0.26	0.04	0.31	0.04	-0.15

Sulfate Profiling

Figure 5.20 shows the quantitative XRD Rietveld analyses of concrete prisms containing Class C fly ash at 0.4 w/cm placed in the modified ASTM C 1012 indoor sodium sulfate conditions. The outer .12in (3mm) layer of the prisms once again shows the highest amount of ettringite formation. Ettringite formation decreased with increasing depth into the specimens. Interestingly, the prisms containing 20% fly ash show more ettringite than the prisms with 40% Class C fly ash. This corresponds to the higher expansions occurring with mixtures containing 20% Class C fly ash. Mixture C1FC20-4 was not shown in the Figure 5.20 due to complete deterioration of the prisms.

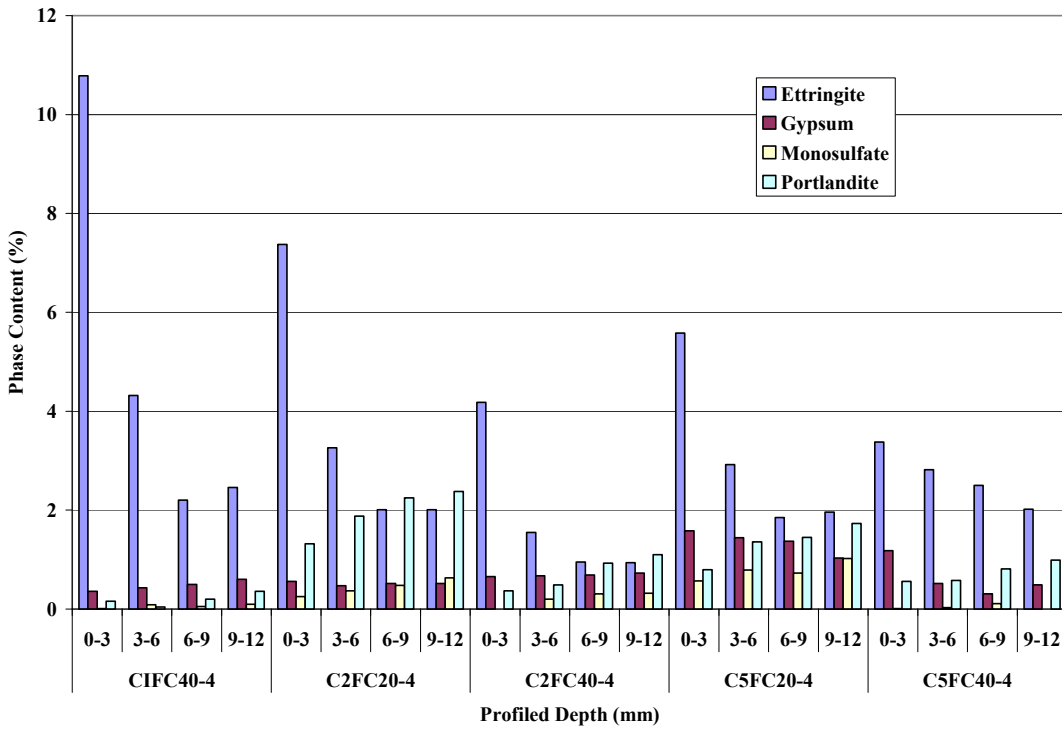


Figure 5.20: Quantitative XRD Analysis of Concrete prisms at 0.4 w/cm placed in sodium sulfate solutions for 18 months

Mixtures C2FC40-7, C5FC20-7, and C5FC40-7 were the only high w/cm ratio mixtures with Class C fly ash to be milled for sulfate profiling. Figure 5.21 presents the phase contents from the milled sections for these three mixtures. Ettringite formation was the greatest in these mixtures. Ettringite formation in mixture C5FC20-7 is greater than C5FC40-7, which again corresponds well with expansion data shown in Table 5.8. The ettringite levels decrease after the first layer in all three mixtures. This did not occur with mixtures with high w/cm and without SCMs, once again illustrating the importance of permeability in combating sulfate attack (both chemical and physical forms of distress).

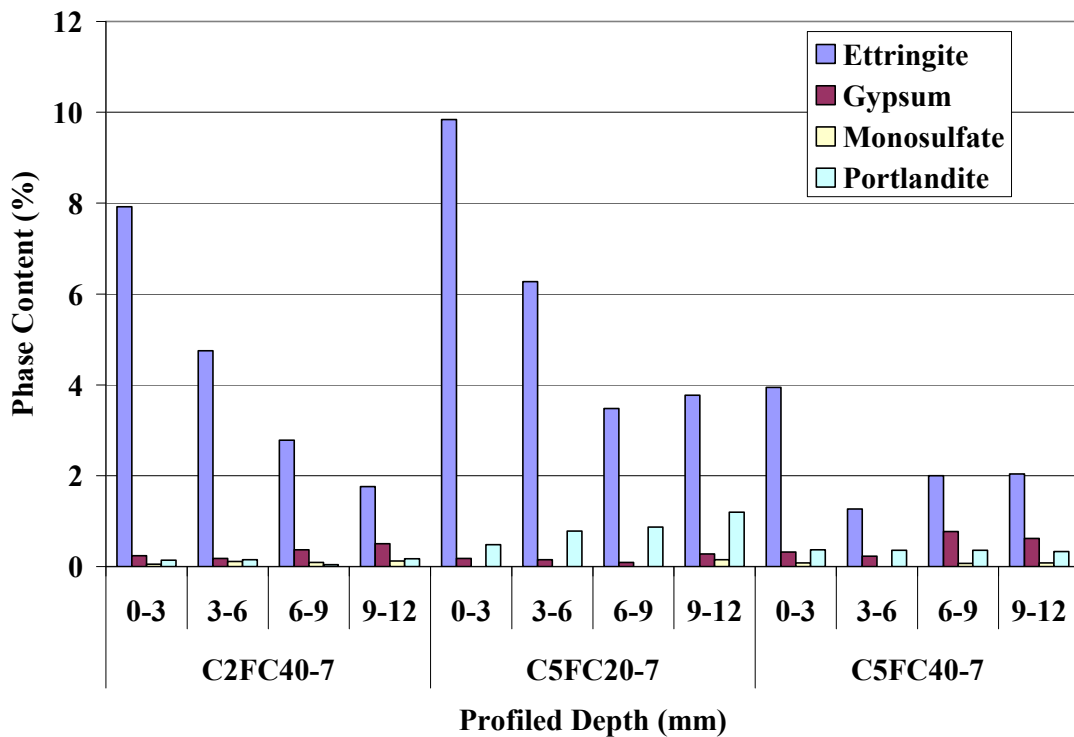


Figure 5.21: Quantitative XRD analysis of prisms at 0.7 w/cm placed tested indoors in sodium sulfate solutions

Comparison of Mortar to Concrete

Several mortar mixtures were tested using ASTM C 1012 that had similar combinations and dosages of cementitious materials, as well as fairly comparable w/cm (0.43 to 0.485) to the concrete mixtures (0.40) tested in sulfate solutions, as previously summarized in Table 5.5. These similar mixtures included control mixtures incorporating Type I, Type I/II, and Type V cements and mixtures containing these cements in combination with either 20 or 40% Class C fly ash. The results of these mortar tests are summarized in Table 5.11, and for convenience, the data from comparable concrete mixtures are also included.

Table 5.11: Comparison between mortar bars and concrete prisms evaluated using sodium sulfate solution in ASTM C 1012 storage

Age (Months)	Mixture	Concrete* Expansion (%)	Mortar** Expansion (%)	Mixture	Concrete* Expansion (%)	Mortar** Expansion (%)	
3	Type I Cement	0.00	0.03	Type I/II Cement	0.00	0.04	
6		0.03	0.07		0.01	0.04	
9		0.04	0.19		0.01	0.08	
12		0.07	0.55		0.01	0.11	
18		1.08	Broken		0.01	0.32	
3	Type I Cement 20% FA1	0.01	0.03	Type I/II Cement 20% FA1	0.01	0.04	
6		0.02	0.04		0.01	0.06	
9		0.02	0.1		0.02	0.1	
12		0.05	0.13		0.00	0.15	
18		Broken	0.9		0.04	0.35	
3	Type I Cement 40% FA1	0.03	0.04	Type I/II Cement 40% FA1	0.01	0.07	
6		0.03	0.12		0.01	0.58	
9		0.08	0.26		0.01	Broken	
12		0.12	0.51		0.04	Broken	
18		0.48	Broken		0.07	Broken	
3	Type V Cement	0.00	0.03	Type V Cement 20% FA1	0.00	0.03	
6		0.01	0.03		0.02	0.04	
9		0.03	0.05		0.03	0.05	
12		0.02	0.06		0.03	0.05	
18		0.03	0.07		0.02	0.05	
3	Type V Cement 40% FA1	0.00	0.06				
6		0.00	0.27				
9		0.03	0.53				
12		0.03	Broken				
18		0.05	Broken				

* w/cm = 0.40

** w/cm = 0.43 – 0.48 (based on meeting target flow value)

As has been the general trend in this experimental program, the expansion and/or deterioration of mortar mixtures has been greater than that observed for similar concrete mixtures. In some cases, there were particularly stark differences in behavior between mortar and concrete exposed to similar sulfate solutions. For example, mortar containing Type V cement and 40% Class C fly ash (FA1) expanded considerably (0.27% at 6 months and 0.53% at 12 months) and were not intact by 12 months. Conversely, a similar concrete mixture (C5FC40-4) expanded by only 0.05% after 18 months. There is a large disconnect between mortar and concrete performance, but as mentioned earlier, the higher paste content and smaller specimen size for the mortar samples may be key factors.

Expansion and Mass loss at 45 months

Damage observed in the sodium sulfate exposure trench has increased from the 18 month measurements presented earlier in the chapter. Damage to upright samples includes sub-grade deterioration as well as physical sulfate attack from the wicking of sodium sulfate. Figures 5.22 and 5.23 shows the damage typical of long-term exposure to sodium sulfate. Table 5.12 provides the expansion and mass change data for the mixtures at 45 months.



Figure 5.22: Damage to prisms exposed to 33000 ppm sodium sulfate

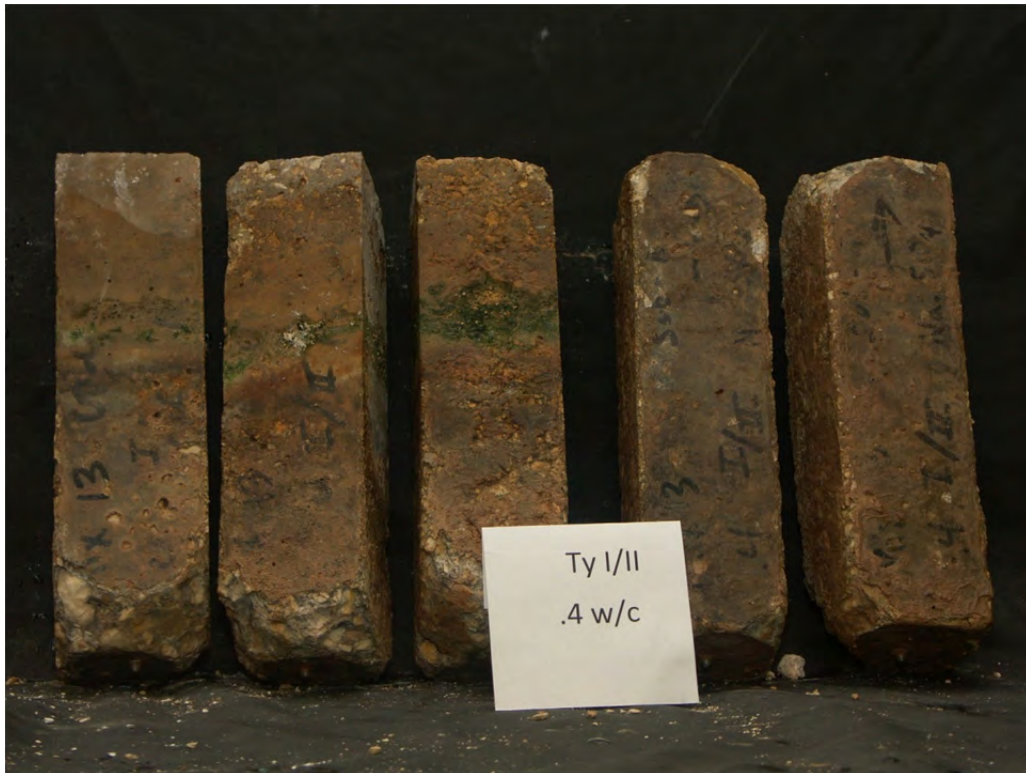


Figure 5.23: Damage to mixtures with Type I/II binders at a 0.4 w/cm in sodium sulfate exposure

However, it is important to note two mixtures that performed very well in the exposure conditions. One mixture, Mix 27, contained Type V cement at a 0.4 w/cm and 20% Class F fly ash. The other mixture, Mix 29, shown in Figure 5.24, contained Type V cement at a 0.4 w/cm as well as 30% Class C fly ash and 3% silica fume. This performance helps validate the concept that Class C fly ash can be used to make durable concrete when used as part of ternary blend. The use of these ternary systems also causes drastic improvements in the performance of physical sulfate attack. It is also important to note that these two mixtures correspond to suggestive preventative measures from ACI 318-08 for S3 exposure.



Figure 5.24: Concrete Prisms Exposed to 33000 ppm Sodium Sulfate exhibiting excellent performance

Table 5.12: Expansion and Mass Change for Phase I Prisms Exposed to a 5% Sodium Sulfate Solution in Outdoor Exposure Site

Mix Description			Age Months	Sodium Sulfate			
				Up Exp %	Mass %	Submerged Exp %	Mass %
1	0.4	Type I	-	45	x	-	x
2	0.7	Type I	-	45	x	-34.0	x
3	0.4	Type I	20% C	45	x	-	x
4	0.7	Type I	20% C	45	x	-	x
5	0.4	Type I	40% C	45	0.34	-3.0	0.28
6	0.7	Type I	40% C	45	x	-17.7	x
7	0.4	Type V	-	45	0.01	-0.4	0.04
8	0.7	Type V	-	45	0.05	-0.6	0.07
9	0.4	Type V	20% C	45	0.06	-0.1	0.13
10	0.7	Type V	20% C	45	x	-19.2	x
11	0.4	Type V	40% C	44	0.03	0.0	0.11
12	0.7	Type V	40% C	44	0.08	-3.2	0.07
13	0.4	Type I/II	-	44	0.25	-0.7	0.51
14	0.7	Type I/II	-	44	0.38	-0.2	0.58
15	0.4	Type I/II	20% C	44	x	-11.7	x
16	0.7	Type I/II	20% C	43	x	-	x
17	0.4	Type I/II	40% C	43	0.08	-0.5	0.85
18	0.7	Type I/II	40% C	43	x	-26.0	x
19	0.4	Type I/II	20% F	42	0.03	0.0	0.10
20	0.7	Type I/II	20% F	42	x	-15.6	x
21	0.4	Type I/II	30%C 3SF	42	0.12	-0.4	0.30
22	0.7	Type I/II	30%C 3SF	42	x	-5.1	0.95
23	0.4	Type I	20% F	41	0.09	-0.8	0.30
24	0.7	Type I	20% F	41	x	-36.0	x
25	0.4	Type I	30%C 3SF	40	0.01	-0.2	0.02
26	0.7	Type I	30%C 3SF	40	x	-17.9	x
27	0.4	Type V	20% F	39	0.00	0.1	0.02
28	0.7	Type V	20% F	39	0.06	-0.3	0.09
29	0.4	Type V	30%C 3SF	38	-0.01	-0.1	-0.01
30	0.7	Type V	30%C 3SF	38	0.01	-0.3	0.05
							0.3

5.2.5 Magnesium Sulfate

Cement Composition and w/cm

Expansions and Mass Change

Table 5.13 summarizes the expansions and mass changes for mixtures without SCMs in all three magnesium sulfate conditions. Regardless of exposure conditions (ASTM C 1012 or outdoor exposure site), only control mixtures containing Type I cement exhibited significant expansion. Mixtures C1-4 and C1-7 both exhibited expansion under ASTM C 1012 storage conditions. In addition, CI-7 expanded in the submerged placement in the outdoor sulfate

exposure site. Prisms that expanded outdoors exhibited mass loss, which was mainly from deterioration of the prisms below the ground level. On the other hand, concrete prisms that expanded under ASTM C 1012 testing conditions gained mass, exhibited large cracks, but were still intact after 18 months of testing.

Table 5.13: Expansion and Mass Change Data for Mixtures without SCMs, exposed to Magnesium Sulfate Solution

Mix	Age (months)	Magnesium Sulfate 1012		Magnesium Submerged		Magnesium Vertical	
		Expansion (%)	Mass Change (%)	Expansion (%)	Mass Change (%)	Expansion (%)	Mass Change (%)
C1-4	3	0.00	0.52	0.01	0.01	0.01	-0.01
C1-4	6	0.02	0.54	0.01	0.02	0.01	0.06
C1-4	9	0.03	0.79	0.02	0.08	0.02	0.21
C1-4	12	0.04	0.87	0.03	0.13	0.02	0.11
C1-4	18	0.44	1.73	0.05	-0.45	0.02	-0.76
C1-7	3	0.01	0.32	0.01	-0.01	0.00	-0.17
C1-7	6	0.03	0.66	0.02	0.14	0.01	0.04
C1-7	9	0.09	0.79	0.07	0.34	0.02	0.16
C1-7	12	0.18	0.97	0.13	0.38	0.04	-0.15
C1-7	18	0.45	1.29	0.61	-1.58	0.06	-0.73
C2-4	3	0.00	0.15	0.00	-0.01	0.00	-0.15
C2-4	6	0.00	0.23	0.00	-0.02	0.01	-0.06
C2-4	9	-0.01	0.33	0.01	-0.02	0.01	-0.07
C2-4	12	0.00	0.38	0.01	0.00	0.01	-0.04
C2-4	18	0.00	0.45	0.02	0.08	0.01	0.03
C2-7	3	-0.01	0.27	0.00	0.05	-0.02	-0.22
C2-7	6	0.01	0.35	0.00	0.12	-0.01	0.02
C2-7	9	0.01	0.32	0.01	0.23	-0.01	0.06
C2-7	12	0.02	0.29	0.01	0.17	-0.01	-0.02
C2-7	18	0.03	0.28	0.01	0.31	0.01	0.16
C5-4	3	-0.01	0.37	0.00	0.00	-0.01	-0.15
C5-4	6	0.00	0.20	0.01	0.03	0.00	-0.03
C5-4	9	0.01	0.21	0.01	0.02	0.00	-0.02
C5-4	12	0.01	0.24	0.02	0.04	0.00	-0.08
C5-4	18	0.02	0.25	0.03	0.07	0.01	0.14
C5-7	3	0.00	0.46	0.02	0.03	0.01	-0.25
C5-7	6	0.01	0.45	0.02	0.01	0.01	-0.07
C5-7	9	0.01	0.56	0.02	0.05	0.02	-0.10
C5-7	12	0.02	0.50	0.03	0.10	0.01	-0.22
C5-7	18	0.03	0.48	0.03	0.12	0.03	-0.07

Sulfate Profiling

Figure 5.25 depicts the XRD results from powders milled at successive depth into the prisms placed in ASTM C 1012 storage conditions in magnesium sulfate solution after 18 months of storage. The three mixtures shown in the Figure 5.25 show a large amount of ettringite in the outer layer followed by an abrupt decrease in ettringite with proximity toward the center of prism. It was originally thought that brucite may have formed due to magnesium sulfate exposure; however, XRD analysis did not confirm this supposition. Gypsum and monosulfate formed in large amounts in these layers. Calcium hydroxide was nearly depleted in the outer layer of the C1-4 mixture. Decalcification of C-S-H could potentially be occurring in this sample. Mixture C2-4 exhibited ettringite formation in the outer layer. Mixture C5-4 does not show any significant reaction products forming that would indicate sulfate attack.

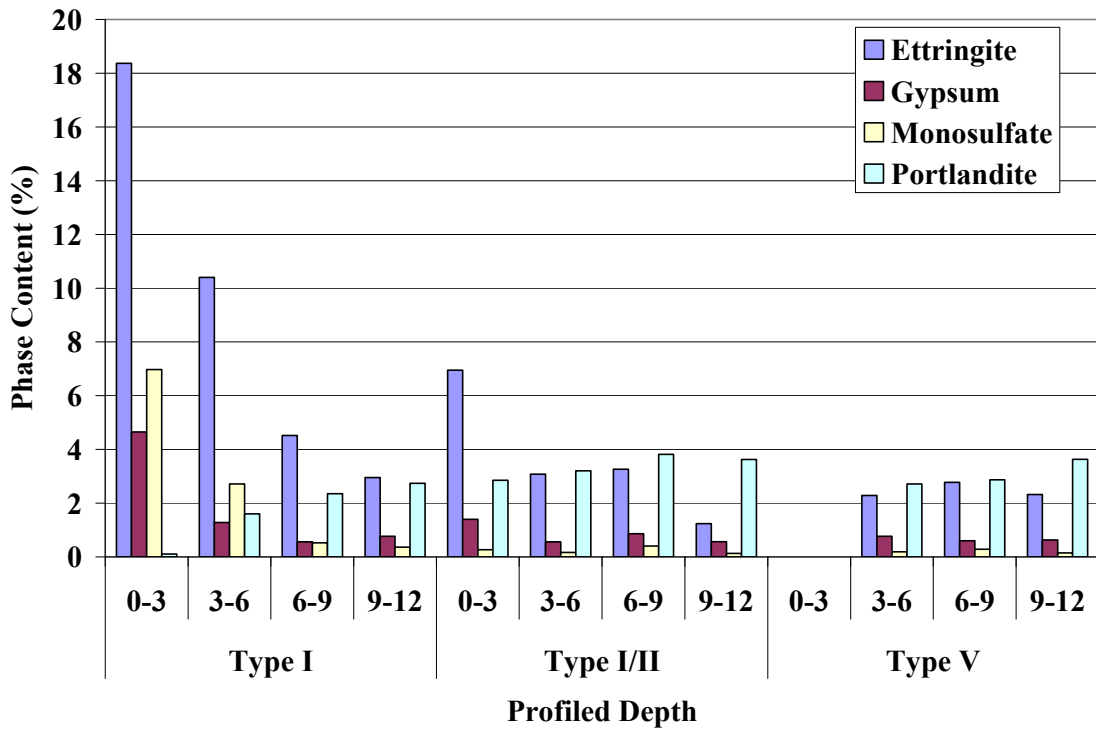


Figure 5.25: Semi-quantitative XRD Analysis of concrete prisms at 0.4 w/cm placed in indoor magnesium sulfate conditions

Figure 5.26 shows mixtures at 0.7 w/cm in ASTM C 1012 storage conditions in magnesium sulfate. Ettringite is highest in the outer layer but does not decline further into the specimen. Gypsum formation is also greatest in the outer layer but does decrease with increasing depth toward the middle of the prism. Calcium hydroxide is depleted towards the outer layer and increases in content further into the prisms.

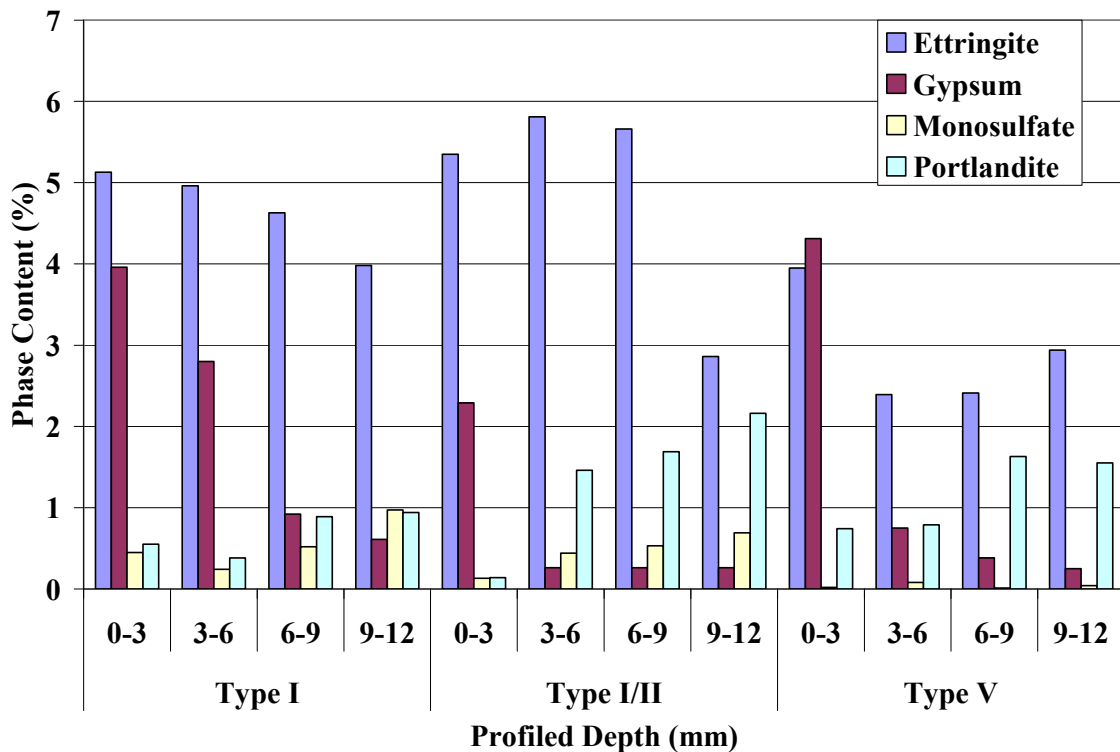


Figure 5.26: Semi-quantitative XRD Rietveld analysis of prisms placed in magnesium sulfate conditions

Supplementary cementing materials

Expansions and Mass Change

Similar to mixtures in sodium sulfate, the addition of 20% Class C fly ash performed worse than a replacement level of 40% Class C fly ash. Table 5.14 provides the expansion and mass change data for mixtures containing Type I cement and SCMs. Prisms in the indoor controlled environment from mixture C1FC20-7 were not measurable at 12 months due to their length being too long for the comparator. The same mixture in the outdoor environment expanded over 1% and did not fully deteriorate. Large cracks in the prisms and physical damage which occurred during removal from the soil made these bars immeasurable. Prisms that did expand too much for the comparator gained mass until they finally fully deteriorated. Mixtures with 40% Class C fly ash did not fail the 0.1% expansion criterion in any of the three environments.

Table 5.14: Expansion and Mass Change Data for Concrete with Type I Cement and Class C fly ash, exposed to magnesium sulfate solution

Mix	Age (months)	Magnesium Sulfate 1012		Magnesium Submerged		Magnesium Vertical	
		Expansion (%)	Mass Change (%)	Expansion (%)	Mass Change (%)	Expansion (%)	Mass Change (%)
C1FC20-4	3	0.01	0.11	0.00	-0.08	0.00	-0.05
C1FC20-4	6	0.01	0.10	0.01	-0.09	0.01	0.03
C1FC20-4	9	0.02	0.17	0.02	-0.06	0.01	0.07
C1FC20-4	12	0.02	0.21	0.03	0.05	0.02	0.06
C1FC20-4	18	Broken	Broken	0.04	-2.13	0.02	0.15
C1FC20-7	3	0.03	0.34	0.03	0.15	0.02	-0.09
C1FC20-7	6	1.07	1.28	0.29	-6.94	0.10	-2.81
C1FC20-7	9	1.52	2.04	1.06	-7.92	0.36	-11.05
C1FC20-7	12	Too Long	1.22	1.28	Broken	Broken	Broken
C1FC20-7	18	--	2.35	Broken	--	--	--
C1FC40-4	3	0.02	0.25	0.00	0.01	-0.01	-0.12
C1FC40-4	6	0.03	0.30	0.00	0.08	-0.01	-0.10
C1FC40-4	9	0.03	0.38	0.00	0.08	-0.01	-0.09
C1FC40-4	12	0.02	0.21	0.02	0.15	0.01	-0.14
C1FC40-4	18	0.04	0.20	0.02	0.06	0.01	-0.20
C1FC40-7	3	0.02	0.18	0.00	0.06	-0.01	-0.11
C1FC40-7	6	0.03	0.09	0.00	0.23	0.00	-0.14
C1FC40-7	9	0.05	0.27	0.01	0.27	0.00	-0.18
C1FC40-7	12	0.05	0.22	0.03	0.28	0.01	-0.43
C1FC40-7	18	0.09	0.18	0.04	0.19	0.02	-0.35

Mixtures with Type I/II cement and Class C fly ash are shown in Table 5.15, along with expansion and mass change data. Similar to mixtures in magnesium sulfate conditions containing Type I cement, 20% Class C fly ash performed worse than 40% Class C fly ash. Reducing the w/cm was effective in improving sulfate resistance. Lastly, for the indoor testing, using ASTM C 1012 storage conditions, mixture C2FC20-4 exhibited better sulfate resistance than C1FC20-4, illustrating the importance of cement composition.

Table 5.15: Expansion and Mass Change Data for Concrete with Type I/II Cement and Class C fly ash, exposed to magnesium sulfate solution

Mix	Age (months)	Magnesium Sulfate 1012		Magnesium Submerged		Magnesium Vertical	
		Expansion (%)	Mass Change (%)	Expansion (%)	Mass Change (%)	Expansion (%)	Mass Change (%)
C2FC20-4	3	0.01	0.14	0.00	0.11	-0.01	-0.04
C2FC20-4	6	0.01	0.17	0.00	0.11	-0.01	-0.05
C2FC20-4	9	0.02	0.36	0.01	0.12	0.01	0.04
C2FC20-4	12	0.01	0.32	0.02	0.10	0.02	0.02
C2FC20-4	18	0.00	0.33	0.02	0.18	0.02	0.09
C2FC20-7	3	0.02	0.59	0.00	0.01	0.00	-0.20
C2FC20-7	6	0.03	0.56	0.01	0.17	0.01	-0.24
C2FC20-7	9	0.60	1.01	0.03	0.31	0.06	-0.08
C2FC20-7	12	Broken	1.63	0.11	-0.58	0.12	-0.12
C2FC20-7	18	--	3.14	Broken	Broken	Broken	Broken
C2FC40-4	3	0.00	0.07	-0.01	-0.04	-0.01	-0.07
C2FC40-4	6	0.01	0.19	0.00	0.01	0.00	-0.02
C2FC40-4	9	-0.01	0.33	0.00	0.11	0.00	-0.06
C2FC40-4	12	0.01	0.22	0.00	0.06	0.00	-0.03
C2FC40-4	18	0.02	0.22	0.00	0.11	0.00	-0.02
C2FC40-7	3	0.04	0.26	0.01	0.30	0.01	0.00
C2FC40-7	6	0.18	0.52	0.03	0.29	-0.01	0.10
C2FC40-7	9	0.27	0.67	0.05	0.56	0.00	-0.26
C2FC40-7	12	0.34	0.67	0.05	0.63	0.01	-0.53
C2FC40-7	18	0.41	0.66	0.07	0.52	-0.02	-0.76

All mixtures containing Type V cement and Class C fly ash performed well except for C5FC20-7 which failed the expansion criteria at 12 months in only the modified ASTM C 1012 magnesium sulfate solution as shown in Table 5.16. Mixtures with Class C fly ash performed better in magnesium sulfate conditions than those in sodium sulfate. These prisms in magnesium sulfate conditions did not fail in many conditions and did not lose mass.

Table 5.16: Expansion and Mass Change Data for Concrete with Type V Cement and Class C fly ash, exposed to magnesium sulfate solution

Mix	Age (months)	Magnesium Sulfate 1012		Magnesium Submerged		Magnesium Vertical	
		Expansion (%)	Mass Change (%)	Expansion (%)	Mass Change (%)	Expansion (%)	Mass Change (%)
C5FC20-4	3	0.00	0.15	0.00	0.26	0.01	0.06
C5FC20-4	6	0.01	0.36	0.01	0.25	0.02	0.14
C5FC20-4	9	0.03	0.23	0.01	0.31	0.02	0.18
C5FC20-4	12	0.03	0.34	0.02	0.34	0.01	0.14
C5FC20-4	18	0.02	0.40	0.00	0.42	0.00	0.26
C5FC20-7	3	0.00	0.10	0.02	0.30	0.02	-0.13
C5FC20-7	6	0.01	0.15	0.02	0.32	0.02	0.08
C5FC20-7	9	0.05	0.26	0.04	0.43	0.03	-0.02
C5FC20-7	12	0.10	0.36	0.06	0.44	0.04	-0.18
C5FC20-7	18	0.36	0.60	0.09	-0.27	0.06	0.01
C5FC40-4	3	0.01	0.16	-0.01	0.05	0.00	-0.09
C5FC40-4	6	0.03	0.22	0.00	0.06	0.01	-0.01
C5FC40-4	9	0.04	0.18	0.00	0.03	0.01	-0.02
C5FC40-4	12	0.03	0.30	0.01	0.10	0.02	-0.04
C5FC40-4	18	0.03	0.56	-0.02	0.06	-0.01	-0.01
C5FC40-7	3	0.00	0.16	0.00	0.07	0.01	-0.11
C5FC40-7	6	0.00	-0.21	0.00	0.13	0.01	-0.06
C5FC40-7	9	0.01	0.20	0.01	0.18	0.04	-0.09
C5FC40-7	12	0.04	0.42	0.01	0.20	0.02	-0.24
C5FC40-7	18	0.06	0.42	-0.02	0.23	0.03	-0.18

Ternary blends exhibited good sulfate resistance in all mixtures. Similar to sodium sulfate, the 30% Class C fly ash and 3% silica fume ternary blend performed well. Every mixture passed the expansion criteria up to the 18 month measurements.

Mixtures containing 20% Class F fly ash are shown in Table 5.17 with their expansion and mass change data. C1FF20-7 was the only mixture that failed the 0.1% expansion criteria. The prisms in the modified ASTM C 1012 magnesium sulfate solutions failed at 9 months while the outdoor submerged and vertical prisms were broken for the 18 month measurements. This failure was surprising since the bars had not expanded prior to 18 months.

Table 5.17: Expansion and Mass Change Data for Concrete with ternary SCM blends exposed to magnesium sulfate solution

Mix	Age (months)	Magnesium Sulfate 1012		Magnesium Submerged		Magnesium Vertical	
		Expansion (%)	Mass Change (%)	Expansion (%)	Mass Change (%)	Expansion (%)	Mass Change (%)
C1FF20-4	3	0.01	-0.24	0.01	-0.02	0.00	-0.08
C1FF20-4	6	0.01	0.27	0.00	0.01	0.00	-0.06
C1FF20-4	9	0.01	0.30	0.01	0.02	0.00	-0.06
C1FF20-4	12	0.03	0.35	0.00	0.07	-0.01	-0.01
C1FF20-4	18	0.02	0.44	0.00	0.10	0.00	0.02
C1FF20-7	3	0.01	0.38	0.02	0.04	0.00	-0.07
C1FF20-7	6	0.03	0.41	0.02	0.09	0.00	-0.05
C1FF20-7	9	0.10	0.51	0.03	0.08	0.01	-0.05
C1FF20-7	12	0.27	0.65	0.02	0.15	0.00	0.10
C1FF20-7	18	broken	broken	Broken	Broken	Broken	Broken
C2FF20-4	3	0.01	0.07	0.00	-0.15	-0.01	-0.07
C2FF20-4	6	0.02	0.10	-0.01	-0.08	0.00	-0.05
C2FF20-4	9	0.02	0.12	0.00	-0.03	0.00	-0.08
C2FF20-4	12	0.03	0.13	0.00	-0.06	0.00	-0.02
C2FF20-4	18	0.03	0.30	0.00	-0.02	0.01	0.05
C2FF20-7	3	-0.02	0.18	0.00	-0.06	0.00	0.03
C2FF20-7	6	-0.01	0.15	0.00	0.03	0.00	-0.02
C2FF20-7	9	0.01	0.22	0.01	0.08	0.00	-0.18
C2FF20-7	12	0.01	0.28	0.02	0.08	0.02	-0.11
C2FF20-7	18	0.06	0.49	0.04	0.20	0.05	0.01
C5FF20-4	3	0.00	0.00	0.00	0.09	0.00	-0.05
C5FF20-4	6	0.00	0.14	0.00	0.04	-0.01	-0.08
C5FF20-4	9	0.01	0.13	0.01	0.09	0.00	-0.12
C5FF20-4	12	0.01	0.13	-0.01	0.17	-0.01	-0.04
C5FF20-4	18	0.01	0.14	-0.01	0.16	-0.01	-0.06
C5FF20-7	3	0.01	0.13	0.01	-0.03	0.00	-0.07
C5FF20-7	6	0.00	0.14	-0.01	-0.13	0.00	-0.06
C5FF20-7	9	0.00	0.11	0.02	-0.06	0.01	-0.18
C5FF20-7	12	0.00	0.12	0.00	0.01	0.00	-0.08
C5FF20-7	18	0.03	0.21	0.01	0.12	0.00	-0.01

Sulfate Profiling

Figure 5.27 shows semi-quantitative XRD Rietveld analyses on concrete prisms placed in the modified ASTM C 1012 storage condition in magnesium sulfate. Specifically, this graph compares the differences between different cements with Class C fly ash at varying replacement levels. Ettringite and gypsum formation were greater in the outer layer of each mixture shown. Both 20% and 40% Class C fly ash replacement resulted in formation of nearly the same amount of ettringite. Portlandite was reduced in mixtures containing higher fly ash replacement due to the pozzolanic reaction occurring with the additional fly ash.

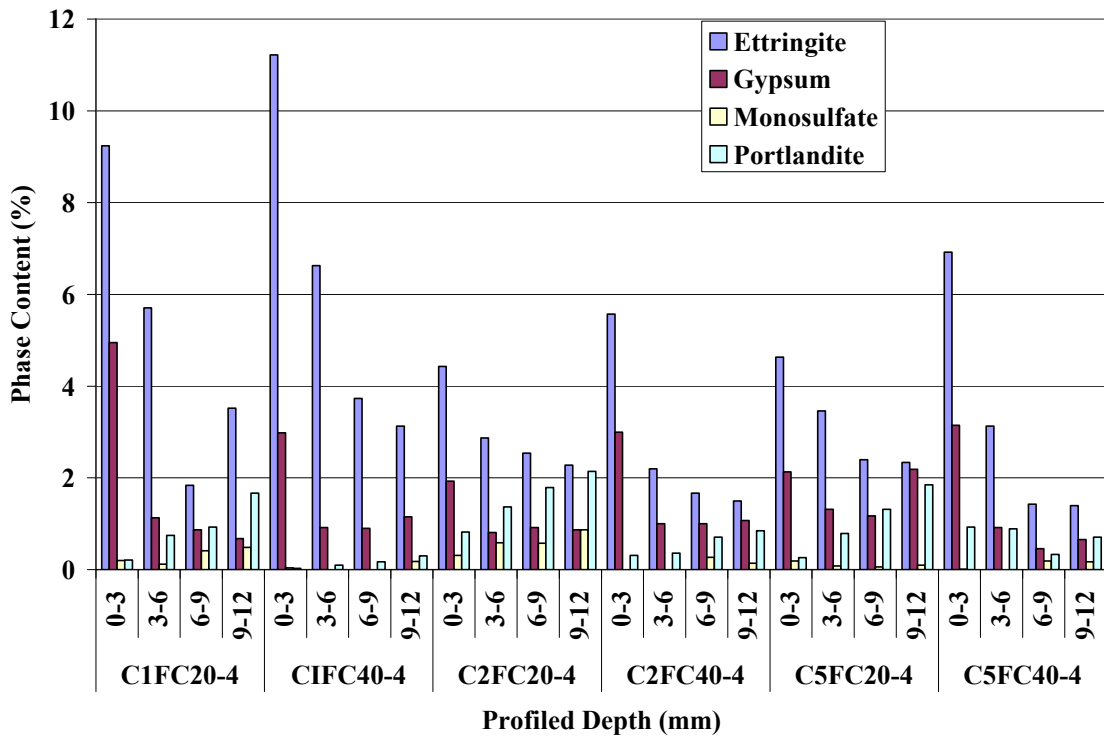


Figure 5.27: Semi-quantitative XRD Rietveld analysis of prisms containing SCMs in indoor magnesium sulfate conditions

Similarly at higher w/cm of 0.7, Figure 5.28 shows ettringite and gypsum formation are greater in the outer layer. At 40% replacement, a decline in ettringite formation can be seen as one move into the concrete, owing to the reduced permeability of the mixtures.

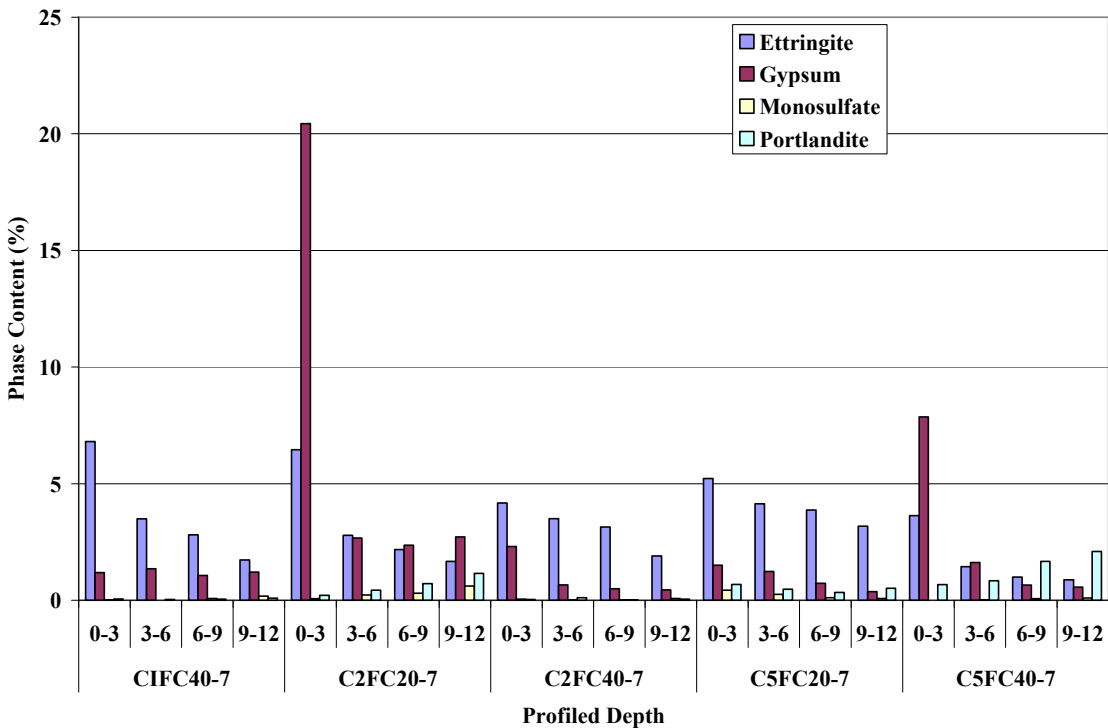


Figure 5.28: Semi-quantitative XRD Rietveld Analysis of prisms with SCMs placed indoors in magnesium sulfate solution

Comparison between concrete and mortars

Expansion results for Type I/II and Type V control mixtures exposed to magnesium sulfate solution are shown in Table 5.18. Mortars made with similar materials performed worse than companion concrete prisms. Concrete control mixtures did not expand at either w/cm whereas control mortar mixture C2 failed at 18 months. Concrete prisms with Class C fly ash did not fail in any of the comparable mortar mixtures. Mortar mixtures containing Class C fly ash expanded past the expansion limit usually within 6 to 9 months.

Table 5.18: Comparison between mortar bars and concrete prisms evaluated using magnesium sulfate solution in ASTM C 1012 storage conditions

Mixture	Age (Months)	Concrete* Expansion (%)	Mortar** Expansion (%)	Mixture	Concrete* Expansion (%)	Mortar** Expansion (%)
Type I/II Cement	3	0.00	0.03	Type V Cement	-0.01	0.02
	6	0.00	0.04		0.00	0.03
	9	-0.01	0.07		0.01	0.05
	12	0.00	0.09		0.01	0.06
	18	0.00	0.2		0.02	0.09
Type I/II Cement 20% FA1	3	0.01	0.03	Type V Cement 20% FA1	0.00	0.03
	6	0.01	0.04		0.01	0.04
	9	0.02	0.1		0.03	0.05
	12	0.01	0.17		0.03	0.07
	18	0.00	0.38		0.02	0.12
Type I/II Cement 40% FA1	3	0.00	0.04	Type V Cement 40% FA1	0.01	0.05
	6	0.01	0.25		0.03	0.21
	9	-0.01	0.74		0.04	0.44
	12	0.01	Broken		0.03	Broken
	18	0.02	Broken		0.03	Broken

* w/cm = 0.40

** w/cm = 0.43 – 0.48 (based on meeting target flow value)

Expansion and Mass Loss at 45 Months

An increase in damage was also observed in samples exposed to magnesium sulfate, but this damage was not to the extent seen in the sodium sulfate trench. The most drastic change to these mixtures was the increase in physical sulfate attack observed in vertical specimens (with damage manifested above grade). Figure 5.29 shows prisms with typical damage due to magnesium sulfate. Table 5.19 provides the expansion and mass loss for the magnesium sulfate prisms at 45 months.

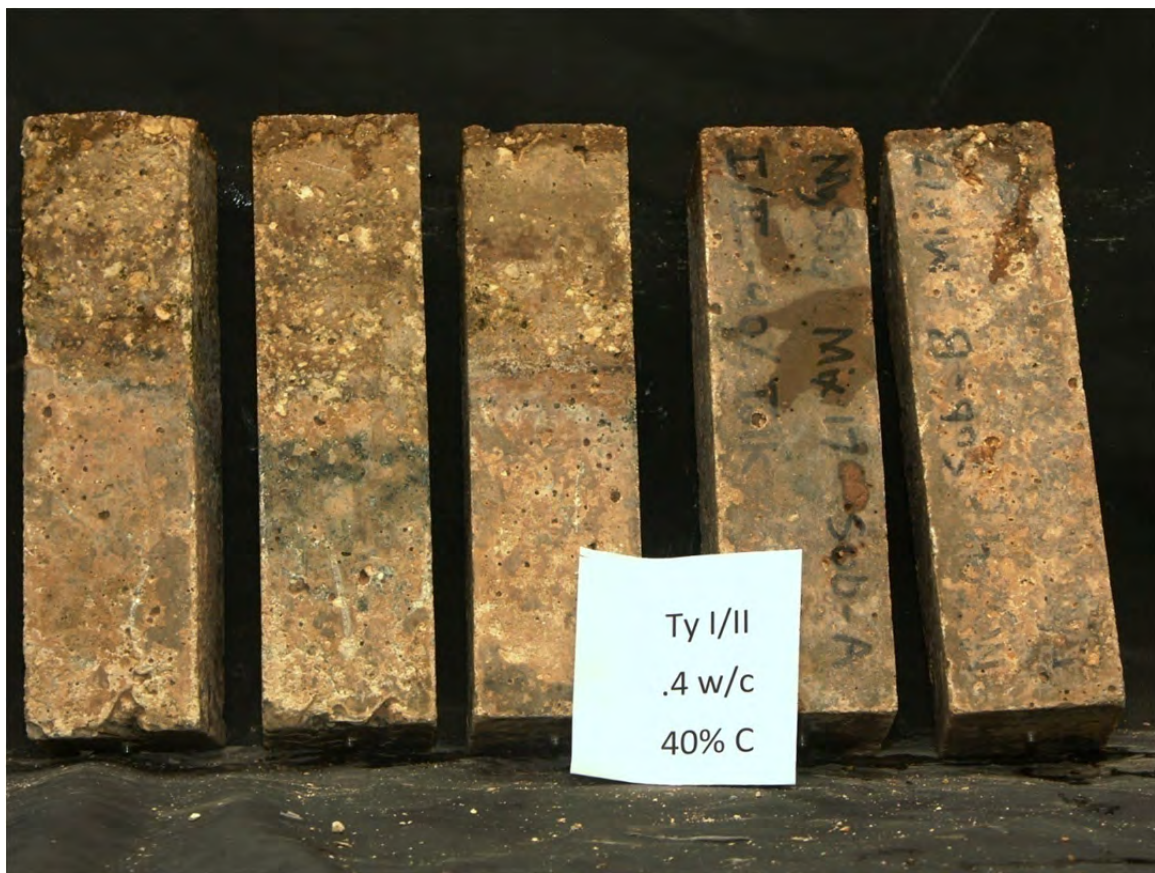


Figure 5.29: Damage to Prisms Exposed to 33000 ppm Magnesium Sulfate

Table 5.19: Expansion and Mass Change for Phase I Prisms Exposed to a 5% Magnesium Sulfate Solution in Outdoor Exposure Site

Mix Description				Age Months	Magnesium Sulfate			
					Up Exp %	Mass %	Submerged Exp %	Mass %
1	0.4	Type I	-	45	x	-34.0	x	-40.0
2	0.7	Type I	-	45	x	-42.0	x	-
3	0.4	Type I	20% C	45	0.34	-2.9	1.10	-19.2
4	0.7	Type I	20% C	45	x	-	x	-
5	0.4	Type I	40% C	45	0.04	-0.5	0.03	0.2
6	0.7	Type I	40% C	45	0.02	-1.4	0.04	0.3
7	0.4	Type V	-	45	-0.01	-0.1	0.04	0.1
8	0.7	Type V	-	45	0.01	-0.6	0.03	0.2
9	0.4	Type V	20% C	45	0.02	0.0	0.05	0.4
10	0.7	Type V	20% C	45	0.16	-0.4	0.31	0.0
11	0.4	Type V	40% C	44	0.02	-0.1	0.03	0.1
12	0.7	Type V	40% C	44	0.03	-0.9	0.01	0.2
13	0.4	Type I/II	-	44	0.00	-0.3	0.01	0.2
14	0.7	Type I/II	-	44	0.11	-0.3	0.11	0.3
15	0.4	Type I/II	20% C	44	0.02	0.0	0.05	0.3
16	0.7	Type I/II	20% C	43	x	-30.0	x	-34.8
17	0.4	Type I/II	40% C	43	0.01	-0.1	0.00	0.2
18	0.7	Type I/II	40% C	43	-0.02	-2.2	0.08	0.5
19	0.4	Type I/II	20% F	42	0.00	-0.1	0.00	0.0
20	0.7	Type I/II	20% F	42	0.10	-0.4	0.09	0.3
21	0.4	Type I/II	30%C 3SF	42	0.01	-0.3	0.01	0.1
22	0.7	Type I/II	30%C 3SF	42	0.03	-0.6	0.11	0.4
23	0.4	Type I	20% F	41	0.00	-0.2	0.00	0.2
24	0.7	Type I	20% F	41	0.11	-0.4	0.09	0.3
25	0.4	Type I	30%C 3SF	40	-0.01	-0.2	0.00	0.2
26	0.7	Type I	30%C 3SF	40	0.03	-0.5	0.06	0.3
27	0.4	Type V	20% F	39	0.00	-0.2	0.01	0.3
28	0.7	Type V	20% F	39	0.01	-0.4	0.02	0.1
29	0.4	Type V	30%C 3SF	38	-0.04	-0.2	-0.01	0.0
30	0.7	Type V	30%C 3SF	38	-0.01	-0.6	0.01	0.1

5.2.6 Prisms Constructed for Phase II

Research Goals

Upon conclusion of Phase I of the study the decision was made to construct additional sulfate exposure trenches to simulate more conditions. Sodium sulfate was determined to be the most damaging form of attack in Phase I. Thus, it was chosen for use in concentrations of 1500 ppm and 10000 ppm to simulate ACI 318-08 S1 and S2 exposure. Calcium sulfate was also chosen at a sulfate ion concentration of 1500 ppm to simulate S1 exposure. The decision to use calcium sulfate at this exposure was based upon the fact that it is the most prevalent form of sulfate in the state, and 1500 ppm is close to the maximum theoretical solubility (1440 ppm) of calcium sulfate in water. A comparison of the performance of prisms in the two calcium sulfate

exposure sites is desired to better understand if damage is similar or drastically different. This will help to answer the question of the effects of soils with an abundance of calcium sulfate, a condition regularly seen in the state.

The more targeted approach of this part of the study made the excavation of large trenches unnecessary. The decision was made to use galvanized steel tanks 8 feet in diameter by 2 feet deep (2.44 m diameter x 0.61 m deep) lined with the same EPDM liner used in Phase I. Sandy loam soil, from the same source used in Phase I, was placed to a depth of 16 inches (.41 m). Testing of this loam confirmed no sulfates were present. Solutions of the new concentrations were then prepared and added to the tanks to provide the same exposure conditions used in Phase I. Figure 5.30 shows the updated sulfate exposure site in Austin, Texas.

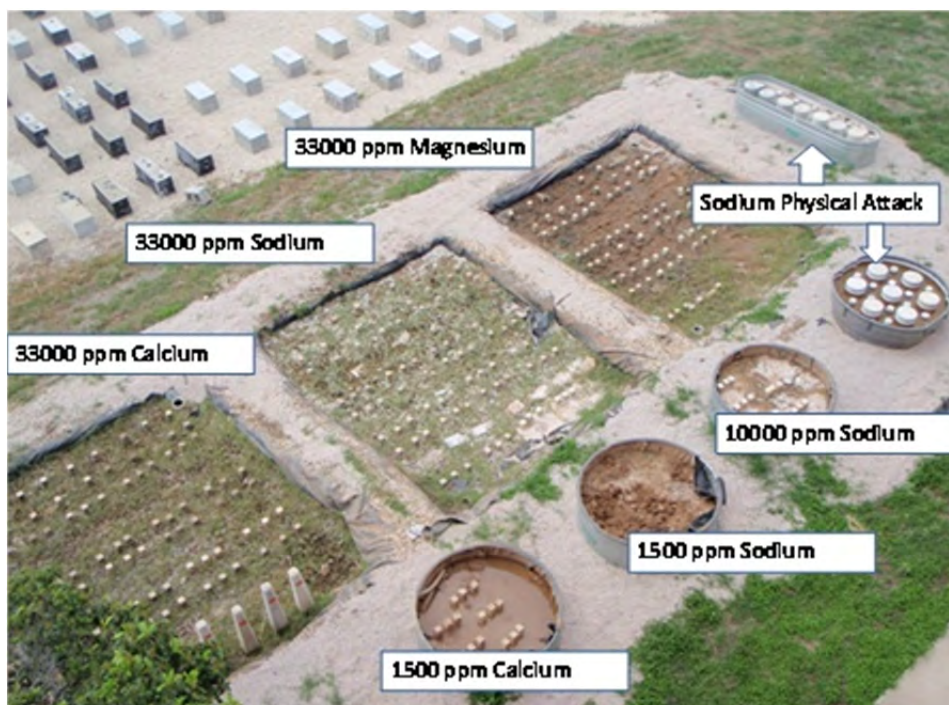


Figure 5.30: Updated Outdoor Sulfate Exposure Site

Specimens Currently Being Tested

Five mixtures were cast in the summer of 2008 and placed in the new outdoor sulfate exposure tanks. A description of these mixtures is given in Table 5.20.

Table 5.20: Mixtures Cast for Phase II Outdoor Sulfate Exposure

Mix #	Cement	SCMs	w/cm
31	Type I	-	0.4
32	Type I	-	0.45
33	Type I	-	0.5
34	Type I	20% C	0.4
35	Type I	40% C	0.7

Care was taken to evaluate w/cm that were not used in the Phase I study, namely 0.45 w/cm and 0.5 w/cm, in order to give a more realistic evaluation of mixtures used for structural concrete. Specimens have reached one year of exposure with none at the limit of 0.1% expansion set in Phase I. The reduction in expansion can be attributed to the reduced concentrations of sulfate to which the samples are exposed. Data for the expansion in 1500 ppm calcium sulfate are presented in Table 5.21.

Table 5.21: Expansion and Mass Change for Phase II Prisms Exposed to a 1500 ppm Calcium Sulfate Solution

Mix Description				Age Days	Calcium Sulfate 1500 ppm					
					Up		Submerged		1012	
					Exp %	Mass %	Exp %	Mass %	Exp %	Mass %
31	0.4	Type I	-	430	-0.01	-0.6	0.00	0.0	0.01	0.2
32	0.45	Type I	-	417	-0.01	-0.6	0.00	-0.3	0.01	0.2
33	0.5	Type I	-	394	-0.02	-0.6	0.00	0.0	0.01	0.3
34	0.4	Type I	20% C	394	-0.01	-0.1	0.00	-0.1	0.02	0.2
35	0.7	Type I	40% C	329	0.00	-0.3	-0.01	0.0	0.01	0.4

It should be noted that samples from Phase I in 5% (33000 ppm) calcium sulfate did not pass 0.1% expansion until 45 months exposure. It is not unlikely that this amount of time or more will be required for expansion to manifest. It is important to note that expansion has occurred in the modified ASTM C 1012 testing.

Expansion values were also low in samples exposed to a 1500 ppm sodium sulfate solution as shown in Table 5.22.

Table 5.22: Expansion and Mass Change for Phase II Prisms Exposed to a 1500 ppm Sodium Sulfate Solution

Mix Description				Age Days	Sodium Sulfate 1500 ppm					
					Up		Submerged		1012	
					Exp %	Mass %	Exp %	Mass %	Exp %	Mass %
31	0.4	Type I	-	430	-0.01	-0.4	0.00	0.1	0.01	0.1
32	0.45	Type I	-	417	0.00	-0.3	0.01	0.0	0.01	-0.1
33	0.5	Type I	-	394	0.00	-0.4	0.00	0.0	0.00	0.1
34	0.4	Type I	20% C	394	0.00	-0.2	0.01	0.0	0.00	0.2
35	0.7	Type I	40% C	329	0.00	-0.1	0.00	0.1	0.00	0.2

Even with these low values of expansion, distress is becoming evident on some samples; Figure 5.31 shows surface scaling on Mixture 33. Samples exposed to a 1500 ppm sodium sulfate solution show negligible expansion. However, there was no shrinkage of vertical samples, which occurred in samples exposed to 1500 ppm calcium sulfate. Minor scaling on the surface of samples in contact with soil had become visible at one year of exposure.



Figure 5.31: Surface Scaling in 1500 ppm Sodium Sulfate in Soil Contact Zone

Expansion was greatest in samples exposed to 10000 ppm sodium sulfate; values are shown in Table 5.23. Samples were damaged to a greater extent than mixtures damaged in 1500 ppm sodium sulfate (Figure 5.32). More surface scaling was visible in samples exposed to 10000 ppm sodium sulfate than on samples in 1500 ppm sodium sulfate. Small cracks had formed on the edges of the submerged samples.

Table 5.23: Expansion and Mass Change for Phase II Prisms Exposed to a 10000 ppm Sodium Sulfate Solution

Mix Description	Age Days	Sodium Sulfate 10000 ppm					
		Up		Submerged		1012	
		Exp %	Mass %	Exp %	Mass %	Exp %	Mass %
31 0.4	Type I	-	430	0.03	-0.3	0.01	0.0
32 0.45	Type I	-	417	0.00	-0.3	0.01	0.2
33 0.5	Type I	-	394	0.00	-0.3	0.02	-0.2
34 0.4	Type I	20% C	394	0.00	-0.3	0.01	0.0
35 0.7	Type I	40% C	329	0.00	-0.2	0.00	0.1
						0.02	0.3

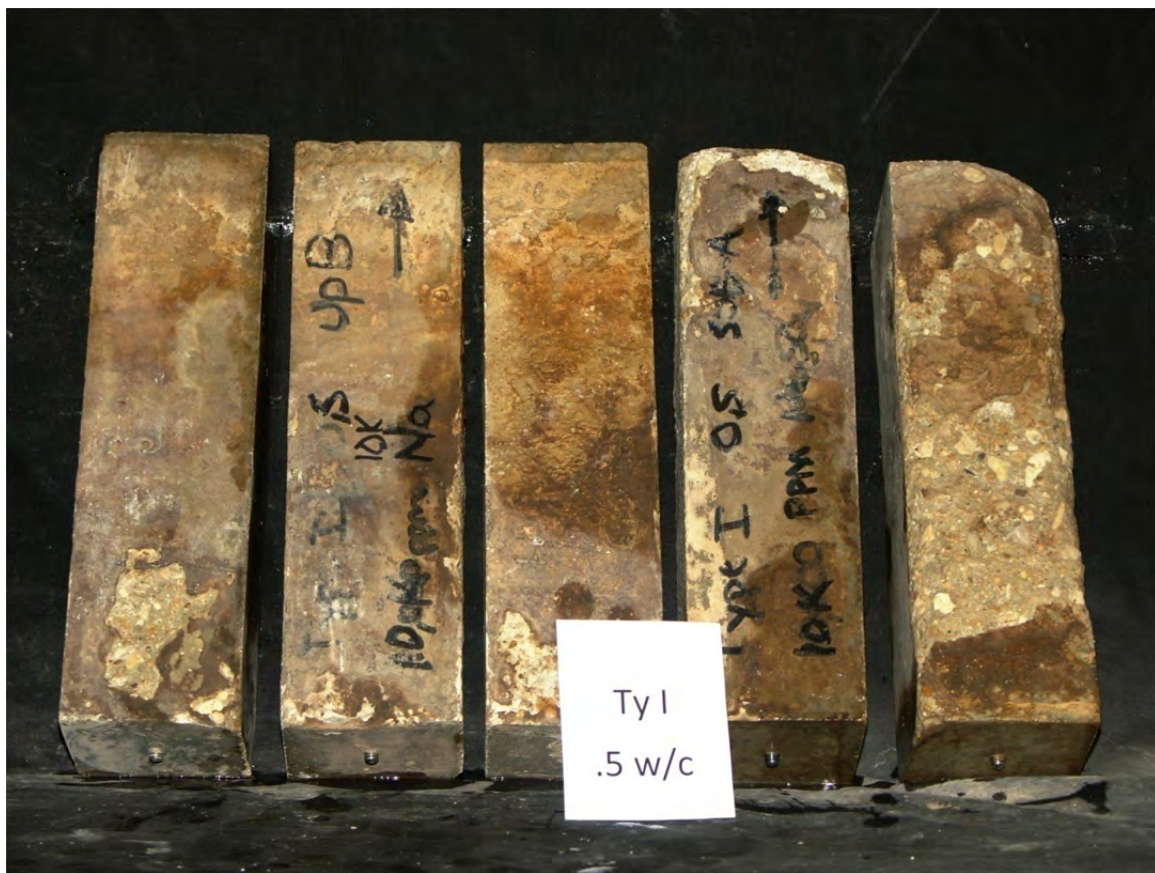


Figure 5.32: Surface Scaling in 10000 ppm Sodium Sulfate in Soil Contact Zone

Mixture 35, 0.7 w/cm, 40% Class C fly ash, is also beginning to show signs of physical sulfate damage (Figure 5.33).



Figure 5.33: Physical Sulfate Attack in 10000 ppm Sodium Sulfate Above Soil Contact Zone

Specimens Recently Constructed

Upon review of the Phase I prisms measured in the summer of 2009, an additional five mixtures were selected for testing in the sulfate exposure trenches at the Austin, Texas exposure site. These mixtures are intended to further investigate the performance in the various classes of exposure as determined by ACI 318-08. They will be placed in S1 calcium sulfate, S1, S2, and S3 sodium sulfate exposure conditions. Special interest in the performance of ternary blends was selected as a key goal. The use of ultra fine fly ash (UFFA) was decided based on results from ASTM C 1012 testing completed in Phase I. Table 5.24 presents the mixtures completed to finish this study.

Table 5.24: Final mixtures for Outdoor Exposure Study.

Mix #	Cement	SCMs	w/cm
36	Type II	-	0.5
37	Type I	25% C 5SF	0.45
38	Type I	25% C 9% UFFA	0.45
39	Type I	25% C 9% UFFA	0.5
40	Type V	-	0.5

Physical Sulfate Testing

As previously discussed, the results of outdoor exposure tests have shown that physical sulfate attack may be a significant cause of distress, especially when considering exposure to sodium sulfate and for exposure conditions in which wicking action results in distress above the soil line. To further evaluate the physical form of sulfate attack, a separate study was initiated in which mortar specimens were immersed in different sulfate solutions and subjected to rapid temperature changes, the type of accelerated testing regime that Folliard and Sandberg (1994) found to be extremely damaging to concrete.

As described in Section 4.2.4, various mortar specimens were cast and immersed in different sulfate solutions (sodium sulfate or magnesium sulfate at concentrations of 10, 20, and 30%), then subjected to rapid temperature changes. Mortar mixtures with different w/cm ratios (0.4 and 0.7), different cement types (Type I and Type V), and with and without air-entraining agent were cast and tested. Mass loss was used as a simple index for quantifying distress.

Some general trends became quite evident after subjecting the various mortar specimens to over 150 cycles of temperature changes. Mortar mixtures with a w/cm of 0.4 showed very little distress, regardless of the cement type or sulfate solution in which they were exposed. Mortar mixtures with a w/cm of 0.7 exhibited significant distress, as manifested in substantial mass loss, when exposed to high concentrations of sodium sulfate solution, as shown in Figure 5.34. This figure shows the mass loss for mortar with a 0.7 w/cm containing Type V cement – similar distress was observed for Type I cement, further suggesting that this form of attack is physical in nature and not sensitive to cement chemistry. No distress was observed for any of the mortar specimens exposed to magnesium sulfate. This observation is consistent with the outdoor exposure site, where the only physical sulfate attack was observed for sodium sulfate.

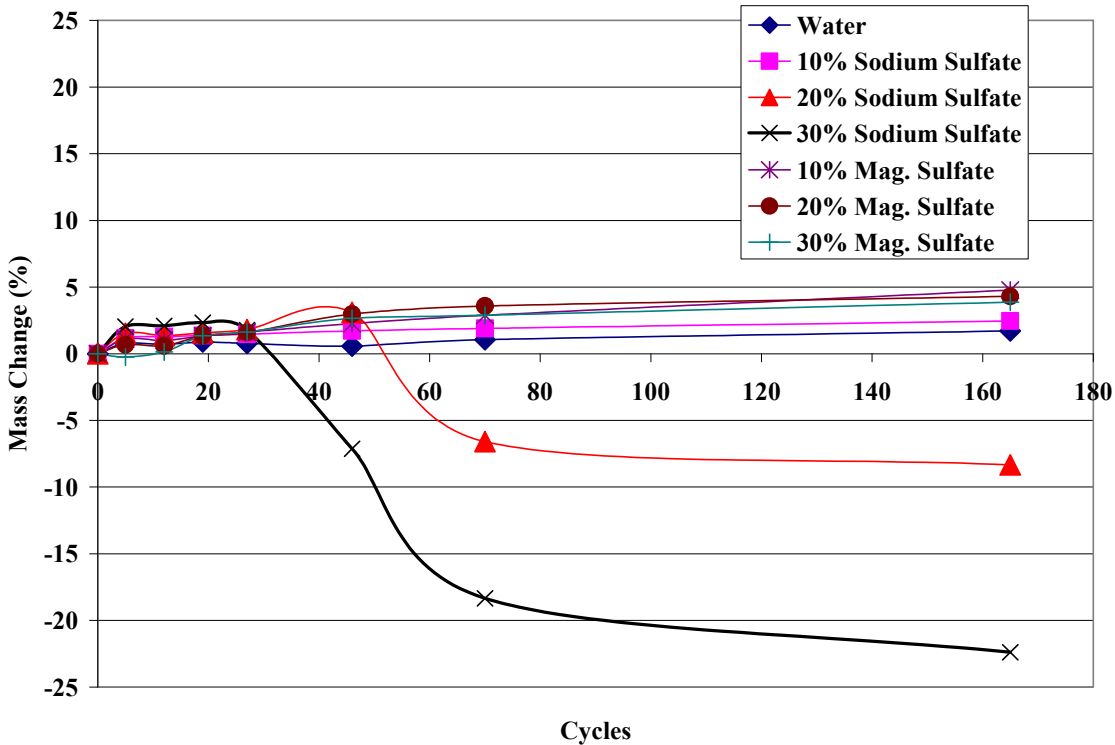


Figure 5.34: Physical sulfate testing of non-air-entrained mortars containing Type V cement ($w/cm=0.7$)

Figure 5.35 shows mass loss results for mortars ($w/cm=0.7$) containing either Type I or Type V cement and for each cement type, non-air-entrained and air-entrained mortars were evaluated. This graph shows that air entrainment slightly delays the onset of deterioration, but as was reported by Folliard and Sandberg (1994), air-entrained voids eventually become filled with sodium sulfate and their effectiveness in alleviating stresses caused by salt crystallization rapidly decreases. This graph also illustrates that the response to physical sulfate attack is quite similar between Type I and Type V cements, as previously discussed. Figure 5.36 shows the before and after images of a specimen that was damaged by physical sulfate attack in this testing regime.

In summary, the most important findings from this study on physical salt attack were that the best method of preventing distress is by using lower w/cm , that sodium sulfate is the main sulfate form causing physical sulfate attack, that cement type has little influence on distress, and that air entrainment provides short-term protection, but not long-term protection, against physical sulfate attack.

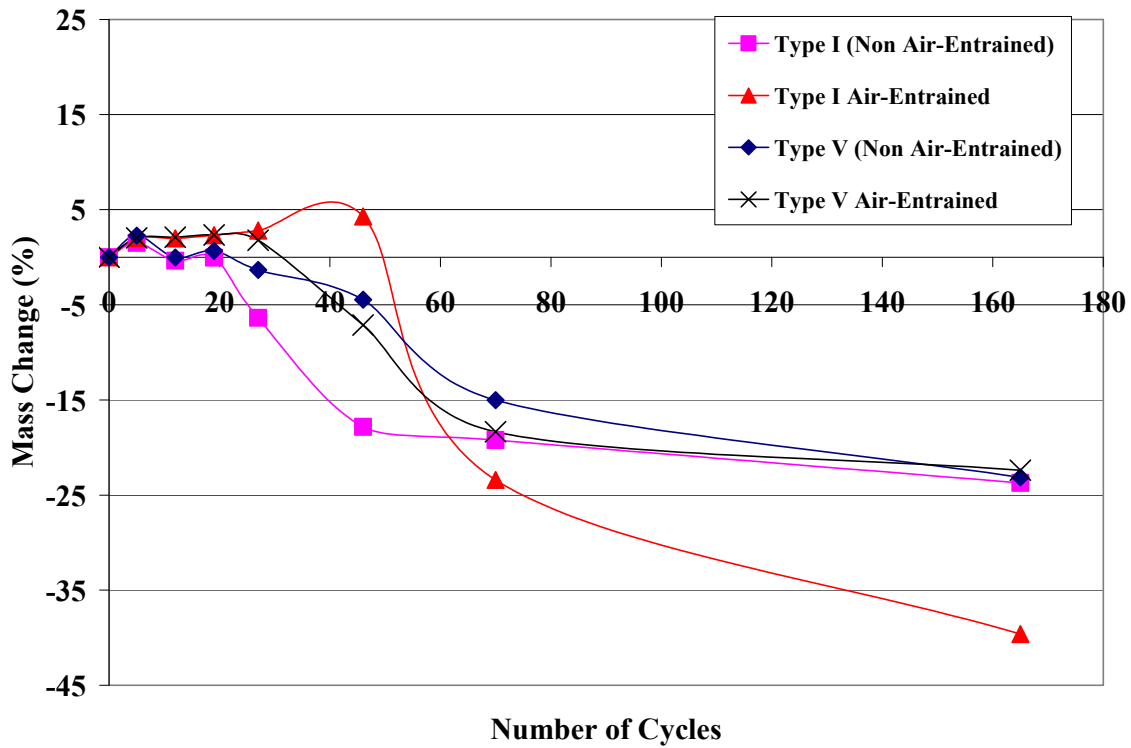


Figure 5.35: Physical sulfate testing of air-entrained and non-air-entrained mortars ($w/cm=0.7$) immersed in 30% sodium sulfate solution and subjected to temperature changes.



Figure 5.36: Mortar specimens before and after physical sulfate testing. The mixture contained Type V cement at 0.7 w/cm . The disk on the left was prior to testing and the disk on the right went through 150 cycles.

5.3 Discussion

In the majority of the concrete testing including outdoor and indoor conditions, prisms in sodium sulfate conditions performed the worst. According to expansion criteria, expansions were first observed in prisms placed in sodium sulfate conditions followed by those in magnesium sulfate. It is usually noted that magnesium is the most severe sulfate that attacks concrete due to the many hydration products that are attacked. However, aggressiveness of sodium sulfate in both mortar and concrete testing showed damage at earlier time periods. The formation of brucite is known to create a protective layer on prisms attacked by magnesium sulfate; which may suggest the delayed attack on the prisms. Mixtures in calcium sulfate did not expand past 0.1% expansion after 18 months in any concrete mixture; however, damage is noticed on the exterior of the prisms. The low solubility of gypsum does not get to the middle of the prisms to show appreciable expansions. The majority of the expansion is near the surface of the sample as shown by ettringite formation from XRD analysis and visibly by the deteriorated corners of the samples. Prisms submerged in the outdoor sodium sulfate conditions performed the worse of all the sodium sulfate conditions. These prisms performed worse than their counterparts indoors due to the wet/dry cycles that occur, extreme temperatures, and the physical sulfate attack.

The deterioration mechanism behind each of the conditions was clearly visible even without any analytical testing. Each of the sulfates deteriorated in different ways. Prisms placed in calcium sulfate began to deteriorate by scaling of the surface. Below the scaling, prisms were still sound, and did not show softening as noticed in the prisms placed in sodium and magnesium sulfate. Prisms placed in sodium sulfate conditions showed deterioration as evidenced by cracking along the corners of the prism before expansions began. A continual layered process of deterioration occurred with prisms in sodium sulfate. The layering attack was similar to findings by Gollop and Taylor (1994) which shows the progression of attack into the concrete from sodium sulfate. The corners eventually fell apart and more cracking occurred at the freshly exposed surface. Physical sulfate attack deterioration occurred on samples that were exposed to the atmosphere (no soil contact zone) in the sodium sulfate outdoor exposure condition. Magnesium sulfate caused a softening on the exterior of the prisms. Once expansion began, large cracks formed on the concrete, and unlike prisms in sodium sulfate, these prisms remained intact with the large cracks. Once significant expansion occurred (>1%), the prisms did eventually fall apart along these cracks.

Mixtures containing 40% Class C fly ash generally exhibited enhanced performance over mixtures containing 20% Class C fly ash, which was generally the opposite when testing similar mortar bars in ASTM C 1012. The curing regime between the mortar and concrete mixtures was different which might suggest reasoning behind the difference. Concrete mixtures were allowed to moist cure for 28 days prior to placement into each of their corresponding solutions. ASTM C 1012 testing provides an accelerated curing regime in a water bath for 24 hours followed by limewater storage until strength of 2850 psi (20 MPa) is achieved. The permeability may be lower for specimens after 28 days of wet curing especially with 40% Class C fly ash. Sulfate milling provided similar results in that ettringite formation was lower in specimens with 40% Class C fly ash.

Sulfate profiling by progressive milling provided an understanding of the chemical formation of hydration and reaction products forming in the different mixtures. In most mixtures, including those that did not exhibit expansion, ettringite formation was identified in the outer layer of the prism. Ettringite formation generally decreased further into the prisms; however, in some high w/cm mixtures, ettringite formation within the bulk of the specimen approached that

near the surface. Gypsum formation increased in content near the outer portion when expansions occurred. The increased gypsum formation is forming and not converting to ettringite if there is not a source of aluminate. The calcium hydroxide increased as the milling depth increased into concrete especially for prisms in sodium sulfate. The decreased depletion of calcium hydroxide did not allow further ettringite formation to occur further into prism. The profiling at regular intervals was a better technique than crushing the entire bulk mortar bar in chapter 3.

ASTM C 1012 mortar mixtures deteriorated more quickly with the addition of Class C fly ash. A large difference was noticed between mortar bar testing and concrete testing that had the same materials. Mortar bars expanded and deteriorated at a faster rate. The concrete prisms did not expand after 18 months where as their comparative mortar mixtures began to fail at 6 months. This was true for all three sulfate types tested. This difference in behavior may be attributed to differences in paste content, specimen size, curing conditions, or other factors. Also, a large disconnect was noticed in XRD compositions between mortars and concretes. Mortar bars provided ettringite contents in Chapter 3 between 40 and 65% which is much greater than those found in the concrete prisms. The paste volume is higher in the mortars which might suggest the greater formation of ettringite. Overall, disconnect does exist between laboratory testing and field concrete suffering from external sulfate attack. The worse conditions with concrete prisms placed in the outdoor sodium sulfate exposure site that had temperature effects responded better than mortar specimens stored indoors.

5.4 Conclusions

This chapter presented and discussed the results of concrete prisms exposed in an outdoor sulfate exposure site in Austin, Texas. Prisms constructed during Phase I were removed to measure the length and mass change for comparison to values last reported in Drimalas 2007.

The most significant findings from these measurements were:

- Concrete prisms constructed with Type I and Type II portland cement concrete without any SCMs showed considerable deterioration in the calcium sulfate outdoor exposure. Damage to these prisms was entirely in the region exposed to soil; above the soil line, no distress was visible on the prisms.
- Concrete prisms exposed to sodium and magnesium sulfate experienced an increased damage above the soil line due to physical sulfate attack. Many of these samples were more severely distressed because of physical sulfate attack than because of external sulfate attack.
- Concrete prisms constructed with Type V cement at a 0.4 w/cm in either a ternary blend or having used Class F fly ash exhibited outstanding performance in solutions containing sodium, magnesium, or calcium sulfate.

Phase II of the study focused on constructing additional outdoor exposure sites at concentrations not used in Phase I. Samples will be monitored for many years to provide an expanded database for external sulfate exposure testing. Findings from this phase of the project included:

- Concrete prisms exposed to S1 and S2 conditions expanded less than concrete prisms from Phase I, which were exposed to S3 conditions. The lower concentrations used for this study are more realistic of field conditions, but these

concentrations will require additional time to cause distress similar to what was seen in Phase I.

- Increasing the w/cm of the prisms caused an increase in the rate of distress to the prisms. This can be related to the increased permeability of the concrete.
- Concrete prisms exposed to S2 conditions in sodium sulfate had the most damage at one year of exposure. These samples had also begun to show signs of physical sulfate attack above the soil line at one year of exposure.

Chapter 6. Sulfate Resistance of High-Calcium Fly Ash Concrete

6.1 Introduction

Chapter 6 provides a summary of a study on the sulfate resistance of high-calcium fly ash concrete that was conducted at the University of New Brunswick (UNB) between September 2005 and August 2009. The study was funded under subcontract from The University of Texas at Austin (UTA) and the funding source was the Texas Department of Transportation (TxDOT) under TxDOT Project 4889, “Sulfate Resistance of Concrete Exposed to External Sulfate Attack.” Full details of the work conducted at UNB were reported in the PhD Dissertation of Dhole (2009).

The UNB study was divided into five phases¹ as follows:

Phase I Combined Physical-Chemical Sulfate Attack on Concrete

Phase II Sulfate Resistance of Mortars Containing Class C Fly Ash Blended with Other Pozzolans

Phase III Strategies for Increasing the Sulfate Resistance of Mortars Containing Class C Fly Ash: Gypsum Addition, Low w/cm and HVFA

Phase IV Characterization of Class C Fly Ashes

Phase V Analysis of Fly Ash Hydration Products in Sulfate Environments

A summary of the details and key findings of each of the five phases is presented next. The overall findings of this study, coupled with the research at The University of Texas at Austin, were synthesized and integrated into the recommendations and guidance provided in the final chapter of this report.

6.2 Materials

Most of the cementing materials used in this study were provided by UTA and are sub-samples of the samples collected and used by Drimalas (2007). Table 6.1 lists brief details of the materials including the C₃A content of the cement and the CaO content of the fly ashes. The table also provides details of where the full chemical analysis of each material can be found in Dhole’s (2009) thesis.

¹ These five phases are reported as Chapters 3 to 7 in the PhD Thesis of Dhole (2009)

Table 6.1: Details of Cementing Materials

Material	Designation	Chemistry	Full Analysis ¹
Portland Cement	PC	11% C ₃ A	Table 3.1
Fly Ashes	BF	1.10% CaO	Table 4.1
	UFFA	10.85%	Table 4.2
	RL	12.76% CaO	Table 3.1
	HN	21.58% CaO	Table 7.1
	TK	23.54% CaO	Table 3.1
	BC	26.92% CaO	Table 4.1
	PS	27.49% CaO	Table 4.1
	WL	28.98% CaO	Table 3.1
	Silica Fume	93.17% SiO ₂	Table 3.1

¹Full analysis available in PhD Thesis of Dhole (2009)

Aggregates used for the production of concrete were siliceous sand and gravel meeting the requirements of ASTM C 33. The sand used for the production of mortars was graded Ottawa silica sand meetings the requirements of ASTM C 778 for graded sand.

6.3 Combined Physical-Chemical Sulfate Attack on Concrete (Phase 1)

In this phase of testing concrete samples were subjected to cyclic wetting and drying in sulfate solution. Five exposure conditions were used as follows:

1. Static Na₂SO₄ exposure (NSS) – 3 prisms were continuously immersed in a solution of 5% Na₂SO₄ at a constant temperature of 21°C (70°F).
2. Static CaSO₄ exposure (CSS) – 3 prisms were continuously immersed in a solution saturated with CaSO₄ at a constant temperature of 21°C (70°F). The saturated solution was prepared by adding CaSO₄ (50g/L) to distilled water. The measured concentration of CaSO₄ in the solution was approximately 2240 ppm. The remaining CaSO₄ produced a solid reservoir.
3. Cyclic Na₂SO₄ exposure (NSD) – 3 prisms were exposed to alternate cycles of immersion in 5% Na₂SO₄ at a constant temperature of 21°C (70°F) for 24 hours and drying in air at 38°C (100°F) for 72 hours.
4. Cyclic CaSO₄ exposure (CSD) - 3 prisms were exposed to alternate cycles of immersion in saturated CaSO₄ solution at a constant temperature of 21°C (70°F) for 24 hours and drying in air at 38°C (100°F) for 72 hours. The saturated CaSO₄ solution was prepared in the same way as for the static CaSO₄ exposure.
5. Two prisms were immersed in water at 21°C (70°F).

Twenty-two concrete mixes were produced with combinations of Type I cement, Class C and Class F fly ashes, UFFA and silica fume, and using w/cm in the range of 0.40 to 0.70. A summary of the mixes is presented in Table 6.2 and full details (materials and proportions) are provided in Tables 6.2 and 6.3 of Dhole (2009).

Table 6.2: Summary of Concrete Mixes

Mix Designation	w/cm	First SCM	Second SCM	Third SCM
Control 40	0.40			
Control 45	0.45			
Control 50	0.50			
Control 70	0.70			
WL4040	0.40	40% WL		
WL2040	0.40	20% WL		
TK4070	0.70	40% TK		
TK2070	0.70	20% TK		
TK 4045	0.45	40% TK		
TK 2045	0.45	20% TK		
TK4040	0.40	40% TK		
TK2040	0.40	20% TK		
RL 4050	0.50	40% RL		
RL 2050	0.50	20% RL		
RL 4040	0.40	40% RL		
RL 2040	0.40	20% RL		
TKRL 15100-50	0.50	15% TK	10% RL	
TKRL 15100-40	0.40	15% TK	10% RL	
TKRL 15104-50	0.50	15% TK	10% RL	4% Silica Fume
TKRL 15104-40	0.40	15% TK	10% RL	4% Silica Fume
TK 2040 SF5	0.40	20% TK	5% Silica Fume	
TK 3040 UFFA	0.40	30% TK	9% UFFA	

Wet-dry cycling was performed in an automated set up to provide a 1-day soak period at 21°C (100°F) followed by a 3-day drying period in air at 38°C (100°F).

The performance of the concrete mixes was studied by monitoring the changes in mass, length, and dynamic modulus of elasticity of specimens over time.

Data for control mixes with w/cm = 0.40, 0.45, 0.50 and 0.70 are shown in Figures 6.1 to 6.6. Clearly the w/cm is very influential in determining the extent of expansion and deterioration. For the control concrete with w/cm = 0.40 there was no significant expansion for specimens after 180 wet-dry cycles in either Na₂SO₄ or CaSO₄ and the dynamic modulus actually increased with time. There was a small mass loss (~ 2%) for specimens after 180 cycles in Na₂SO₄ solution (NSD) and this was manifested as slight spalling at the edges and corners of specimens. Little damage was observed for specimens from the same mix that were continuously immersed in Na₂SO₄ (NSS) or CaSO₄ (CSS) although a small expansion (0.11 to 0.13%) and minor spalling at the edges and corners was observed after 750 days (Figure 6.5). Little difference was observed between in the performance of concrete with w/cm = 0.40 and 0.45 as the expansion and changes in dynamic modulus were similar in all four sulfate environments. However, specimens from the mix with w/cm = 0.45 did exhibit slightly greater mass loss and show more visible signs of damage in the Na₂SO₄ solution (NSS) compared with concrete with w/cm = 0.40 (see Figure 6.5).

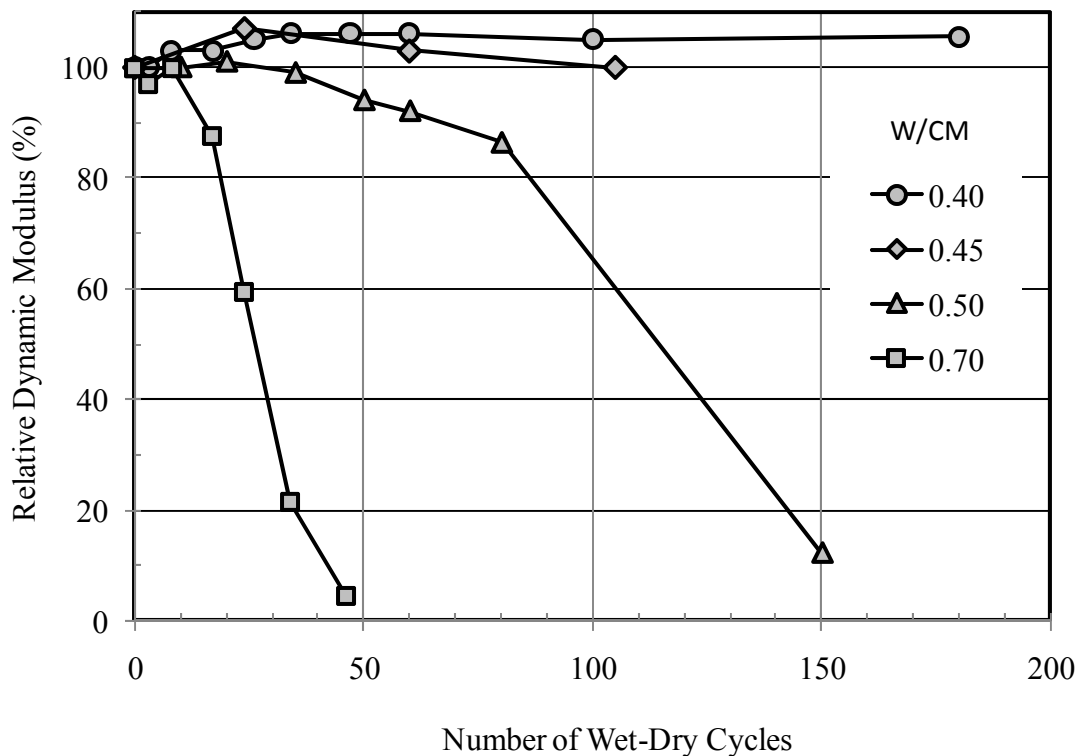


Figure 6.1: Effect of w/cm on the Change in Relative Dynamic Modulus of Control Mixes Exposed to Wet-dry Cycling in 5% Na_2SO_4 Solution (NSD)

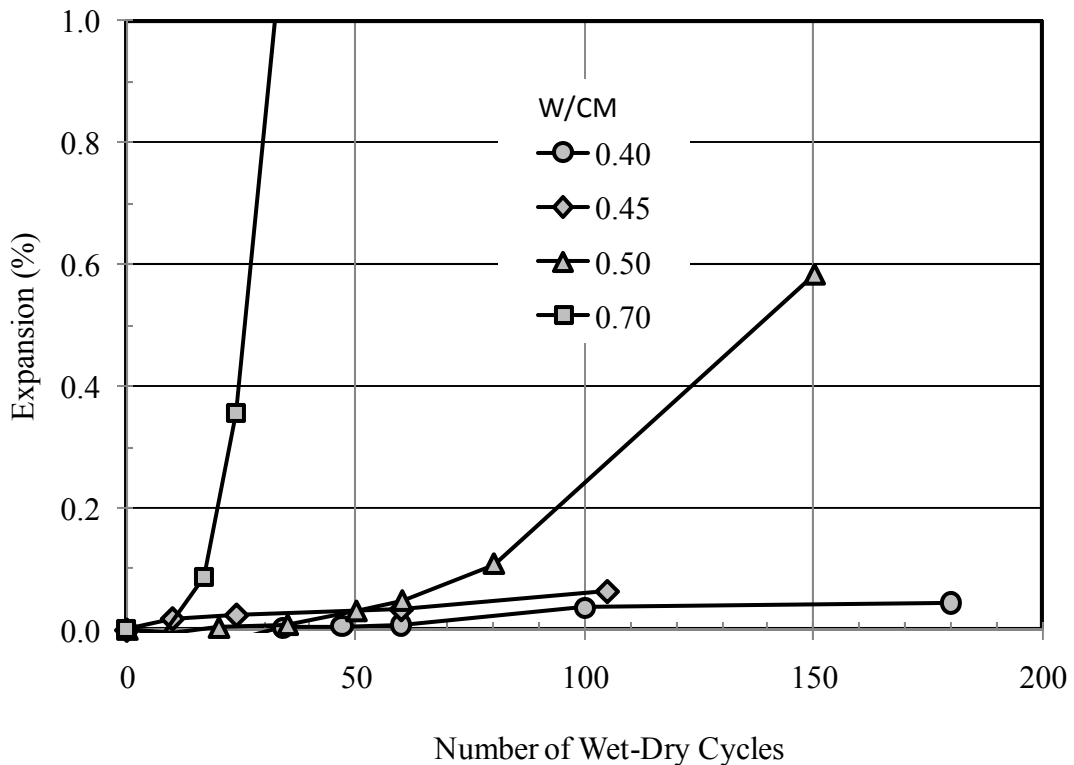


Figure 6.2: Effect of w/cm on the expansion of Control Mixes Exposed to Wet-Dry Cycling in 5% Na_2SO_4 Solution (NSD)

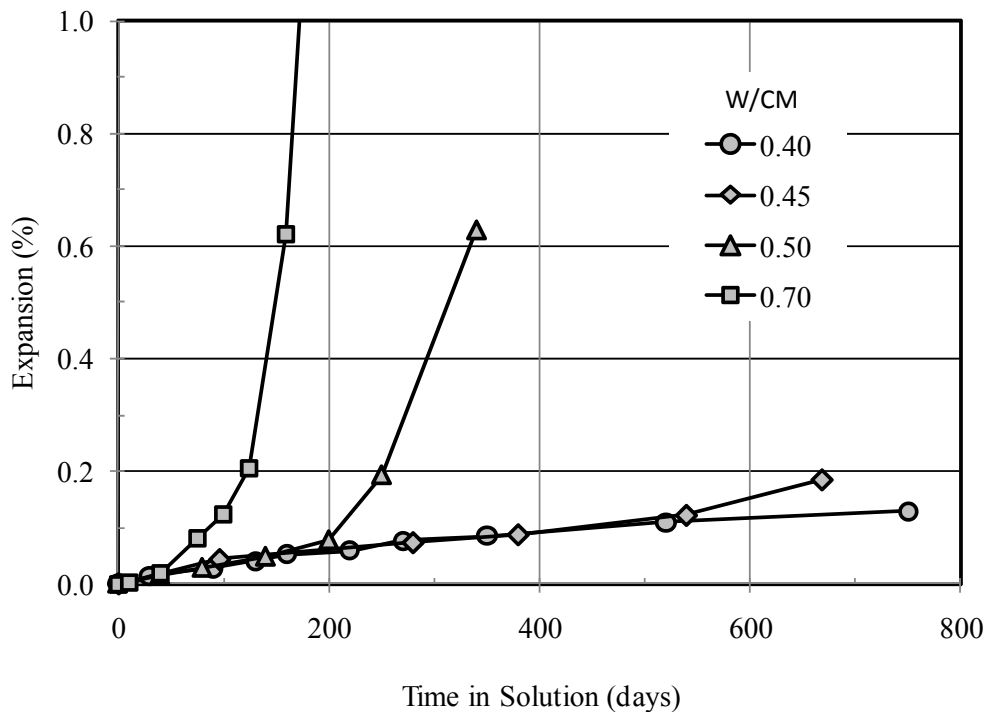


Figure 6.3: Effect of w/cm on the Expansion of Control Mixes Immersed in 5% Na_2SO_4 Solution (NSS)

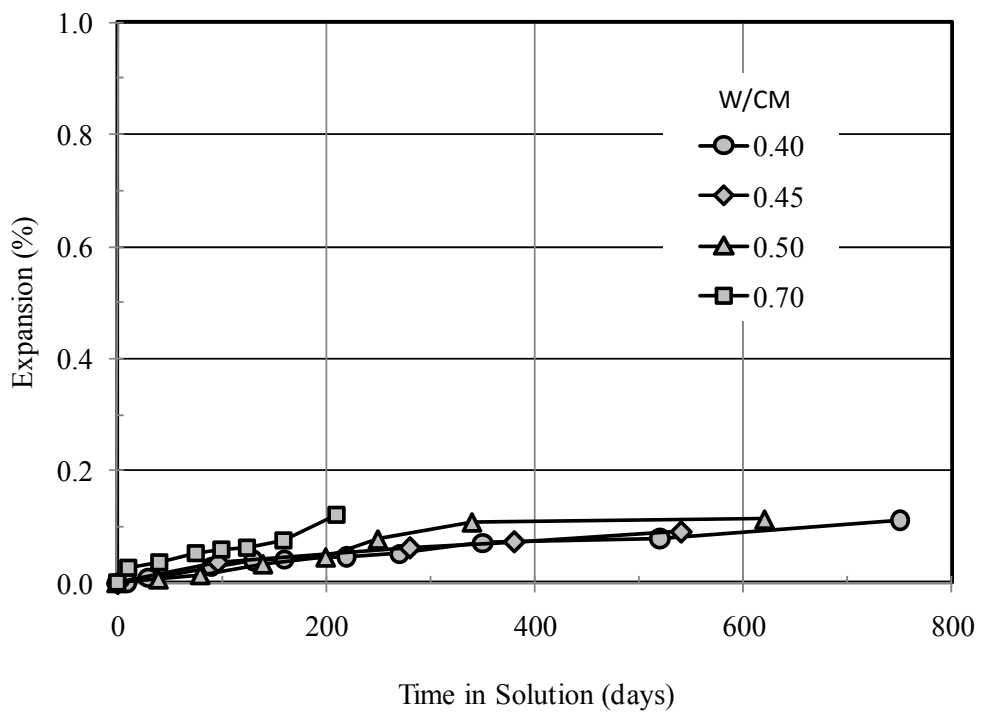


Figure 6.4: Effect of w/cm on the Expansion of Control Mixes Immersed in Saturated- CaSO_4 Solution (CSS)



w/cm = 0.70, 200 days in Na_2SO_4



w/cm = 0.50, 320 days in Na_2SO_4



w/cm = 0.45, 280 days in Na_2SO_4



w/cm = 0.40, 520 days in Na_2SO_4

Figure 6.5: Visual Appearance of Control Mixtures after Immersion in 5% Na_2SO_4 Solution (NSS)



w/cm = 0.70, 200 days in static CaSO_4



w/cm = 0.50, 320 days in static

Figure 6.6: Visual Appearance of Control Mixtures after Immersion in Saturated CaSO_4 Solution (CSS)

Specimens from mixes with $w/cm = 0.50$ started to deteriorate after approximately 75 wet-dry cycles in 5% Na_2SO_4 solution (NSD) and after about 200 days immersion in Na_2SO_4 (NSS). Little significant deterioration was observed for specimens subjected to cyclic wetting and drying in saturated CaSO_4 solution (CSD) although a significant mass loss (5%) was observed after just over 600 days immersion in saturated CaSO_4 solution (CSS). Specimens from the control mix with $w/cm = 0.70$ deteriorated more rapidly showing significant expansion and reduction in dynamic modulus after just 25 cycles in NSD and 200 days immersion in NSS.

As expected significantly more deterioration (expansion, mass loss, and reduction dynamic modulus) occurred with concrete exposed to sodium sulfate (NSS and NSD) as compared with calcium sulfate solution (CSS and CSD). Indeed, none of concrete mixes showed significant signs of damage when exposed to cyclic wet-dry cycles in CaSO_4 solution (CSD) and the damage that occurred in continuous immersion in CaSO_4 solution (CSS) was limited to softening and scaling of the surfaces with some mass loss at the corners and edges of some mixes with higher w/cm ; expansion was generally close to or less than 0.10%.

Figures 6.7 and 6.8 show data for concretes with fly ash TK (23.54% CaO) in NSD exposure. Concretes with $w/cm = 0.40$ and 0.45 provide satisfactory performance for 60 wet-dry cycles, whereas concrete with $w/cm = 0.70$ deteriorated rapidly. Figures 6.9 and 6.10 show similar data for fly ashes WL (28.98% CaO) and RL (12.76% CaO). Mix WL4040 with 40% WL fly ash and $w/cm = 0.40$ started to deteriorate after approximately 30 to 40 cycles and was severely deteriorated after 60 cycles. This mix was the only concrete with SCM and $w/cm \leq 0.45$ that showed expansion $> 0.15\%$ or a reduction in the relative dynamic modulus $> 20\%$ after 60 wet-dry cycles.

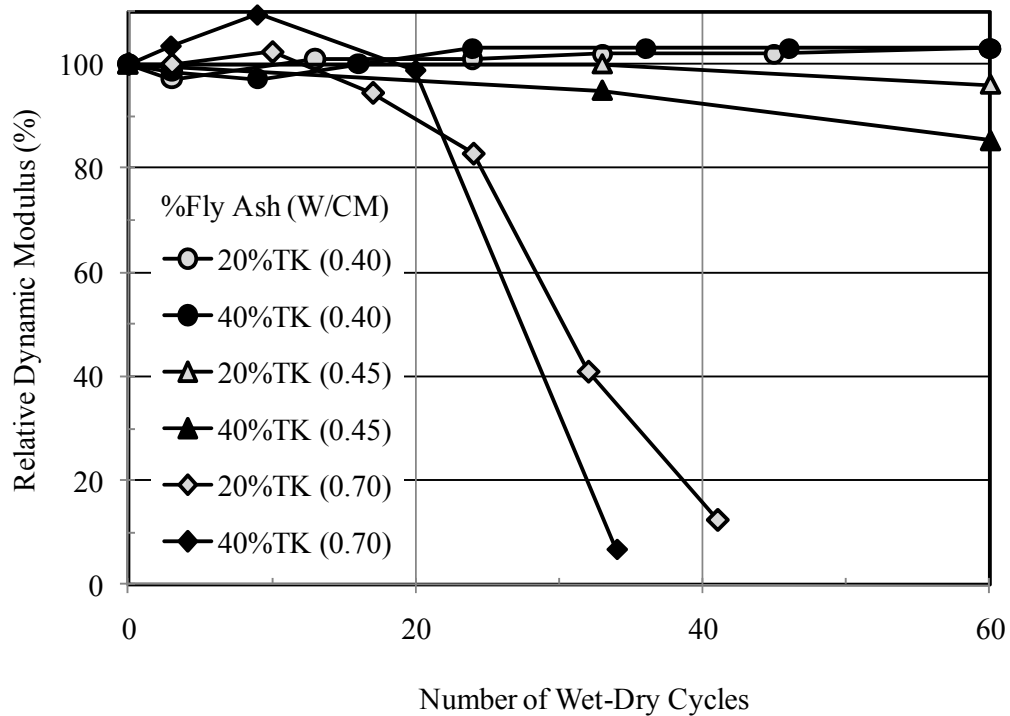


Figure 6.7: Change in Relative Dynamic Modulus of Concrete with TK Fly Ash (23.54% CaO) Exposed to Wet-Dry Cycling in 5% Na_2SO_4 Solution (NSD)

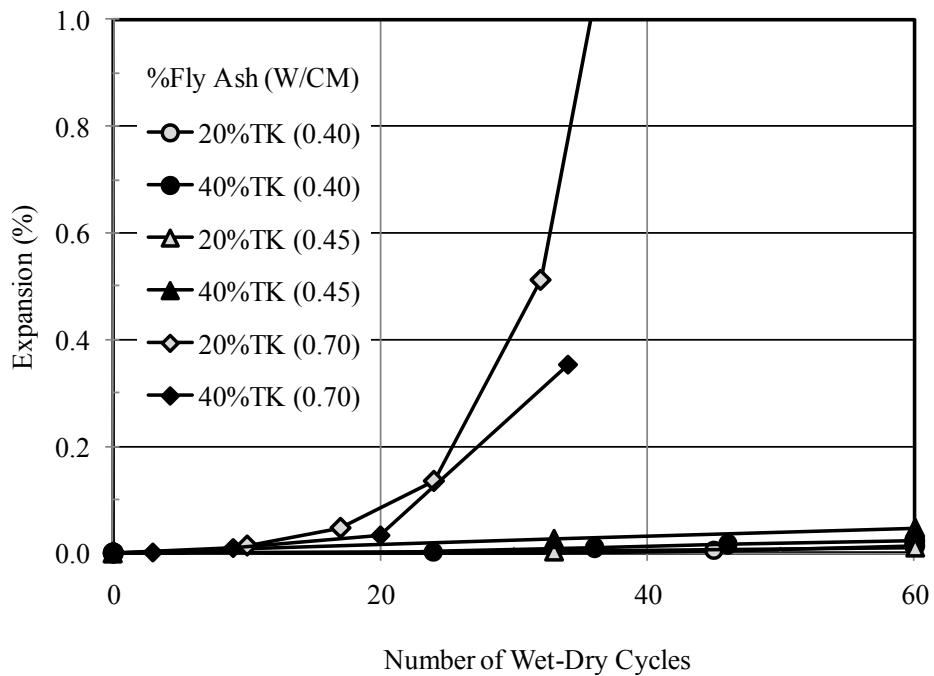


Figure 6.8: Expansion of Concrete with TK Fly Ash (23.54% CaO) Exposed to Wet-Dry Cycling in 5% Na_2SO_4 Solution (NSD)

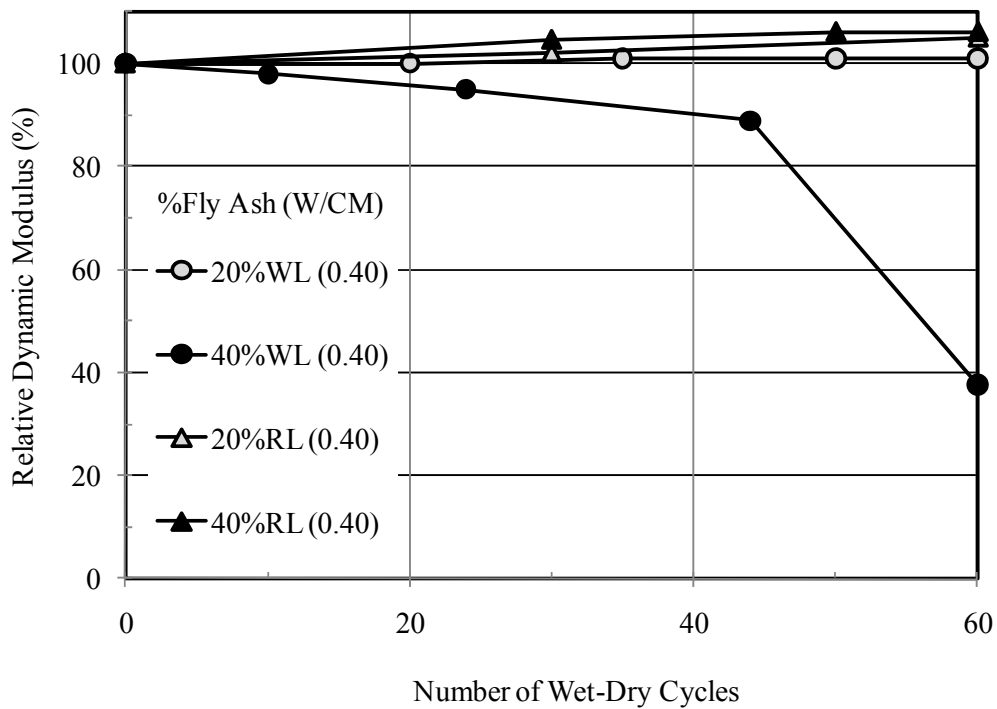


Figure 6.9: Change in Relative Dynamic Modulus of Concrete with Fly Ash WL (28.98% CaO) and RL (12.76% CaO) Exposed to Wet-Dry Cycling in 5% Na_2SO_4 Solution (NSD)

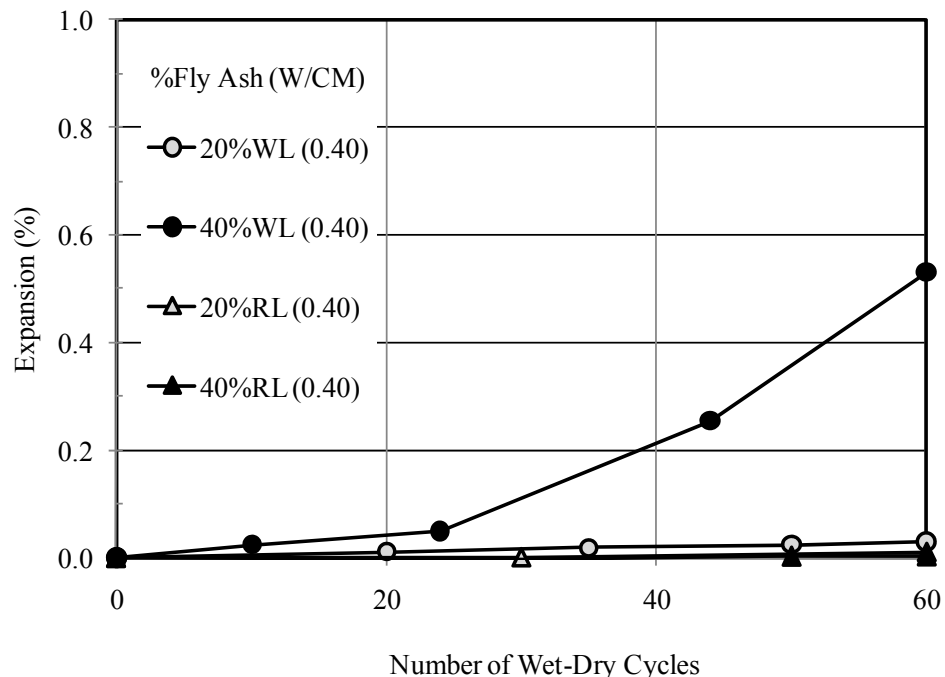


Figure 6.10: Expansion of Concrete with Fly Ash WL (28.98% CaO) and RL (12.76% CaO) Exposed to Wet-Dry Cycling in 5% Na_2SO_4 Solution (NSD)

Figure 6.11 and 6.12 show the expansion of the same concrete mixtures in NSS exposure. All of the concretes with $w/cm \leq 0.45$, even WL4040, expanded $< 0.15\%$ during the test period. On the other hand, mixes with TK fly ash and $w/cm = 0.70$ deteriorated rapidly in NSS exposure.

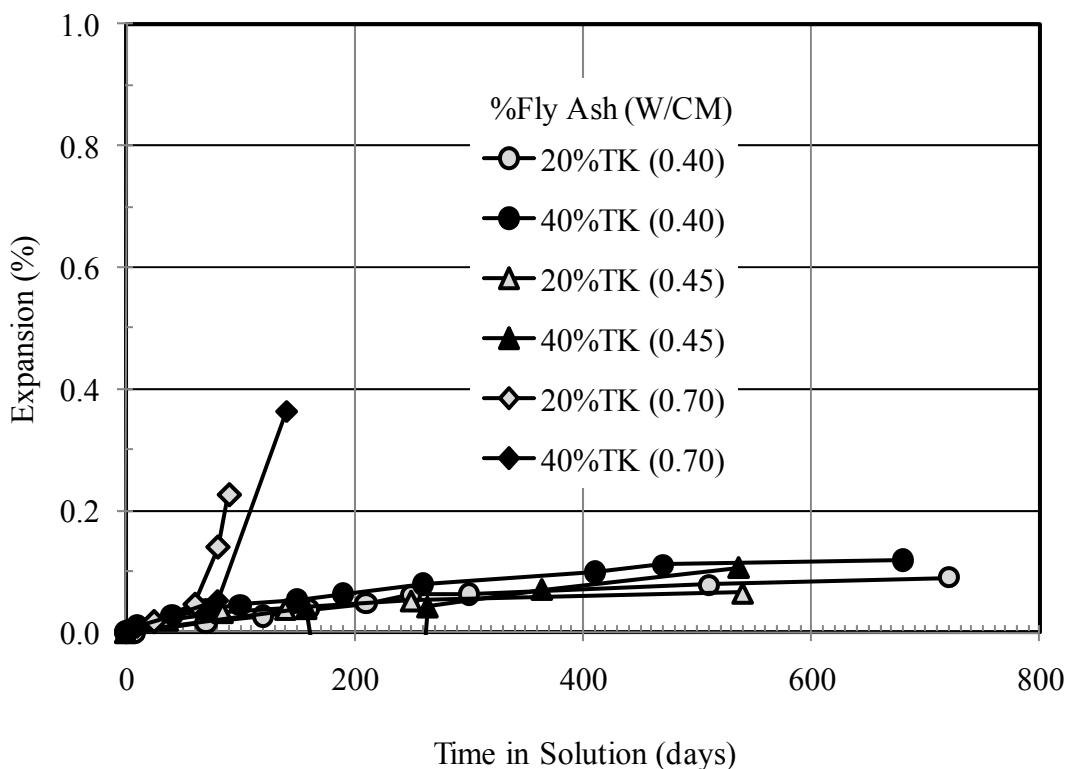


Figure 6.11: Expansion of Concrete with Fly Ash TK (23.54% CaO) Immersed in 5% Na_2SO_4 Solution (NSS)

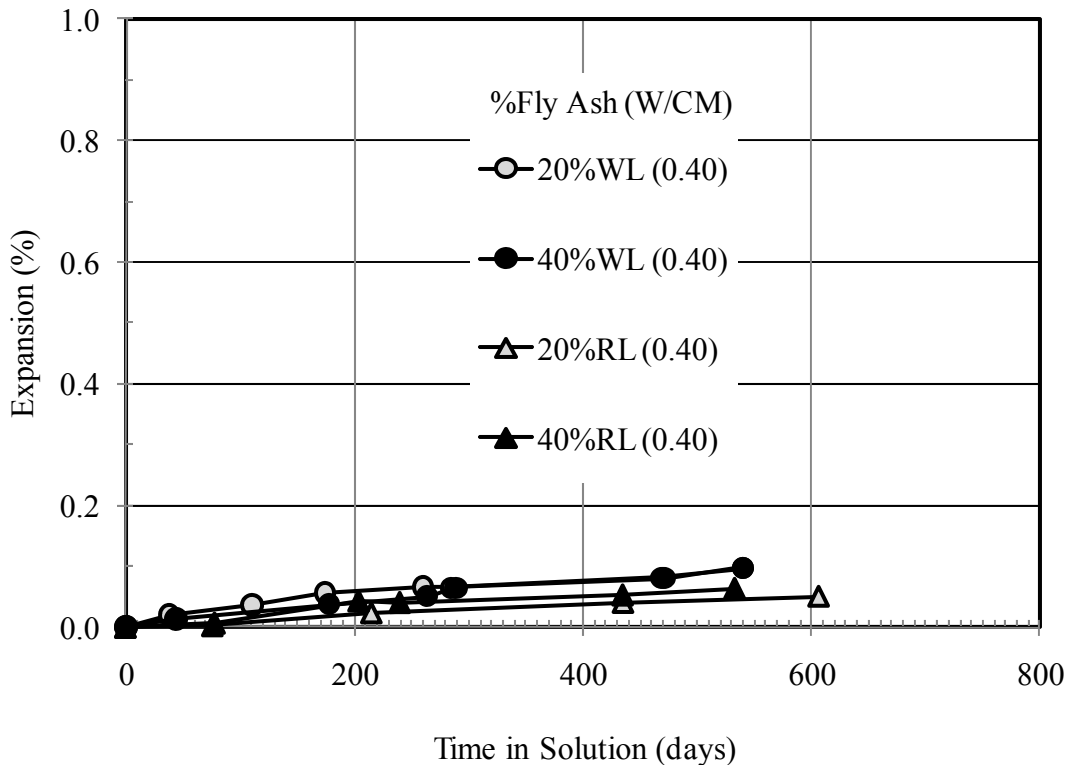


Figure 6.12: Expansion of Concrete with Fly Ash WL (28.98 CaO) and RL (12.76% CaO) Immersed in 5% Na_2SO_4 Solution (NSS)

Summary expansion data for NSD, NSS and CSS exposures and changes in relative dynamic modulus for NSD and NSS exposure are shown in Figures 6.13 and 6.14, respectively. In each case, the last data point before the end of test or before the sample completely deteriorated is shown. Consequently, the number of cycles or the duration of immersion may differ between mixes. With the exception of Mix WL4040, all of the mixes with $w/cm \leq 0.45$ behave in a similar manner in these exposure conditions. As discussed above, Mix WL4040 deteriorated in cyclic exposure (NSD), but not when continuously immersed (NSS). Mix TKRL15100-50 with 15% TK and 10% RL fly ashes and $w/cm = 0.50$ showed the opposite trend. This mix expanded significantly during immersion (0.47% after 500 days in NSS) but not during wet-dry cycling (NSD). However, it was unusual that the expansion was not accompanied by a reduction in the relative dynamic modulus.

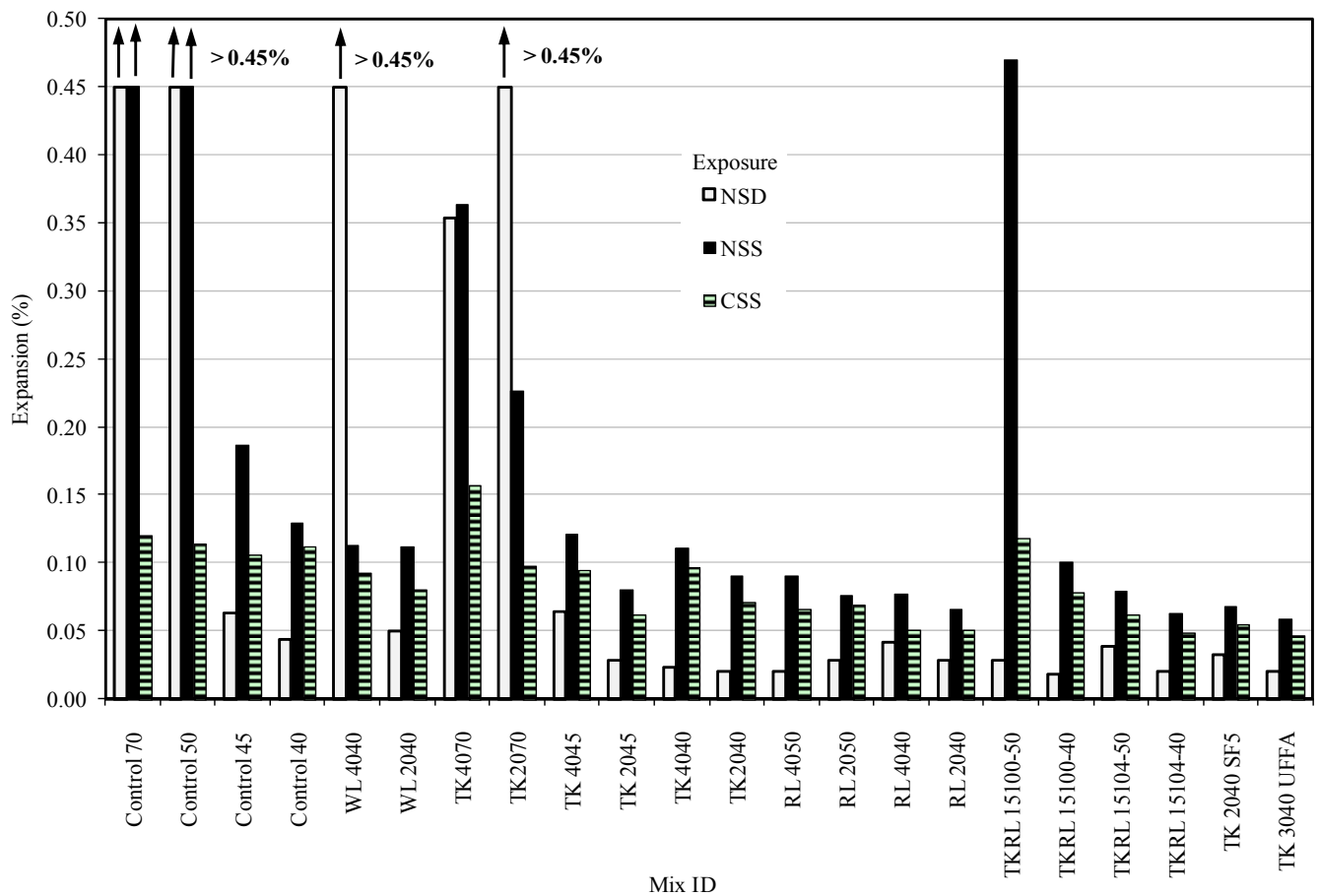


Figure 6.13: Summary of Expansion Data for Concrete Mixes

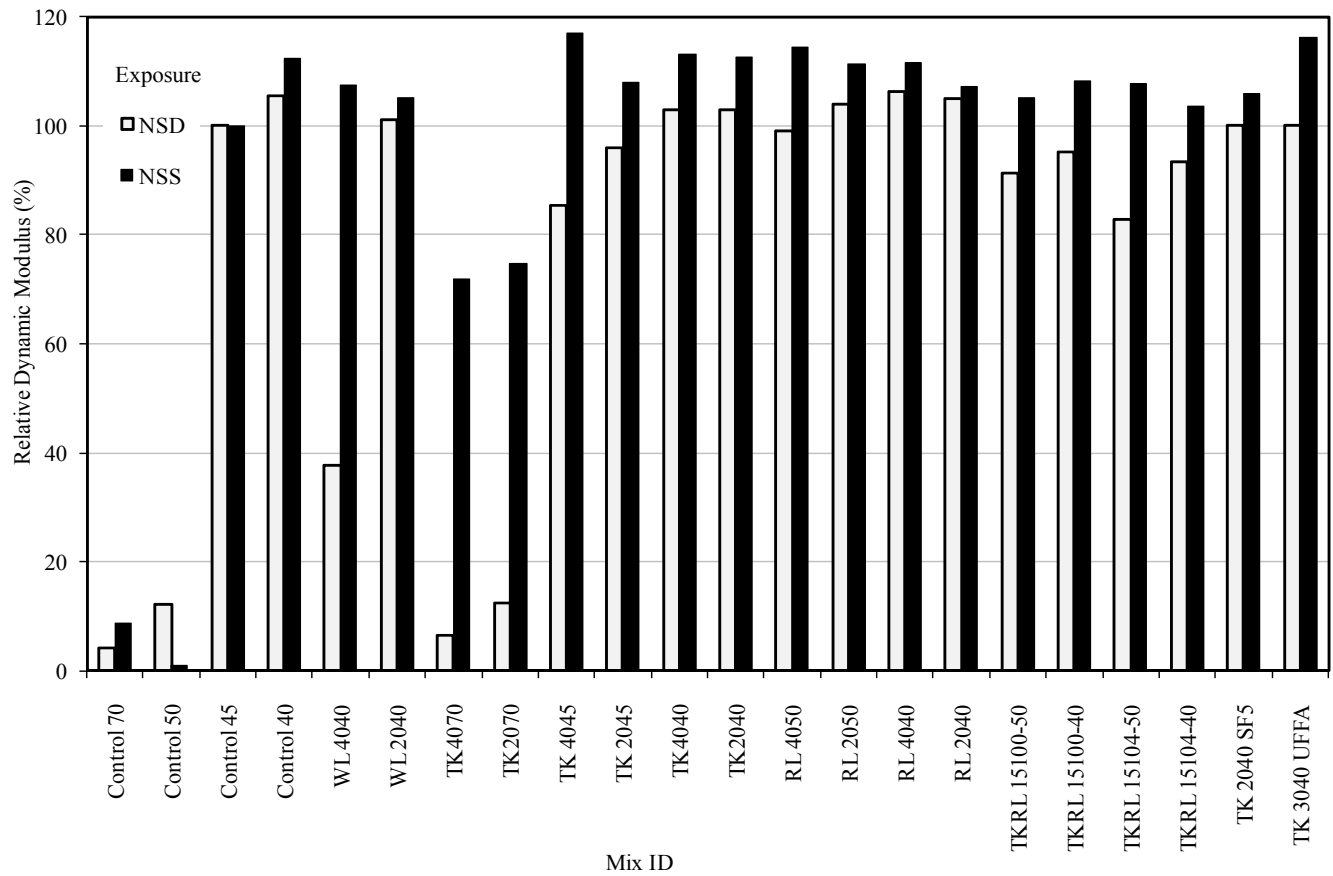


Figure 6.14: Summary of Relative Dynamic Modulus Data for Concrete Mixes

Dhole (2009) ranked the 22 mixes according to the performance of the concrete in the four exposure environments using the criteria in Table 6.3. Table 6.4 presents the results of the ranking exercise. The two mixes containing a ternary blend of portland cement, TK fly ash and either silica fume (SF) or ultra-fine fly ash (UFFA) performed the best. These mixes showed a very small amount of expansion (0.050 to 0.075%), but no sign of visual deterioration or loss of relative dynamic modulus. Concrete with 20 or 40% RL (Class F) fly ash also performed well, especially with $w/cm = 0.40$. The combination of TK and RL (Class C and Class F) fly ash provided satisfactory performance at $w/cm = 0.40$. The ranking highlights the importance of the water-to-cementing materials even in the relatively small range from 0.40 to 0.50 and provides support for maintaining the $w/cm \leq 0.45$ for concrete exposed to sulfates.

Table 6.3: Performance Criteria

Rating	Visual Observation	Expansion (%)	Relative Dynamic Modulus (%)
0	No damage	< 0.050	> 100
1	Slight loss of corners	0.050 to 0.075	95 to 100
2	Loss of corners & edges	0.075 to 0.100	90 to 95
3	Significant loss of mass & softening	0.100 to 0.200	80 to 90
4	Cracking and spalling	0.200 to 0.300	60 to 80
5	Complete deterioration	> 0.300	< 60

Table 6.4: Ranking of Concrete Based on Performance

Rank	Mix Designation	Performance in Na₂SO₄	Performance in CaSO₄
1	TK 3040 UFFA	1	0
2	TK 2040 SF5	1	1
3	RL 2040	2	0
4	TK2040	2	1
5	RL 2050	2	1
6	RL 4040	2	1
7	TKRL 15104-40	3	0
8	TKRL 15100-40	3	2
9	TK4040	4	2
10	RL 4050	5	1
11	TKRL 15104-50	5	1
12	WL 2040	5	2
13	TK 2045	7	2
14	Control 40	8	4
15	Control 45	10	5
16	TKRL 15100-50	11	3
17	TK 4045	13	3
18	WL 4040	22	3
19	Control 50	28	9
20	TK4070	29	3
21	TK2070	29	4
22	Control 70	30	6

6.4 Sulfate Resistance of Mortars Containing Class C Fly Ash Blended with Other Pozzolans

In this phase of testing 49 combinations of fly ash, ultrafine fly ash and silica fume were tested in mortar bars exposed to 5% Na₂SO₄ solution in accordance with test method ASTM C 1012. Details of the mixtures and the expansion results at 6, 12 and 18 months are presented in Tables 6.5 to 6.7.

Table 6.5: Details of Binary Mixes with Class F or Class C Fly Ash for ASTM C 1012 Tests

Mix No.	Mix ID	Class C (Type, %)	Class F (Type, %)	Exp (%) at 6m	Exp (%) at 12m	Exp (%) at 18m
1	TK 25	TK 25.0	-	0.083	0.366	Fail
2	BC 25	BC 25.0	-	0.272	>0.326	Fail
3	PS 30	PS 30.0	-	0.125	>0.572	Fail
4	WL 75	WL7.5	-	0.159	Fail	-
5	WL 15	WL 15.0	-	0.182	Fail	-
6	WL 225	WL22.5	-	0.283	Fail	-
7	WL 30	WL 30.0	-	0.458	Fail	-
8	RL 75	-	RL 7.5	0.108	0.656	Fail
9	RL 15	-	RL 15.0	0.065	0.115	0.189
10	RL 225	-	RL 22.5	0.059	0.090	0.108
11	RL 25	-	RL 25.0	0.060	0.085	0.115
12	RL 30	-	RL 30.0	0.065	0.096	0.117
13	BF 25	-	BF 25.0	0.058	0.086	0.118

Table 6.6: Details of Ternary Mixtures with Blends of Class F and Class C Fly Ash for ASTM C 1012 Tests

Mix	Mix ID	Class C (Type, %)	Class F (Type, %)	Exp % at 6m	Exp % at 12m	Exp % at 18m
1	Control	0	0	0.155	> 1.36 %	Fail
2	TKRL 2005	TK 20	RL 5	0.080	0.184	0.479
3	TKRL 1510	TK 15	RL 10	0.082	0.180	0.440
4	TKRL 1015	TK 10	RL 15	0.078	0.152	0.382
5	TKRL 0520	TK 5	RL 20	0.060	0.085	0.118
6	BCBF 2005	BC 20	BF 5	0.153	0.242	Fail
7	BCBF 1510	BC 15	BF10	0.073	0.164	0.586
8	BCBF 1015	BC 10	BF15	0.068	0.124	0.270
9	BCBF 0520	BC 5	BF 20	0.068	0.107	0.226
10	PSRL 75225	PS 7.5	RL 22.5	0.053	0.085	0.114
11	PSRL 1515	PS 15	RL 15	0.065	0.150	0.192
12	PSRL 22575	PS 22.5	RL 7.5	0.091	>0.275	Fail
13	WLRL 75225	WL 7.5	RL 22.5	0.072	0.114	0.155
14	WLRL 1515	WL 15	RL 15	0.065	0.107	0.182
15	WLRL 22575	WL 22.5	RL 7.5	0.075	0.148	0.547

Table 6.7: Details of Mixes with Blends of Fly Ash, Ultra-Fine Fly Ash and Silica Fume for ASTM C 1012 Tests

Mix	Mix ID	Class C (Type, %)	Class F (Type, %)	UFFA %	SF %	Exp % 6m	Exp % 12m	Exp % 18m
1	WLUFFA 2010	WL 20	0	10	-	0.047	0.051	0.052
2	WLUFFA 3010	WL 30	0	10	-	0.054	0.061	0.063
3	WLUFFA 4010	WL 40	0	10	-	0.063	0.069	0.069
4	PSSF 3006	PS 30	0	-	6	0.056	0.084	0.110
5	TKSF2005	TK 20	0	-	5	0.042	0.074	0.261
6	TKSF3005	TK 30	0	-	5	0.034	0.074	0.138
7	WLRL 75225SF3	WL 7.5	RL 22.5	-	3	0.049	0.076	0.102
8	WLRL 1515SF3	WL 15	RL 15	-	3	0.054	0.087	0.119
9	WLRL 22575SF3	WL 22.5	RL 7.5	-	3	0.058	0.099	0.163
10	WLRL 75225SF6	WL 7.5	RL 22.5	-	6	0.037	0.064	0.084
11	WLRL 1515SF6	WL 15	RL 15	-	6	0.042	0.068	0.088
12	WLRL 22575SF6	WL 22.5	RL 7.5	-	6	0.044	0.074	0.096
13	TKRL 75225SF3	TK 7.5	RL 22.5	-	3	0.039	0.075	0.106
14	TKRL 1515SF3	TK 15	RL 15	-	3	0.043	0.078	0.105
15	TKRL 22575SF3	TK 22.5	RL 7.5	-	3	0.053	0.086	0.118
16	TKRL 75225SF6	TK 7.5	RL 22.5	-	6	0.026	0.054	0.074
17	TKRL 1515SF6	TK 15	RL 15	-	6	0.029	0.057	0.076
18	TKRL 22575SF6	TK 22.5	RL 7.5	-	6	0.029	0.058	0.079
19	PSRL 75225SF6	PS 7.5	RL 22.5	-	6	0.038	0.066	0.088
20	PSRL 1515SF6	PS 15	RL 15	-	6	0.041	0.072	0.089
21	PSRL 22575SF6	PS 22.5	RL 7.5	-	6	0.052	0.075	0.093

According to ASTM C 595 specification for blended cements and ASTM C 1157 performance specification for hydraulic cements sulfate resistant cements should meet the following criteria:

Type of Cement	Maximum Expansion (%)	
	At 6 months	At 12 months
Moderate sulfate-resistance, Type MS	0.10	-
High sulfate-resistance, Type HS	0.05	0.10

Figure 6.15 shows the expansion of mortars produced with binary blends of high-C₃A (11%) portland cement and 25 to 30% fly ash (Class F and Class C). The data in the figure and in Table 6.5 indicate that blends with Class F fly ashes will meet the 12-month requirement for Type HS cement provided sufficient fly ash is present in the blend (> 20%), whereas blends with Class C fly ash do not meet sulfate-resistance requirements. Note that the mixture with 25% TK fly ash did meet the 6-month requirement for Type MS cement, but the mortar bars subsequently expanded rapidly and disintegrated shortly after 12 months.

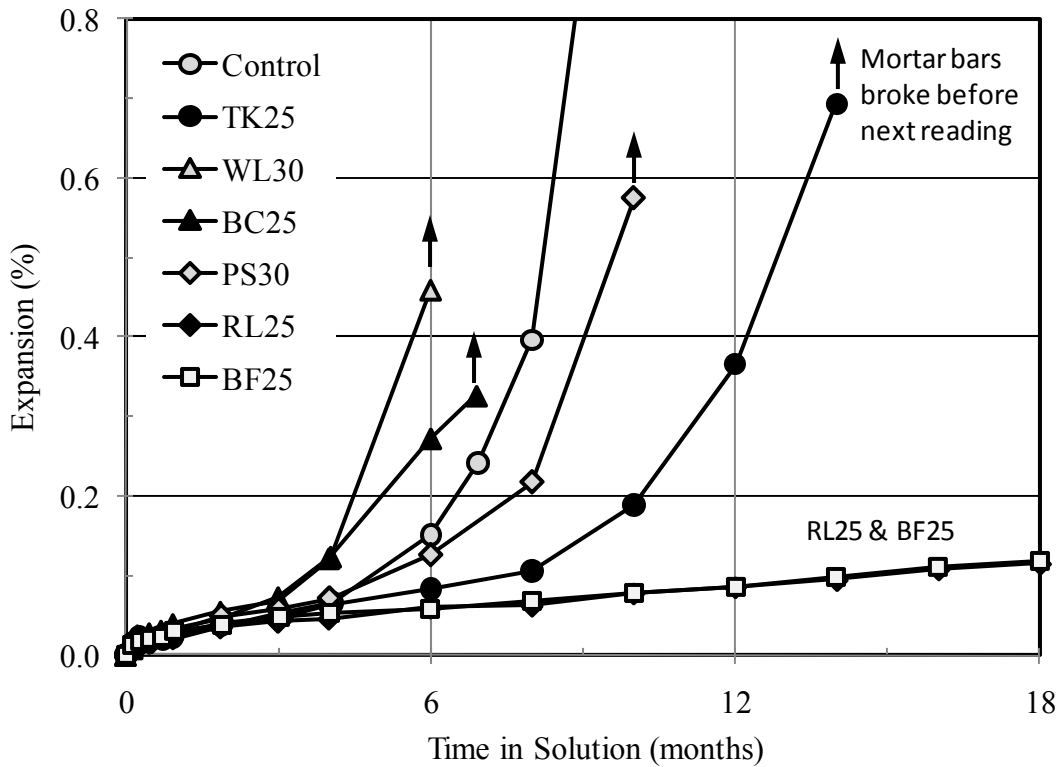


Figure 6.15: Expansion of Mortar Bars with Different Fly Ashes (ASTM C 1012 – 5% Na_2SO_4 Solution)

Figure 6.16 shows the expansion of mortars produced with 25% blended fly ash, using various proportions of TK (Class C) and RL (Class F fly ash). Data for blends of other fly ashes are presented in Table 6.6. Only two blends actually meet the 12-month expansion limit and these blends both contain 20% Class F fly ash and just 5% Class C fly ash.

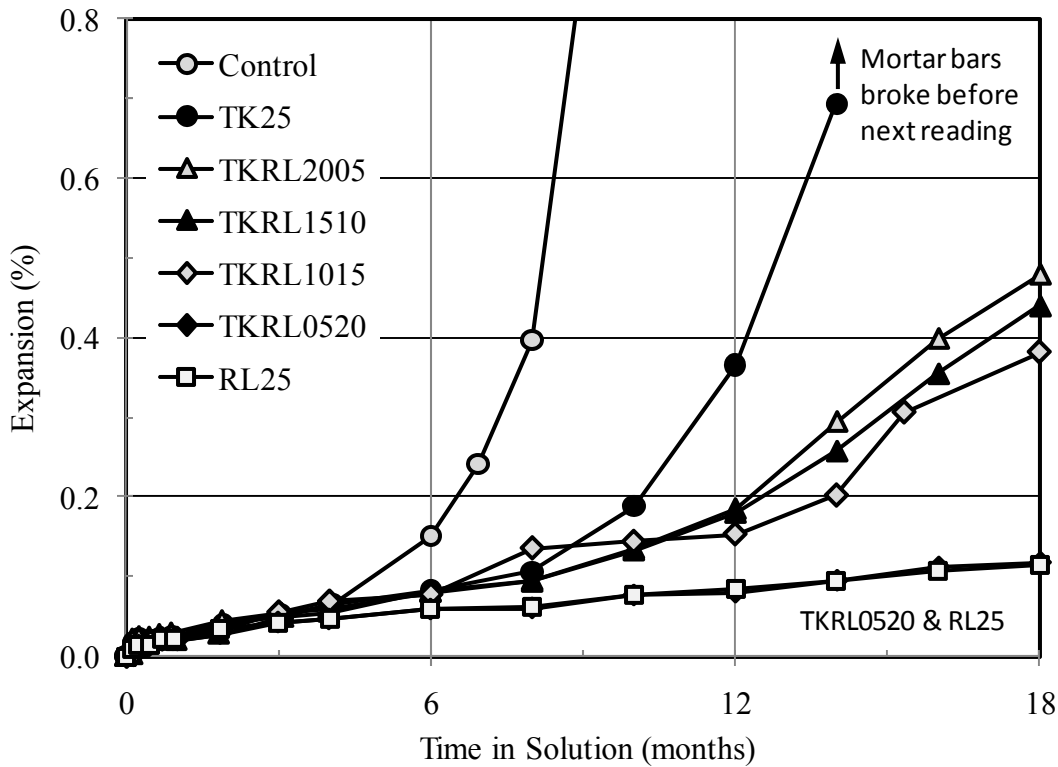


Figure 6.16: Expansion of Mortar Bars with Blended (Type F – Type C) Fly Ashes (ASTM C 1012 – 5% Na_2SO_4 Solution)

Figures 6.17 and 6.18 show the 12-month expansion of mortars containing 25 to 30% of a single fly ash and 25 to 30% of a blend of two fly ashes, respectively, plotted against the calcium content of the fly ash. Included in this figure are some unpublished data from previous studies at the University of Toronto and UNB. The calcium content of the fly ash or the blended fly ash appears to provide a reasonable indicator of the efficacy of the material with regards to controlling expansion in the ASTM C 1012 test. Fly ashes or blends of fly ashes with less than 15% CaO are likely to produce Type HS performance when they are used at a replacement level of 25 to 30%. The performance for materials with more than 15% CaO is variable, whereas materials with more than 25% CaO invariably show poor performance.

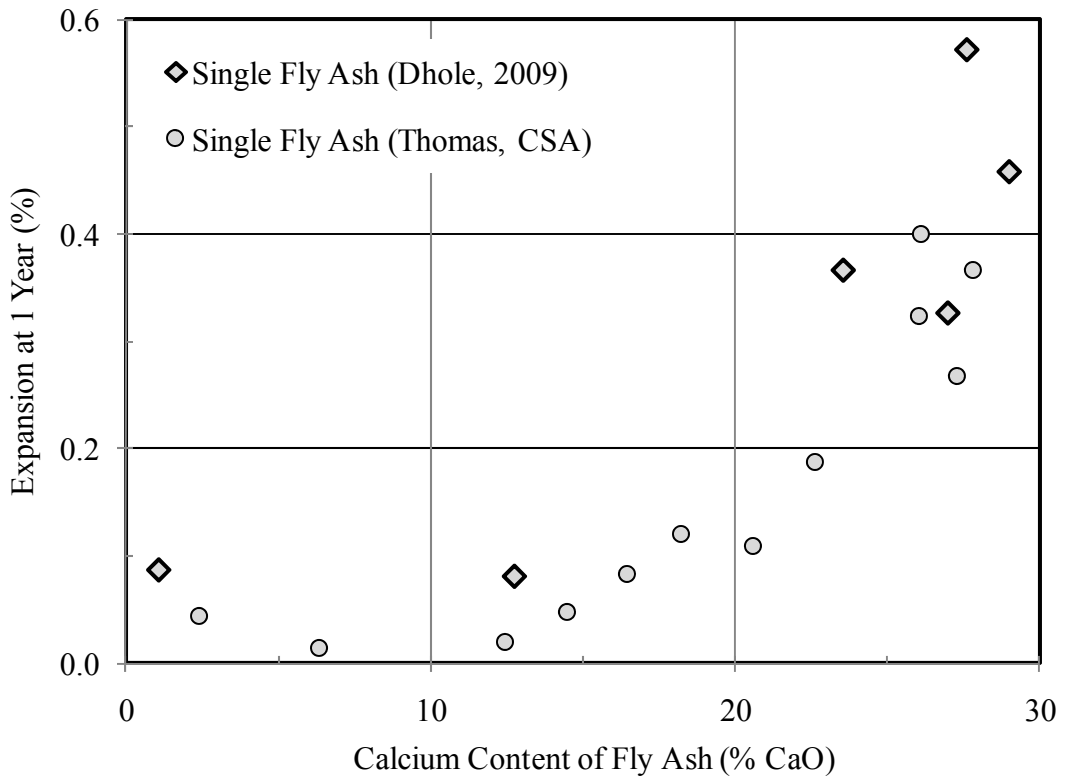


Figure 6.17: Effect of the CaO Content of Fly Ash on the Expansion of Mortar Bars with 25 to 30% Fly Ash (ASTM C 1012 – 5% Na_2SO_4 Solution)

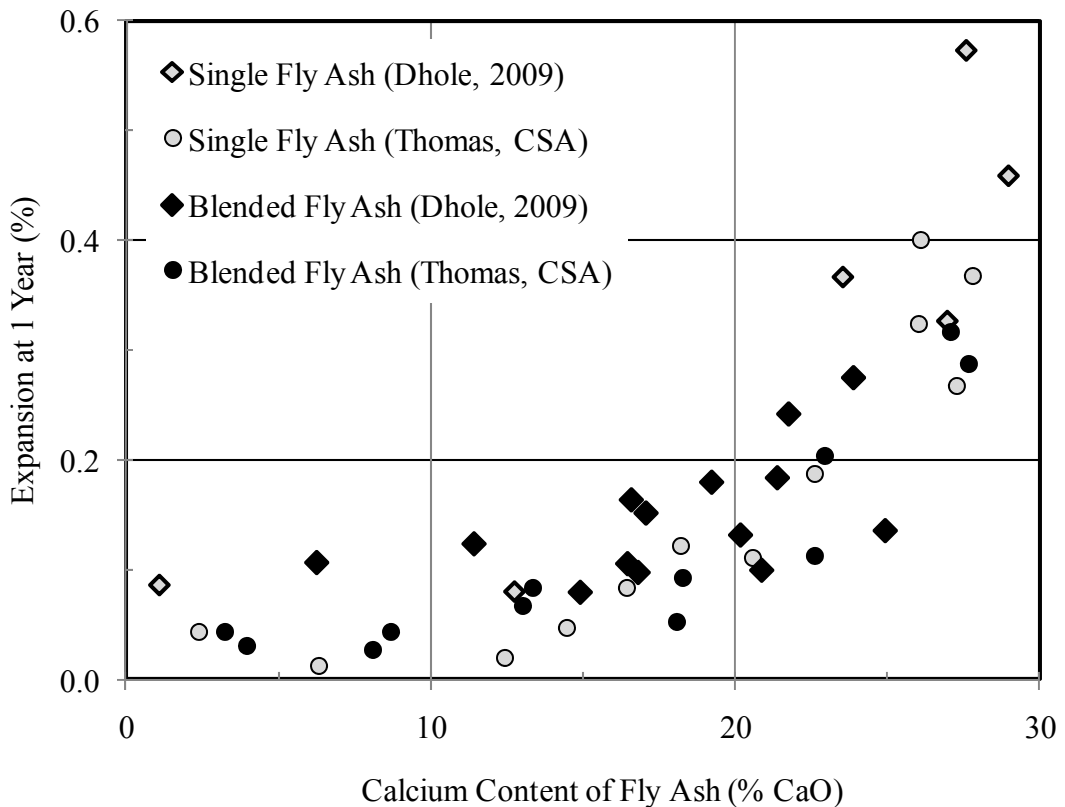


Figure 6.18: Effect of the CaO Content of Blended Fly Ash on the Expansion of Mortar Bars with 25 to 30% Fly Ash (ASTM C-1012 – 5% Na_2SO_4 Solution)

Expansion data for mortar mixes containing fly ash plus either ultra-fine fly ash (UFFA) or silica fume (SF) are presented in Figure 6.19 and Table 6.8. All of these mixes meet the 12-month expansion criteria for Type HS cement. Many of them also meet the requirement in the ACI 318 Building Code for cement for use in an S-3 (very severe) sulfate exposure class (expansion less than 0.10% at 18 months).

Table 6.8: Details of Mixes with Blends of Fly Ash, Ultra-Fine Fly Ash and Silica Fume for ASTM C 1012 Tests

Mix	Mix ID	Class C (Type, %)	Class F (Type, %)	UFFA %	SF %	Exp % 6m	Exp % 12m	Exp % 18m
1	WLUFFA 2010	WL 20	0	10	-	0.047	0.051	0.052
2	WLUFFA 3010	WL 30	0	10	-	0.054	0.061	0.063
3	WLUFFA 4010	WL 40	0	10	-	0.063	0.069	0.069
4	PSSF 3006	PS 30	0	-	6	0.056	0.084	0.110
5	TKSF2005	TK 20	0	-	5	0.042	0.074	0.261
6	TKSF3005	TK 30	0	-	5	0.034	0.074	0.138
7	WLRL 75225SF3	WL 7.5	RL 22.5	-	3	0.049	0.076	0.102
8	WLRL 1515SF3	WL 15	RL 15	-	3	0.054	0.087	0.119
9	WLRL 22575SF3	WL 22.5	RL 7.5	-	3	0.058	0.099	0.163
10	WLRL 75225SF6	WL 7.5	RL 22.5	-	6	0.037	0.064	0.084
11	WLRL 1515SF6	WL 15	RL 15	-	6	0.042	0.068	0.088
12	WLRL 22575SF6	WL 22.5	RL 7.5	-	6	0.044	0.074	0.096
13	TKRL 75225SF3	TK 7.5	RL 22.5	-	3	0.039	0.075	0.106
14	TKRL 1515SF3	TK 15	RL 15	-	3	0.043	0.078	0.105
15	TKRL 22575SF3	TK 22.5	RL 7.5	-	3	0.053	0.086	0.118
16	TKRL 75225SF6	TK 7.5	RL 22.5	-	6	0.026	0.054	0.074
17	TKRL 1515SF6	TK 15	RL 15	-	6	0.029	0.057	0.076
18	TKRL 22575SF6	TK 22.5	RL 7.5	-	6	0.029	0.058	0.079
19	PSRL 75225SF6	PS 7.5	RL 22.5	-	6	0.038	0.066	0.088
20	PSRL 1515SF6	PS 15	RL 15	-	6	0.041	0.072	0.089
21	PSRL 22575SF6	PS 22.5	RL 7.5	-	6	0.052	0.075	0.093

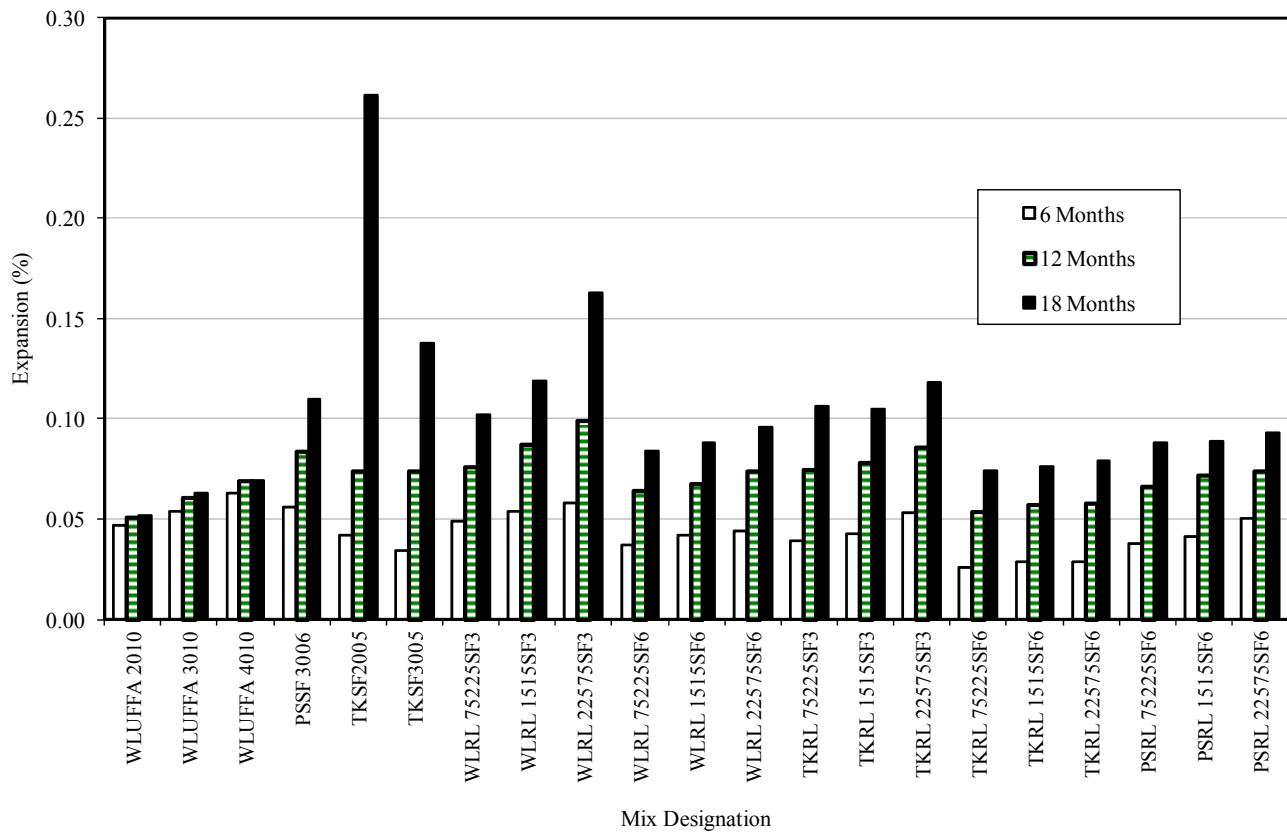


Figure 6.19: Summary of Expansion Results for Mortars Containing Ultra-Fine Fly Ash (UFFA) or Silica Fume (SF) – ASTM C 1012)

6.5 Strategies for Increasing the Sulfate Resistance of Mortars Containing Class C Fly Ash: Gypsum Addition, Low w/cm and HVFA

6.5.1 Gypsum Addition

Mortar mixes were produced with fly ashes TK and WL with added gypsum; details are given in Table 6.9. The theoretical quantity of gypsum required to balance the aluminates in the TK mixes was calculated using a procedure developed by Tikalsky and Carrasquillo (1989) and Van Aardt and Vissar (1985). The theoretical quantity was used in addition to three smaller levels of addition as described in Dhole (2009). Figure 6.20 shows the expansion of mortar bars containing fly ash TK and varying levels of gypsum. The mortar mix with the theoretical calculate gypsum content ($12.9\% \text{ CaSO}_4 \cdot 2\text{H}_2\text{O}$) expanded rapidly reaching a total expansion of more than 3% after 18 months. The mix with 8.51% gypsum also expanded rapidly initially, but the rate of expansion slowed and the expansion after 12 and 18 months was less than that for the mix with 25% TK fly ash but no gypsum. Lower amounts of gypsum (1.95 and 4.26%) were very effective in reducing expansion in mortar mixtures with 30% TK.

Table 6.9: Details of Mortar Mixes with Added Gypsum for ASTM C 1012 Tests

Mix	Mix ID	Exp % at 6m	Exp % at 12m	Exp % at 18m
1	25 % TK + 0.00 % Gy	0.083	0.365	Fail
2	30 % TK + 1.94 % Gy	0.042	0.091	0.142
3	30 % TK + 4.26 % Gy	0.068	0.115	0.142
4	30 % TK + 8.51% Gy	0.201	0.293	0.320
5	30 % TK + 12.90 % Gy	1.839	2.966	3.398
6	30 % WL + 0.00 % Gy	0.459	Fail	Fail
7	20 % WL + 2.50 % Gy	0.118	0.251	0.466
8	30 % WL + 2.50 % Gy	0.098	0.219	0.296
9	40 % WL + 2.50 % Gy	0.059	0.069	0.074

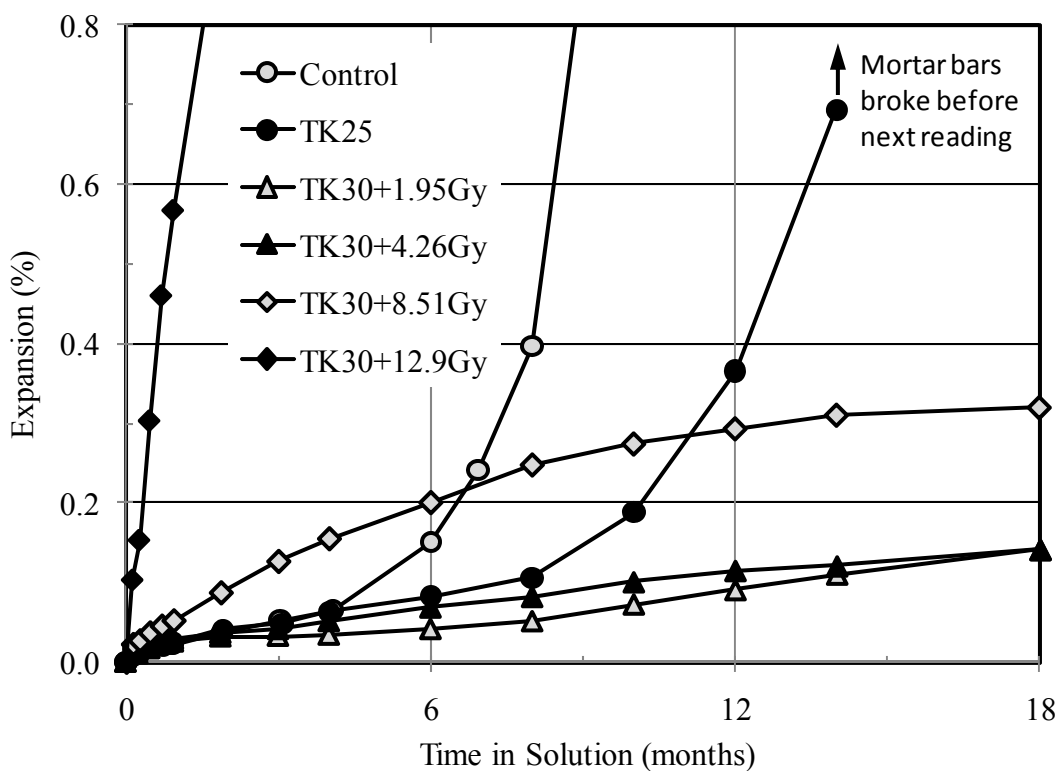


Figure 6.20: Expansion of Mortar Bars with TK Fly Ash and Added Gypsum (ASTM C 1012 – 5% Na_2SO_4 Solution)

Based on the results of the tests with TK fly ash, mortar mixes with WL fly ash were produced with a gypsum content of 2.5%. Figure 6.21 shows that this level of gypsum was very effective in controlling expansion with 40% WL, but mixes with the same level of gypsum and lower amounts of WL (20 and 30%) expanded by more than 0.2% after 12 months. However, the expansion was significantly reduced compared with mortars with WL fly ash and no gypsum.

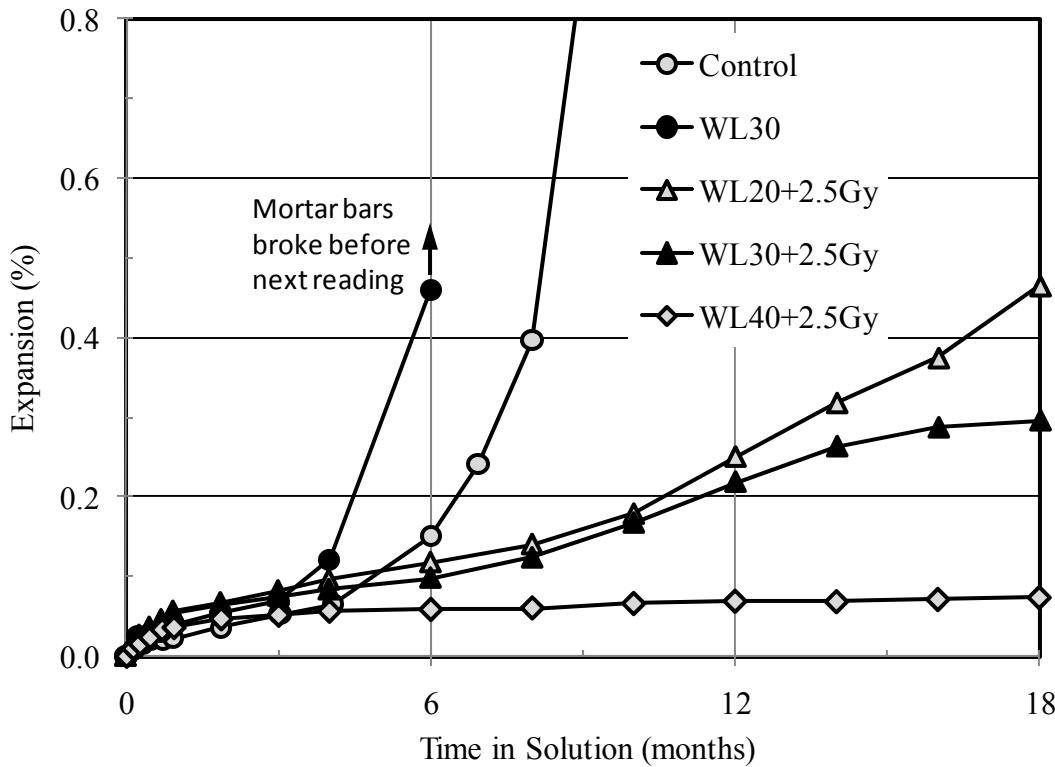


Figure 6.21: Expansion of Mortar Bars with WL Fly Ash and Added Gypsum (ASTM C 1012 – 5% Na_2SO_4 Solution)

6.5.2 Low w/cm

Three mortar mixes were produced with varying amounts of WL fly ash and a reduced w/cm = 0.40 (standard w/cm = 0.485 in ASTM C 1012). The details of the mixes are given in Table 6.10 and Figure 6.22 compares the expansion curves of the mixtures at 2 different w/cm. Even at the reduced w/cm, the mortar bars expanded rapidly in sulfate solution and none of the bars could be measured after 8 months exposure.

Table 6.10: Details of Mortar Mixes with Lower w/cm for ASTM C 1012 Tests

Mix	Mix ID	Exp % at 6m	Exp % at 12m	Exp % at 18m
1	15% WL, w/cm = 0.40	0.152	Fail	Fail
2	22.5% WL, w/cm = 0.40	0.164	Fail	Fail
3	30% WL, w/cm = 0.40	0.236	Fail	Fail

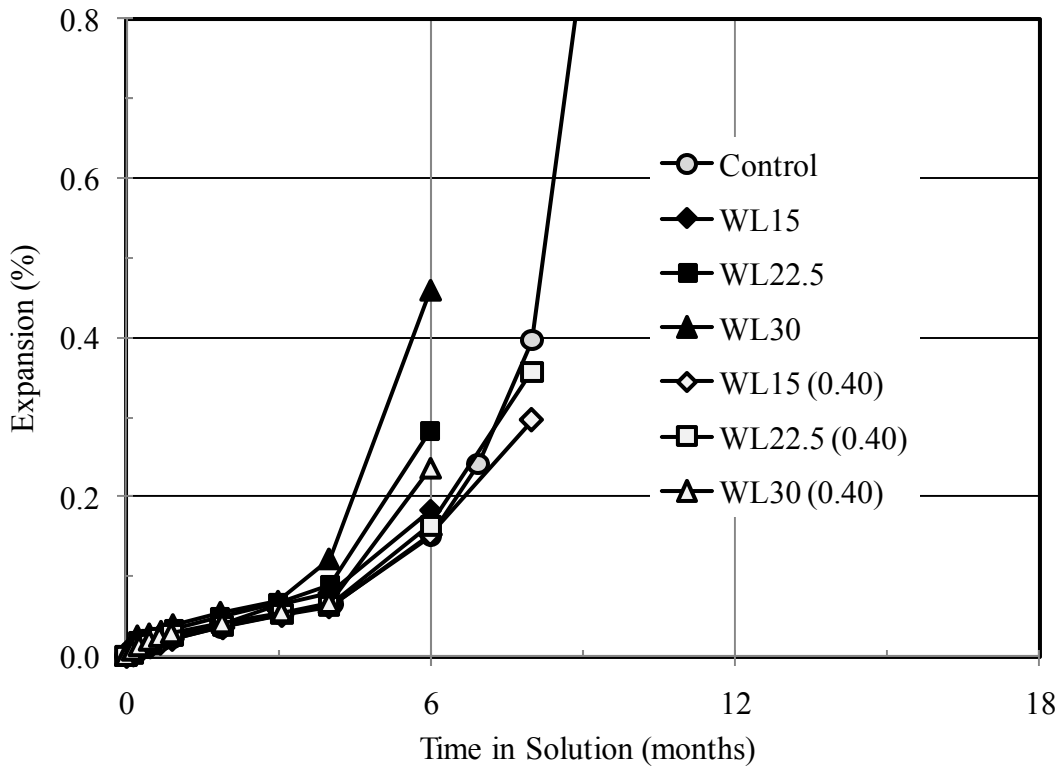


Figure 6.22: Effect of w/cm on the Expansion of Mortar Bars with WL Fly Ash (ASTM C 1012 – 5% Na_2SO_4 Solution)

6.5.3 High-Volume Fly Ash Mortars

A series of 20 mortar mixtures were cast with high-volumes of fly ash ($\geq 50\%$ by mass). The details of the mixes are presented in Table 6.11 and expansion data are shown in Figures 6.23 to 6.27. Fly ashes TK and PS were effective in controlling sulfate expansion when used at replacement levels of 50% or more (Figures 6.23 and 6.24). Fly ash WL was not effective at 50% replacement and specimens from this mixture disintegrated rapidly and could not be measured beyond 4 months (Figure 6.25). However, specimens from the mixture with 60% or more WL performed very well. Mortar mixtures with 40 to 70% of a blend of PS and RL fly ashes also performed very well (Figure 6.26) and further improvements in performance were produced by reducing the w/cm from the standard value of 0.485 to 0.40 (Figure 6.27).

Table 6.11: Details of Mortar Mixes with High-Volume Fly Ash for ASTM C 1012 Tests

Mix	Mix ID	Exp % at 6m	Exp % at 12m	Exp % at 18m
1	50 % TK (HVFA)	0.084	0.107	0.115
2	60 % TK (HVFA)	0.069	0.089	0.095
3	70 % TK (HVFA)	0.056	0.077	0.082
4	30% PS	0.125	Fail	Fail
5	40% PS	0.076	0.131	0.235
6	50 % PS (HVFA)	0.078	0.097	0.109
7	60 % PS (HVFA)	0.074	0.094	0.104
8	70 % PS (HVFA)	0.063	0.076	0.077
9	50 % WL (HVFA)	Fail	Fail	Fail
10	60 % WL (HVFA)	0.022	0.100	0.103
11	70 % WL (HVFA)	0.061	0.085	0.090
12	80 % WL (HVFA)	0.044	0.067	0.069
13	20 % PS + 20 % RL	0.066	0.092	0.101
14	25 % PS + 25 % RL	0.077	0.12	0.130
15	30 % PS + 30 % RL	0.068	0.106	0.115
16	35 % PS + 35 % RL	0.062	0.078	0.089
17	20 % PS + 20 % RL, w/cm = 0.40	0.045	0.065	0.070
18	25 % PS + 25 % RL, w/cm = 0.40	0.048	0.063	0.067
19	30 % PS + 30 % RL, w/cm = 0.40	0.050	0.062	0.062
20	35 % PS + 35 % RL, w/cm = 0.40	0.056	0.067	0.067

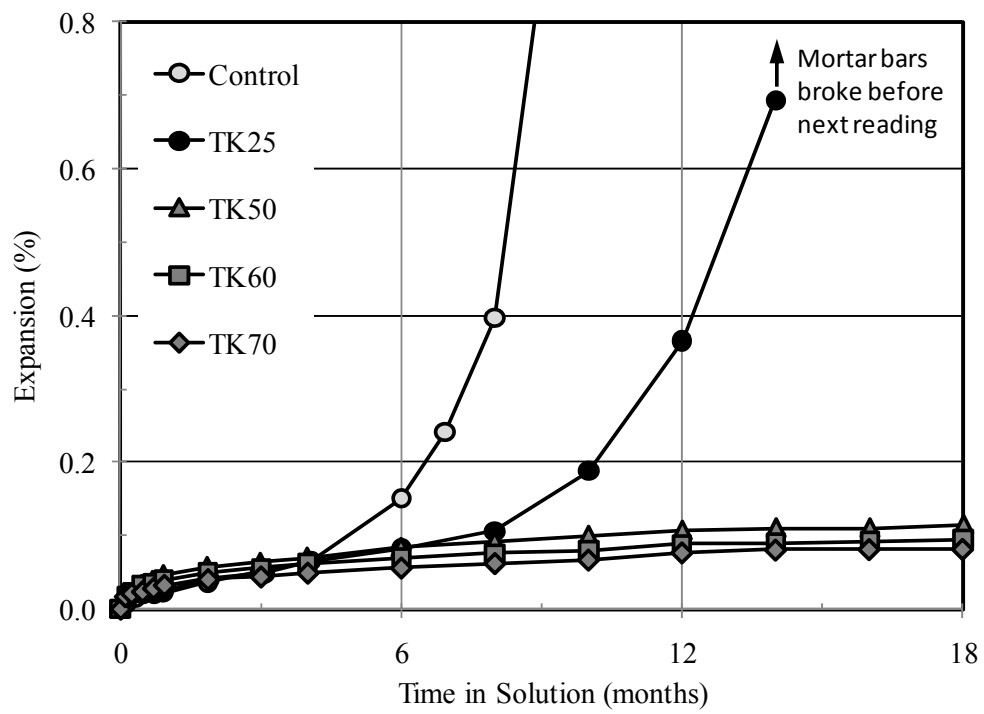


Figure 6.23: Expansion of HVFA Mortar Bars with TK Fly Ash (ASTM C 1012 – 5% Na₂SO₄ Solution)

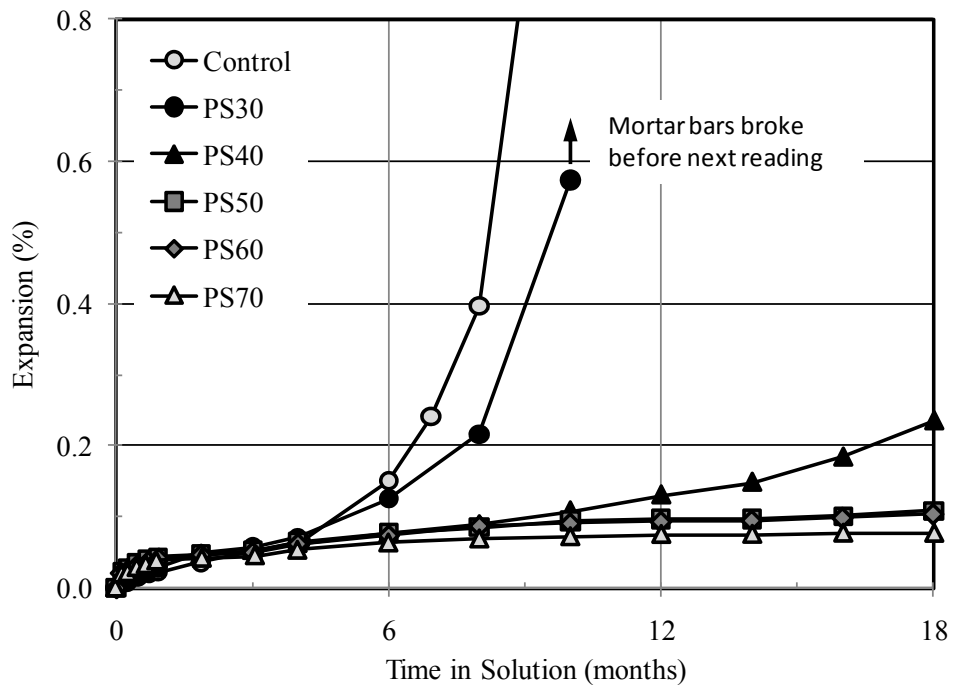


Figure 6.24: Expansion of HVFA Mortar Bars with PS Fly Ash (ASTM C 1012 – 5% Na_2SO_4 Solution)

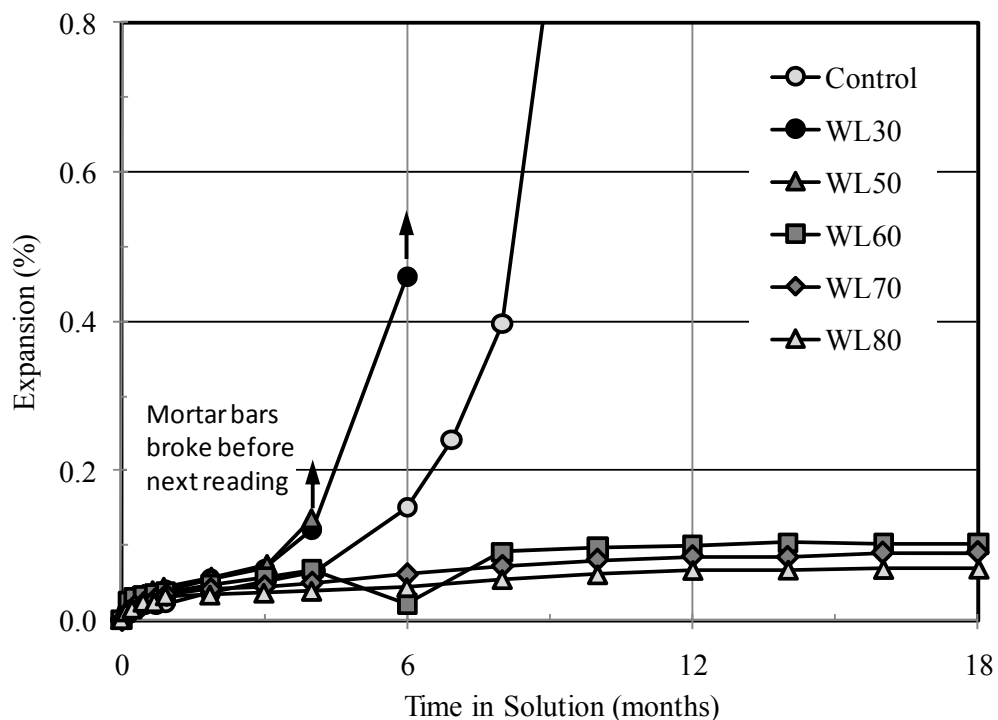


Figure 6.25: Expansion of HVFA Mortar Bars with WL Fly Ash (ASTM C 1012 – 5% Na_2SO_4 Solution)

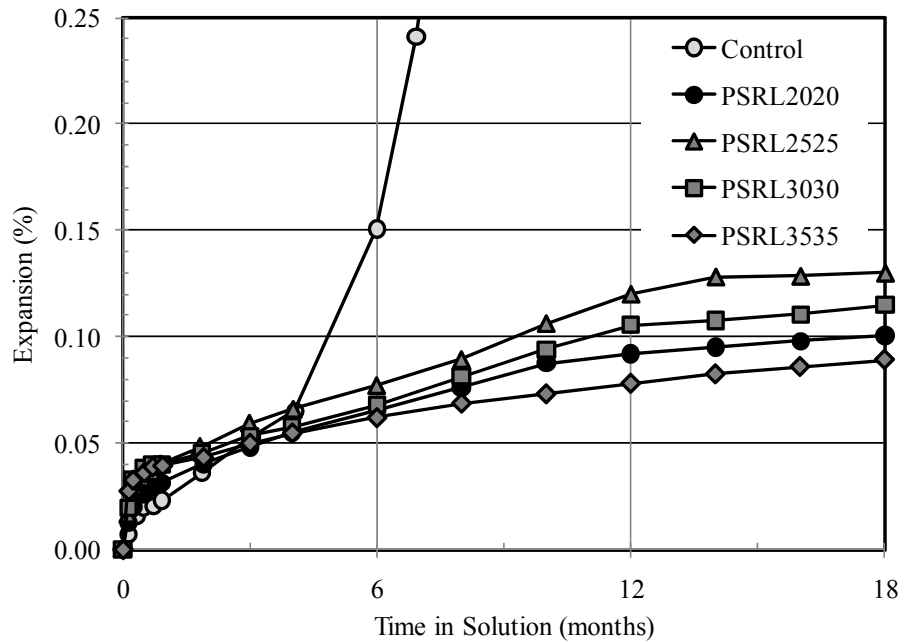


Figure 6.26: Expansion of HVFA Mortar Bars with Blends of PS and RL Fly Ash (ASTM C 1012 – 5% Na_2SO_4 Solution)

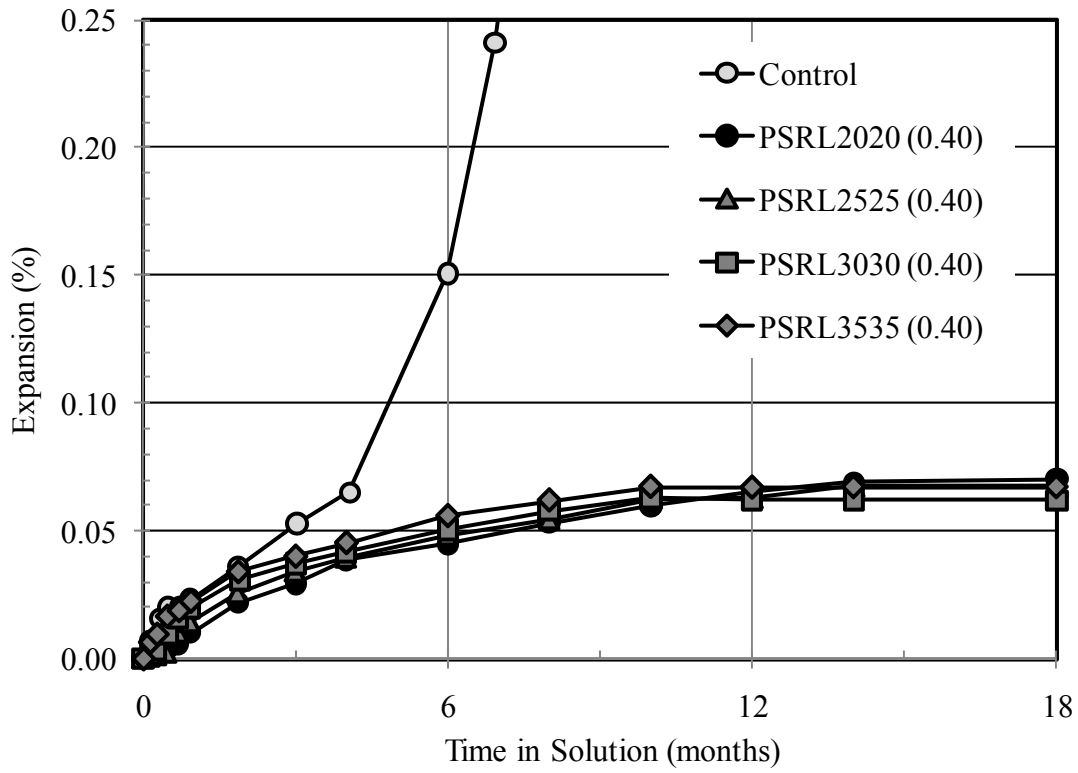


Figure 6.27: Expansion of HVFA Mortar Bars with Blends of PS and RL Fly Ash and Reduced $w/cm = 0.40$ (ASTM C 1012 – 5% Na_2SO_4 Solution)

Many of the high-volume Class C fly ash mixtures meet the requirement for Type HS cement with expansion values less than 0.10% at 12 months. Some mixes even meet the ACI 318 requirement for an S-3 (very severe) sulfate exposure condition (expansion \leq 0.10% at 18 months).

6.6 Characterization of Class C Fly Ashes

6.6.1 Characterization using X-Ray Diffraction

Four Class C fly ashes (BC, TK, PS, and WL) and two Class F fly ashes (BF and RL) were examined using XRD with quantitative analysis undertaken using the Rietveld method. Full details of the experimental procedure can be found in Chapter 6 of Dhole's (2009) thesis.

The crystalline content of the Class F and Class C fly ashes is shown in Figures 6.28 and 6.29, respectively. The Class F fly ashes both contain approximately 28% crystalline material, the remainder (\sim 72%) being amorphous glass. The mineralogy of the crystalline phases is dominated by quartz and mullite. Approximately 2% magnetite is also present and the remaining crystalline phases detected were each less than 1%. The Class C fly ashes contained more crystalline material (32 to 36%) with the exception of TK fly ash which comprised 28% crystalline components. The mineralogy of the Class C fly ashes is very different from the Class F fly ashes as these fly ashes contain significant quantities of crystalline phases some of which, C₃A and C₂AS (gehlenite), are known to be reactive in the presence of sulfates. Significant quantities of reactive periclase (MgO) and anhydrite (CaSO₄) are also present in the Class C fly ashes. It is interesting to note that when comparing the Class C fly ashes, WL fly ash, which generally gave the most expansion in sulfate tests, contains the greatest amount of these potentially deleterious phases and TK fly ash, which gave the best performance in sulfate exposure, contains the least amount.

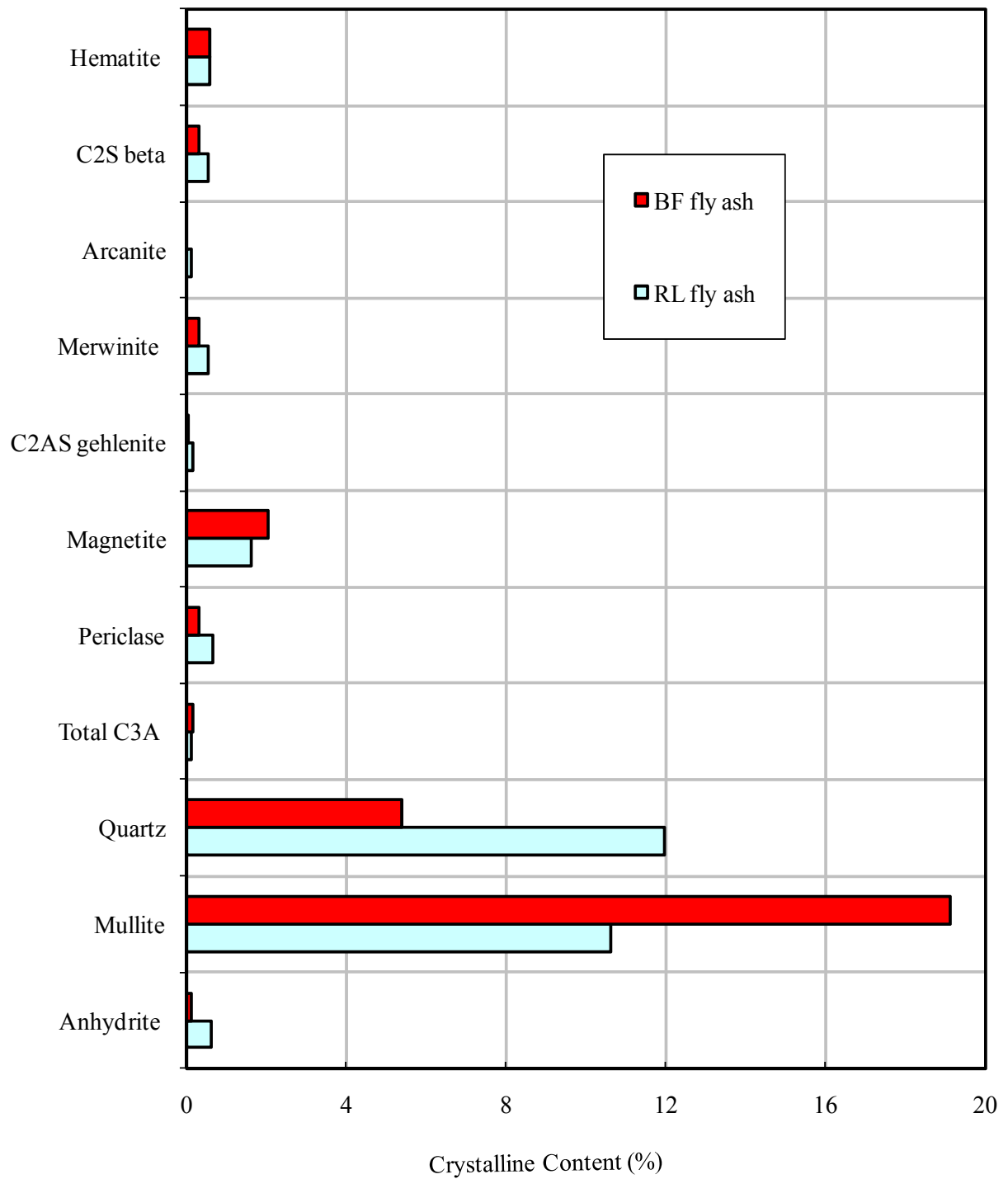


Figure 6.28: Crystalline Composition of Class F Fly Ashes Determined by XRD Rietveld Method

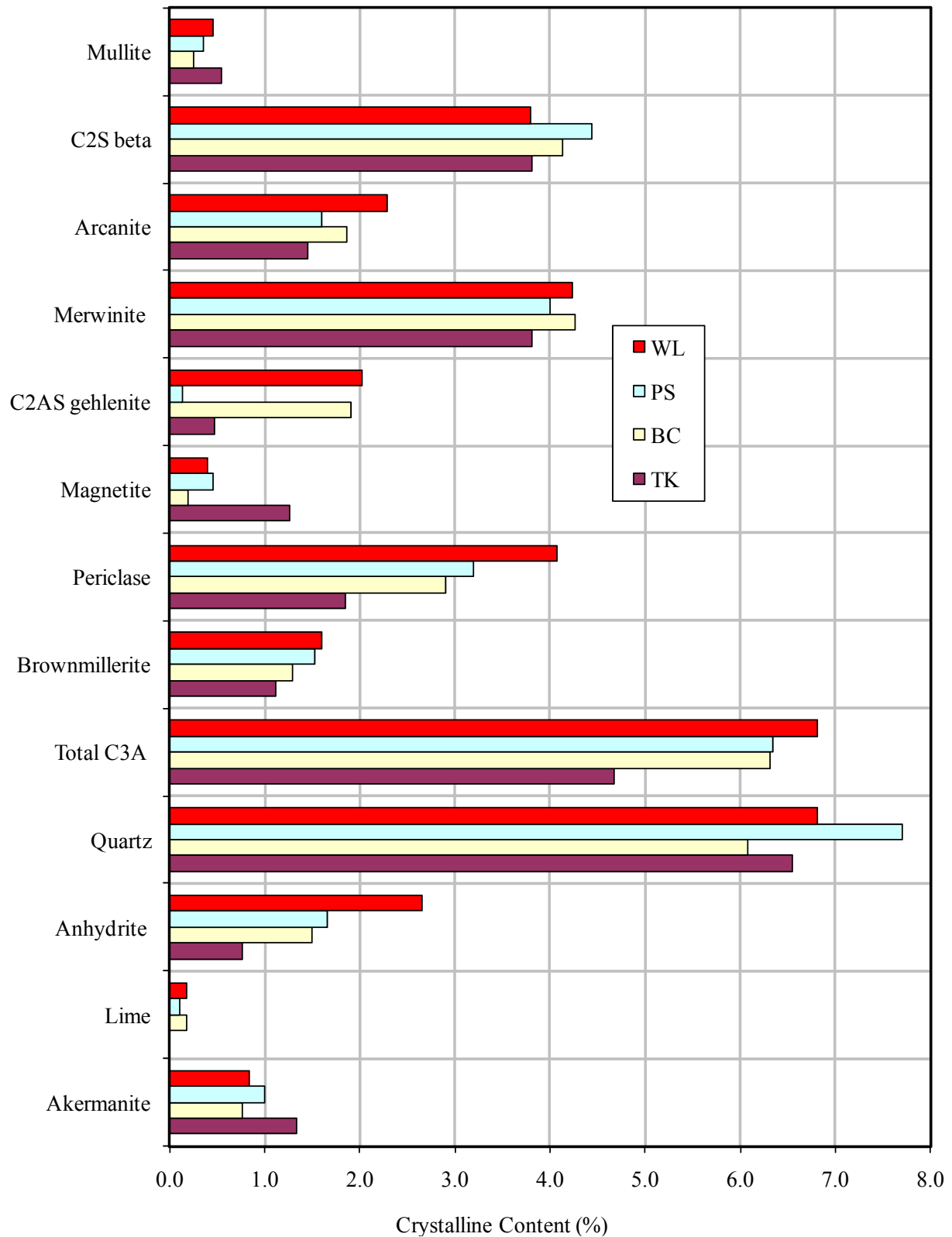


Figure 6.29: Crystalline Composition of Class C Fly Ashes Determined by XRD Rietveld Method

The chemical composition of the glass in the six fly ashes was calculated by subtracting the oxide composition of the crystalline phases from the bulk composition of the fly ash. The normalized glass composition for the six fly ashes is shown in Figure 6.30. The glass composition closely follows the bulk composition. The glass in BF fly ash, which has the lowest bulk CaO content, is almost entirely composed of silica and alumina with minor amounts of iron² and almost no calcium (< 1%). As the bulk CaO content of the fly ash increases, so does the CaO content of the glass with concomitant reductions in the SiO₂ content; the Al₂O₃ content remains relatively stable.

² Note that the iron content in the glass needs to be corrected (reduced) as it currently includes iron III present in magnetite (Fe₃O₄)

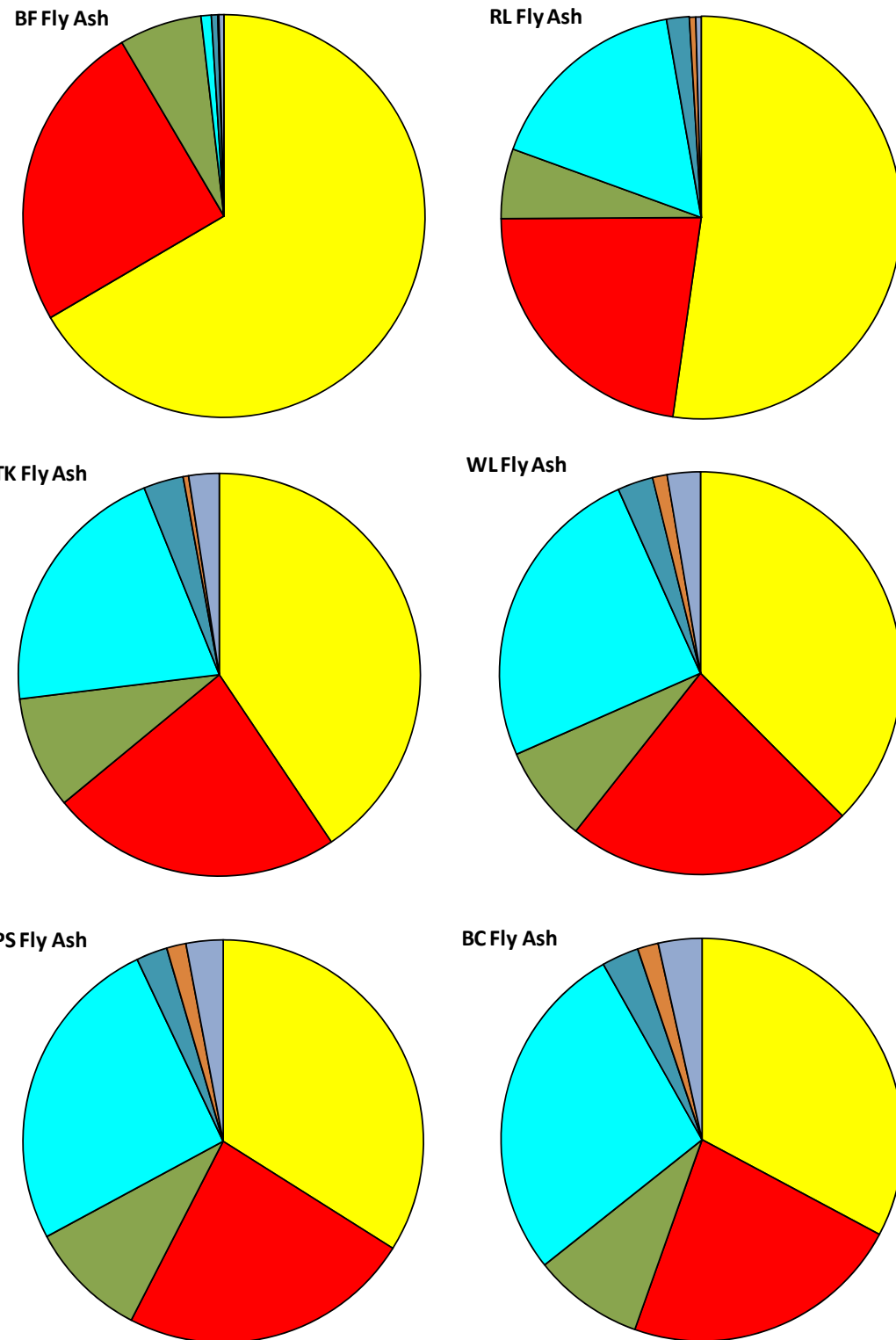


Figure 6.30: Normalized Glass Composition of Fly Ashes Determined by Subtraction of Oxide Content of Crystalline Components from Bulk Oxide Composition

Figure 6.31 shows the glass composition (determined from XRD analysis) of the fly ashes plotted on a ternary $\text{CaO}-\text{SiO}_2-\text{Al}_2\text{O}_3$ diagram.

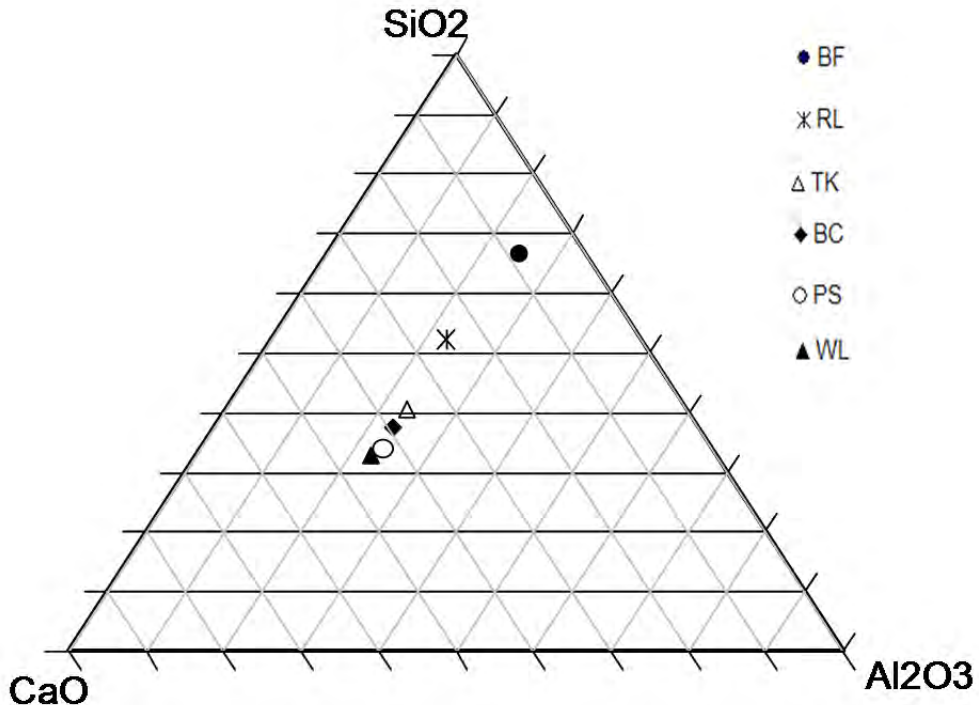


Figure 6.31: Ternary $\text{CaO}-\text{SiO}_2-\text{Al}_2\text{O}_3$ Diagram Showing Location of Glass in Six Fly Ashes Glass Composition Determined by Rietveld Analysis

6.6.2 Characterization using SEM-EDXA

Five Class C fly ashes (BC, TK, PS, HN, and WL) and two Class F fly ashes (BF and RL) were also examined by scanning electron microscopy (SEM) equipped with energy-dispersive x-ray analysis (EDXA). Polished samples were made from each fly ash and the chemical composition of at least 100 particles of each fly ash was determined by SEM-EDXA.

The data from this study are discussed in detail in Dhole (2009).

Figure 6.32 shows the glass composition determined from the analysis of 100 glass particles of each fly ash using SEM-EDXA. The data are plotted on the ternary $\text{CaO}-\text{SiO}_2-\text{Al}_2\text{O}_3$ diagram and it can be seen that there is good agreement with the results from XRD analysis (plotted in Figure 6.31).

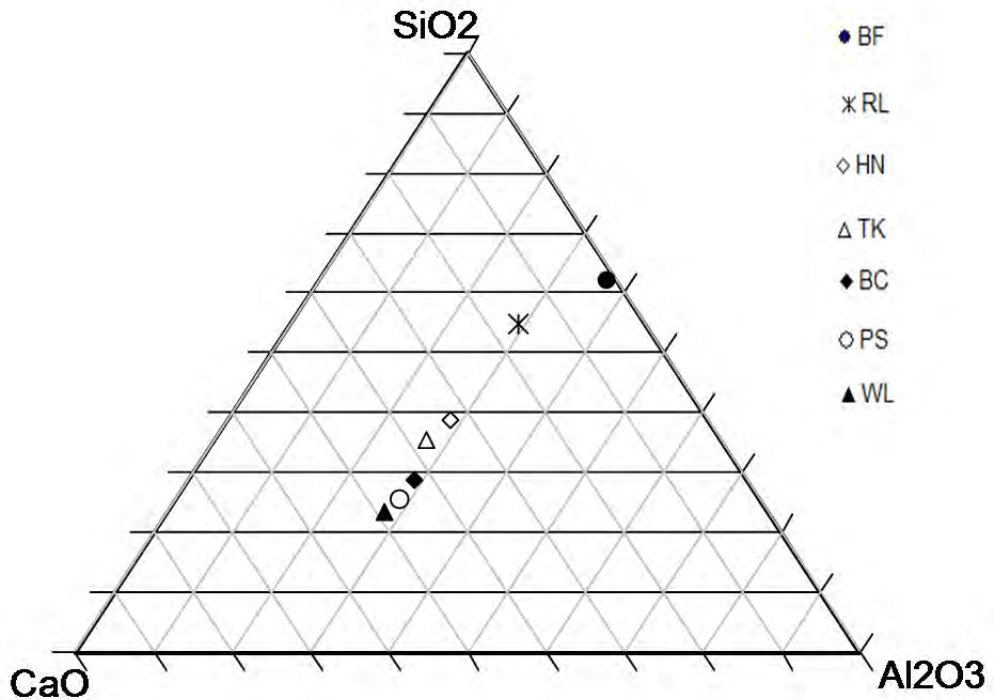


Figure 6.32: Ternary $\text{CaO}-\text{SiO}_2-\text{Al}_2\text{O}_3$ Diagram Showing Location of Glass in Seven Fly Ashes Glass Composition Determined by SEM-EDXA

Figure 6.33 shows the bulk composition of the fly ashes, determined by chemical analysis. The bulk composition of the ashes plots in similar locations as the glass composition determined by XRD or SEM-EDXA although the calcium is generally lower in the bulk composition. This means that the bulk composition underestimates the relative proportion of calcium in the glass phase.

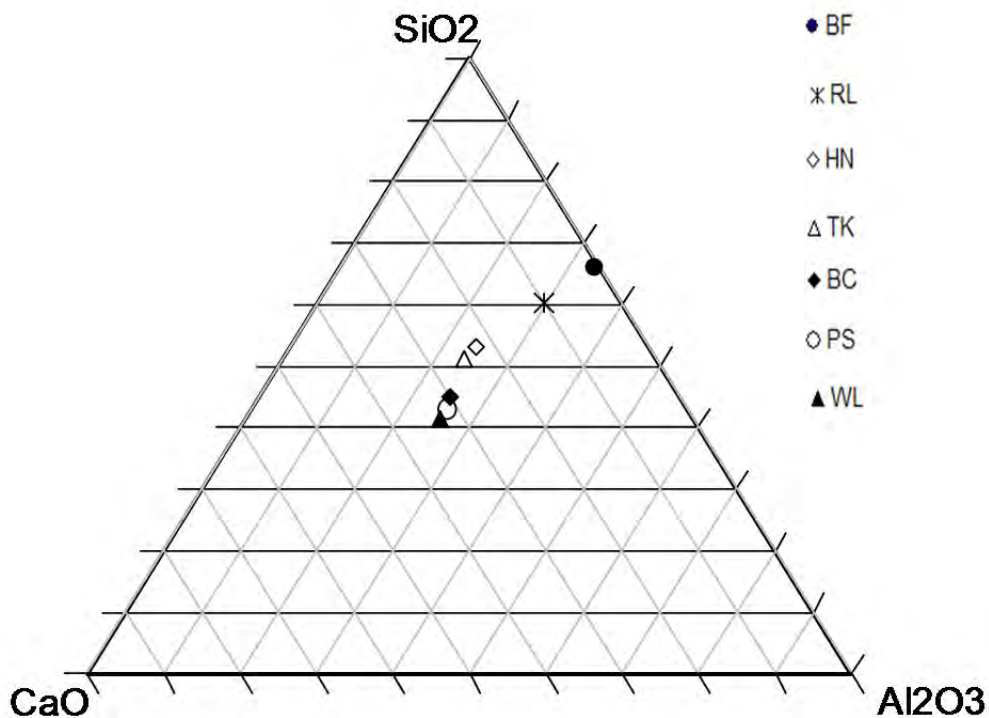


Figure 6.33: Ternary $\text{CaO}-\text{SiO}_2-\text{Al}_2\text{O}_3$ Diagram Showing Location of Glass in Seven Fly Ashes Bulk Composition of Fly Ash Determined by Chemical Analysis

6.7 Analysis of Fly Ash Hydration Products in Sulfate Environments

The purpose of this study was to determine the nature and quantity of reaction products when lime-fly ash hydration products are exposed to sulfate solutions. Fly ash (FA) samples were mixed with calcium hydroxide (CH), FA:CH = 3:2, and a solution of 0.15 M NaOH + 0.35 M KOH, using a water-to-solids ratio of W/S = 0.45. The pastes were sealed in plastic containers and cured at 38°C (100°F) for 28 days. A control paste was produced with Type I cement for comparison. After curing the pastes were crushed to pass a 200-micron (#70) sieve. A sub-sample of the crushed material was then subjected to XRD using rutile as an internal standard to determine the relative quantities of CH, ettringite and monosulfate. The remaining sample was exposed to various sulfate solutions (15 g of paste in 300 ml of solution) and continuously shaken to prevent particles from settling. The pH of each solution was monitored and sodium sulfate solutions were changed weekly during the first month and thereafter every second week. After 90 days exposure paste samples were analyzed by XRD to determine the quantities of phases present. Full details of the methodology are provided in the thesis of Dhole (2009). Only the data for pastes exposed to 5% Na_2SO_4 are presented in this summary report; results for other sulfate solutions can be found in Dhole (2009).

Table 6.12 shows the quantities of phases present in the lime-fly ash pastes after curing and prior to exposure to sulfate. A significant quantity of unreacted CH remains (original content was 40%) the amount increasing with the CaO content of the fly ash. This indicates that the Class F fly ashes consume more CH during curing and this is probably a result of the higher

pozzolanic activity of low-CaO fly ashes. Figure 6.34 shows the amount of monosulfate and ettringite that formed in the pastes prior to sulfate exposure. The amount of monosulfate formed increases with increasing CaO content in the fly ash. The amount of ettringite formed is also on average higher in the pastes produced with Class C fly ashes (mean = 4.34%) compared to those produced with Class F fly ashes (mean = 2.55%), however the trend between ettringite and CaO content of the fly ash is not as clear as the trend for monosulfate.

Table 6.12: Quantities of Phases in Lime-Fly Ash Pastes Prior to Sulfate Exposure

Fly Ash		Phase content after 28 days curing		
Type	CaO (%)	Monosulfate (%)	Ettringite (%)	CH (%)
BF	1.1	1.41	2.5	11.55
RL	12.76	1.21	2.59	12.63
HN	21.58	3.28	4.69	13.93
TK	23.54	3.13	5.47	16.47
BC	26.92	5.21	3.28	14.99
PS	27.49	7.50	3.36	19.62
WL	29.09	7.87	4.91	18.62

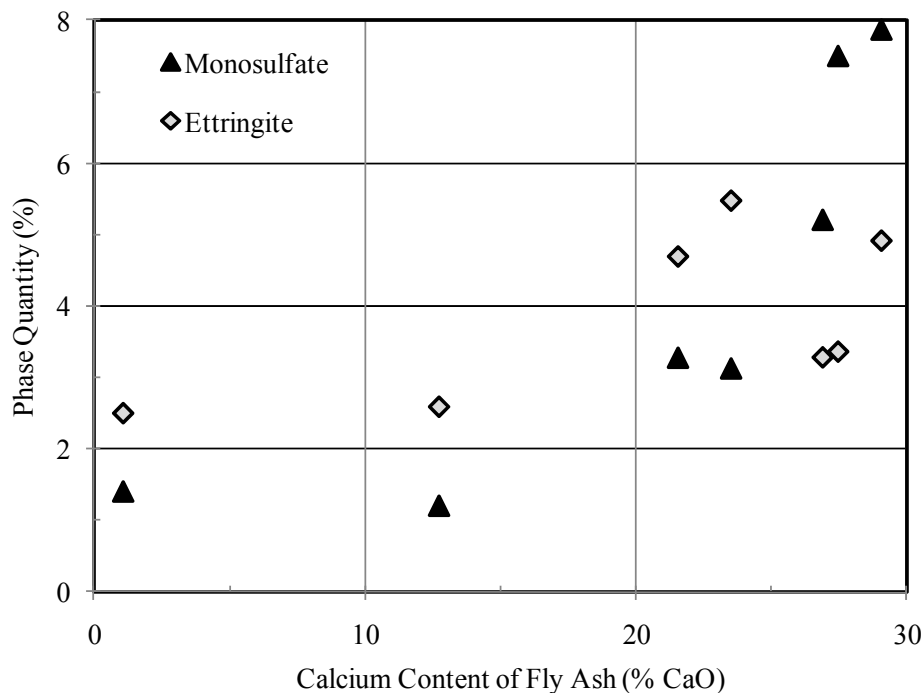


Figure 6.34: Relationship between the CaO Content of Fly Ash and the Quantity of Sulfate Phases produced in Lime-Fly Ash Pastes after Curing (prior to sulfate exposure)

Table 6.13 and Figure 6.35 show the quantities of phases after 90 days exposure to 5% Na₂SO₄. No monosulfate remains in any of the pastes after exposure and only negligible amounts of CH remain. Ettringite is abundant in all seven pastes ranging in quantity from 36 to 72%. The amount of ettringite clearly increases with the CaO content of the fly ash. The paste

with WL fly ash (with the highest CaO content) contains almost twice the ettringite as the paste with fly ash BF (lowest CaO content).

Table 6.13: Quantities of Phases in Lime-Fly Ash Pastes after Exposure to 5% Na₂SO₄ for 90 days

Fly Ash	Monosulfate (%)	Ettringite (%)	Gypsum (%)	CH (%)
BF	0.00	36.52	0.80	0.22
RL	0.00	36.11	0.62	0.18
HN	0.00	47.67	0.57	0.15
TK	0.00	55.64	1.34	0.00
BC	0.00	62.21	1.11	0.00
PS	0.00	68.28	1.15	0.18
WL	0.00	71.68	0.94	0.00

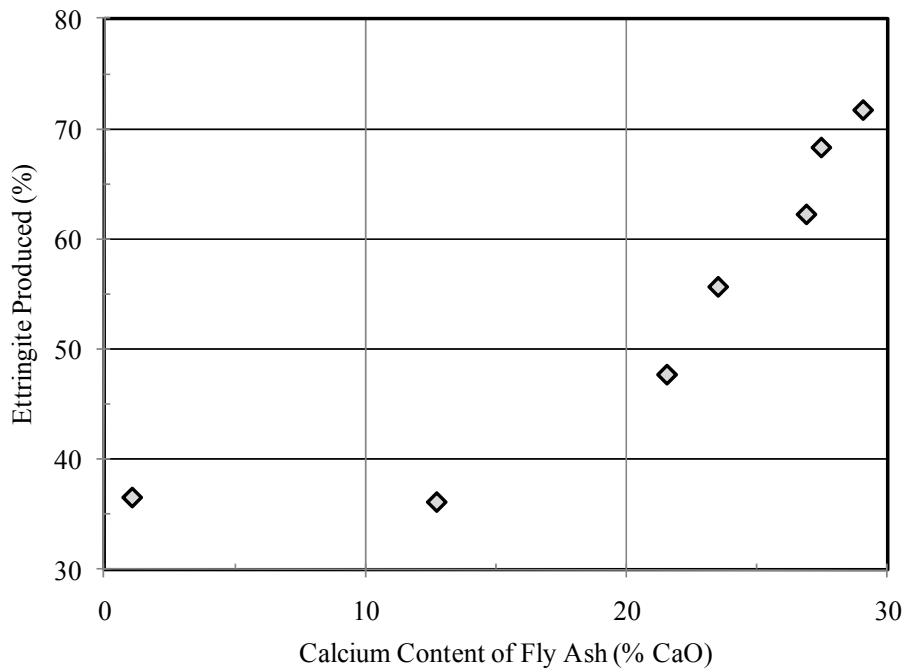


Figure 6.35: Relationship between the CaO Content of Fly Ash and the Quantity of Ettringite produced in Lime-Fly Ash Pastes exposed to 5% Na₂SO₄

Figure 6.36 shows the relationship between the ettringite produced by the seven different fly ash pastes and the expansion of mortar bars produced with 25 to 30% of the same fly ash. The expansion value corresponds to the 12-month reading or, in the case of mortars that deteriorated before 12 months, the latest reading available. There is clearly a relationship between the expansion of mortars containing fly ash and the potential for the fly ash to produce ettringite.

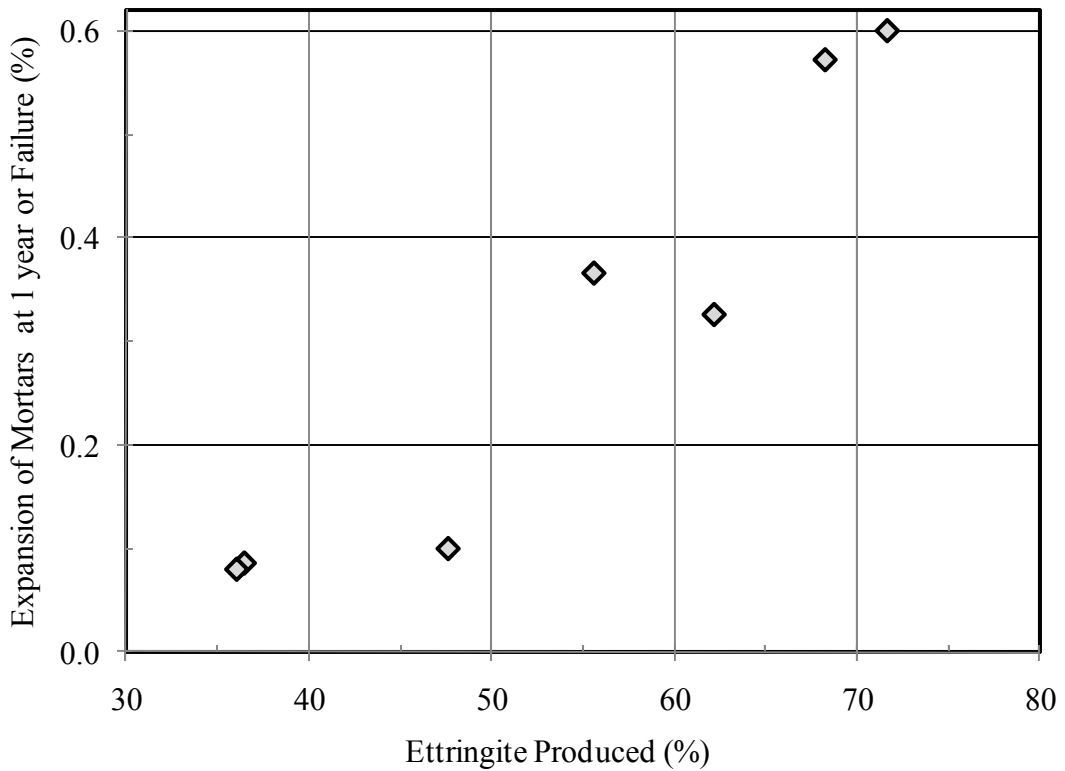


Figure 6.36: Relationship between the CaO Content of Fly Ash and the Quantity of Ettringite Produced in Lime-Fly Ash Pastes exposed to 5% Na₂SO₄

6.8 Summary

This chapter summarized the key findings of research performed at UNB and described in detail in Dhole (2009). The work described in this chapter made significant progress in better understanding the mechanisms of sulfate attack, the effects of fly ash mineralogy on sulfate resistance, and the combined effects of chemical and physical sulfate attack. The most important and implementable findings from this work were integrated into the main conclusions and recommendations provided in Chapter 8 of this report.

Chapter 7. Evaluation of Concrete Structures for Potential Deterioration to External Sulfate Attack

This chapter presents the results of a comprehensive evaluation of transportation structures exposed to gypsiferous soils or gypsum-bearing groundwater. The structures investigated were all in the state of Texas. To pinpoint areas of possible sulfate attack, agricultural maps identifying sulfate-bearing soils, were utilized. According to these maps, several TxDOT-defined “districts” were selected. The El Paso, Paris, and Childress Districts showed the most promise for areas containing sulfate-bearing soils in the state of Texas. Over 200 concrete bridges, culverts, columns, and other transportation structures were visually inspected, and a subset of these were selected for further, detailed investigations. Figure 7.1 provides the locations of each site investigated in this chapter. For the sites selected for more detailed evaluation, soil samples and groundwater samples (when available) were procured for subsequent laboratory testing, as were concrete powder samples for x-ray diffraction analysis and sulfate concentration determination. For certain structures, cores were extracted for more detailed laboratory-based evaluations, such as petrographic evaluation and scanning electron microscopy (SEM) analysis.

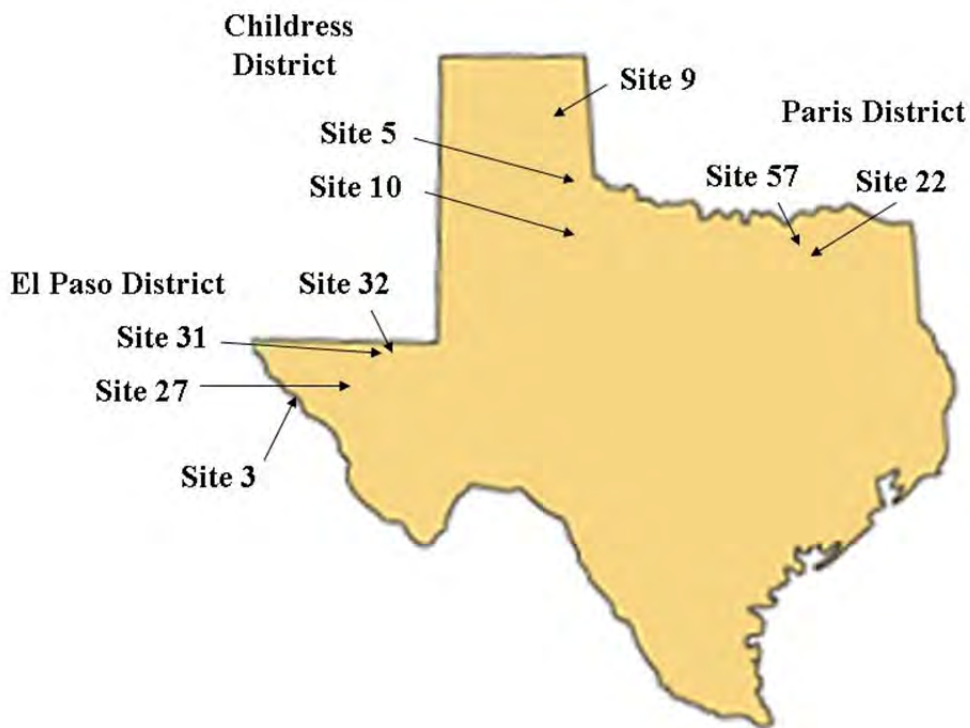


Figure 7.1: Site Locations evaluated within this chapter

7.1 Experimental Methods

The following section provides the methodology and testing program for samples taken from areas of probable external sulfate attack in field structures. Samples taken included: water samples, soil samples, concrete powder samples, and concrete cores.

7.1.1 Water Samples

When available, water samples were taken near the concrete structures where potential damage from sulfate attack was observed. Samples were retrieved by placing a 1 L Nalgene bottle into the source of water and collecting a full bottle of water. Samples were retrieved at multiple locations (e.g. upstream, downstream, etc.) at a given site. Once the samples were returned to the laboratory, a turbidimeter was used to measure the sulfate content. The turbidimeter measures the scattering of light that is being passed through a suspension of materials. The water samples were mixed with barium chloride, which reacts to form barium sulfate, which creates a suspension in the solution. The solution was then placed into the turbidimeter which measures NTU (Nephelometric Turbidity Units). A calibration curve was then created to relate the NTU to sulfate concentration. Figure 7.2 provides a calibration curve for calcium sulfate, sodium sulfate, and magnesium sulfate. The calibration curve was nearly the same for all three sulfate types. The unknown field samples were then measured against the calibration curve. Any readings above the calibration range were diluted to fit into the range of the calibration curve.

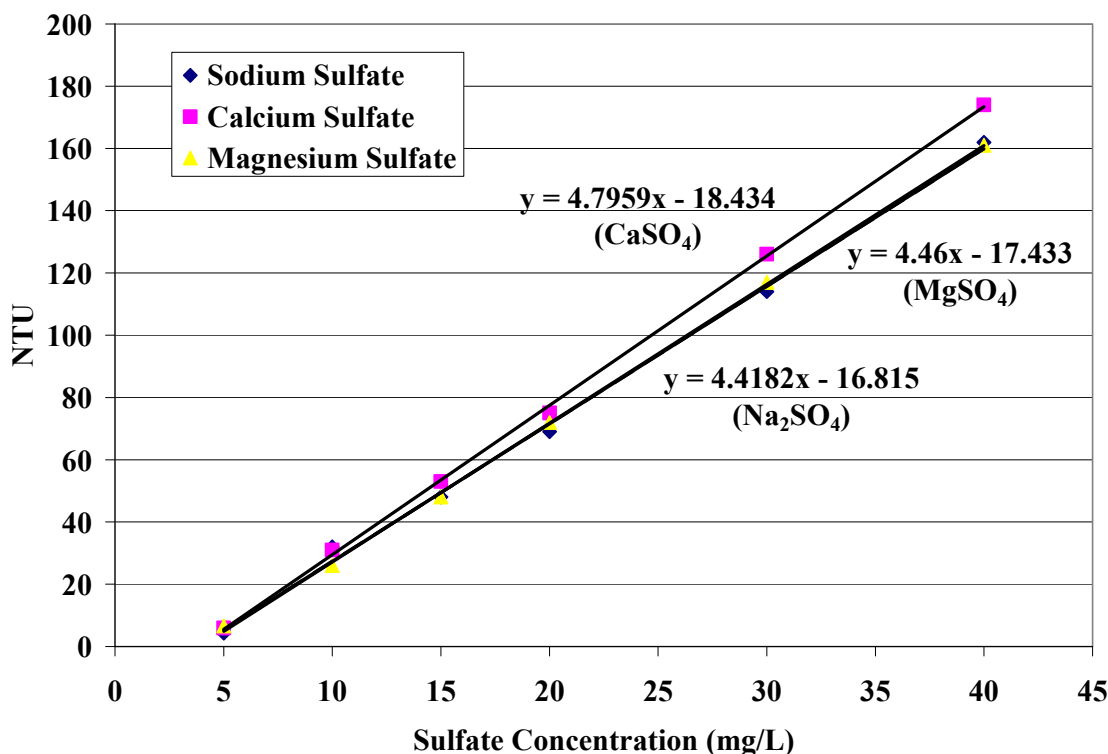


Figure 7.2: Calibration curve for sulfate using the turbidimeter

7.1.2 Soil Samples

Soil samples were taken from different locations at each field site where sulfate attack was suspected. Two testing standards were used for the evaluation of sulfates in soils: TxDOT specification TEX-135-E that uses an extraction ratio of 20:1 and ASTM C 1580 that uses an 8:1

and 80:1 extraction ratio (TxDOT 1991, ASTM C 1580 2005). The two extraction ratios used in ASTM C 1580 provide a large enough range to determine if gypsum is present in the soil. The 80:1 extraction should provide enough water to accommodate the low solubility of gypsum. Table 7.2 provides the exposure class table from ACI 201.2R. The exposure class is based on sulfate concentrations obtained from either water or soil samples collected from a given site. A higher exposure class corresponds to greater sulfate content in the soils. Each exposure class specifies w/cm and cementitious material requirements for concrete to be resistant to the amount of sulfate corresponding to the given exposure class.

7.1.3 Concrete Powder Samples

Concrete powder samples were taken for sulfate content and x-ray diffraction. Powder samples were taken from both deteriorated and non-deteriorated surfaces using a power drill. The determination of sulfate content was based on a method discussed by Hime (2001). Samples were passed through a No. 30 sieve and then 5 grams of the sieved material was digested in 20 ml of 1:4 HCl solution. The sample was then filtered and tested for sulfate content with a turbidimeter following the same methodology discussed in section 5.2.1. The samples were also tested in the XRD following the test procedure in section 3.2.3

7.1.4 Concrete Cores

Concrete cores were taken from the most accessible locations on the affected structures. Core diameters of 2 in (50 mm) and 4 in (100 mm) were taken. Five cores were removed from most of the structures, with two to three from either a deteriorated or non-deteriorated section of the structure. After the cores were removed, they were labeled and placed into individual plastic bags. Samples of the cored concrete were used for scanning electron microscopy. The SEM sample preparation procedure for the SEM is given in section 3.2.4.

7.2 Results and Discussion

This section is divided into the three TxDOT districts investigated: Childress, Paris, and El Paso Districts. Each district contains geographical areas where deterioration from external sulfate attack is possible. In total, over 200 sites were investigated and they were numbered sequentially, whether deterioration due to external sulfate attack was suspected or not. Due to the large number of sites investigated, only the results from selected sites will be presented herein. The last section of this chapter presents preliminary results on a long-term study underway in the El Paso District. Appendix C in Clement (2009) provides agricultural maps with the site locations of the districts investigated. The site locations are not in continuous order since many sites visited did not have any deterioration.

7.2.1 Childress District

In general, the least amount of damage was observed in the Childress District. The location of the Childress District is southeast of Amarillo and west of Fort Worth. Three potential sites were investigated for possible damage from external sulfate attack. Site 5 consisted of damage to a concrete wall below a bridge on US 83. Site 9 had riprap damage below a bridge. Riprap is a sloped wall of concrete used hold back earth/soil to prevent erosion. Site 10 was a bridge on FM 2278 that had deteriorating columns.

Site 5

Site 5 has damage to the concrete base that supports an old steel bridge on US 83. Figure 7.3 shows the damage on the wall. The sulfate content of the soil was analyzed according to ASTM C 1580 and was found to be 0.04%, which constitutes a Class 0 exposure. This location is in the lowest classified exposure classification. The XRD Rietveld analysis from the concrete powder only showed an increase in monosulfate in the area of deterioration. In addition, the amount of ettringite and gypsum detected did not change between the two areas. Concrete cores taken from this location were not analyzed since the sulfate content was low in the soil and the XRD results did not show any significant deleterious reaction products.



Figure 7.3: Damage to the lower part of a wall below US 83 in Childress District

Site 9

The location of Site 9 is on FM 1547 in Shamrock, Texas which is east of Amarillo, Texas. Deterioration at this site is occurring on the riprap. Riprap is concrete that is used along the embankments below a bridge to hold back earth/soil. It is a low quality concrete. The sulfate content in the soil was 0.04% which is classified as Class 0 exposure. The concrete powder samples analyzed by XRD did not show any ettringite or gypsum formation.

Site 10

The last sampled site in the Childress District showed the most potential for external sulfate attack by visual inspection. Figure 7.4 shows one of the six columns sampled at site 10 which is a bridge on FM 2278 located south of Childress, Texas.



Figure 7.4: Damage to a bridge column on FM 2278, south of Childress, Texas

Sulfate content in the soils was 0.05%, which falls into a Class 0 exposure. Table 7.1 shows the sulfate content in the powder collected from this bridge. The sulfate content is greater near the top of the columns. An in-situ milling method to provide a sulfate profile would likely be more suitable for such an analysis but was not employed here.

Table 7.1: Sulfate content of concrete powders from locations in the Childress District

Location	%SO4
FM 2278 SO Bottom	0.51
FM 2278 SO Middle	0.40
FM 2278 SO TOP	0.47
FM 2278 SM Bottom	0.26
FM 2278 SM Middle	0.50
FM 2278 SM TOP	0.66
FM 2278 NO Bottom	0.26
FM 2278 NO Middle	0.42
FM 2278 NO TOP	0.46
FM 2278 NM Bottom	0.33
FM 2278 NM Middle	0.33
FM 2278 NM TOP	0.89

Table 7.2 provides the XRD quantitative results from the two outer columns at this location. The XRD results from this location did not indicate any signs of sulfate attack occurring in the concrete. A total of 12 powder samples were analyzed from this site and all XRD results showed similar products indicating little to no sulfate attack.

Table 7.2: Quantitative XRD Rietveld Analyses from columns SO and NO in the Childress District

Location	Ettringite (%)	Gypsum (%)	Portlandite (%)
SO Bottom	1.43	0.33	0.50
SO Middle	0.07	0.82	0.76
SO Top	0.13	0.62	0.89
NO Bottom	0.30	0.55	0.59
NO Middle	0.09	0.54	0.25
NO Top	0.25	0.52	0.30

Summary of Childress District Findings

This district had few structures affected from external sulfate attack. Findings concluded that the locations sampled were located in Class 0 exposure which suggests that no sulfate damage would be expected. In the case of Site 10 that had visible damage possibly from external sulfate attack, the XRD scans did not indicate any deleterious reaction products resulting from external sulfate attack for any of the six columns. Only a small percentage of all the concrete structures in this district were visually inspected, but those that showed the most signs of distress were selected for evaluation and these were not found to be suffering from external sulfate attack. Further investigations that are beyond the scope of this research project would be needed to determine the type of attack causing the visible deterioration evidenced in a small number of structures in this district.

7.2.2 Paris District

The Paris district is located between Dallas and Texarkana, in the northeast part of the state of Texas. A total of 100 bridges, culverts, and other concrete structures were inspected. A total of five structures were selected for detailed evaluation; Sites 22 and 57 are discussed below. Site 22 is a culvert on Highway 19, north of Sulphur Springs and Site 57 is a bridge showing signs of distress in the columns that is located on State Highway 11 northwest of Sulphur Springs.

Site 22

Site 22, located on Highway 19 north of Sulphur Springs has several deteriorating culverts. The distress shown in Figure 7.5 is one of the culverts observed at site 22. It was common to see this distress throughout the majority of this district. The distress begins near the base of the culvert and continues upward to 2 ft. (.66 m). The observed distress appears similar to acid attack; however, external sulfate attack and and/or freeze thaw attack may lead to such observed distress. While the paste remains intact, the aggregate has dissolved or lost its cohesion to the cement paste matrix. Similar distress was found on bridge columns. Based on the water samples (10 ppm SO₄) taken from this location had minimal sulfates which would place this location into Class 0 exposure. ASTM C 1580 was used for measuring the sulfate content of the

soil for this location. The sulfate content for this location was 0.07%, which would place this location into Class 0 exposure. There was not a significant change between the two extraction ratios tested which might mean that gypsum may not be the main sulfate. At this location, one of the culverts was being excavated to remove the soil from the bottom. Figure 7.6 shows the partially excavated soil in the culvert. It has not yet been determined, but the area above the soil level shows signs of distress which is often associated with physical salt attack. Table 7.3 provides the semi-quantitative results on a deteriorated and non-deteriorated section of the culvert. There are no formations of ettringite or gypsum in any of the XRD scans from any of the deteriorated culverts/columns in the district. Physical salt attack does not form any deleterious products as no chemical changes are occurring to the paste.

Table 7.3: Quantitative Rietveld analyses taken from two sections from a culvert at Site 22

Location	Ettringite (%)	Gypsum (%)	Monosulfate (%)	Portandite (%)
Site 22 Deteriorated	0.76	0.22	4.3	0.04
Site 22 Undeteriorated	1.39	0.07	2.99	0.11



Figure 7.5: Deterioration commonly found in culverts in the Paris District. The distress begins near the base of the culvert and continues up the side, likely in line with the highest level of water.



Figure 7.6: Deterioration of a culvert above the soil level, with no deterioration visible below the level of the soil (after excavation)

Site 57

This bridge is situated on SH 11 northwest of Sulphur Springs, Texas. Figure 7.7 shows the observed deterioration. A large portion of the cross section of the columns has deteriorated with reinforcing bars visibly showing. Similar to Site 22, the sulfate levels in the soils (0.08%) tested with TEX-135-E classify it as a class 0 exposure. Table 7.4 provides the XRD Rietveld analyses from the damaged and undamaged sections of the columns.



Figure 7.7: Deteriorated concrete columns from a bridge in the Paris District

Table 7.4: XRD results from Site 57 in the Paris District

Location	Ettringite (%)	Gypsum (%)	Monosulfate (%)	Portlandite (%)
Site 57 Deteriorated	1.39	0.07	2.99	0.11
Site 57 Non-deteriorated	0.76	0.22	4.31	0.04

The XRD results did not show significant amounts of ettringite or gypsum in either sample. Further testing is needed to determine the cause of the damage occurring to these structures. Sample retrieval for future powder samples may consist of taking powders at specified depth intervals. The creek below was dry on the day of sample retrieval which did not allow for water samples to be collected.

Summary of Paris District Findings

The damage shown in the culverts in this district is very widespread and further investigations are needed to identify the cause(s) of distress. Preliminary results may suggest physical salt attack on these structures as distress was primarily observed at evaporative fronts. The sulfate levels from the soil samples were quite low, generally below a Class 1 exposure according to ACI Exposure Table. Site 22 had sulfate contents of 0.07% and site 57 had sulfate contents in the soil of 0.08%. Site 57 did provide a significant loss on cross section from each column, but XRD analyses concluded that sulfate attack may not be occurring. The retrieval process may not be providing an accurate measurement of the concrete powder collected. Future testing should include milling into the concrete to provide different depths to determine a

sulfate concentration profile in the concrete, and cores should be extracted and examined petrographically.

7.2.3 El Paso District

Sites in the El Paso district exhibited the most significant sulfate attack signs of distress in Texas. The four most distinct cases will be discussed. Three of the locations include riprap damage while the fourth case involves concrete right of way (ROW) markers in the area. Sites 3, 31 and 32 all have riprap damage and Site 27 is the location of the deteriorated ROW markers.

Site 3

Site 3 is located on Interstate 10 near mile marker 57, just outside of El Paso. Figure 7.8 shows the damage to the riprap under the bridge. Several other bridges in the area show similar distress in the riprap. The paste is lost on the surface and many of the aggregates are loosened while others are barely clinging onto the paste below. In a few areas, the top layer of the concrete has separated from the layer below. A soil sample taken at the base of the riprap shows 0.01% SO₄ using ASTM C 1580 and 0.06% SO₄ using TEX-135-E. According to ACI 201.2R, both of these would be classified as Class 0 exposure according to ACI Exposure Class Table. Powder samples were taken from the base (0.06% SO₄) and top (0.14% SO₄) of the riprap embankment. The sulfate content is greater in the upper part of the embankment. Sulfates may concentrate on the surface of the concrete further up the embankment away from running water that may remove the sulfates off of the concrete on the bottom section. Riprap is usually made with a high w/cm and could lead to accelerated damage, compared to concrete with a lower w/cm.



Figure 7.8: Riprap deterioration occurring on the embankment below a bridge

Site 31

Another location with riprap damage is on FM 652, east of Guadalupe National Park, near the Texas and New Mexico Border. Figure 7.9 shows the disintegrated riprap at this location. The riprap damage is more severe than the damage seen in the Childress District and Site 3 in this district.



Figure 7.9: Riprap deterioration at Site 31 in the El Paso District

The sulfate content in the soil was 0.07% as per ASTM C 1580 and 0.18% SO₄ as per TEX-135-E, which brackets the cut-off point between Class 0 and Class 1 exposures of 0.1% SO₄. Table 7.5 shows the sulfate content in the concrete taken from the bottom, middle and top of the embankment. Sulfate levels in the riprap increase in the vertical direction, as was the case for Site 3.

Table 7.5: Sulfate content of concrete powder taken from the riprap at site 31

Location	SO ₄ (%)
Bottom	0.68
Middle	0.83
Top	1.38

Quantitative XRD Rietveld analysis conducted on the same powders showed an increase in gypsum content from one sample to the next as one moves vertically up the embankment. The gypsum content was 3% at the base of the embankment, 10% in middle, and 15% at the top. The increase in gypsum may suggest wicking of salts up the embankment leading to concentrations increasing near the top. Ettringite formation was minimal at each of the three locations on the embankment suggesting little transformation of hydration products to ettringite.

Site 32

This site is very near Site 31 and exhibits the same type of deterioration in the riprap. Figure 7.10 shows the riprap damage at this location. The sulfate content at this location fits into the Class 1 exposure classification (0.1% SO₄ as per ASTM C 1580 and 0.15% SO₄ as per TEX-620-E).



Figure 7.10: Deteriorated Riprap at Site 32 located on FM 652 in the El Paso District

Site 27

The most significant signs of attack on concrete specimens occurred on right-of-way (ROW) markers along the roadways. The ROW markers are pyramid shaped with a height of 48 in (1.2 m) consisting of an 8 in (200 mm) square base and 4 in (100 mm) square top. The marker is positioned 30 in (.75 m) into the soil. The TxDOT ROW Marker specification is in Appendix D. The ROW markers are constructed with two #3 reinforcement bars. Depending on the roadway, there are about 20 ROW markers per mile and more markers occur on curves which are used as station points for surveying. On a roadway, two ROW markers are placed directly across from each other. The initial discovery of a deteriorated ROW marker was at Site 27, located on SH 54 north of Van Horn, Texas. Figure 7.11 shows a photograph which is typical of the many deteriorated ROW markers in this region. The sulfate content of the soil on the surface was

0.91% SO₄, classifying it as very severe Class 3 exposure. Based on preliminary evaluations of these ROWs, a more detailed investigation was launched as discussed next.



Figure 7.11: ROW marker deteriorating in West Texas.

A long-term study on ROW markers located in the El Paso District which began in April 2007 is underway at the Concrete Durability Center (CDC) at The University of Texas at Austin to investigate the mechanisms of deterioration and to determine if external sulfate attack has occurred. According to preliminary tests, sulfate content in the soils in El Paso fell into a Class 3 exposure and gypsum was the primary type of sulfate. To allow for a detailed laboratory-based evaluation of deteriorated ROW markers, a total of eight ROW markers were removed and brought back to the CDC for subsequent testing. Six of these ROW markers were replaced with new ROW markers, cast at the CDC using selected concrete mixtures and constructed as per TxDOT specifications. Figure 7.12 shows the location of the ROW markers removed and replaced north of Van Horn, Texas. Table 7.7 shows the mixtures used in replacing the existing ROW markers. Two types of fly ashes were tested in addition to two different w/cm. These materials and mixture proportions were selected based on previous testing at the CDC (see Chapter 4) to produce some mixtures that were expected to perform and other mixtures that were expected to perform poorly in a sulfate environment (Class C fly ash with high w/cm).

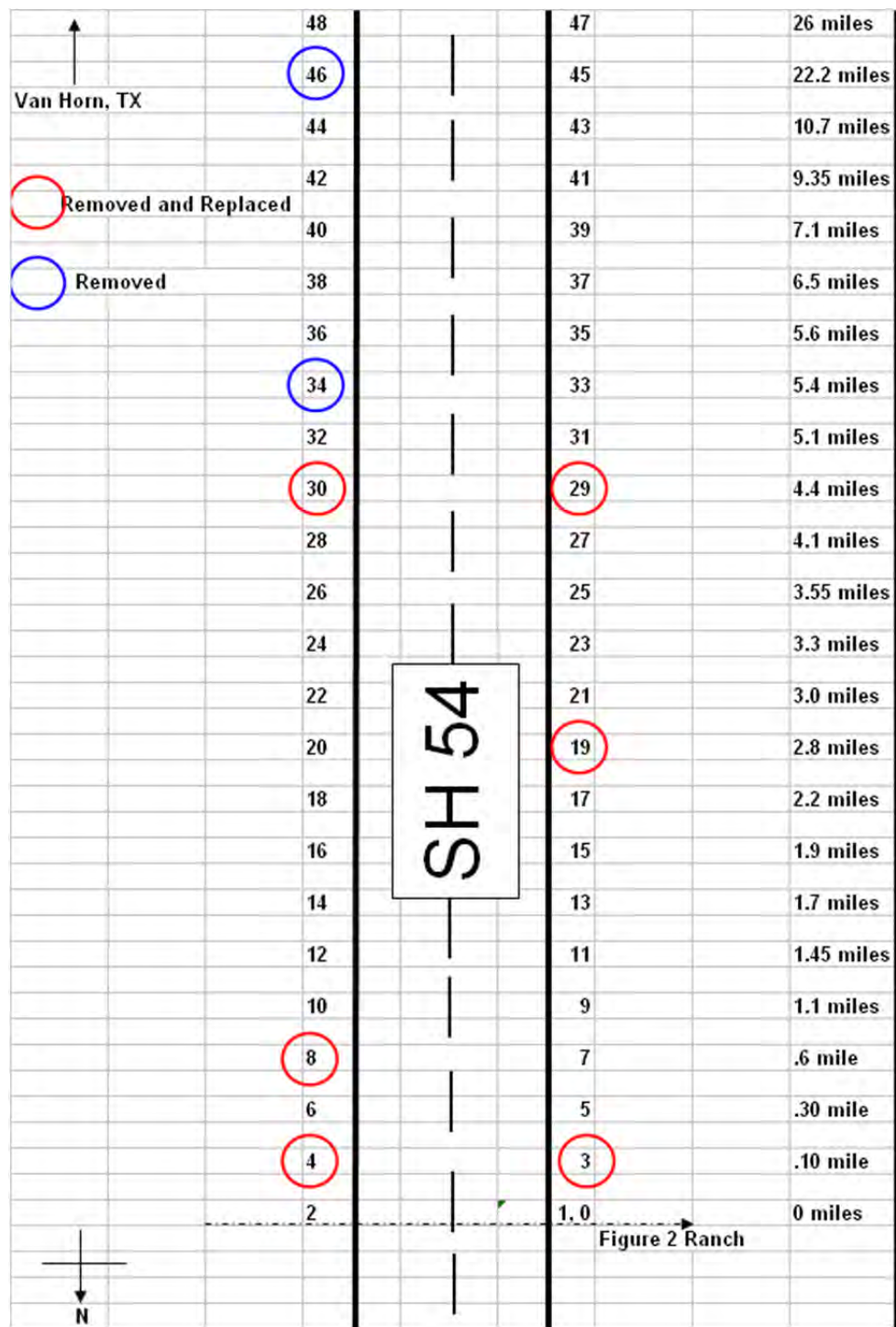


Figure 7.12: Location of the removed and replaced ROW markers along SH 54 north of Van Horn, TX

Table 7.6: Concrete Mixtures made for ROW Markers in West Texas

Mix #	Cement	Fly Ash	w/cm
1	Type I	-	0.4
2	Type I	-	0.7
3	Type I	40% C	0.4
4	Type I	40% C	0.7
5	Type I	20% F	0.4
6	Type I	20% F	0.7

Figure 7.13 shows an image of the placement of a new ROW marker in the existing hole left by the removal of a deteriorated ROW marker. At each ROW marker location, soil samples were removed from the top, middle, and bottom of the hole corresponding to depths of 0, 15 in (380 mm), and 30 in. (760 mm).



Figure 7.13: Placement of new ROW marker in the existing location of the deteriorated ROW marker

Figure 7.14 shows the sulfate content of the soil for each of the locations. The sulfate percentage from the 8:1 and 80:1 extraction ratio are shown to highlight the large difference between the two ratios. A difference of magnitude 10 is noticed between the two ratios which suggest gypsum is present in the soil. TEX-135-E, which uses a 20:1 extraction ratio, yielded sulfate contents near 2% for all the locations. Following the ACI 201.2R classification of severity of soils, both 20:1 and 80:1 extraction methods would fall into the most severe levels of exposure. The 8:1 extraction ratio would be considered a moderate sulfate exposure.

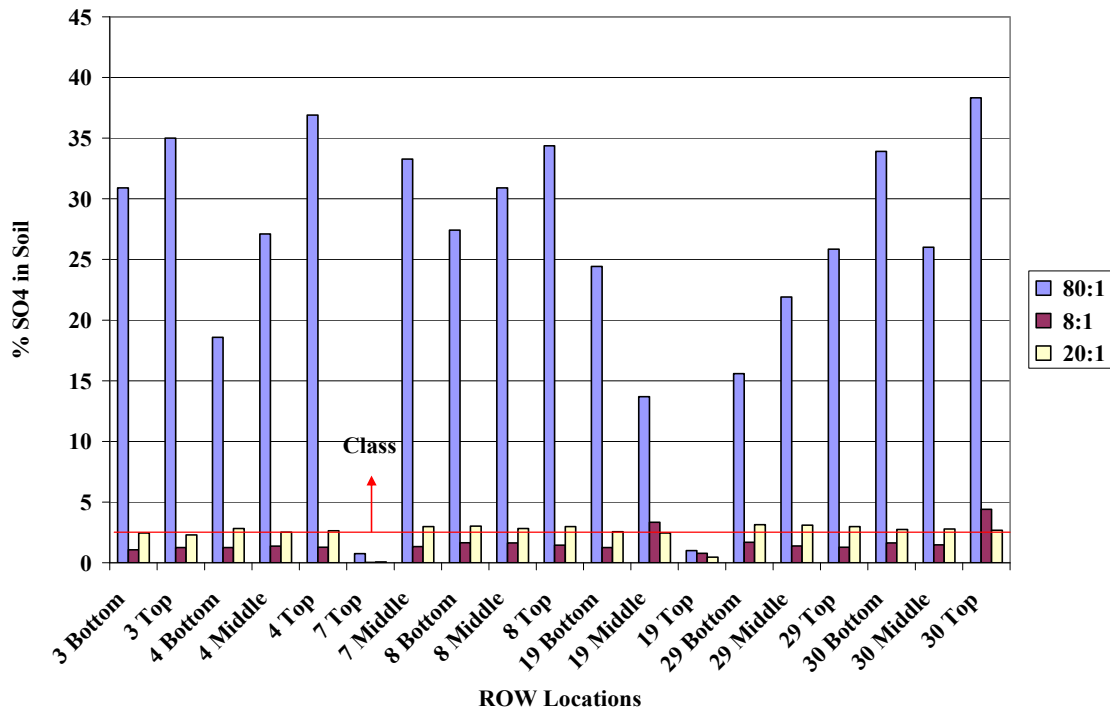


Figure 7.14: The sulfate content of soils taken from each of the ROW locations using ASTM C 1580 and TEX-135-E Test Methods

Preliminary results showed signs of sulfate-related deteriorations occurring in the ROW markers. Figure 7.15 provides the XRD Rietveld analysis from the ROW markers. Concrete powder was taken near the ground level of the marker. Quantitative XRD Rietveld analysis yielded 12% ettringite, which is clearly seen in the XRD scan. Chemical attack from gypsum (calcium sulfate) is known to produce ettringite formation. All but one of the markers removed showed significant ettringite and gypsum formation. The high level of sulfates in the soil and the deleterious products formed indicate damage induced by external sulfate attack from gypsumiferous soils.

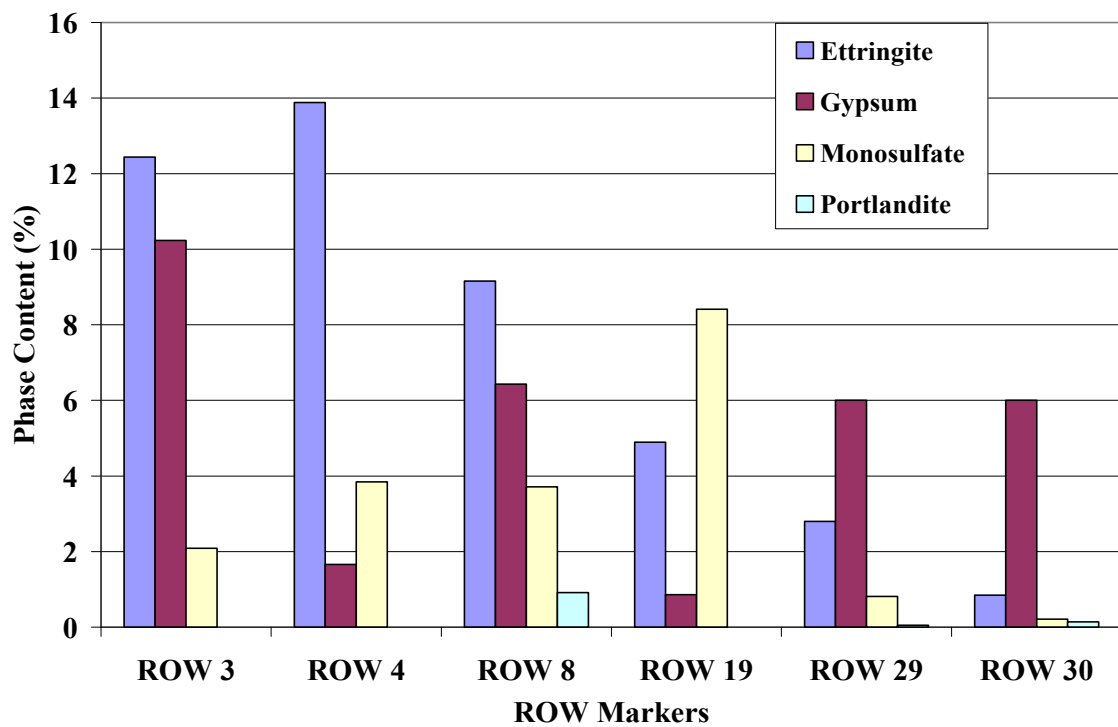


Figure 7.15: Rietveld Analyses from ROW markers in the El Paso District

Ongoing testing on the ROW markers includes milling for sulfate profiles on three different locations on the marker. Profiling was performed every 0.12 in (3 mm) to a depth of 0.48 in (12 mm) on the following sections of the marker: near the bottom of the marker (bottom of the hole), middle of the marker, (soil level), and top of the marker(exposed area). In addition, samples are being prepared for analysis by scanning electron microscopy.

The long-term study of these ROW markers began in April 2007 when the newly constructed ROW markers were placed into each of the existing ROW marker locations. Figure 7.16 shows a new ROW marker with Class C fly ash at 0.4 w/cm after three months of exposure. It will likely take several years to see any deterioration for the new ROW markers cast specifically to show deterioration (i.e. specific water/cm, fly ash combinations). ROW markers with Class F Fly ash at 0.4 w/cm should perform the best; while ROW markers with Class C fly ash at 0.7 w/cm would be expected to fail the earliest. The performance of these ROW markers will be tracked and reported in future publications. In addition, selected ROW markers were cast and are being monitored at the outdoor sulfate exposure site at the CDC in Austin. The sulfate soil concentrations at both sites are past the solubility limit of gypsum which should allow for similar progression of attack between the two sites.



Figure 7.16: New ROW marker with Class C fly ash at 0.4 w/cm after 3 months of exposure in gypsiferous soils

Summary of El Paso Findings

The visual damage to structures in this district and the subsequent forensic evaluations have shown that external sulfate attack in gypsiferous soils is occurring in the El Paso district, although this distress appears to be limited to relatively poor quality concrete used for non-structural applications (ROW markers, riprap, etc.) Additional research is in progress, but the findings are significant in that it has been confirmed that external sulfate attack has occurred in Texas, albeit on a limited number of non-critical structures.

7.3 Conclusions

The investigation into external sulfate attack in Texas resulted in examining over 250 concrete structures in three districts. The following are conclusions made from the investigation of concrete structures for external sulfate attack:

- 12 structures throughout the three districts have shown visual signs of deterioration similar to sulfate attack in the state of Texas.
- It was concluded that the Childress District did not have any structures deteriorated from external sulfate attack.
- The Paris District had many culverts and bridges potentially damaged from physical salt attack. Preliminary results indicate that chemical attack is not occurring on these structures. The deterioration is occurring in the evaporative section of the structures usually above a water line or soil level.

- The El Paso District showed the most deterioration. Riprap, constructed from high w/cm concrete, exhibited some distress in relatively low sulfate concentrations, perhaps due to the relatively poor quality of the concrete. Gypsum formation within the matrix was detected, and sulfate concentrations were found to increase vertically as one moves up the embankments, suggesting that sulfates are rising by wicking action and accumulating towards the top of the elements.
- ROW markers in the El Paso district showed significant deterioration, which was confirmed to be caused by external sulfate attack. Rietveld analyses show ettringite formation occurring in the ROW markers. More detailed evaluation of ROWs, removed from service, is in progress and will be presented in future publications and in the final project report to be submitted to TxDOT in 2009.

The use of varying sulfate extraction ratios, through the combined use of ASTM C 1580 and TEX-135-E, did allow for the identification of gypsum in soils. More research is needed to determine how best to analyze the results from sulfate extracts and how to apply these results to specifications aimed at preventing external sulfate attack.

Chapter 8. Conclusions, Recommendations, and Guidelines for Sulfate Resistant Concrete

This research project covered a comprehensive laboratory and field evaluations of mortars and concretes exposed to external sulfates. The research summarized in this report and described in detail by Drimalas (2007), Clement (2009), and Dhole (2009) has made significant progress in better understanding the underlying mechanisms of external sulfate attack, especially with regard to the use of Class C fly ash in sulfate-rich environments. Based on this research, the following conclusions, recommendations (e.g., test methods), and guidance (e.g., w/cm ratio) can be presented, all of which can be implemented into specifications aimed at ensuring the durability of concrete in sulfate environments.

In general, the use of high-calcium fly ash in moderate dosages (e.g., 20 to 40 percent by mass of cementitious materials) in the study showed poor sulfate resistance. The deterioration tended to increase as the dosage of Class C fly ash was increased. However, the incorporation of a second SCM (silica fume, slag, UFFA) helped to substantially improve the sulfate resistance of mixtures containing these Class C fly ashes, as did the addition of small amounts of gypsum. Although the research performed under this project has clearly shown that adding gypsum to concrete containing Class C fly ash can significantly improve sulfate resistance of various mixtures, this is likely not a viable option in the field because excessive additions of gypsum can adversely impact performance and adding gypsum to concrete not containing Class C fly ash may in fact increase the potential for internal or external sulfate attack. It was also found that increasing the Class C fly ash dosage to higher levels (e.g., 60 to 70 percent by mass of cementitious materials) resulted in satisfactory sulfate resistance, regardless of the CaO content of the fly ash.

Characterization of fly ashes used in this program was carried out successfully by using XRD and SEM techniques. This study gave good insight into the reasons behind satisfactory performance of the Class F fly ashes and poor performance of the Class C fly ashes. A good link between chemical composition of the glass in fly ashes, mineralogy of the crystalline components and sulfate resistance was established. The glass composition of a fly ash expressed by its location in the mullite, anorthite or gehlenite field on the Dunstan's Ternary diagram, reveals its performance more precisely than its bulk composition. The Rietveld method of analysis was used as the technique to determine the crystalline portion.

Quantitative analysis of the hydration products formed in fly ash mixes confirmed that fly ashes generating more ettringite than monosulfate before they are exposed to sulfates solution, yield better sulfate resistance. On the other hand, fly ashes generating more monosulfate than ettringite prior to exposures offered poor performance. Using this method of quantifying early hydration products and resultant product formation after exposure to sulfates, it is thus possible to predict sulfate resistance of a given fly ash by determining its ettringite potential. The overall sulfate resistance of a fly ash may also be indicated by other parameters such as SO₃ content and CaO/SiO₂ which are closely related to the CaO content of the corresponding fly ash.

Concrete prisms placed in sodium sulfate expanded the quickest and showed faster deterioration than prisms placed in magnesium and calcium sulfate. Prisms in the submerged sodium sulfate conditions deteriorated quicker than control prisms kept indoors at 73 °F (23 °C). Prisms in magnesium sulfate ultimately expanded the greatest of all the sulfate types and showed large cracks rather than deteriorating/expansion noticed in sodium sulfate prisms.

Prisms in the different calcium sulfate conditions did not expand at 18 months but did show signs of deterioration on the surface of the prisms. The sulfate concentration in the trench matched the total sulfate in ppm from the sodium sulfate trench (33000ppm SO₄) which is far beyond the solubility limit of gypsum. In the outdoor calcium exposure site, prisms only show deterioration below the soil level. Due to visible damage on prisms, prisms in the indoor calcium solutions were kept for 2 years, after which they began to expand. This helps to confirm that concrete exposed to external sources of gypsum can, in fact, suffer from sulfate-related deterioration.

XRD Rietveld analysis highlighted the strong impact that w/cm has on sulfate resistance of concrete. In lower w/cm mixtures, less destructive products, such as ettringite, formed as a function of distance from the exposed surface. For higher w/cm mixtures, levels of ettringite were nearly the same for milled powder samples taken from the exposed surface and similar samples taken from within the bulk of concrete prisms.

The w/cm ratio was found to be the most important factor that determines the susceptibility of mixtures to combined (chemical and physical) sulfate attack. Concrete specimens cast with w/cm of 0.50 and 0.70 undergo significant level of deterioration in both static and cyclic exposures to Na₂SO₄ and static exposure to CaSO₄. Sulfate attack cannot be prevented by limiting the w/cm of concrete to 0.45. Reducing the w/cm to 0.40 can provide satisfactory sulfate resistance to the concrete mixes with Type I cement, or Class C fly ash mixes containing 20% fly ash. However concrete produced with a low w/cm of 0.40 and with 40% Class C fly ash can still undergo deterioration during the combined (physical-chemical) sulfate attack of Na₂SO₄, in the form of scaling, mass loss, and cracking.

A comprehensive field survey was performed in the three TxDOT-defined districts in Texas (Childress, Paris, and El Paso) with the highest sulfate contents in soil and/or groundwater. A total of 12 structures throughout these three districts have shown visual signs of deterioration similar to sulfate attack. Right-of-Way (ROW) markers in the El Paso district were the only concrete structures that had a correlation between sulfates in soils and deleterious products forming within the concrete. Calcium sulfate (gypsum) did produce damage on these concrete markers in West Texas, which suggests that gypsum may cause damage in the field. This was confirmed in long-term exposure site testing in Austin, TX. This combination of field performance data, outdoor exposure site results, and laboratory tests show the sulfate attack in gypsiferous soils is a potential concern and justifies the requirements for preventive measures in such environments.

Although the degree of deterioration was generally less in soils (or solutions) containing gypsum than those containing magnesium or sodium sulfate, it not possible at this time to establish separate guidance for gypsum compared to the other sulfates. An approach similar to that in ACI 318 (and ACI 201) is thus recommended at this point, where the requisite preventive measures are based on total sulfate concentration (in soil or groundwater), regardless of cation type. It is hoped that in the future, and with the aid of long-term field data from exposure sites in Austin and other parts of Texas, it will be possible to develop gypsum-specific guidance.

The use of ASTM C 1012 is still the recommended test for determining the sulfate resistance of concrete mixtures. It uses sodium sulfate solution which did prove to be the most aggressive solution in the majority of testing. Texas predominately has calcium sulfate (gypsum) soils but the use of calcium sulfate in ASTM C 1012 only delayed the onset of expansion. The use of mortar bars compared to the modified version with concrete prisms tended to decrease the time until the onset of expansion. A correlation did exist between ASTM C 1012 and the

outdoor exposure concrete prisms, but once again the mortar bars began to expand at earlier time periods.

ASTM C 1580 is recommended as a suitable test method for measuring sulfates in soils. The varied extraction ratios used in this method allow the engineer to determine whether the soil contains gypsum or other more soluble sulfate types (sodium or magnesium sulfate). This test method is particularly useful in Texas, where gypsiferous soils are very common. Also, this test does not rely on the determination of cation type or concentration, thus making it more practical for TxDOT or other agencies to implement.

References

ACI 201.2R, "Guide to Durable Concrete," Manual of Concrete Practice, 2001

Al-Amoudi, OSB "Attack on plain and blended cements exposed to aggressive sulfate environments," *Cement and Concrete Composites*, Vol. 24, pp. 305-316, 2002.

ASTM C 452, "Standard Test Method for Potential Expansion of Portland-Cement Mortars Exposed to Sulfate," ASTM International, West Conshohocken, PA, 2006.

ASTM C 1012, "Standard Test Method for Length Change of Hydraulic-Cement Mortars Exposed to a Sulfate Solution," ASTM International, West Conshohocken, PA, 2004.

ASTM C 1293, "Standard Test Method for Determination of Length Change of Concrete Due to Alkali-Silica Reaction," ASTM International, West Conshohocken, PA. 2006

ASTM C 1580, "Standard Test Method for Water-Soluble Sulfate in Soil," ASTM International, West Conshohocken, PA. 2005.

Bellmann, F., Stark, J., "New Findings when Testing the Sulfate Resistance of Mortars," *ZKG International*, Vol. 59, No. 6, 2006.

Bensted, J. "Thaumasite - Background and Nature in Deterioration of Cements, Mortars and concretes," *Cement & Concrete Composites*, Vol. 21, No. 2, pp 117-121, April, 1999.

Berkeley, E. "On Some Physical Constants of Saturated Solutions," *Philosophical Transactions of the Royal Society of London. Series A, Containing Papers of a Mathematical or Physical Character*, Vol. 203, pp. 189-215, 1904.

Clement, C., "Laboratory and Field Evaluations of External Sulfate Attack – Phase II," Ph.D. Dissertation, The University of Texas at Austin, 2009.

Dhole, R. (2009). "Sulfate resistance of high-calcium fly ash concrete." PhD Thesis, University of New Brunswick, Fredericton, NB, Canada.

Drimalas, T., "Laboratory Investigations of Delayed Ettringite Formation," Thesis. The University of Texas at Austin (2004) Austin, Texas

Drimalas, T. 2007. "Laboratory and field evaluation of external sulfate attack." PhD Thesis, University of Texas at Austin, Austin, TX.

Dunstan, E. R., "A possible method for identifying Fly Ashes That Will Improve the Sulfate Resistance of Concretes," *American Society of Testing and Materials*, 1980.

Eglinton, M., "Resistance of Concrete to Destructive Agencies," *Lea's Chemistry of Cement and Concrete*. Editor. 4th Edition, pp. 299-342, 1998.

Famy, C. (1999). "Expansion of Heat-Cured Mortars," Dissertation. University of London. London, England

Flatt, R.J., and Scherer, G. W. "Hydration and Crystallization Pressure of Sodium Sulfate," Material Research Society Symposium, Vol. 712, Princeton University, Civil and Environmental Engineering, Princeton NJ. 2002

Folliard, K.J. and Sandberg, P., "Mechanisms of Concrete Deterioration by Sodium Sulfate Crystallization," *Proceedings, Third International ACI/CANMET Conference on Concrete Durability*, Nice, France, pp. 933-945, 1994.

Gollop, R.S., Taylor H.F.W., "Microstructural and MicroAnalytical Studies of Sulfate attack III. Sulfate-Resisting Portland Cement: Reactions with Sodium and Magnesium Sulfate Solutions," *Cement and Concrete Research*, Vol. 25, No. 7, pp.1581-1590, 1995.

Haynes, H, O'Neill, R., and Mehta, P.K., "Concrete Deterioration from Physical Attacks by Salts," *Concrete International*, V.18, No. 1, pp. 63-68, January 1996.

Heinz, D., and Ludwig, U., "Mechanism of Secondary Ettringite Formation in Mortars and Concretes Subjected to Heat Treatment," *Concrete Durability: Katherine and Bryant Mather International Conference*, Vol. 2, pp 2059-2071, 1987.

Hime, W.D, and Mather, B., "Sulfate Attack" or is it?" *Cement and Concrete Research*, V.29. No.5, pp. 789-791, 1999.

Hooton, D. R. and Emery J., "Sulfate Resistance of a Canadian Slag Cement," *ACI Materials Journal*, Vol. 87, No. 6, pp. 547-555, Nov-Dec, 1990.

Khatib, J.M., Wild S., "Sulfate Resistance of Metakaolin Mortar," *Cement and Concrete Research*, Vol. 28, No 1, pp 83-92, 1998.

Khatri, R.P, Sirivivatnanon V., and Yang J.L., "Role of permeability in sulfate attack," *Cement and Concrete Research*. Vol. 27 No. 8, pp 1179-1189, 1997.

Lee, S.T., Moon, H.Y., Hooton, R.D., Kim, J.M., "Effect of Solution Concentration and Replacement Levels of Metakaolin on the Resistance of Mortars Exposed to Magnesium Sulfate Solutions," *Cement and Concrete Research*. Vol. 35, pp. 1314-1323, 2005.

Mehta, P.K, Gjorv O.E., "A New Test for Sulfate Resistance of Cements," *Journal of Testing and Evaluations, KTEVA*. Vol.2 No. 6, pp. 510-514, Nov 1974.

Mehta, P.K., "Sulfate attack on concrete: separating myths from reality," *Concrete International*. Vol. 22 Issue 8, pp 57-61, 2000.

Mehta, P.K., "Sulfate attack on concrete: a critical review," *Materials Science of Concrete*, Vol. III, American Ceramic Society, Westerville, Ohio, pp 105-130, 1993.

Neville, A. M., Properties of Concrete, 4th edition, John Wiley & Sons, 1996.

Neville, A.M., "The Confused World of Sulfate Attack" Cement and Concrete Research. Vol. 34, No. 8, pp 275-1296, 2004.

Powers, T.C., Copeland L.E., Hayes, J.C., Mann H.M., "Permeability of Portland Cement Paste," *ACI Journal Proceedings 51 (3)* pp. 285-298, 1954.

Hime, W.G., "Chemical Methods of Analysis of Concrete" *Handbook of Analytical Techniques in Concrete Science and Technology*. Editors Ramachandran, V.S., and J.J. Beaudoin, Noyes Publications / Willam Andrew Publishing, Norwich, New York, pp. 105-126, 2001.

Ramlochan, T. "The Effect of Pozzolans and Slag on the Expansion of Mortars and Concrete Cured at Elevated Temperature," Dissertation. University of Toronto, Toronto, Canada, 2003.

Rebel, B., Detwiller, R.J., Gebler, S.H., and Hooton, R. D. "The Right Sulfate Test Makes a Difference," *Concrete International*, February, 2005.

Santhanam, M., M.D. Cohen and Olek, J, "Sulfate Attack Research –Whither now?," *Cement and Concrete Research*, V31. pp. 845-851, 2001.

Shashiprakash, S. and Thomas, M. "Sulfate Resistance of Mortars containing high calcium fly ashes and combinations of highly reactive pozzolans and fly ash," *Seventh CANMET/ACI International Conference on Fly Ash, Silica Fume, Slag, and Natural Pozzolans in Concrete, American Concrete Institute*. SP 199.201. Volume 1. pp. 221-237, 2001.

Stark, D. "Durability of Concrete in Sulfate-Rich Soils," *Research and Development Bulletin RD 097*. Portland Cement Association. Skokie IL. 1989

Stark, D. "Performance of Concrete in Sulfate-rich soils," *Research and Development Bulletin RD 129*. Portland Cement Association, Skokie, IL. 2002

Taylor, H.F.W. and Gollop, R. S., "Some Chemical and Microstructural Aspects of Concrete Durability," *Mechanisms of Chemical Degradation of Cement-Based Systems*, pp.177-184. 1997

Tian, B, M.D. Cohen, "Expansion of alite paste caused by gypsum formation during sulfate attack," *Journal of Materials in Civil Engineering*. Vol. 12 No. 1, pp. 24–25, February, 2000.

Tikalsky, P.J and Carrasquillo R.L. (1989) "The effect of Fly Ash on the sulfate resistance of concrete, "Centre for Transportation Research, University of Texas, Austin, Research Report No. 481-5, 317p.

Tikalsky P.J. and R.L. Carrasquillo. "Fly Ash Evaluation and Selection for Use in Sulfate-Resistant Concrete," *ACI Materials Journal*. pp. 545-551, November-December, 1993.

Tikalsky P.J. and R.L. Carrasquillo, "Influence of Fly Ash on Sulfate Resistance of Concrete" *ACI Material Journal*, pp. 69-75, January-February, 1993.

Tulliani, Jean-Marc, Montanaro, L., Negro, A., Collepardi, M., "Sulfate Attack of Concrete Building Foundations induced by sewage waters," *Cement and Concrete Research*, Vol. 32, No. 6, pp. 843-849, June, 2002.

Van Aardt, J.H.P. and Vissar, S. (1985) "Influence of alkali on the sulfate resistance of ordinary portland cement mortars," *Cement and Concrete Research*, Vol. 15, pp. 485-494.